Dissecting Tumor Heterogeneity and Cancer Stem Cell Properties in Clear Cell Renal Cell Carcinoma

---

Dissertation

zur

Erlangung der naturwissenschaftlichen Doktorwürde

(Dr. sc. nat.)

vorgelegt der

Mathematisch-naturwissenschaftlichen Fakultät

der

Universität Zürich

von

Claudia Corrò

aus

Italien

Promotionskommission

Prof. Dr. Beat Schaefer (Vorsitz)
Prof. Dr. Holger Moch (Leitung der Dissertation)
Prof. Dr. Bernd Bodenmiller
Prof. Dr. Ian Frew
Dr. Markus Rechsteiner

Zürich, 2018

To my family

TABLE OF CONTENTS

ABBREVIATIONS

ABCB5: ATP-binding cassette, sub-family B, member number 5

ALDH1: aldehyde dehydrogenase 1

AML: acute myeloid leukemia

BHD: Birt-Hogg-Dubé

BMDC: bone marrow-derived cell

BMP: bone morphogenetic protein

BMPC: bone marrow-progenitor cell

CAF: cancer associated fibroblast

CA-IX: carbonic anhydrase-IX

ccRCC: clear cell RCC

CD105: Endoglin

CD133: Prominin-133

cfDNA: circulating free DNA

CFS: cancer-free survival

chRCC: chromophobe RCC

c-MET: tyrosine-protein kinase Met

CRC: colorectal carcinoma

CSC: cancer stem cell

CSS: cancer-specific survival

CT: computed tomography

CTC: circulating tumor cell

ctDNA: circulating tumor DNA

CTLA-4: cytotoxic T-lymphocyte-associated antigen 4

CXCL8: CXC motif ligand 8

CXCR4: CXC-chemokine receptor 4

DC: dendritic cell

DFS: disease-free survival

ECM: extra-cellular matrix

EGF: epidermal growth factor

EGFR: EGF receptor

EMT: epithelial-mesenchymal transition

EPO: erythropoietin

ERK: extracellular signal-regulated kinase

EV: extracellular vesicle

FACS: fluorescent-activated cell sorting

FAK: focal adhesion kinase

FGF: fibroblast growth factor

FGFR: FGF receptor

FISH: fluorescence in situ hybridization

Glut1: glucose transporter 1

GPCR: G protein-coupled receptor

HA: glycosaminoglycan hyaluronan

HCC: hepatocellular carcinoma

HDAC1: histone deacetylase 1

HGF: hepatocyte growth factor

HIF: hypoxia-inducible factor

HLA-G: human leukocyte antigen G

HLRCC: hereditary leiomyomatosis RCC

HRE: hypoxia-responsive elements

HSP: heat shock family proteins

IFNα: interferon-α

IGF-1: insulin-like growth factor-1

IHC: immunohistochemistry

IL-15: interleukin-15

IL-1β: interleukin-1β

JAK: Janus kinase

LDA: limiting dilution assay

LOH: loss of heterozygosity

MACS: magnetic beads-conjugated antibodies

MAPK: mitogen-activated protein kinase

MDSC: myeloid-derived suppressor cell

MEK: mitogen-activated protein kinase kinase

MET: mesenchymal-epithelial transition

miRNA: microRNA

MMP: matrix metalloproteinases

OCD: dissociated tumor cells

OS: overall survival

PCR: polymerase chain reaction

PD-1: programmed death 1

PDGF: platelet-derived growth factor

PDGFR: PDGF receptor

PD-L1: PD-1 ligand

PHD: prolyl hydroxylase domain protein

PI3K: phosphatidylinositol-3 kinase

PKC: protein kinase C

PLC: phospholipase C

pRCC: papillary RCC

RCC: renal cell carcinoma

RFS: recurrence-free survival

Rh123: Rhodamine 123

IL-2: interleukin-2

IL-6: interleukin-6

IL-8: interleukin-8

MRI: magnetic resonance imaging

MSC: mesenchymal stem cell

mTOR: mammalian target of rapamycin

MVB: multivesicular body

n.s.: non-significant

NF-kB: nuclear factor-kappa B

NK: natural killer

NSCLC: non-small-cell lung cancer

NSG: NOD scid gamma

RT-PCR: real time-PCR

SCF: stem cell factor

SDF1: CXC chemokine stromal cell-derived factor 1

SDH-RCC: succinate dehydrogenase RCC

siRNA: small interfering RNA

SNP: single nucleotide polymorphism

SP: side population

STAT: signal transducers and activators of transcription

TAM: tumor-associated macrophage

TEM: transmission electron microscopy

TGF: transforming growth factor

TGFβ: transforming growth factor β

TKI: tyrosine kinase inhibitor

TMA: tissue microarray

TMA: tumor-associated macrophage

TME: tumor microenvironment

TNA: tumor-associated neutrophil

TNFα: tumor necrosis factor α

VEGF: vascular endothelial growth factor

VEGFR: VEGF receptor

TNM: tumor, lymph nodes, metastasis

TS: tuberous sclerosis

UCH: ubiquitin C-terminal hydrolase

VHL: von Hippel-Lindau

ABSTRACT

Renal cell carcinoma (RCC) represents the most common malignancy affecting the adult kidney. Accounting for 2 % of all cancers, RCC lays among the 10 most common cancers worldwide. In particular, clear cell renal cell carcinoma (ccRCC) is the most frequent RCC subtype. ccRCC is characterized by inactivation of the *von Hippel-Lindau* (*VHL*) tumor suppressor gene by chromosomal loss of one allele located at position 3p combined with a mutation on *VHL* on the second allele resulting in loss of heterozygosity (LOH). The protein pVHL is involved in many different biological processes, therefore, drugs targeting VHL downstream pathways are now standard therapies used for treating ccRCCs. However, these drugs show only moderate overall survival benefit and have significant side effects for patients. Recently, several additional tumor suppressor genes have been found frequently mutated in ccRCC such as genes involved in the chromatin-remodeling process: *SETD2*, *BAP1*, *PBRM1*, *JARID1c*, *TP53* and some other genes involved in PI3K-mTOR pathway: *PIK3CA*, *MTOR* and *PTEN*. Interestingly, phylogenic evaluation revealed these genes to be mutated together or separately in different tumor regions analyzed from the same primary ccRCC tumor. Additionally, comparison of multiple samples derived from the same ccRCC patient revealed 25 % higher similarity to unrelated ccRCC samples, indicating that ccRCC is characterized by extensive inter- and intra-tumor heterogeneity. Indeed, tumor heterogeneity is one of the major limitation in the treatment of epithelial tumors. Poor response is observed upon chemotherapy and radiotherapy in ccRCC patients, whereas targeted therapies such as TKIs are only palliative in advanced ccRCCs. It is becoming increasingly clear that genetic and epigenetic factors are not just the only two factors contributing to tumor heterogeneity. The tumor microenvironment, stroma cells, soluble molecules and extracellular vesicles (i.e. exosomes) play an important role in modulating metastatic properties and sensitivity of tumor cells to therapy. Moreover, cancer stem cells (CSCs) are recognized being the major cause of tumor recurrence and resistance to therapy. They are characterized by unlimited cell division, self-renewal, capability to differentiate into several cell types, and tumorigenicity. Therefore, the identification of a specific subpopulation of cells within a tumor

that either initiate or maintain tumorigenesis is of utmost importance for understanding tumor biology and in the development of novel therapies.

During my Ph.D. studies, I focused on the investigation of the clinical applicability of circulating tumor DNA (ctDNA) and exosomes as potential prognostic and diagnostic biomarkers showing that the development of non-invasive methods to detect *de novo* or to monitor already known tumor specific signatures continue to be a major challenge in renal cancer. Nevertheless, genomic investigation of exoDNA together with ctDNA might prove to successfully detect new mutations harboring during tumor progression and therapeutic intervention. Moreover, primary tumor cultures were exploited in order to dissect tumor heterogeneity in the context of a personalized medicine approach. We showed that patient-derived cultures are more accurate in retaining patient-specific molecular features compared to immortalized cell lines and, therefore, are a promising tool for translational cancer research studies. Finally, new biomarkers for renal cancer stem cells with potential therapeutic implications were investigated. IL-8/CXCR1 were found associated with cancer stem cell properties *in vivo* and *in vitro* representing a potential therapeutic target for renal cancer. Moreover, IL-8 and CXCR1 were found correlated with clinical prognosis in ccRCC patients. For this reason, targeting CSCs through IL-8/CXCR1 in combination with conventional chemotherapy agents and/or immunotherapy would be the next step towards overcoming tumor recurrence. In conclusion, understanding the mechanisms underlying tumor heterogeneity and cancer stem cell contribution to tumor progression, metastasis formation and therapy failure, together with the use of primary cell cultures, may ultimately promote the discovery of more accurate and reliable diagnostic and prognostic tools as well as provide the instruments for precise and patient-oriented therapeutic intervention.

KURZFASSUNG

Das Nierenzellkarzinom ist das häufigst auftretende bösartige Nierenkrebsleiden und wird in 2 % aller neudiagnostizierten Krebsfälle nachgewiesen. Somit steht das Nierenzellkarzinom an zehnter Stelle aller Krebsleiden weltweit. Das klarzellige Nierenzellkarzinoms ist des weiteren der häufigste Subtyp und ist durch die Inaktivierung des *von Hippel-Lindau* (*VHL*) Tumorsuppressorgens charakterisiert. Häufig ist die Inaktivierung des *VHL* Gens durch einen 3p-Allelverlust und einer weiteren Mutation auf dem zweiten Allel gekoppelt, was zu einem sogenannten 'loss of heterozygosity' (LOH) Genotyp führt. Das VHL Protein ist in vielen biologischen Prozessen involviert, welche durch verschiedene Inhibitoren reguliert werden können. Einige dieser Inhibitoren sind bereits zugelassene Standardtherapien, wobei leider nur bei einem kleinen Prozentsatz der Patienten ein verlängertes Gesamtüberleben nachgewiesen wurde. Kürzlich wurden im klarzelligen Nierenzellkarzinom nebst Mutationen im Gen *VHL* auch häufig genetische Alterationen in anderen Tumorsuppressorgenen *(SETD2*, *BAP1*, *PBRM1*, *JARID1c*, *TP53)* und in Genen der PI3K-mTOR Signalkaskade (z.B. *PIK3CA*, *MTOR, PTEN)* gefunden. Phylogenetische Analysen zeigten zudem, dass Mutationen in diesen Genen entweder zusammen oder einzeln in verschiedenen Regionen des ein und demselben Primärtumors auftreten können. Des Weiteren konnte gezeigt werden, dass Tumorproben von Patienten mit klarzelligem Nierenzellkarzinom untereinander sogar eine 25 % höhere Übereinstimmung der genetischen Alterationen aufwiesen, als mit einzelnen Metastasen und des Primärtumors von demselben Patienten. Dies lässt auf einen hohen Grad an inter- und intra- Tumorheterogenität im klarzelligen Nierenzellkarzinom schliessen. Dieser Fact ist auch gut vereinbar mit dem schlechten Ansprechen von Patienten mit einem klarzelligen Nierenzellkarzinom auf Chemo- und Radiotherapie und der nur palliative angewandten Therapien mittels TKIs. Zunehmend wird klarer, dass nicht nur genetische und epigenetische Faktoren zur Tumorheterogenität beitragen sondern auch die umliegenden Zellen, wie Stromazellen, oder zellfreie Moleküle und extrazelluläre Vesikel, wie Exosomen, welche das metastasierende Potential eines Tumors oder die Sensitivität gegenüber einer Therapie beinflussen. Zusätzlich rücken sogennante Krebsstammzellen weiter in den Fokus und werden haupsächlich für das erneute Auftreten eines Tumors nach Behandlung und dessen Resistenz verantwortlich gemacht. Krebsstammzellen sind durch unlimitiertes

Wachstum, Selbsterhaltung und Tumorgenität charakterisiert und können in verschiedene Zelltypen differenzieren. Deshalb ist es von grösstem Interesse eine solche Stammzellpopulation innerhalb der Tumormasse ausfindig zu machen, um die Tumorevolution besser zu verstehen und geeignete Behandungsoptionen anbieten zu können.

Während meinem Ph.D. Studium fokussierte ich mich zuerst auf die klinische Anwendbarkeit von zirkulierender Tumor-DNA (ctDNA) und Exosomen als prognostische und prediktive Biomarker im klarzelligen Nierenzellkarzinom. Die Anwendung sollte einerseits zur Detektierung von schon bekannten Mutationen, welche bereits vor Therapiestart bekannt waren, genutzt werden. Andereseits sollte es aber auch möglich sein, neue sogenannte Resitenzmutationen nachzuweisen. Der Nachweis solcher Mutationen im klarzelligen Nierenzellkarzinom erwies sich als schwierig und wurde auch als solches publiziert (Corrò C. et. al., 2017: Detecting circulating Tumor DNA in renal cancer: An open challenge). Als zweites Haupziel meiner Dissertation vertiefte ich mich in die Etablierung und Analyse von primären Zelllinien, welche von Nierenzellkarzinom-Patienten stammten. Dieser Ansatz erlaubte es, gezielt die Tumorheterogenität zu untersuchen und mögliche personaliserte Therapien auszuarbeiten. Wir konnten zeigen, dass diese primären Patientenzelllinien das molekulare Profil besser erhalten als z.B. immortalisierte Zelllinien. Ein weiteres Ziel im Rahmen der Dissertation war, Stammzell-Biomarker im klarzelligen Nierenzellkarzinom zu finden und zu untersuchen. Dabei zeigte sich, dass Nierenkrebszellen, welche IL-8 und CXCR1 exprimierten zu einer Nischenpopulation gehörten, welche Stammzelleigenschaften aufwiesen. Demzufolge wäre eine Kombinationstherpaie von konventioneller Chemotherapie gekoppelt mit einer Immuntherapie ein möglicher nächster Schritt, um eine Therapie einzusetzten, welche die Wahrscheinlichkeit eines Wiederauftretens des Tumor verkleiner würde. Zusammengefasst erarbeitete ich in meiner Dissertation neue Einblicke in die Tumorheterogenität des klarzelligen Nierenzellkarzinoms, insbesondere in dessen Krebsstammzelleigenschaften, und wie diese sich auf die Tumorprogression, Metastasierung und Therapieansprechen auswirken können. Diese Ergebnisse bieten eine Möglichkeit neue und bessere Therapieansätze zu entwickeln, welche den Nierenzellkarzinom-Patienten helfen können.

INTRODUCTION

1. Renal Cell Carcinoma

Cancer is one of the leading cause of morbidity and mortality worldwide. Despite of the significant progress made in understanding and treating cancer in the last decades, cancer still represents a major public health problem (WHO factsheet 2017). In 2016, 1'685'210 new cancer cases and 595'690 cancer deaths are projected to occur in the United States (1).

Cancer assembles a group of diseases engaging dynamic chances in the genome (2). Tumorigenesis is a multi-step process, which involves the malignant transformation of normal cells into tumor cells. Cancer cells can grow beyond their usual boundaries, invade nearby tissues and spread to other organs forming metastases, which are the major cause of death (WHO factsheet 2017) (Fig. 1.1A). It is a complex phenomenon, which not only requires tumor cells to acquire sustaining proliferative signaling, evasion of programmed cell death (apoptosis), reprogramming metabolic pathways and activating tissue invasion and metastasis, but also involves all the cellular components neighboring tumor cells, and that contribute to the acquisition of another dimension of complexity by creating the "tumor microenvironment". These hallmark traits are represented by evasion from the immune system, genome instability and inflammation (3) (Fig. 1.1B).

Renal cell carcinoma (RCC), a malignant tumor affecting the adult kidney, accounts for 2 % of all cancers. Affecting 64'000 people every year with 20 % death incidence, RCC is among the 10 most common cancers worldwide (4) (Fig. 1.2). Arising from the renal tubular epithelial cell, RCC is the most frequent malignancy affecting the adult kidney (87 %), whereas the remainder are 11 % urothelial carcinomas of the renal pelvis and rare others (2 %) (5). Incidence and mortality rate of RCC have been raising in many countries, in particular in highly developed countries most likely due to risk factors prevalent in these areas like cigarette smoking, analgesic use, hypertension and obesity as well as a longer period of life (6,7). RCC occurs preferentially in men then in women with a ratio of approximately 2:1. The RCC incidence increases with age reaching a peak at 60-70 years of age.

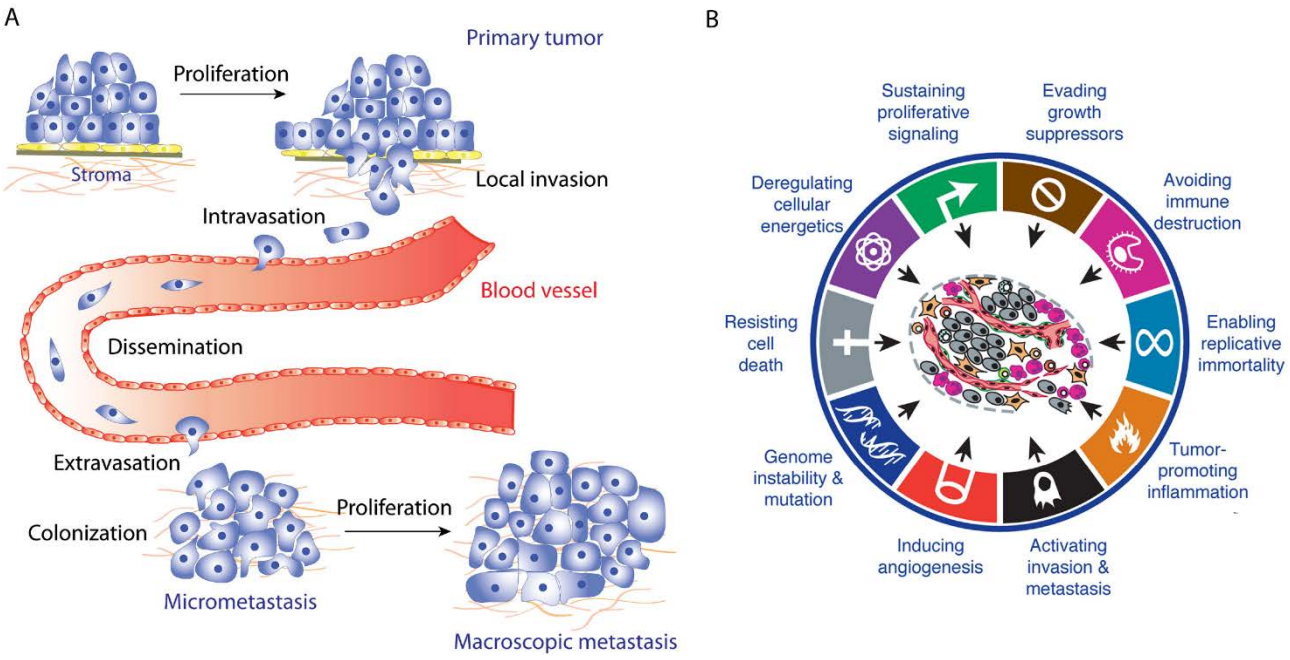

Figure 1.1. Dissecting cancer. Adapted from Hanahan D. and Weinberg R.A., "Hallmarks for cancer: the next generation", Cell, 2011; and Saxena M. and Christofori G., "Rebuilding cancer metastasis in the mouse", Molecular Oncology, 2013. **A)** Schematic representation of the metastatic cascade. Proliferating tumor cells from the primary tumor disseminate into the blood circulation and colonize distant secondary sites initially forming micrometastases and, finally, outgrowing as a macroscopic mass. **B)** The hallmarks of cancer.

Estimated New Cases

			Males	Females			
Prostate	180,890	21%			Breast	246,660	29%
Lung & bronchus	117,920	14%			Lung & bronchus	106,470	13%
Colon & rectum	70,820	8%			Colon & rectum	63,670	8%
Urinary bladder	58,950	7%			Uterine corpus	60,050	7%
Melanoma of the skin	46,870	6%			Thyroid	49,350	6%
Non-Hodgkin lymphoma	40,170	5%			Non-Hodgkin lymphoma	32,410	4%
Kidney & renal pelvis	39,650	5%			Melanoma of the skin	29,510	3%
Oral cavity & pharynx	34,780	4%			Leukemia	26,050	3%
Leukemia	34,090	4%			Pancreas	25,400	3%
Liver & intrahepatic bile duct	28,410	3%			Kidney & renal pelvis	23,050	3%
All Sites	**841,390**	**100%**			**All Sites**	**843,820**	**100%**

Figure 1.2. Kidney cancer statistics. Adapted from Siegel R.L. et al., "Cancer statistics", ACJC, 2016.

1.1 Renal cell carcinoma classification

Morphologically RCCs are a very heterogeneous class of tumors. According to the WHO 2016 classification which combines histological and genetic characteristics and clinical implications, RCC can be subdivided into three different entities (WHO 2016; Fig 1.3). Clear cell renal cell carcinoma which is the most common subtype of RCC, representing up to 80 % of all RCCs; papillary renal cell carcinoma accounting for 10-15 %; and chromophobe renal cell carcinoma representing only 5 % of all RCCs. These tumor subtypes have different prognosis and response to novel therapies might be different (8). Five years survival for metastatic RCC is 12 % (9). The classification is continuously evolving and tumor entities can be differently grouped.

The majority of RCC tumors occur in a sporadic form. However, 2-4 % of cases are associated with inherited tumor syndromes, such as von Hippel-Lindau (VHL) tumor syndrome, hereditary papillary RCC (HPRCC), Birt-Hogg-Dubé (BHD) syndrome, hereditary leiomyomatosis RCC (HLRCC), succinate dehydrogenase RCC (SDH-RCC), tuberous sclerosis (TS) and Cowden's disease (10,11). Patients carrying germ line mutations in one of the predisposing genes to hereditary RCC are likely to develop renal cancers: *VHL*, *MET*, *FH*, *BHD* and *HRPT2*, *TSC*, *TFE*, *SDH* and *PTEN*. Each of these genes plays an essential role in pathways involved in cell metabolism leading to changes in proliferation and survival.

1.1.1 Clear cell renal cell carcinoma

Accounting for almost 80 % of all RCCs, clear cell renal cell carcinoma (ccRCC) is the most frequent and studied RCC subtype. It arises from the proximal tubular epithelial cells probably through dedifferentiation (12). The name clear cell RCC reflects the fact that this tumor entity is composed of cells contained within a delicate vascular system with clear or eosinophilic cytoplasm due to high lipid content which is lost during routine histological processing (12,13). The presence of necrotic areas and highly vascularized tumor stoma as well as sarcomatoid differentiation and tumor infiltrating lymphocytes are associated with tumor aggressiveness and poor prognosis (8). ccRCC frequently metastasize through the vena cava to lungs or through the urogenital tract to bone, liver and brain. Many patients present metastasis at the time of diagnosis, and 20 % of them present with brain metastasis. Additionally, late metastasis can appear at 10 years of distance (8).

1.1.2 Papillary renal cell carcinoma

Accounting for 10-15 % of all RCCs, papillary renal cell carcinoma (pRCC) represent the second most frequent malignancy affecting the adult kidney after ccRCC. It arises from the proximal tubular epithelial cells undergoing malignant transformation and formation of tubules and papillae (8,14). The 5 years survival rate for this tumor type lays around 90 % (13). Characteristic of pRCCs is the presence of bilateral or multifocal tumors accompanied by necrosis. Sarcomatoid differentiation is also seen in pRCC and correlates with poor prognosis (8).

pRCC is characterized by trysomy or polysomy of chromosomes 3q, 7, 8, 12, 16, 17 and 20, and loss of Y chromosome. Treatment of pRCC is very similar to that of ccRCC. For localized pRCC radical nephrectomy or nephron-sparing surgery is applied. Anti-angiogenesis agents such as bevacizumab, sunitinib, and sorafenib are used in first-line therapy for metastatic pRCC. Temsirolimus, which targets the mammalian target of rapamycin (mTOR) receptor pathway, also appears to improve overall survival in patients with metastatic pRCC (14,15).

Two morphological subtypes of pRCC have been identified. pRCC type I, also known as basophilic, is the major pRCC subtype accounting for 70 % of all pRCCs (8,16). It is characterized by a single layer of epithelial cells with scant cytoplasm covering the tubules. pRCC type II, also known as eosinophilic, is the least frequent pRCC subtype but more aggressive (poor prognosis) (16). It shows eosinophilic cytoplasm and pseudo-stratified nuclei.

1.1.3 Chromophobe renal cell carcinoma

Accounting for 5 % of all RCCs, chromophobes renal cell carcinoma (chRCC) is the third most frequent RCC subtype. It originates from the distal nephron. It is characterized by polygonal cells delineated by a prominent cell membrane and a transparent reticulated cytoplasm due to the high content of microvesicles. Some cells are irregular and multinucleate. Macroscopically, chRCC appears grey-brown.

Contrary to ccRCC, chRCC occurs in patients with a wide age range and with a male:female ratio of 1:1. The mortality rate is less than 10 % and metastases affect lung, liver, and pancreas. Rarely occurring sarcomatoid differentiation is a sign of poor prognosis.

chRCC harbors extensive chromosomal loss involving chromosome Y, 1, 2, 6, 10, 13, 17 and 21 (17). It has been proposed that chRCC may evolve from oncocytoma. Oncocytoma is a benign neoplasm (18). Moreover, mutations in *TP53* tumor suppressor gene were found together with loss of heterozygosity around *PTEN* gene in 27 % of chRCCs (19).

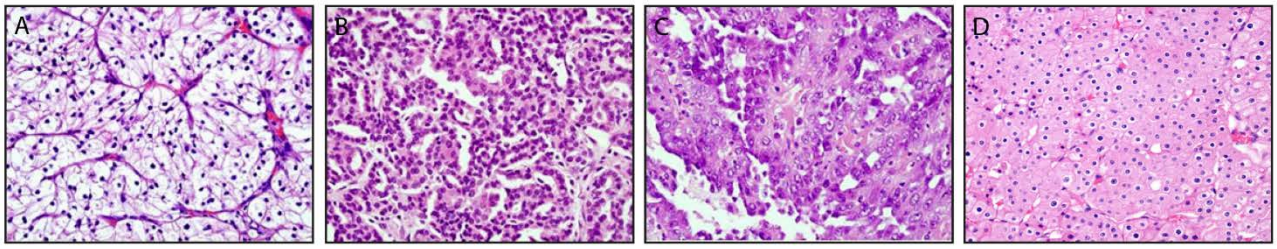

RCC subtype	ccRCC	pRCC type I	pRCC type II	chRCC
Frequency	80 %	10 %	5 %	5 %
Gene	*VHL*	*cMET*	*FH*	*BHD*

Figure 1.3. Renal cell carcinoma subtypes. In the upper panel are depicted the three most common RCC subtypes stained by H&E: **A**) clear cell renal cell carcinoma (ccRCC), **B**) papillary RCC type I and type II (**C**), **D**) chromophobe RCC (chRCC). In the lower panel frequencies and the gene of interest for each subtype is described.

1.2 Diagnosis, prognosis and therapeutic treatments

Renal cancer is often asymptomatic in early stage and it is usually detected by chance during examination or illness. Clinical presentation of a palpable mass on the flank, pain in the abdomen, anemia, loss of weight and the presence of blood in the urine is very uncommon (20). However, the most common clinical signs may appear with the tumor growth. Following presentation of one or more of these symptoms, different tests are performed such as blood and urine test, ultrasound, computed tomography (CT) scan, magnetic resonance imaging (MRI), and finally biopsy.

Determine tumor stage and grade is fundamental in order to stratify treatment options, and assess prognosis and survival. The most common staging system for kidney cancer is the TNM system introduced by the American Joint Committee on Cancer (AJCC), where "T" indicates tumor size, "N" describers whether the primary tumor has spread to the nearby lymph nodes, and "M" stands for presence of disseminated metastases (Table 1.1). Common metastatic sites include bone, liver, lung, brain, and distant lymph nodes (AJCC 6th edition 2017). According to the TNM values, the overall stage can be assigned (Table 1.1).

Several grading systems for RCC have been discussed over the years. The Fuhrman system is based on the microscopic evaluation of the uniformity of the nuclear size, shape and nucleolar prominence (21,22). It was the most frequently used but it couldn't be applied to chRCC and to the new entities (23). Therefore, a new grading system has been introduced by the WHO in 2016 (24). The new four-tired WHO/ISUP system defines tumors of grade 1-3 based on nucleolar prominence, whereas grade 4 is defined by the presence of nuclear pleomorphism, big tumor cells and sarcomatoid differentiation (25)(Table 1.2).

Table 1.1. Renal cancer staging.

TNM classification			
T	**Information concerning the primary tumor**		
TX		Information not available	
T0		Primary tumor not detectable	
T1		Primary tumor confined to the kidney and no longer than 7 cm in size	
	T1a	Tumor size is no longer than 4 cm across	
	T1b	Tumor size is no longer than 7 cm across	
T2		Primary tumor larger than 7 cm but still confined to the kidney	
	T2a	Tumor size between 7 and 10 cm across	
	T2b	Tumor size larger than 10 cm	
T3		Tumor is growing into a major vain or in the tissue surrounding the kidney, but not in the adrenal gland or beyond the Gerota's fascia	
	T3a	Tumor is growing into the renal vain or in the fatty tissue surrounding the kidney	
	T3b	Tumor is growing into the vena cava leading to the heart	
	T3c	Tumor has grown into the vena cava within the chest	
T4		Primary tumor has spread beyond the Gerota's fascia	
N	**Information concerning regional lymph node involvement**		
NX		Information not available	
N0		No lymph node is involved	
N1		Tumor has spread to nearby lymph nodes	
M	**Information concerning the presence of metastasis**		
M0		Tumor has not spread to other organs	
M1		Tumor has spread to other organs	
Staging classification			
Stage I			
T1	N0	M0	Primary tumor is no larger than 7 cm across. There is no lymph nodes or other organs involvement
Stage II			
T2	N0	M0	Primary tumor is larger than 7 cm across. There is no lymph nodes or other organs involvement
Stage III			
T3	N0	M0	Primary tumor is growing into a major vain but not in the adrenal gland or beyond the Gerota's fascia. There is no lymph nodes or other organs involvement
T1-3	N1	M0	Primary tumor can be of any size and it has spread to the nearby lymph nodes, but it has not spread beyond the Gerota's fascia or to any other organ.
Stage IV			
T1-4	N0-1	M1	Primary tumor can be of any size. It may or may not have spread to nearby lymph nodes, but it has spread to distant lymph nodes or other organs.

Table 1.2. Renal cancer tumor grade.

Grading classification		
Grade I		
Nuclear size	Nuclear outline	Nucleoli
10 mm	Round, uniform	Absent
Grade II		
Nuclear size	Nuclear outline	Nucleoli
15 mm	Slightly irregular	Small (400x magnification)
Grade III		
Nuclear size	Nuclear outline	Nucleoli
20 mm	Markedly irregular	Prominent (100x magnification)
Grade IV		
Nuclear size	Nuclear outline	Nucleoli
>20 mm	Bizarre	Large

Treatment options depends on the staging of the tumor, on the tumor type, on the markers expressed by the tumor and on the patient's age and general health (5).

Curative surgical resection is the only effective therapeutic option for localized RCCs (5,26,27). Radical nephrectomy represents the method of choice for significantly big tumors (>pT2). It is achieved by removal of the entire kidney, perirenal fat and adrenal gland accompanied by lymph nodes dissection. Nevertheless, high cardiovascular events and mortality rate is associated with this method. Partial nephrectomy (nephron sparing) represents a less invasive technique which requires the removal of the tumor mass and the surrounding tissue (safe margins) without impairing the renal function. Nephron sparing nephrectomy applies to all pT1 tumors where the relationship between the tumor size and the rest of the kidney is less than 50 %. Both resections can be performed laparoscopically reducing periperative morbidity and the length of the hospitalization. If the renal tumors are not in close proximity to susceptible organs, thermal ablation can be an alternative option for selected patients (5).

At the time of diagnosis, 3-22.5 % of the patients have nodal involvement, 20-35 % of the patients present tumor extension into renal veins, whereas 30 % of patients have already developed metastases and 50 % of those with localized disease will develop metastatic lesions. In these patients treatment is palliative to relief symptoms and concentrated on prolonging survival time and preserving the quality of life (94, 95). Local recurrence in the nephrectomy bed is 20-40 %.

Some patients may receive radiotherapy or chemotherapy before or after surgical resection of the tumor in to shrink the tumor size or further kill cancer cells, respectively (neo-adjuvant versus adjuvant therapy). Nevertheless, chemotherapy, radiotherapy and hormonal therapy showed a very little benefit to the patients (18).

Due to the much higher prevalence of ccRCCs, very few clinical trials have been carried out considering other histological RCC subtypes. Therefore, most of the drugs have been developed based on ccRCC, and they are currently applied to all RCC patients. Treatment of advanced or metastatic RCC patients is achieved primarily by targeted therapy. Tyrosine kinase inhibitors (TKIs) play an important role in modulating growth factor signaling acting on epidermal growth factor (EGF), fibroblast growth factor (FGF), platelet-derived growth factor (PDGF), and vascular endothelial growth factor (VEGF) receptors (28). First line treatment of such patients relies on the usage of VEGF-inhibitors such as the VEGF-neutralizing antibody bevacizumab, the VEGF receptor antagonists sorafenib, sunitinib and pazopanib (29,30). Although pazopanib showed enhanced quality of life and safety advantages compared to sunitinib, it is still regarded as second treatment option against sunitinib (31-33). Interestingly, EGF-inhibitors showed to be ineffective in the treatment of RCCs. More traditional cytokine therapy includes interferon-α (IFNα) and interleukin-2 (IL-2) treatment, which is effective only for a small group of patients (34).

Tumor angiogenesis is also stimulated by growth factors through the phosphatidylinositol-3 kinase (PI3K)-AKT-mTOR signal transduction pathway. Agents targeting this pathway can also be expected to have antitumor activity (34). Therefore, second line treatment is managed by axitinib, everolimus and temsirolimus (35). Axitinib is a selective TKI for VEGFR-1, -2 and -3 (36). Whereas, everolimus and temsirolimus are mTOR inhibitors. Interestingly everolimus is also considered as third line treatment option (Table 1.3).

Several approaches to immunotherapy are currently investigated for RCC patients such as vaccines, adoptive cell therapy and T-cell modulation (37,38). In this regard, the anti-CTLA-4 antibody (ipilimumab) prevents CD80 and CD86 from binding to CTLA-4 receptor and, thereby, promotes T-cell activation. Evidence also

shows that CTLA-4 antibodies can deplete regulatory T cells contributing to the activation of the immune system (38). Antibodies against programmed death 1 (PD-1, nivolumab) and its ligand PD-L1 (durvalumab and atezolizumab) have been developed and act by blocking the interaction between T-cells and cancer cells at the tumor site leading to the activation of the T-cell response (38).

Despite all the progress made in the development of novel anti-cancer compounds, the management and treatment of RCC patients still remains a crucial aspect in the clinics. Improving the understanding of morphologic features and molecular genetics of renal cancers as well as the discovery of prognostic and predictive biomarkers will improve the identification of more efficient therapeutic strategies.

Table 1.3. Therapeutic options for renal cancer. Adapted from Bukowski R.M. et al., "Pazopanib", Nature Reviews, 2010 (39).

Treatment	Drug	Target
First line	Bevacizumab Sorafenib Sunitinib Pazopanib	Multiple RTKs (VEGFR, PDGFR)
Second line	Axitinib Everolimus Temsirolimus	PI3K-AKT-mTOR
Third line	Different TKIs New agents: Cabozatinib	Growth factors (EGF, FGF, PDGF, VEGF)

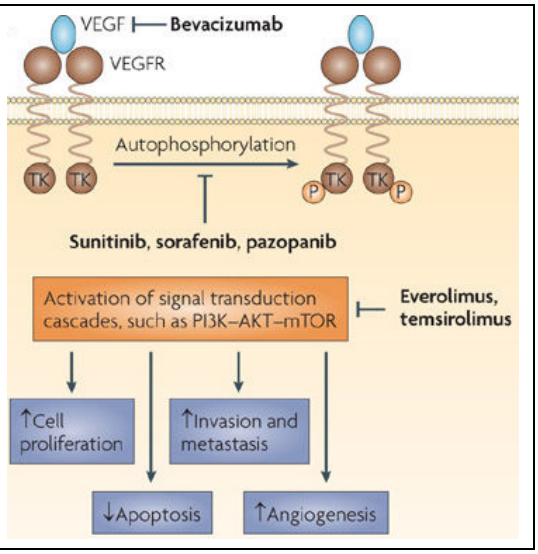

1.3 Biomarkers in renal cancer

Diagnosis and classification of RCC subtypes can be usually accomplished by morphological evaluation of the tumor specimen. Occasionally, evaluation of immunohistochemical staining (IHC), which allow the detection of antigens expressed on tumor cells, may be used to verify unclear diagnosis. For instance, ccRCC shows reactivity for Vimentin, Cytokeratin, CD10, Pax2, and Carbonic anhydrase-IX (CA-IX); pRCC is positive for Vimentin, Cytokeratin, and CK7; whereas chRCC is positive for E-cadherin, CD117 and CK7 (40) (Table 1.4).

Due to the high tumor heterogeneity which characterize RCCs, employment of such panel of markers is often speculative and limited. Besides immunohistochemistry other techniques are adopted such as molecular cytogenetics (41), fluorescence in situ hybridization (FISH) (42), gene expression profiling (43-45), single nucleotide polymorphism (SNP) array (46,47), methylation status, mutational analysis and proteomics (48). To date no prognostic and diagnostic biomarker is routinely used in the clinics. Several studies proposed new potential biomarkers for RCCs. However, most of them need further validation. Among them, the most significative are: VHL (49,50), HIF1α (51,52), CA-IX (52,53), survivin (54), Ki-67 (55), fascin (56), c-MET (57), family of the ligands B7-H (58,59), VEGF (60), CAF (46) and IL-8 (47,61).

The majority of biomarkers require invasive procedure such as biopsies and surgical intervention. Blood and urine represent two valuable sources of cancer-derived molecules being proteins, nucleic acids, extracellular vesicles (EVs) and circulating tumor cells (CTCs). Detection of changes in the level of these molecules in the body fluids have been associated with tumor load and malignant progression, proposing these liquid biopsies as a novel prognostic, diagnostic and predictive tool for cancer patients. Additionally, the possibility to analyze the genetic content of CTCs and EVs as well as determine *de novo* mutations in the circulating tumor DNA (ctDNA) over time is regarded as an important step towards personalized medicine and treatment monitoring.

The presence of nucleic acids circulating in the blood have been shown for the first time in 1948 by Mandel and Metais who discovered the presence of DNA and RNA in the plasma of healthy and diseased donors (62). After this study, several others have identified the presence of circulating free DNA (cfDNA) in the

bloodstream of patients and changes in the levels of these circulating nucleic acids have been associated with tumor load and malignant progression proposing these liquid biopsies as a novel prognostic, diagnostic, and predictive tool for cancer patients, including renal cancer (63-65). However, correlation of cfDNA levels to tumor stage and grade in renal cancer revealed discordant results (65-68).

In particular, it has been shown that the amount of ctDNA shed by cancer cells represents up to 10 % of total cfDNA derived from blood in patients with advanced tumors (69). Thus, ctDNA opens the possibility to detect the mutational profile of a specific cancer during tumor evolution, metastasis formation and therapy. Indeed, different mutations have been identified in cfDNA of patients affected by colon, lung, ovarian and breast cancers (63,70-74). More recently, Bettegowda and co-workers detected ctDNA in more than 75 % of the patients with advanced pancreatic, ovarian, colorectal, bladder, gastro-oesophageal, breast, melanoma and head and neck cancers but in less than 50 % of patients presenting with renal and prostate cancers (75). In particular, the release of ctDNA was investigated in five ml of plasma derived from five metastatic RCC patients. Prior analysis of the tumor tissue revealed in one RCC patient a *MET* mutation, in one a *HOOK2* mutation, and in three a *VHL* mutation. When analysing the ctDNA, only one *VHL* mutation and the *MET* mutation were successfully detected (40 %). For the detection of *VHL*, the authors used PCR-ligation and for the detection of the *MET* mutation SafeSeqS. Both methods are highly sensitive with detection limits below 1 % allele count. However, for both assays the mutation of interest has to be identified in the tumor tissue before analysis of the blood samples. Therefore, the development of non-invasive methods to detect *de novo* or to monitor already known tumor specific signatures continue to be a major challenge in renal cancer.

Table 1.4. Renal cancer subtype discrimination using immunohistochemical markers.

RCC subtype	**IHC positive markers**	**IHC negative markers**
ccRCC	Vimentin, Keratin, CD10, Pax2/8, CA-IX, CK18	CK7, Ksp-cadherin, E-cadherin, CK19
pRCC	Keratin, CK7, Vimentin	CD117, Ksp-cadherin
chRCC	E-cadherin, CD117, CK7	Vimentin, CA-IX

1.4 Tumor heterogeneity in clear cell renal cell carcinoma

Clear cell renal cell carcinoma is the most common RCC subtype. Inactivation of *VHL* tumor suppressor gene by mutation or promoter methylation has been found responsible for about 80 % of ccRCC cases (76). Characteristic for the majority of sporadic ccRCC is the chromosomal loss of one allele located at position 3p combined with a mutation on *VHL* on the second allele resulting in loss of heterozygosity (LOH) (77). In several cases amplification of chromosome 5q and loss of 14q were reported (78).

Recently, several additional tumor suppressor genes have been found frequently mutated in ccRCC such as genes involved in the chromatin-remodeling process: *SETD2* (16 %), *BAP1* (15 %), *PBRM1* (33 %), *JARID1c* (4 %), *TP53* (2 %) and some other genes involved in PI3K-mTOR pathway: *PIK3CA* (3 %), *MTOR* (6 %) and *PTEN* (4.3 %) (78-83). *PBRM1*, *SETD2* and *BAP1* are located on chromosome 3p suggesting they might be involved in large deletions together with *VHL* (84). Mutations in *PBRM1* and *BAP1* were mutually exclusive, whereas, mutations in *PBRM1* and *SETD2* were appearing together as well as individually (83).

BAP1 encodes a nuclear deubiquitinase of the ubiquitin C-terminal hydrolase (UCH) family. Mutations in this gene promotes mTOR signaling activation. *BAP1* mutations in ccRCC patients have been correlated to decreased cancer specific survival (85), overall survival (TCGA, 2013), and lower recurrence free survival (80). Additionally, BAP1 loss of expression assessed by immunohistochemistry correlated with lower overall survival (86).

The *PBRM1* gene encodes the polybromo BAF180 protein. PBRM1 loss induces cytoskeleton remodeling, cell mobility and cell proliferation via inhibition of the cyclin-dependent kinase inhibitor p21 (79). Loss of PBRM1 expression correlates with high tumor grade, late tumor stage and worse patient outcome (87). However, patients carrying a mutation only in the *PBRM1* gene showed favorable clinical outcome compared to *BAP1*-mutant (82).

SETD2 has been found linked to DNA mismatch repair, microsatellite instability and DNA methylation in ccRCCs (78). However, the role of SETD2 in ccRCC is still unclear (79). SETD2 was shown to be a potential

prognostic biomarker for overall survival and progression-free survival prediction in patients with metastatic renal cell carcinoma receiving targeted therapy as well as in non-metastatic RCCs (88,89).

According to their significance, mutations can be classified into driver and passenger mutations. Driver mutations are implicated in tumor initiation and progression, whereas passenger mutations are transitory (90). Interestingly, these genes have been found to be mutated separately or together in the same primary ccRCC in different tumor regions analyzed (91). Comparison of multiple samples derived from the same ccRCC revealed in 25 % a higher similarity to unrelated ccRCC samples (92) (Fig. 1.4). These findings hint to a high degree of parallel evolution of tumor subclones in ccRCC resulting in tumor heterogeneity, which opens the discussion about tumor stem cells and the metastatic-initiating tumor cell population.

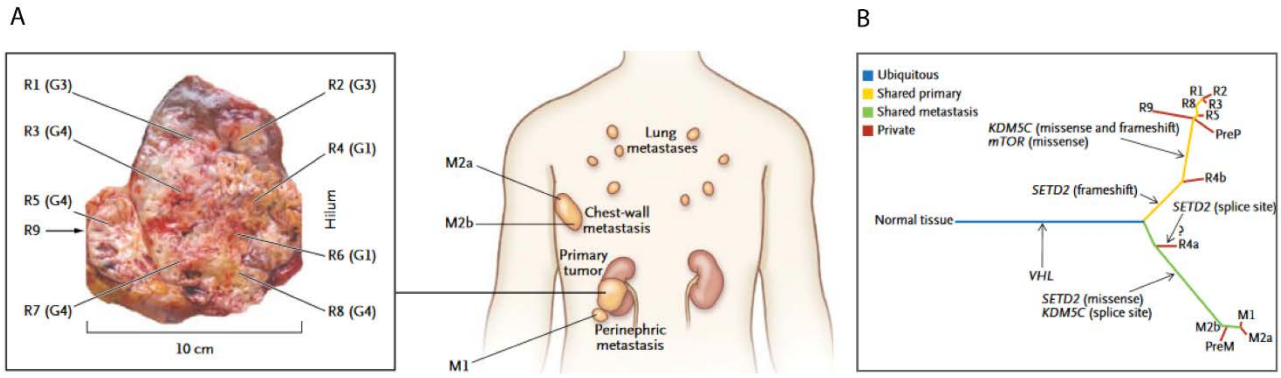

Figure 1.4. Intra-tumor heterogeneity. Adapted from Gerlinger M. et al., "Intratumor Heterogeneity and Branched Evolution Revealed by Multiregion Sequencing", The New England Journal of Medicine, 2012. **A)** Different regions and metastatic sites were resected and analyzed by whole exome sequencing. **B)** Phylogenic evaluation revealed mutations in *VHL*, *SETD2*, *BAP1* and in the mTOR pathway appearing together or separately in different tumor regions analyzed from the same primary ccRCC tumor. At the same time, comparison of multiple samples derived from the same ccRCC patient revealed 25 % higher similarity to unrelated ccRCC samples.

1.5 VHL and HIFs

The *VHL* gene encodes for two proteins by alternative splicing. The full length isoform p-VHL_{30}, so-called because of a molecular weight of 30 KDa, consists of 213 amino acids and it is localized in the cytoplasm. On the other hand, p-VHL_{19} consists of 160 amino acid residues and it is equally distributed between the cytoplasm and the nucleus.

P-VHL is part of the E3 ubiquitin ligase complex containing elongin B, elongin C, Cul2 and Rbx1 (93). The VHL protein contains two domains: the α domain is responsible for binding to elongin C triggering the formation of the complex, the β domain is responsible for the binding to HIFα (94).

In presence of normal oxygen tension (normoxia), this complex binds to the α subunit of the heterodimeric transcription factor hypoxia-inducible factor (HIF) leading to polyubiquitination and proteosomal degradation (76). Under low oxygen levels (hypoxia), HIFα is not hydroxylated on the proline residues (Pro-402 and Pro-564), therefore, it escapes the recognition by p-VHL, dimerizes with HIFβ, translocates into the nucleus, and by binding to the hypoxia-responsive elements (HRE) transcriptionally activates genes involves in metabolism, angiogenesis, cell migration, resistance to apoptosis and cytoskeletal remodeling (95). These genes are VEGF, PDGF, EGFR, transforming growth factor α (TGFα), c-Met, Cyclin D1, glucose transporter 1 (GLUT1), CA-IX, and erythropoietin (EPO) (35) (Fig. 1.5).

All the mutations found in *VHL* compromise the ability to either suppress HIF or bind to the complex. Interestingly, nonsense and frameshift mutations abrogate p-VHL, whereas missense mutations may have different effects (77). Nevertheless, pVHL-deficiency alone is not sufficient to initiate tumor formation (96), and therefore, VHL status was not found correlated with the clinical outcome in ccRCC patients (97-100). Recently, it was shown that out of the remaining 8 % *VHL* wt ccRCC cases, 42 % harbor biallelic inactivation of the elongin B gene (*TCEB1*).

There are three HIFα family members (HIF1α, HIF2α, HIF3α) and two HIFβ family members (HIF1β, HIF2β). The α subunit is oxygen sensitive, whereas the β subunit is constitutively expressed (76). The HIF proteins are

members of the basic helix-loop-helix PAS family of DNA-binding transcription factors. Both HIF1α and HIF2α have two dedicated transcriptional activation domains that can activate transcription when bound to DNA. The core sequence of the HRE recognized by HIF is 5'-RCGTG-3', where R stands for purine. Both HIF1 and HIF2 share common but also distinct transcription patterns. HIF1 drives the expression of genes involved in apoptosis and metabolism acting as a tumor suppressor gene (101). HIF2 activates genes involved in cell proliferation and angiogenesis. For this reason, it was suggested that HIF2 is more oncogenic than HIF1. HIF1α has been found involved in early lesions, whereas HIF2α plays an important role in malignant progression and metastasis formation (102).

Finally, the protein pVHL is involved in many other different biological processes, such as organization of extracellular matrix and microtubules (93), cell polarity, inhibition of NF-kB activity (103), maintenance of chromosome stability (104), differentiation, and growth arrest (105).

Drugs that inhibit specifically members of the VHL-HIF-VEGF pathway are now standard therapies used for treating ccRCC cases (35,93)(Fig. 1.5). However, these drugs show only moderate overall survival benefit and have significant side effects for patients. Therefore, development of new prognostic and diagnostic markers are needed.

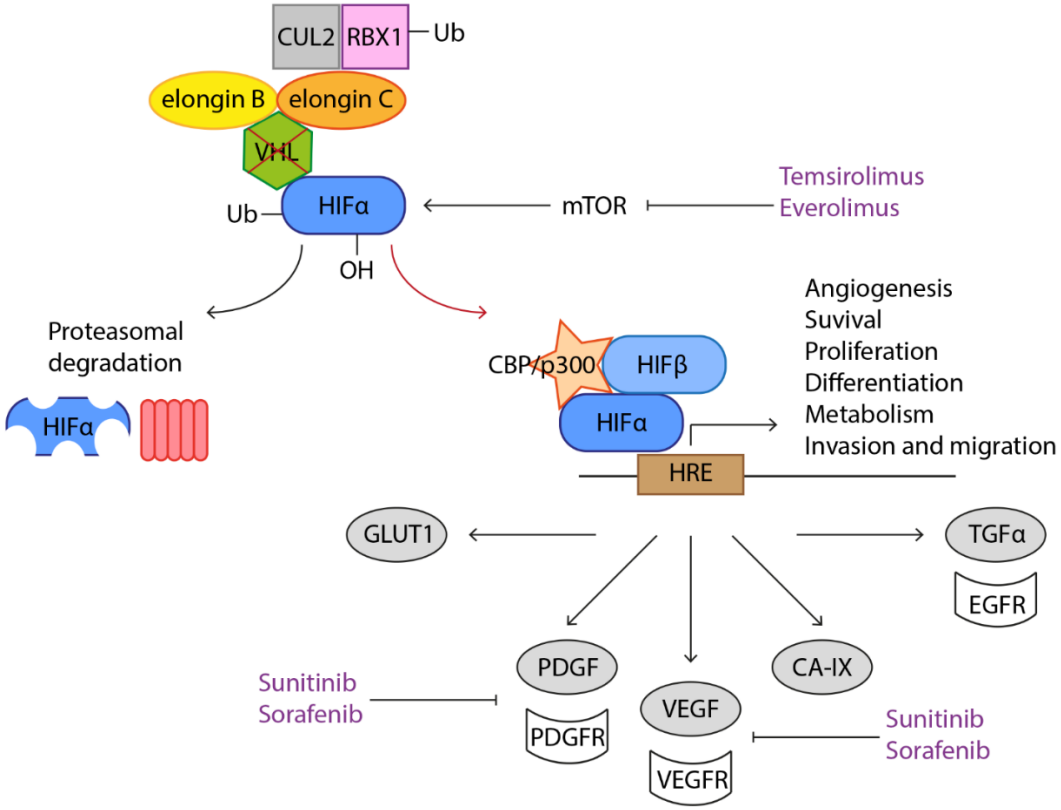

Figure 1.5. The pVHL-HIF axis. Adapted from Clark P.E., "The role of VHL in clear-cell renal cell carcinoma and its relation to targeted therapy.", Kidney International, 2009. Under normoxia conditions HIFα subunits are hydroxylated by a member of the PHDs protein family, which leads to E3 ubiquitin ligase complex formation and HIF1α and HIF2α are targeted for proteasomal degradation. During hypoxia or loss of functional pVHL, HIFα subunits are stabilized and HIF target genes are transcribed. Drugs that inhibit specifically members of the VHL-HIF-VEGF/mTOR pathway are now standard therapies used for treating ccRCC cases.

2. Cancer stem cells

In particular, intra-tumor and inter-tumor heterogeneity is one of the major limitation in the treatment of epithelial tumors (106). Two different tumor models have been proposed playing a role in tumor development, progression and tumor heterogeneity. The cancer stem cell (CSC) model or hierarchical model proposes that tumor growth and propagation is driven by a small subpopulation of cells with pluriproliferative features (107,108). According to this model, a pool of CSCs can only be maintained by cells that have both stem cell potential and the ability to give rise to progeny with self-limited proliferative capacity (109). The clonal evolution model or stochastic model implies the presence of a tumor cell population, derived from a normal cell that underwent malignant transformation known as cell-of-origin or tumor initiating cells, carrying different mutations which are accumulated during time and then selected under different selective pressure (110).

Genetic and epigenetic factors are not just the only two factors contributing to tumor heterogeneity. Tumor heterogeneity is in fact, further enhanced by clonal variation and tumor microenvironment (TME) (111). Therapy itself may act as selection mechanism that shapes tumor evolution. More recently, a unifying model of clonal evolution applied to CSCs has been proposed by Kreso et al., whereby CSCs can acquire mutations and generate new stem cell branches contributing to tumor heterogeneity (108) (Fig. 2.1).

Therefore, the identification of a specific subpopulation of cells within a tumor that either initiate or maintain tumorigenesis is of utmost importance for understanding tumor biology and in the development of novel therapies.

CSCs are a small population of neoplastic cells within a tumor presenting characteristics reminiscent of normal stem cells. In particular, they are capable to give rise to all the cell types present in the tumor tissue which they derive from (differentiation). They are characterized by unlimited cell division, maintenance of the stem cell pool (self-renewal), give rise to tumor and metastasis *in vivo* (tumorigenicity), resistance to therapies and recurrence. These cells divide asymmetrically resulting in a CSC identical to the parental cell and on the other hand to a more differentiated cell responsible for establishing the tumor bulk.

Dick and co-authors performed the first experimental study on CSCs in 1994. They isolated $CD34^{+}/CD38^{-}$ cells from acute myeloid leukemia (AML) patients and showed they could initiate AML *in vivo* upon transplantation into NOD/SCID mice (112). Subsequently, several others have showed the presence of CSCs in colorectal cancer, breast cancer, glioblastoma, melanoma, lung cancer, liver and prostate cancer (113-122). Growing evidence suggests that renal cancer, as many other solid tumors, possesses a rare population of cells capable of self-renewal that contribute to metastasis and resistance to therapy. So far, many studies tried to identify biomarkers in order to isolate CSC populations in RCC (123-127). Some of these markers are CD105, ALDH1, OCT4, CD133 and CXCR4, which have been found specifically expressed in CSC and cancer stem-like cells derived from RCC (Table 2.1).

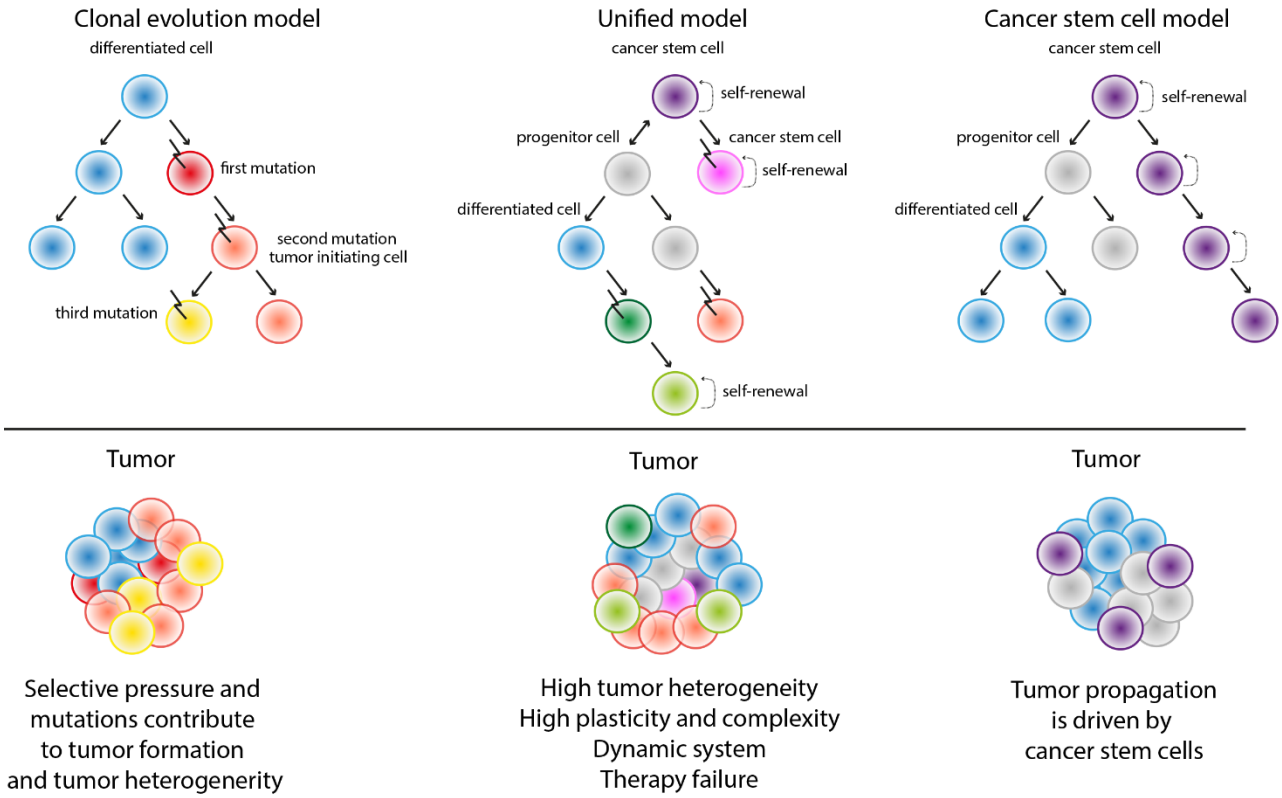

Figure 2.1. Model of tumorigenesis. This figure illustrates three models of tumorigenesis. The clonal evolution model or stochastic model which implies the presence of a tumor cell population carrying multiple mutations which is transformed over time by selective pressure resulting in tumor heterogeneity and progression. The CSC model or hierarchical model which proposes that tumor growth and propagation is driven by a small subpopulation of cells with pluriproliferative features namely CSCs. More recently, a unifying model characterized by high tumor heterogeneity, plasticity and complexity has bene proposed. According to this model CSCs can acquire mutations and generate new stem cell branches, on the other hand, tumor cells in the non-CSC subpopulation can undergo EMT and acquire CSC-like features contributing to tumor heterogeneity. Moreover, tumor microenvironment and therapy add another layer of complexity.

Table 2.1. Summary of putative CSC markers.

Sample	*Assay*	*Putative marker of the study*	*Positive markers*	*Negative markers*	*CSC features*	*Reference*
769P	side population		ABCB1	ABCC1, ABCG2	clonogenic, tumorigenicity, resistance to chemo and radiotherapy	Huang et al. (128)
786O	sphere formation assay		CD73		tumorigenicity, resistance to radiotherapy	Song et al. (129)
786O	flow cytometry	Rh123			spheroids in soft agar, proliferation, differentiation, tumorigenicity, resistance to radiotherapy	Lu et al. (130)
786O, 769P, A704, Caki1, Caki2	Flow cytometry	USP21	ALDH		sphere formation, clonogenic, proliferation, invasion	Peng et al. (131)
ACHN	side population		ALDH1	CD105, CD133	sphere formation, self-renewal, tumorigenicity	Ueda et al. (126)
ACHN, Caki1	sphere formation assay		Oct4, Nanog, LIN28, KL4, Zeb1, Zeb2, N-cadherin, Vimentin, CD44, CD24	miR17	sphere formation, self-renewal, differentiation, tumorigenicity	Lichner et al. (132)
ACHN, Caki1	flow cytometry	CD105	CD105, Oct4, Nanog, CD90, CD73	CD24, CD34, CD11, CD19, CD45	spheroids in soft agar, hanging drops	Khan et al. (133)
ACHN, Caki1	MACS		$CD133^+/CD24^+$, Oct4, Notch1, Notch2, Jagged1, Jagged2, DLL1, DLL 4		self-renewal, invasion and migration, tumorigenicity, resistance to chemotherapy (sorafenib and cisplatin)	Xiao et al. (134)
ACHN, Caki1, SMKTR2, SMKTR3, RenCa	side population		DNAJB8		tumorigenicity	Nishizawa et al. (135)
ACHN, Caki2	flow cytometry	ALDH1	Oct4, Nanog, Pax2		self-renewal, clonogenic, tumorigenicity	
Caki1, Caki2, 786O, 769P	sphere formation assay		CXCR4		sphere formation, tumorigenicity	Micucci et al. (136)
HEK293T	sphere formation assay		$ALDH^+$, CD44, β-catenin, Notch1, Survivin, Vimentin, N-cadherin, Zeb1, Snail, Slug	CD24	sphere formation, resistance to radiotherapy	Debeb et al. (137)
RCC xenograft	sphere formation assay		CD133/CXCR4		sphere formation, tumorigenicity, resistance to chemotherapy	Varna et al. (127)
RCC26, RCC53	flow cytometry	CXCR4	CXCR4, CD24, CD29, CD44, CD73, Nanog, Oct4, Sox2	CD90, CD105, CD133, CXCR1,	sphere formation, tumorigenicity, resistance to chemotherapy	Gassenmeier et al. (138)

				Vimentin, β-catenin		
RCCs	flow cytometry	CD105	CD105, CD44, CD90, CD73, CD29, Nanog, Oct4, Vimentin, Nestin	CD133	sphere formation, clonogenic, differentiation, tumorigenicity	Bussolati et al. (139)
RCCs	flow cytometry	$CD133^+$/ $CD34^-$	CD73, CD44, CD29, Vimentin		non tumorigenic	Bruno et al. (140)
RCCs	flow cytometry	$CD133^+$/ $CD24^+$	CTR2, Nanog, Oct4, Sox2	CD105, CD90	resistance to chemotherapy	Galleggiante et al. (141)
RCCs	side population		CD133		spheroids in soft agar, differentiation	Addla et al. (142)
RenCa			DNAJB8		side population, sphere formation, tumorigenicity	Yamashita et al. (143)
SK-RC-42	sphere formation assay		Oct4, Nanog, BMI, β-catenin	MHC-II, CD80	sphere formation, tumorigenicity, resistance to radio and chemotherapy	Zhong et al. (144)

2.1 Cancer stem cell markers

2.1.1 CD105

Among those, CD105 (Endoglin) is a transmembrane glycoprotein encoded by the *endoglin* gene located on chromosome 9q34. This protein is composed of two constitutively phosphorylated subunits of 95 KDa each, forming a 180 KDa homodimeric mature protein (145). CD105 is an accessory protein of the TGFβ complex. Upon activation of the TGFβ complex, the binding of endoglin results in the activation of Smad proteins regulating cell proliferation, migration, differentiation and angiogenesis (146). Endoglin is predominantly expressed in endothelial cells where it is activated by hypoxia and TGFβ stimulation, whereas it is decreased by tumor necrosis factor α (TNFα)(147). In breast, prostate and gastric cancer, CD105 was present in endothelial cells forming the immature tumor vasculature.

CD105 was shown to be expressed on a ccRCC subpopulation representing <10 % of the tumor mass. These cells isolated my magnetic sorting showed potent capability to grow as spheres and initiate tumors and metastasis recapitulating the histological pattern in mice (124,139). $CD105^+$ cells expressed mesenchymal markers CD44, CD90, CD29, CD73 and Vimentin; embryonic stem cell markers Oct3/4, Nanog and Nestin and embryonic renal marker Pax2 (139). However, $CD105^+$ cells did not express CD133 also known as human tubular progenitor cell marker (148). $CD105^+$ CSCs were able to differentiate into epithelial and endothelial cells and generate $CD105^-$ cells. Additionally, IHC of tumoral CD105 was found positively correlated to nuclear

grade and tumor stage, whereas endothelial expression negatively correlated with clinicopathological features (149). Interestingly, $CD105^+$ CSCs released microvesicles/exosomes containing pro-angiogenic mRNAs (VEGF, FGF, MMP2 and 9) that triggered angiogenesis and promoted the formation of a premetastatic niche *in vivo* (124). EVs derived from renal CSCs impaired T cell activation and dendritic cell differentiation by the human leukocyte antigen G (HLA-G) promoting escape from the immune system (150).

Nevertheless, the use of CD105 as a renal CSC marker was questioned in many studies where also $CD105^-$ cells showed CSC-like features (129).

2.1.2 CD133

Prominin-1 (CD133) is a transmembrane glycoprotein of 865 amino acids (120 KDa) encoded by the gene *PROM1* on chromosome 4p15 (151). The protein consists of an N-teminal extracellular domain, five transmembrane domains with two large extracellular loops, and a cytoplasmic tail (152). Phosphorylation of CD133 results in the activation of PI3K/AKT signaling pathway (153,154). Hypoxia, mTOR inhibition and TGFβ1 were shown to increase CD133 expression in lung cancer, pancreatic cancer and hepatocellular carcinoma (HCC). Interestingly, Oct4 and Sox2 have been found binding the promoter region of CD133 inducing its activation in lung cancer cell lines.

$CD133^+$ cancer cells were able to form spheres, give rise to tumors *in vivo*, and exhibit chemoresistance properties in colorectal carcinoma, HCC, lung cancer, glioblastoma, pancreatic cancer and ovarian cancer. On the contrary, sorted $CD133^+$ cells from RCC patients did not show tumorigenic capability *in vivo* although they expressed stem cell markers such as CD44, CD29, Vimentin, and Pax2 (148). When co-transplanted with renal carcinoma cells, $CD133^+$ progenitors significantly enhanced tumor development and growth. The same result was obtained using $CD133^+$ cells derived from normal kidney tissue (140). Of note, $CD105^+$ cells did not express CD133, suggesting that $CD133^+$ cells may represent renal resident adult progenitor cells.

Interestingly, $CD133^+/CD24^+$ cells derived from ACHN or Caki1 RCC cell lines displayed sphere formation capability, enhanced invasion and migration properties, high colony formation efficiency in soft agar, and resistance to sorafenib and cisplatin (134).

Another interesting publication identified CD133 and CXCR4 coexpressing CSCs in spheres derived from RCC xenografts and tumor tissues. Increased expression of these markers was found in RCC patients after sunitinib treatment (127). However, the coexpressing cells increased only from 4 % to 8 % in average of total cells in the spheres investigated upon treatment. Nevertheless, whether the CD133 and CXCR4 positive or negative cells had detectable levels of CD105 was not assessed. Additionally, the gene expression profile as well as the tumorigenic potential of the spheres was not deciphered.

Lastly, CD133 expression was found strongly correlated with nuclear HIF1α in RCC patients (155,156). CD133 mRNA levels in blood showed to be useful for identifying metastasis, predicting recurrence, and stratifying the patients into different risk groups for possible adjuvant treatment (157). Nevertheless, CD133 expression analyzed by IHC in RCC patients was inconsistent and varied among different studies (146,158).

2.1.3 CD44

CD44 is a transmembrane glycoprotein of 85 KDa (742aa) encoded by the gene *CD44* located on chromosome 11. *CD44* consists of 20 exons. Exons 1-17 are responsible for different regions of the extracellular domain, whereas exons 18-20 are responsible for the cytoplasmic tail. CD44 has more than 20 isoforms due to RNA alternative splicing, giving rise to different proteins in different cancer subtypes. It is involved in many different biological processes such as cell-cell interaction, cell adhesion, migration, proliferation, differentiation and angiogenesis (159). CD44 transcription was found activated by Wnt and β-catenin signaling pathway. It increases secretion of cytokines such as interleukin-8 (IL-8), TNFα and interleukin-1β (IL-1β).

CD44 binds primarily to the extracellular glycosaminoglycan hyaluronan (HA), promoting homing of CSCs in many tumor types. CSCs synthetize HA to attract tumor-associated macrophages (TAMs) in CSC niches. Stromal cells will in turn produce growth factors that regulate stem cell activity (159). Enhanced CD44 expression was observed in RCC cell lines after co-culture with macrophages. This effect was the result of the activation of NF-kB pathway by the TNFα derived from TAMs (160). TNFα enhanced migration and invasion of ccRCC cells together with down-regulation of E-cadherin expression and upregulation of matrix

metalloproteinase 9 and CD44 expression (161). Knockdown of CD44 increased sensitivity to doxorubicin in hepatic cancer cells. Monoclonal antibodies against CD44 are now in clinical trial for patients affected by AML.

Spheres derived from HEK293T, ACHN, Caki-1 and 786O renal cancer cell lines as well as $CD105^+$ cells isolated from RCC specimens showed the presence of a $CD44^+$ population having self-renewal properties, sphere formation capability and resistance to therapy (130,132,137).

Moreover, CD44 expression was found correlated with Fuhrman grade, tumor stage, histological type, and poor prognosis in RCC patients (162). Upregulation of TNF-α together with CD44 was associated with primary tumor stage, distant metastasis, and poor treatment outcome (146,161). Therefore, CD44 expression may serve as a predictor of the number of metastases sites in RCC (158).

2.1.4 CD24

CD24 is a small cell surface protein molecule. It is composed by only 27 amino acids, and its molecular weight ranges between 20 and 70 KDa depending on the glycosylation. CD24 is encoded by the *CD24* gene located in the chromosome 6q21. CD24 is expressed in a wide variety of cell types, including hematopoietic cells (163). Nevertheless, it is preferentially expressed in progenitor/stem cells. CD24 is an important maker for cancer diagnosis and prognosis in breast, non-small cell lung, colon, ovarian and prostate cancer (163,164).

High CD24 expression was observed in CSCs derived from the RCC cell line Caki2 (165). Nevertheless, CD24 expression together with the CSC marker CD44 showed contrasting results. CD24 expression was found correlated to tumor grade, overall survival and disease-free survival in RCCs suggesting its prognostic significance (164).

2.1.5 CXCR4

The CXC-chemokine receptor 4 (CXCR4 or CD184) is a seven transmembrane G protein-coupled receptor (GPCR) on the cell membrane. It is encoded by the *CXCR4* gene located on chromosome 2q22. CXCR4 selectively binds to the CXC chemokine stromal cell-derived factor 1 (SDF1 or CXCL12) leading to the

activation of a variety of biological processes such as stemness, survival, proliferation, migration, angiogenesis and differentiation (166). A number of signaling pathways are involved in the signal transduction. For instance, PLC/MAPK, PI3K/AKT, JAK/STAT and the Ras/Raf pathway.

CXCR4 was found expressed in many different tumor tissues. It has been shown in breast, small cell lung cancer and neuroblastoma that $CXCR4^+$ cells migrate towards tissues expressing high levels of SDF1 to metastasize (167,168). Therefore, CXCR4/SDF1 is involved in cell to stroma interaction creating a permissive niche for metastasis (146).

$CXCR4^+$ cells derived from RCC cell lines (RCC26 and RCC53; Caki1, Caki2, 786O and 769P) expressed high levels of stem cell-associated genes, resistance to therapy (TKI) and showed high capability to form spheres *in vitro* and tumors *in vivo*. Additionally, CXCR4 expression correlated with the tumorigenic potential in the cell lines. Inhibition of CXCR4 by ADM3100 or small interfering RNA (siRNA) impaired tumor formation (136,138). Moreover, overexpression of Notch1 upregulated CXCR4 in ACHN and Caki1 cell lines promoting SDF1 induced chemotaxis *in vitro* (134).

Interestingly, loss of pVHL in ccRCCs as well as hypoxia showed increased CXCR4 and MMPs expression indicating HIF1α may be responsible for expansion of the CXCR4 population (169).Varna and co-authors showed that $CD133^+/CXCR4^+$ cells coexpressed HIF1α and were located in perinecrotic areas in RCCs (127). Moreover, hypoxia promoted $CD133^+/CXCR4^+$ cells tumorigenicity. HIF2α was shown to be involved in the expansion of $CXCR4^+$ CSCs in four RCC cell lines (136).

High mRNA levels of CXCR4 in primary tumors from RCC patients with localized disease predicted shorter survival. Analysis of 2’673 RCC patients by meta-analysis revealed CXCR4 overexpression correlated to worse overall survival (OS), cancer-free survival (CFS) and disease-free survival (DFS) (170).

2.1.6 ALDH1

Aldehyde dehydrogenase 1 (ALDH1) is an enzyme involved in the alcoholic pathway. It catalyzes dehydrogenation of aldehydes to carboxylic acids. It has also been reported its role in stem cells through the retinoid signaling pathway. It is encoded by the *ALDH1* gene located in the chromosome 9q21.

ALDH1 plays an important role in cellular differentiation, proliferation, mobility, embryonic development and organ homeostasis(126). ALDH1 has been identified as a CSC marker many tumor types including breast, prostate and bladder (171,172). Its prognostic significance in RCC is still unclear (173), although ALDH1 was found correlated with tumor grade in RCC by Ozbek and co-authors (174). High expression of ALDH1 was found in the side population (SP) derived from the RCC cell line ACHN compared to the non-SP. Analysis of the $ALDH1^+$ cells revealed enhanced ability to sphere formation, self-renewal, tumorigenicity and high expression of stemness genes compared to $ALDH1^-$ cells. Moreover, drug treatment or hypoxia increased the $ALDH1^+$ cell population (126).

2.1.7 ABCB5

The drug efflux transporter ABCB5 (ATP-binding cassette, sub-family B, member number 5), is an integral membrane glycoprotein encoded by the gene *ABCB5* located in the chromosome 7p21. It is composed of 812 amino acids for an overall molecular weight of 90 KDa. This protein is involved in the transport of small ions, sugar, peptides and organic molecules across the plasma membrane (175).

ABCB5 has been found overexpressed in CSCs in melanoma, liver and colorectal cancers. Moreover, it has been found associated with tumor progression, chemotherapy resistance and recurrence (176).

$ABCB5^+$ cells showed self-renewal and tumorigenic potential as well as differentiation capacity *in vivo*. Moreover, ABCB5 controls IL-1β secretion which, in turn, stimulates IL-8 production by $ABCB5^-$ cells present in the tumor bulk. IL-8 activates CXCR1 expressed by the $ABCB5^+$ cells through paracrine and autocrine signaling (176).

2.1.8 Others

DNAJB8 is part of the heat shock family proteins (HSP40) that regulate chaperone activity. It is encoded by the gene *DNAJB8* located in chromosome 3q21. DNAJB8 is commonly expressed by the testis. Recently, Nishizawa et al., showed that DNAJB8 is expressed in different cancer cells including RCCs (135). In particular, the expression of DNAJB8 correlated with the SP compartment, and overexpression of the protein increased SP cells. Interestingly, DNAJB8 immunization completely abolished tumor formation in mice, indicating that DNAJB8 can be a target for immunotherapy (135).

MicroRNAs (miRNAs) are non-coding small RNA molecules (~22 nucleotides) involved in regulating gene expression by translational repression, mRNA cleavage, and deadenylation. The role of miRNAs in CSCs has been described for different tumor types (177). Six miRNAs involved in TGFβ and Wnt signaling pathways showed the most significant variations in expression by RT-PCR between spheres and parental cells derived from two metastatic RCC cell lines, ACHN and Caki1. Among those, miR17 was significantly downregulated in Caki1 and ACHN spheres. Upon miR17 inhibition sphere formation was enhanced. This result showed that TGFβ signaling plays an important role in renal CSCs and that miR17 impairs the signaling cascade by targeting TGFβ receptor 2 (132).

Galleggiante et al. isolated a subpopulation of cancer cells expressing CD133 and CD24 from 40 RCC samples. This population showed stem cell properties such as self-renewal, differentiation, tumorigenicity and expression of stemness-related transcription factors (141). $CD133^{+}/CD24^{+}$ cells appeared to be more undifferentiated compared to tubular adult renal progenitor cells. Interestingly, these cells also expressed on the cell membrane the amino acid transporter CTR2 which was found involved in resistance to cisplatin (141).

Rhodamine 123 (Rh123) is a fluorescent dye that permeates the cell membrane and accumulates in the mitochondria proportionally to the mitochondrial membrane potential (178). 786O cells were stained with Rh123 and sorted by flow cytometry into two population: $Rh123^{high}$ and $Rh123^{low}$. $Rh123^{high}$ exhibited high proliferative activity, differentiation, resistance to radiation, tumorigenic potential and spheroid formation in soft agar, indicating Rh123 as an alternative method to isolate CSCs (130). Moreover, spheres derived from

786O cell line expressed high levels of CD73 together with Rh123. $CD73^+$ cells expressed high levels of stemness-related transcription factors. These cells were resistant to radiotherapy and were able to initiate tumors *in vivo* (129).

2.2 Cancer stem cell isolation techniques

Stemness traits can be acquired via genetic, epigenetic modification as well as interaction with the tumor microenvironment. This entire process has to be considered reversible, plastic and dynamic. All these mechanisms contributing to cellular plasticity render difficult to discover unique biomarkers. In fact, CSC markers are not unique across tumor types. Several studies have shown that non-CSCs can acquire CSC-like properties under certain conditions. At the same time, CSCs display different stemness features depending on the microenvironment, and these features may be transient. For this reason, different approaches for CSC isolation have been developed over the years (Fig. 2.2).

Antigen-based methods require labelling of the cells based on the expression of specific markers. These include magnetic beads-conjugated antibodies (MACS) (179,180), fluorescent-activated cell sorting (FACS) (181,182), and side population (SP) analysis (183,184). However, dissociation of the tumor tissue into single cell suspension may damage surface antigens limiting the isolation of CSCs exploiting the use of cellular markers (183). In addition, no generally applicable markers are known so far, thus, characterization of putative CSC markers is often based on functional assays (148). 3D culture systems based on the use of scaffolds which recapitulate spatial organization and cell-matrix interactions as well as scaffold-free (anchorage-independent) methods are commonly employed in stem cell studies. These methods comprehend spheroid (185,186) and organoid cultures (187-189), sphere formation assay (144,182,186) and hanging drops (190,191), respectively.

Finally, in order to evaluate tumorigenic potential of a tumor cell population expressing CSC features, cancer cells are serially transplanted into immunocompromised mice (serial tumor transplantations) at low cell density (limiting dilution assay, LDA). Cancer cells capable to develop tumors repeatedly and to recapitulate the histological features and heterogeneity of the parental tumor are defined as CSCs (106).

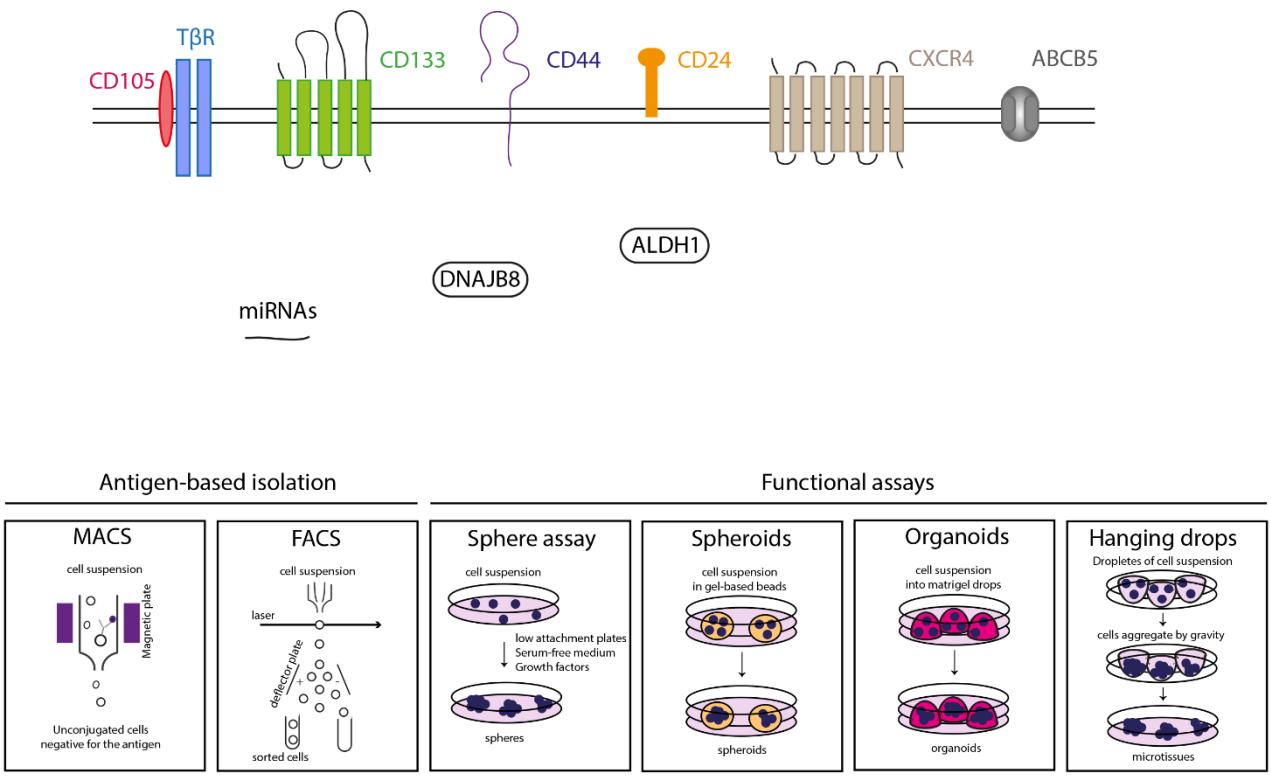

Figure 2.2. Identification and isolation of cancer stem cells. Several potential CSC markers are here depicted. CD105, TβR, CD133, CD44, CD24, CXCR4 and ABCB5 are some of the most studied membranous CSC markers. Whereas, miRNAs, DNAJB8, ALDH1 stand out among the intracellular CSC markers. Based on these markers, FACS and MACS have been adopted as isolation methods for the separation of CSCs from other tumor cells. More recently, other techniques exploiting CSC properties have been developed with the aim to discover potentially new biomarkers such as sphere assay, spheroid and organoid formation and hanging drops.

3. Tumor microenvironment and cancer stem cells

It is becoming more important that tumor microenvironment, stroma cells, soluble molecules (i.e. cytokines and chemokines) and extracellular vesicles play an important role in modulating metastatic properties and sensitivity of tumor cells to therapy by promoting stem cell features (192).

The tumor microenvironment is composed of extra-cellular matrix (ECM), cancer-associated fibroblasts (CAFs), endothelial and immune cells. ECM is composed of collagen, proteoglycans and all the non-cellular components present in the tissues. The ECM exerts its effect through so called mechano-transduction. Differential matrix stiffness and geometry are transmitted through cell contacts to the cytoskeleton and cells change their behavior according to such stimuli. YAP/TAZ, transcriptional coactivators of the Hippo pathway, were shown to be sensors and mediators of these mechano-stimuli enhancing CSC features. Moreover, an increased ECM stiffness can act as physical barrier blocking therapeutic agents.

CAFs arise from multiple sources including tissue-resident fibroblasts, mesenchymal stem cells and endothelial cells. Compared to normal fibroblasts they exhibit high proliferative capacity, enhanced ECM production, release of matrix metalloproteinases (MMPs) and release of other mediators of intercellular communication such as SDF1, interleukin-6 (IL-6), VEGF, EGF, FGF, PDGF, and hepatocyte growth factor (HGF). Hence, CAFs stimulate stemness via activation of Wnt and Notch pathways (193). MMPs also contributes to Wnt signaling and stemness (194).

Mesenchymal stem cells (MSCs) are adults stem cells involved in promoting cancer cell proliferation, angiogenesis, metastasis and immune escape (195). MSCs induce stemness in cancer cells through NF-kB signaling pathway by secreting SDF1, IL-6 and IL-8 and producing BMP antagonists (196).

Lastly, the microvasculature surrounding the tumor is important component that supports cancer growth. And it is also a factor that determine dormancy. CSCs can transdifferentiate into endothelial cells and support their growth forming a niche. Stem cell niches are often localized in hypoxic region.

Approximately 1-1.5 % of the human genes are regulated by HIFs (137). Studying the role of HIFs and the pseudo-hypoxic condition in RCC has always been crucial to fully understand RCC tumorigenesis, and yet this process remains still unclear.

It has been observed that hypoxia and enhanced expression and activity of HIF1 and HIF2 in cancer stem/progenitor cells and their progeny frequently occur during disease progression and metastases, and may induce the expression of several genes involved in self-renewal, survival, metabolism, angiogenesis, invasion, migration and resistance to therapy. Gene products involved in these pathways are Oct3/4, Nanog, Sox2 (189) (190) (191), Snail, Twist, VEGF, TGFβ, CXCR4 and EMT-associated molecules (192).

At the same time, the sustained stimulation of EGFR, insulin-like growth factor-1 receptor (IGF-1R), stem cell factor (SCF) receptor KIT, TGFβRs, Notch and their downstream signaling elements such as PI3K/Akt/mTOR may lead to an enhanced activity of HIFs creating a positive feedback loop.

Chronic exposure to elevated oxidative stress is sufficient to induce malignant transformation in kidney epithelial cells (HK2) through acquisition of stem cell characteristics such as CD44, CD24, CD133, ALDH1, Oct4, Nanog, E-cadherin, Vimentin, β-catenin, and Snail (193). Antagonistic effect of HIF1/2 towards c-Myc and TP53 appear to influence RCC development and progression. HIF1α antagonizes c-Myc activation, slowing down cell cycle and protecting CSCs from DNA damage and enhancing stemness features. In addition, Snail has been reported to reduce the expression of p53 by formation of the Snail-histone deacetylase 1 (HDAC1)-p53 complex which leads to p53 proteasomal degradation (194).

In the tumor, tumor microenvironment is characterized by chronic inflammation, which support tumor cell proliferation and progression (196). Tumor-associated macrophages (TMAs), tumor-associated neutrophils (TANs) and myeloid-derived suppressor cells (MDSCs) are recruited in the tumor milieu by cancer cells secreting cytokines and chemokines. These cells contribute to immunosuppression by secreting TGFβ, inflammatory cytokine and other factors, which maintains chronic inflammation. Additionally, TAMs and MSCs can produce exosomes, involved in promoting multidrug resistance and niche preparation.

The most common inflammatory molecules (i.e. IL-6, IL-8, TGFβ, NF-kβ, TNFα, and HIF) present in the tumor microenvironment during chronic inflammation activate downstream pathways such as TGFβ signaling, canonical and non-canonical Wnt, growth factor-receptor tyrosine kinase, and ECM-integrin signaling pathway which overlap with the process of epithelial-mesenchymal transition (EMT) (196). The EMT is a biological process that allows polarized epithelial cells to assume mesenchymal phenotype which includes enhanced migratory capacity, invasion and cell survival (197). The EMT program is often activated reversibly and partial EMT characterized by concomitant expression of epithelial and mesenchymal markers represent one of the most frequent state of a tumor cell. One of the characterizing features of a stem cell is the expression of mesenchymal markers. Interestingly, tumor cells in the non-CSC compartment can spontaneously undergo EMT changes and acquire CSC-like phenotype and surface marker expression.

In conclusion, all these processes undergoing in the TME such as inflammation, hypoxia, angiogenesis and EMT contribute to maintenance of the CSC fate by acting on the most known pathways regulating CSCs: Wnt, SHH, Notch, TGFβ, and growth factor-receptor tyrosine kinase (RTK) (Fig. 3.1).

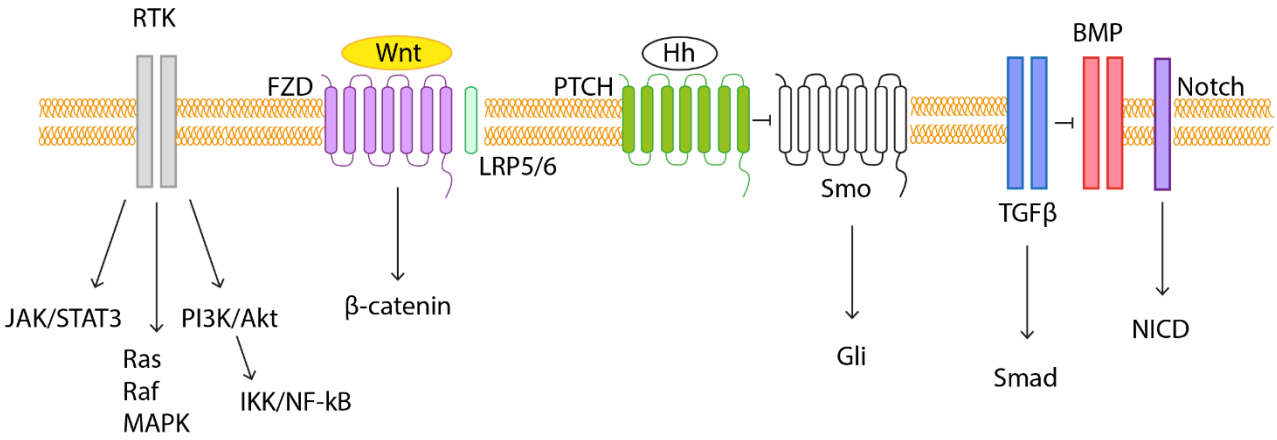

Signaling pathway	CSCs	Angiogenesis	Inflammation	EMT	Hypoxia
RTK	+	+	+	+	+
Notch	+	+		+	+
TGFβ/BMP	+	+	+	+	+
Wnt	+		+	+	+
NF-kB	+		+	+	
Hedgehog	+			+	

Figure 3.1. Cancer stem cell signaling pathways. Stemness is determined by the activation of several signaling pathways. Many of these pathways overlap with some of the biological processes acting during tumor progression. Hence, inflammation, hypoxia, angiogenesis and EMT contribute to maintenance of the CSC properties.

3.1 Exosomes

Exosomes are small membrane vesicles (40-100 nm) of endocytic origin formed within multivesicular bodies (MVBs) secreted by most of the cell types in response to hypoxia, change in pH and oxidative stress (198-201). The exact mechanism of formation and secretion of these EVs is not fully clarified. RAB1A, RAB5A, RAB7, and in particular RAB27A, were found involved in exosomes secretion in melanoma cell lines (202). Exosomes contain functional nucleic acids (mRNAs, microRNAs and DNA), proteins and lipids (200,203). The exosomal protein content may vary depending on the cellular origin of the parental cells. These proteins include adhesion molecules, trafficking molecules, cytoskeleton molecules, chaperones, enzymes and signal transduction proteins (204-207). Released EVs may remain in close proximity to the place of origin or enter biological fluids and reach distant sites (208). Exosomes have been found in various biological fluids including blood, urine, breast milk and saliva (192). It has been shown that exosomes are involved in many different signaling processes related to intercellular communication, protein secretion pathway, immune system function, cancer progression and treatment failure (201,209). They may interact with target cells directly, by transferring receptors or delivering proteins and genetic information to other cells (208). They can be isolated from body fluids or culture supernatant by differential ultracentrifugation, immunoprecipitation or ELISA according to the surface marker expression (199). The top five oncogenic proteins found expressed in exosomes are CD9, HSPA8, CD63, GAPDH, and CD81 (210-212). Importantly, exosomes also contain Alix and TGS101, which are involved in formation of MVBs (195).

Interestingly, cancer patients displayed an increased exosome content in the body fluids compared to healthy donors (213). Exosomes have been found also involved in the pathogenesis of Alzheimer disease by spreading β-amyloid peptides to the surrounding cells (214).

Accumulating evidence shows that exosomes are mediators of metastasis contributing to the generation of the metastatic niche by exchange of molecules stimulating angiogenesis, modulating stromal cells, and remodeling ECM. Tumor-derived exosomes promote education and mobilization of bone marrow-derived cells (BMDCs) such as MSCs, mesenchymal stromal cells, dendritic cells (DCs) and bone marrow-progenitor cells (BMPC), that support angiogenesis, invasion and migration (202,215,216). Exosomes from highly

metastatic melanoma cell lines increased metastatic behaviors of primary tumors in mice by educating BMDCs through MET (202). They were also found to stimulate endothelial signaling promoting angiogenesis, preparation of the lymph nodes niche and acceleration of metastasis (217,218).

Interestingly, cancer cells and stem cells seem to shed increased numbers of exosomes compared to other cell types (219). CSC-derived exosomes have been found involved in promoting angiogenesis in xenograft mice with renal cancer (124,220) and metastatic niche formation in lung carcinoma (221). Moreover, they enhanced invasion, migration and tumorigenic properties of cancer cells in colorectal cancer, breast cancer and glioblastoma (212,222-225). Several studies have shown that a cross-talk between CSCs and the tumor microenvironment indeed exist, thereby, not only CSCs may secrete exosomes which are taken up by other cells to model the tumor microenvironment in a favorable manner, but also cancer cells or stromal cells may shed exosomes to affect CSC fate (226). For instance, fibroblast-derived exosomes were found involved in promoting CSC features *in vitro* and *in vivo*.

At the same time, exosomes play important roles the normal immune system as well as in tumor immunomodulation (201). Exosomes can negatively regulate T cells and natural killer (NK) cells. An increased number of exosomes was detected in patients with poor prognosis and resistance to chemotherapy (208). Exosome release has been found enhanced upon chemotherapy. In gastric cancer exosomes induced chemo-resistance *in vitro* and *in vivo* by activation of the calcium/calmodulin-dependent protein kinases and the Raf/MEK/ERK kinase cascade in association with enhanced expression of multidrug resistance associated proteins (227).

Exosomes can bind the antibody directed against specific receptors expressed by tumor cells reducing its efficacy as well as export anticancer drugs. On the other hand, exosomes have been explored as a vehicle to deliver miRNAs and drugs to cancer cells, perhaps exploiting the expression of tumor-specific markers on their membrane and the homing capacity (195). To date, exosomes are extensively used in regenerative medicine. In conclusion, exosomes represent a valuable tool to investigate cancer pathogenesis and to provide new insights into cancer diagnostics and therapeutics.

4. IL-8/CXCR1-2

CXCL8 (CXC motif ligand 8 or IL-8), represents one of the major chemokines associated with the promotion of neutrophils and inflammatory response (228). IL-8 is undetectable under physiological state but it is rapidly induced by inflammatory cytokines such as TNFα and IL-1β as well as by hypoxia and hormones (229,230). IL-8 belongs to the CXC chemokines family. It is encoded by the gene *IL-8* located in chromosome 4 q12-q21. Initially produced as a 99 aa protein, it is rapidly cleaved to form a 72 aa (8-10 KDa) active form. Previous studies have demonstrated that IL-8 is involved in proliferation and survival of neoplastic cells. IL-8 is also associated with apoptosis, multidrug resistance, angiogenesis and metastasis-related tissue remodeling.

Interestingly, IL-8 promotes the recruitment of bone marrow-derived MSCs to the tumor region, which support angiogenesis and tumor aggressiveness (231). For instance, kidney cancer cells were capable to secrete IL-8 and activate Akt signaling pathway via CXCR2 in MSCs inducing homing of MSCs (232). Additionally, activated MSCs efficiently recruited $CXCR2^{+}$ neutrophils to the tumor region. The interaction between neutrophils and tumor cells resulted in elevated metastasis-related genes by tumor cells in breast cancer and lymphoma (233,234). IL-8 was also found recruiting macrophages in RCC (235).

Dimerization of IL-8 is necessary for the receptor binding. IL-8 interacts with CXCR1 and CXCR2 with different affinities to mediate several cellular responses. CXCR1 receptors can be activated only by binding of IL-8, whereas CXCR2 is activated in response to multiple chemokines, neutrophil-activating peptide and granulocyte chemotactic protein 2 (230). CXCR1/2 are members of the GPCR family which contains seven transmembrane domains. They are encoded by the genes *IL8RA* and *IL8RB* located in chromosome 2q33-q36. CXCR1/2 have recently been demonstrated to be associated with CSC populations as well as proliferation, migration and invasion in certain type of human cancers such as breast, prostate, colon and pancreatic cancers (236-239).

In particular, a recent study on pancreatic cancer showed that positive CXCR1 but not CXCR2 expression correlates with metastasis and poor survival rate in patients (236). Further, IL-8 increased sphere formation, migration and invasion, and these effects could be reversed by CXCR1 blockade. CXCR1 stimulation by

applying exogenous IL-8 increased the SP fraction, the expression of ABC transporters and decreased drug sensitivity in HCC (228). On the other hand, CXCR2 was found playing a critical role in tumor growth and metastasis formation in colon cancer (239). Ginestier et. al. developed a strategy to target breast CSCs using either CXCR1-specific antibodies or repertaxin. Repertaxin, a small molecule blocking CXCR1/2, was able to specifically target breast cancer xenografts retarding tumor growth and reducing metastasis (238). Additionally, ABX-CXCL8 treated mice exhibited significant reduction in tumor growth, angiogenesis and metastasis in bladder and melanoma xenograft models (229,240).

The drug efflux transporter ABCB5 identifies CSCs in various cancers. Its expression is associated with clinical disease progression and tumor recurrence. Interestingly, the drug efflux transporter ABCB5 has been found functionally involved in the regulation of IL-8/CXCR1 signaling through IL-1β in melanoma cells and has therefore been associated with cancer stem-like cells, clinical disease progression and tumor recurrence (176). The correlation between IL-8 and ABC transporters has been proposed in ovarian and colon cancer as well (228).

CXCL8 acts through several signaling pathways (Fig. 4.1). IL-8 activates PI3K followed by phosphorylation of Akt resulting in increased angiogenesis, cell migration and proliferation (230). IL-8 signaling also regulates MAPK signaling through PI3K in neutrophils and via EGFR resulting in Ras-GTPase activation in ovarian and lung cancers (241-243). It also stimulates PLC signaling which in turn induces the phosphorylation of protein kinase C, and promotes migration by increasing Ca+ concentration and regulating actin cytoskeleton (229). IL-8 has been shown to promote activation of EGFR and VEGFR promoting downstream activation of MAPK cascade (230). IL-8 is positively correlated with an increased phosphorylation of Src-kinases and focal adhesion kinase (FAK) in cancer cells which contributes to cell proliferation, cell survival and chemoresistance. Moreover, the Rho-GTPases may promote phosphorylation of Src and FAK with further impact on downstream transcriptional factors (229). IL-8 signaling induces β-catenin nuclear translocation and HIF1α in prostate cancer (244).

High IL-8 levels in blood samples correlated with shorter progression free survival in patients non-small-cell lung cancer (NSCLC) and colorectal carcinoma (CRC) (239,245). IL-8 confers resistance to EGFR inhibitors by inducing stem cell properties in lung cancer (245). In ccRCC, increased IL-8 expression was associated with sunitinib resistance *in vitro* and *in vivo* (61). Moreover, increased expression of IL-8 is a potential independent adverse prognostic biomarker for cancer-specific survival (CSS) and recurrence-free survival (RFS) in patients with ccRCC after nephrectomy (246).

Nevertheless, the role of the IL-8/CXCR1 axis in ccRCC pathogenesis and CSC properties is currently unknown.

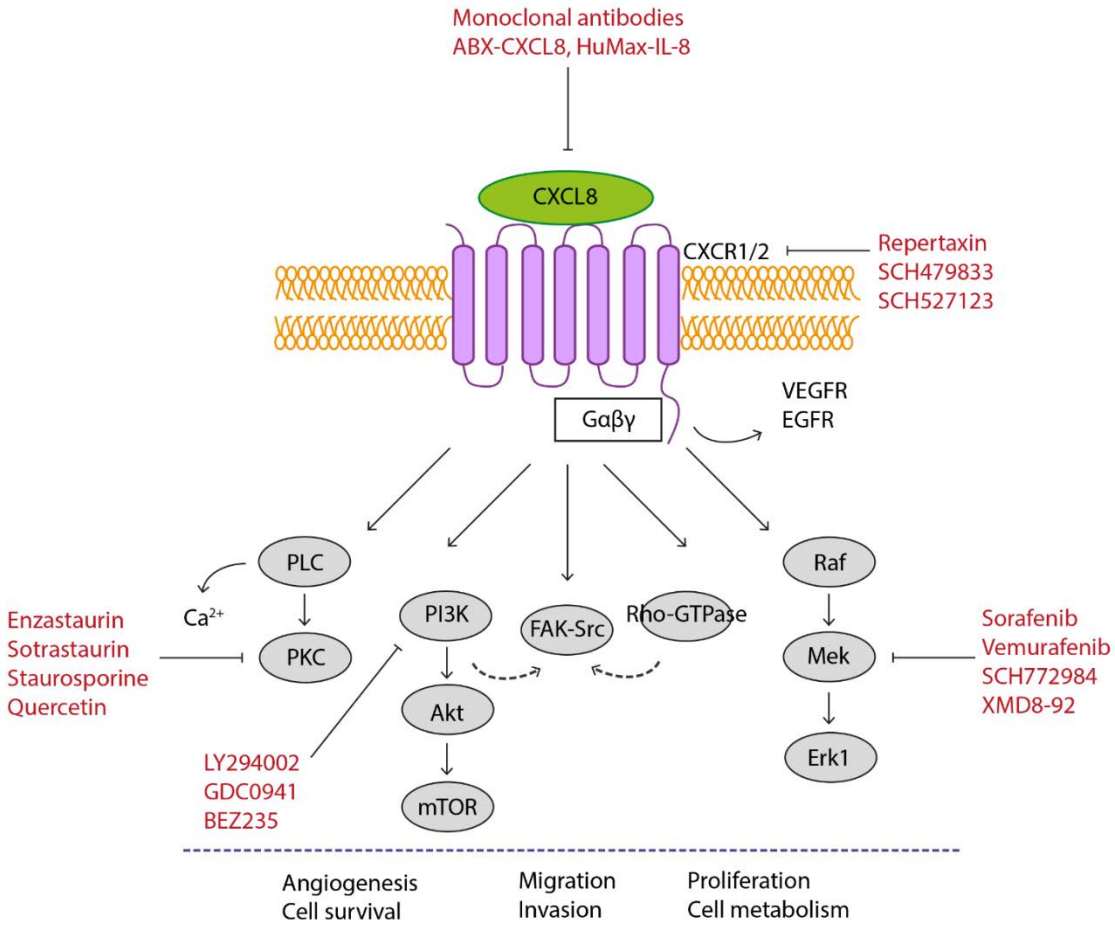

Figure 4.1. IL-8 signaling pathways. Adapted from Liu Q. et al., "The CXCL8-CXCR1/2 pathways in cancer", Cytokine & Growth Factors Reviews, 2016; and Waugh D.J.J. and Wilson C., "The interleukin-8 pathway in cancer ", Clinical Cancer Research, 2008. The diagram illustrates the major signaling pathways of IL-8 including PI3K or PLC, promoting activation of Akt, PKC calcium mobilization and MAPK singaling cascade. In addition, IL-8 activates member of the RhoGTPase family with effects on FAK/Src (dashed lines).

4.1 Cancer stem cell-targeted therapies

Several therapeutic agents have been proposed targeting CSCs based on molecular mechanisms that regulate stem cell features. Interleukin-15 (IL-15) induced loss of the stem cell makers, tumorigenicity and sphere formation capability via differentiation of $CD105^+$ cells from human RCC. Differentiated $CD105^+$ CSCs became sensitive to chemotherapy (247-249). A phase I clinical trial on IL-15 is ongoing for melanoma and metastatic RCC patients (NTC01021059, http://clinicaltrails.gov/). As previously discussed, CSCs activate PI3K/Akt/mTOR singling pathway. Therefore, mTOR inhibitors have been proposed as potential therapeutic agents against CSCs. However, contrasting results have been reported in the literature so far. Bone morphogenetic protein 2 (BMP2) has been shown capable to inhibit tumorigenicity of CSCs in osteosarcoma and renal cancer (250). However, no clinical trial involving BMP2 is registered for cancer patients. Among the agents targeting IL-8/CXCR1-2 axis (Fig. 4.1), a clinical phase II study using repertaxin in combination with chemotherapy in metastatic triple negative breast cancer is running (FRIDA, http://clinicaltrials.gov/). Targeting CXCR1/2 using orally active small molecule antagonist (SCH-527123, SCH-479833) inhibited human colon liver metastasis by diminished angiogenesis and increased apoptosis. However, there was no difference in primary tumor growth (251). Navarixin blocks CXCR2 signaling inhibiting tumorigenesis in xenograft models of breast cancer, CRC, and melanoma (252). Moreover, the administration of humanized antibodies against IL-8 (ABX-IL8) has shown to attenuate the growth of bladder cancer and melanoma in xenograft models (230). A strategy using small interfering RNA has been shown to suppress ovarian tumor xenografts (253). Although IL-8 expression has been described associated with the multidrug resistance ABC transporters, conventional chemotherapy itself has been shown to induce IL-8 expression and secretion by cancer cells increasing the level of autocrine and paracrine IL-8 signaling. Thus, targeting IL-8 in combination with conventional chemotherapy agents and/or immunotherapy would be the next step towards overcoming tumor recurrence. Several other strategies have been proposed to target CSCs, which have not been experimented on RCC so far. They include targeting ABC transporters, CSC surface markers, inhibiting CSC related signaling pathways and delivering CSC-specific therapeutics (146).

OBJECTIVES OF THE STUDY

5. Objectives of the study

The project I have been carrying out during my Ph.D. focuses on understanding the mechanisms underlying tumor heterogeneity and cancer stem cell contribution to tumor progression, metastasis formation and therapy failure, which may ultimately promote the discovery of more accurate and reliable diagnostic and prognostic tools as well as provide the instruments for precise and patient-oriented therapeutic intervention.

As an outline of the whole project, the workflow depicted in the figure 5.1 was established with the aim to address the following questions:

1. Liquid biopsies as a potential diagnostic and prognostic tool for ccRCC patients;
2. Dissecting tumor heterogeneity and personalized medicine using primary cultures;
3. Identifying new biomarkers for renal cancer stem cells with potential therapeutic implications.

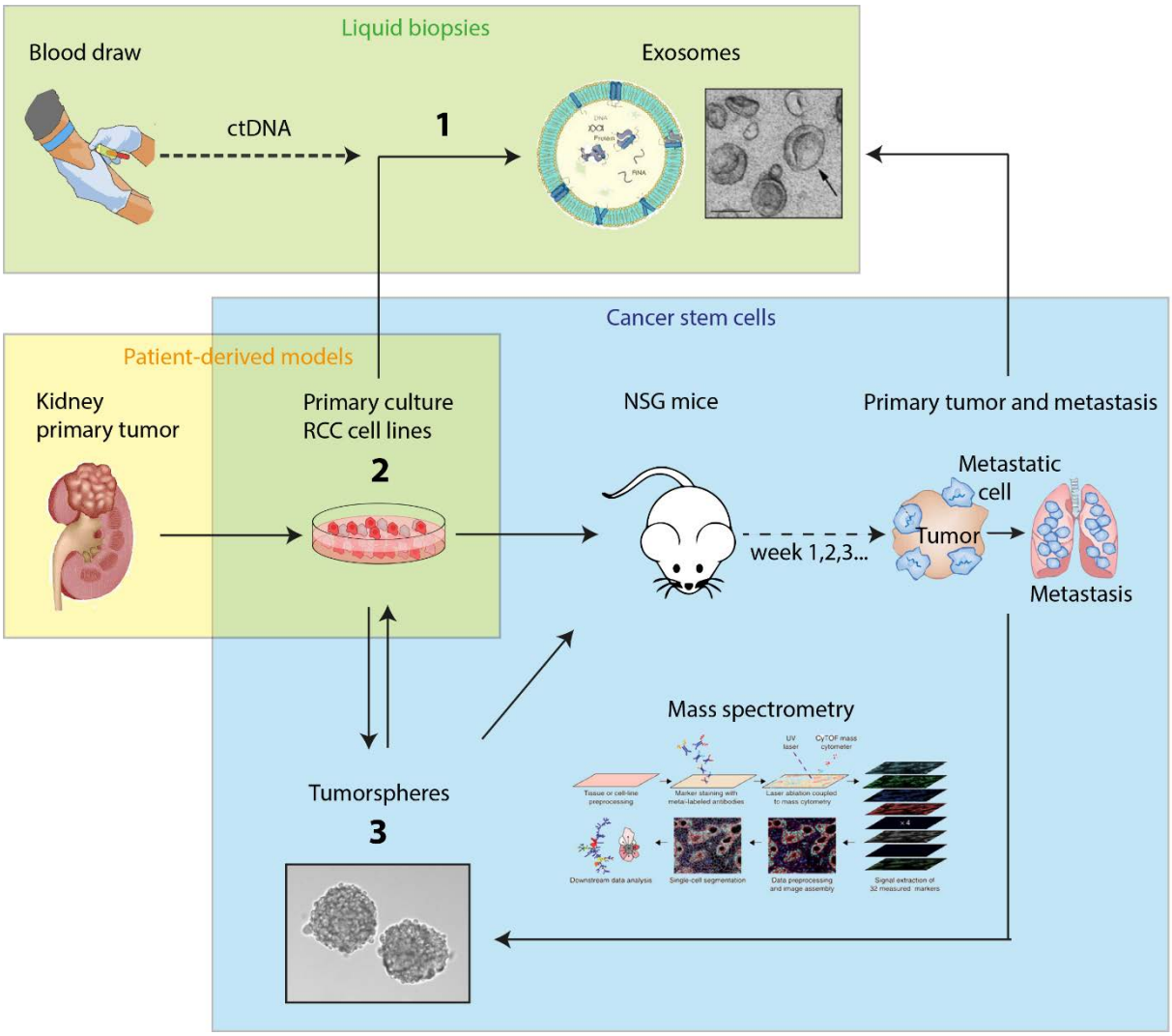

Figure 5.1. Dissecting tumor heterogeneity and cancer stem cell properties in clear cell renal cell carcinoma. Experimental workflow where liquid biopsies, patient-derived models and the investigation of cancer stem cell properties will lead to a better understanding of tumor heterogeneity and, therefore, RCC pathogenesis and therapeutic interventions. Mass spectrometry workflow adapted from Giesen C. et al., "Highly multiplexed imaging of tumor tissues with subcellular resolution by mass cytometry", Nature Methods, 2014 (254).

RESULTS

6. Results

In the following section, I will present three manuscripts I have completed during my Ph.D. work aiming to understanding tumor heterogeneity and cancer stem cell properties in clear cell renal cell carcinoma.

6.1 Liquid biopsies as a potential diagnostic and prognostic tool for ccRCC patients

6.1.1 Detecting circulating tumor DNA in renal cancer: An open challenge

Author contributions

The experiments were conceived and designed by **C.C., H.M.** and **M.R.**

C.C. was involved in the development of the methodology and in the design of the workflow, in the data acquisition, in the analysis and interpretation of the results as well as in the manuscript writing. **T.H.** conducted animal experimentation and acquired xenograft data. Patients were recruited and informed by **C.P.**, **T.S.** and **T.H.**

G.P. and **T.W.** supported this work by collecting samples from colon cancer patients. **P.J.W** contributed in the administrative and NGS infrastructure support. **I.F** revised the manuscript and provided with critical support during the conception of the animal experimentation. Finally, **H.M.** and **M.R.** assisted in the manuscript writing, provided administrative support, study supervision.

Experimental and Molecular Pathology 102 (2017) 255–261

Contents lists available at ScienceDirect

Experimental and Molecular Pathology

journal homepage: www.elsevier.com/locate/yexmp

Detecting circulating tumor DNA in renal cancer: An open challenge

Claudia Corrò [a], Tomas Hejhal [b], Cédric Poyet [c], Tullio Sulser [c], Thomas Hermanns [c], Thomas Winder [d], Gerald Prager [e], Peter J. Wild [a], Ian Frew [b], Holger Moch [a,1], Markus Rechsteiner [a,*,1]

[a] Institute of Surgical Pathology, University Hospital Zurich, Switzerland
[b] Institute of Physiology, University of Zurich, Switzerland
[c] Department of Urology, University Hospital Zurich, Switzerland
[d] Department of Oncology, University Hospital Zurich, Switzerland
[e] Department of Oncology, University Hospital Vienna, Austria

ARTICLE INFO

Article history:
Received 18 October 2016
Accepted 11 February 2017
Available online 23 February 2017

Keywords:
Circulating tumor DNA
Clear cell RCC
VHL
Colon cancer
KRAS
Next generation sequencing

ABSTRACT

Background: Detection of circulating tumor DNA (ctDNA) in blood of cancer patients is regarded as an important step towards personalized medicine and treatment monitoring. In the present study, we investigated the clinical applicability of ctDNA as liquid biopsy in renal cancer.
Methods: ctDNA in serum and plasma samples derived from ccRCC and colon cancer patients as well as ctDNA isolated from RCC xenografts with known *VHL* mutation status was investigated using next generation sequencing (NGS). Additionally, a Taqman mutation specific assay was used for specific *VHL* mutation detection in blood.
Results: In our study, we successfully identified *KRAS* mutation in colon cancer patients. We also confirmed the presence of specific *VHL* mutations in ctDNA derived from RCC xenografts indicating the capability of renal tumors to release DNA into the blood circulation. However, we could not detect any *VHL* mutation in plasma or serum samples derived from nine ccRCC patients. To increase the sensitivity, a *VHL* mutation specific Taqman assay was tested. With this approach, the pVHL mutation p.Val130Leu in exon 2 in one patient was successfully detected.
Conclusion: These data suggest a reduced tumor DNA shedding and an increased clearance of the tumor DNA from the circulation in renal cancer patients independently of tumor size, metastases, and necrosis. This implies that highly sensitive detection methods for mutation calling and prior knowledge of the mutation are required for liquid biopsies in ccRCC.

1. Introduction

The presence of nucleic acids circulating in the blood have been shown for the first time in 1948 by Mandel and Metais who discovered the presence of DNA and RNA in the plasma of healthy and diseased donors (Mandel and Metais, 1948). After this study, several others have identified the presence of circulating free DNA (cfDNA) in the bloodstream of patients and changes in the levels of these circulating nucleic acids have been associated with tumor load and malignant progression proposing these liquid biopsies as a novel prognostic, diagnostic, and predictive tool for cancer patients, including renal cancer (Esposito et al., 2014; Fleischhacker and Schmidt, 2007; de Martino et al., 2012). However, correlation of cfDNA levels to tumor stage and grade in renal cancer revealed discordant results (de Martino et al., 2012; Feng et al., 2013; Perego et al., 2008; Jung et al., 2010).

In particular, it has been shown that the amount of circulating tumor DNA (ctDNA) shed by cancer cells represents up to 10% of total cfDNA derived from blood in patients with advanced tumors (Schwarzenbach et al., 2011). Thus, ctDNA opens the possibility to detect the mutational profile of a specific cancer during tumor evolution, metastasis formation and therapy. Indeed, different mutations have been identified in cfDNA of patients affected by colon, lung, ovarian and breast cancers (Esposito et al., 2014; Kukita et al., 2013; Forshew et al., 2012; Diehl et al., 2008; Schwarzenbach et al., 2008; Hashad et al., 2012). More recently, Bettegowda and co-workers detected ctDNA in >75% of the patients with advanced pancreatic, ovarian, colorectal, bladder, gastro-esophageal, breast, melanoma and head and neck cancers but in <50% of patients presenting with renal and prostate cancers (Bettegowda et al., 2014). In particular, the release of ctDNA was investigated in 5 ml of plasma derived from five metastatic RCC patients. Prior analysis of the tumor tissue revealed in one RCC patient a *MET* mutation, in one a *HOOK2* mutation, and in three a *VHL* mutation. When analyzing the ctDNA, only one *VHL* mutation and the *MET* mutation were successfully detected (40%). For the detection of *VHL*, the authors used PCR-ligation and for the detection of the *MET* mutation SafeSeqS. Both methods are highly sensitive with

* Corresponding author at: Institute of Surgical Pathology, University Hospital Zurich, Schmelzbergstrasse 12, 8091 Zurich, Switzerland.
E-mail address: Markus.Rechsteiner@usz.ch (M. Rechsteiner).
[1] Shared senior authorship.

http://dx.doi.org/10.1016/j.yexmp.2017.02.009
0014-4800/

detection limits below 1% allele count. However, for both assays the mutation of interest has to be identified in the tumor tissue before analysis of the blood samples. Therefore, the development of non-invasive methods to detect de novo or to monitor already known tumor specific signatures continue to be a major challenge in renal cancer.

Renal cell carcinoma (RCC), a malignant tumor affecting the adult kidney, is among the 10 most common cancers, affecting around 64,000 people every year with 5% death incidence (Siegel et al., 2012). Nearly half of all patients with RCC die within 5 years of diagnosis and 5-year-survival for those with metastatic disease is 5–10% (Moch et al., 2000). This is mainly due to the fact that RCC is characterized by asymptomatic manifestation in early stage and a poor response to radiotherapy and chemotherapy in metastatic stage, making this tumor type very difficult to diagnose and treat (Baldewijns et al., 2008; Moch et al., 2016). In particular, clear cell renal cell carcinoma (ccRCC) is the most common type of RCC (Baldewijns et al., 2008; Moch et al., 2016). Inactivation of the von Hippel-Lindau (*VHL*) tumor suppressor gene by mutation or promoter methylation has been found responsible for about 80% of ccRCC cases (Sato et al., 2013; Nickerson et al., 2008; Gnarra et al., 1994; Latif et al., 1993; Zhang and Yang, 2012). The majority of sporadic ccRCCs are characterized by chromosomal loss of one allele located at chromosome 3p combined with a mutation in *VHL* on the second allele (Beroukhim et al., 2009; Rechsteiner et al., 2011).

In the present study, the amount of cfDNA will be exploited as a possible biomarker for ccRCC. We aimed to identify parameters which might increase the presence of ctDNA such as tumor size or necrosis. Additionally, ultra-deep next-generation sequencing and Taqman mutation specific PCR assay will be employed to detect specific tumor mutations in ctDNA, i.e., the tumor suppressor gene *VHL*, next to normal cfDNA with high sensitivity.

2. Materials and methods

2.1. Ethics statement

This study was conducted in strict accordance with the recommendations in the Swiss regulations on animal welfare and experimentation. The protocol was approved by the Ethics committee of the Zurich Cantonal Veterinary Office (license 06/2013).

2.2. Cell lines

The RCC cell lines A-498, HEK293, and SLR26, were purchased from ATCC-LGC Standards (Manassas, VA). The cell lines were additionally authenticated by IdentiCell. Cells were cultured using Dulbecco's Modified Eagle Medium (Sigma) containing 10% vol/vol dialyzed fetal calf serum (FCS) and 2 mM glutamine and they were split when reaching 80% confluence.

2.3. Study cohort and sample collection

Peripheral blood (5 ml) was collected from nine consecutive ccRCC patients shortly before surgery with a written informed consent of the patients. None of the patients received treatments before surgery. In parallel, tissue specimens derived from the partial or radical nephrectomy were fixed and embedded in paraffin and evaluated by one pathologist (H.M.). Tumors were histologically classified and graded according to the World Health Organization classification (Moch et al., 2016). Tumor staging was performed according to the current TMN system. The research protocol was approved by the local commission of ethics (KEK-ZH-Nr. 2011-0072).

In addition, plasma from four colon cancer patients with tumor stage IV was kindly provided by our collaborators Dr. T. Winder and Dr. G. Prager (PASSION-trail, NCT02119026).

2.4. Processing of blood

Peripheral blood (5 ml) was collected in serum (BD Vacutainer, Plymouth, UK) or EDTA-containing tubes (BD Vacutainer, Plymouth, UK) and processed immediately at 3500 rpm for 15 min at 4 °C after collection. Serum and plasma samples were stored at −80 °C.

2.5. Circulating free DNA extraction

Circulating free DNA (cfDNA) was extracted from 1 ml of serum or plasma EDTA using the QIAamp Circulating free DNA Kit (Qiagen, Hilden, Germany) according to the manufacturer's instructions. CfDNA concentration was then measured using a fluorometric assay (High Sensitivity dsDNA Assay, Qubit, Thermo Fisher Scientific/Life Technologies, Zug, Switzerland). Additionally, DNA fragment distribution was analyzed using the Agilent 2100 Bioanalyzer (Agilent Technologies, Basel, Switzerland) in order to determine the quality of the DNA extracted and the DNA fragment size.

2.6. Next-generation sequencing

Sequencing libraries of cfDNA samples were constructed with the Ion AmpliSeq library preparation Kit 2 according to manufacturer's instructions. A human specific gene target set of primers (Cancer Hotspot Panel (CHP2), Life Technologies) including *BRAF*, *KRAS* and *VHL* was used in the amplification process. The libraries were then quantified by qPCR with the Ion Library Quantitation kit (Thermo Fisher Scientific) and amplicon distribution analyzed using the Agilent 2100 Bioanalyzer. Subsequently, the libraries were diluted to 12 pM, mixed and used for template preparation (Ion One Touch™ 200 Template Kit v2, Ion PI Template OT2 200 Kit v3 or Ion PI Hi-Q OT2 200 Kit; Thermo Fisher Scientific). The template Ion Sphere Particles (ISPs) were then enriched, loaded on an Ion 318 Chip v2 or Proton chip and sequenced on the Ion Torrent PGM System (Ion PGM Sequencing 200 Kit v2; Thermo Fisher Scientific) or Proton platform (Ion Proton Sequencing 200 Kit v3 or Ion Pi Hi-Q Sequencing 200 Kit; Thermo Fisher Scientific).

2.7. Sequence alignment and mutation detection

The sequences were aligned to the human genome hg19 (GRCh37.p5). The RefSeq for *VHL* was NM198156.4. The sequencing run performance evaluation, the mutation detection (variant calling) and the data analysis were performed using the Ion Torrent Browser and Ion Reporter Software 4.2 using default settings of the integrated analysis workflows(Thermo Fisher Scientific). Filter criteria for variant calling included variant allele read count >10× and total coverage >50×. All variants were inspected using the Broad Institute's Integrated Genome Viewer (IGV).

2.8. Xenograft

SCID-beige mice (10 weeks old) were maintained in a specific pathogen-free facility (Prof. I. Frew, license 06/2013, LASC Irchel Facility, Zurich University, Switzerland). Mice were subcutaneously injected with the A-498 cell line (5×10^6 cells) in BD Matrigel GFR (BD Biosciences) and euthanized when the tumor size reached 1 cm^3. Blood from mice was collected, tumors were excised and the DNA isolated. Part of the tumor tissue was used for histological preparation and evaluation.

2.9. PCR-specific mutation detection

The Taqman mutation detection assay kit (Cat #4465804) was purchased from Applied Biosystems (Foster city, CA, USA) in order to detect the mutation c.388G>C p.Val130Leu located in the exon 2 of the *VHL* gene.

A mutation specific primer was used to detect either the wt or the mutated DNA template. The assay was performed according to the manufacturer's instruction in 10 μl reaction volume and run on an ABI ViiA7 Real-Time PCR machine (Applied Biosystems). T138 DNA was derived from human tumor tissue as described by Rechsteiner and co-workers (Rechsteiner et al., 2011) and was used as a negative control in the Taqman assay.

2.10. Sanger sequencing

The PCR amplification was performed with the same DNA as was used for library preparation for next-generation sequencing (Table S9). The sequencing run was performed as previously described (Rechsteiner et al., 2013). Sanger sequencing data was analyzed by Sequencher 5.1.

2.11. Statistical and computational analyses

Student's *t*-test was performed using SPSS Statistics 22 (IBM). *P*-values < 0.05 were considered statistically significant.

3. Results

3.1. ctDNA in renal cancer patients

Plasma and serum samples were collected from nine consecutive ccRCC patients. Presence of metastases at diagnosis, tumor stage and tumor necrosis was analyzed retrospectively. These factors potentially increase the probability to detect ctDNA in the blood (Table S1).

The total cfDNA extracted from either serum or plasma ranged from 9.3–48.6 ng with a concentration of 0.31–1.62 ng/μl (Table S2). Moreover, the cfDNA fragment length was determined using the Bioanalyzer and resulted in ~170 bp for all nine samples which was similar to the fragment length detected in the plasma-derived cfDNA isolates from colon cancer patients and xenografts. CfDNA and genomic DNA isolated from the corresponding primary tumor tissue (FFPE) of the ccRCC cases was then amplified using the Cancer Hotspot Panel (CHP2) and sequenced on the PGM platform. The sequencing metrics are summarized in the supplementary Table S3.

We identified six different *VHL* mutations in the DNA derived from the nine primary tumors of ccRCC patients (67%) which was in line with ccRCC frequency described in previous studies (Rechsteiner et al., 2011; Brugarolas, 2014). Three ccRCC patients (#P78; #P163 and #P172) were wild-type for *VHL*. #P68 (primary tumor) showed the *VHL* mutation c.345insC/p.Leu116ProfsX15 located in exon 2 with 15% variant frequency. In #P69 (primary tumor) two *VHL* mutations were detected in exon 2 with 10% variant frequency. In #P84 (primary tumor) the *VHL* mutation c.300_315del16/p.Leu101AlafsX26 located in exon 1 was present with 6% variant frequency, whereas #P115 (primary tumor) showed the *VHL* mutation in exon 2 c.345C>G/p.His115Gln with 25% variant frequency (Table 1). Moreover, we could identify the *VHL* mutation c.578insA/p.Asp193LysfsX63 in exon 3 in #P155 and, in the same exon, #P159 showed the following mutation: c.488T>C/p.Leu163Pro. These data were confirmed by Sanger sequencing (Fig. 1), but we could not identify the same *VHL* mutations in the corresponding cfDNA derived from serum or plasma of ccRCC patients although having a sequencing depth at these specific locations ranging from 7880 to 10,895×. To increase the sensitivity of mutation detection, a second sequencing run was performed on the Proton platform using the same NGS-libraries as used on the PGM platform. Again, no single read with the appropriate mutation was detected.

The sequencing metrics for the Proton run are as well summarized in the supplementary Table S4.

3.2. ctDNA detection in colon cancer patients

Since no *VHL* mutation was detected in cfDNA derived from *VHL*-mutated renal cancer patients, a proof-of-concept study with four colon cancer patients was initiated to determine whether we could detect ctDNA in general. The total cfDNA extracted from the colon cancer patients ranged from 12.3–87 ng with a concentration of 0.41–2.90 ng/μl (Table S5). Moreover, the size of the DNA fragments was determined using Bioanalyzer and yielded ~170 bp in all the samples (Fig. S1a–d). Subsequently, cfDNA samples were amplified using the CHP2 and sequenced on the PGM platform. The performance of the sequencing run and the sequencing metrics are summarized in Table S6. Different mutations in the *KRAS* gene were detected in three out of four samples analyzed. In particular, in patient #1 (#P1) the *KRAS* mutation c.T>C/p.Ala146Thr in exon 4 was detected with 8% variant frequency. In patient #2 (#P2) no mutation was identified. Patient #3 (#P3) showed the *KRAS* mutation c.G>T/p.Gln61His located in exon 3 with 12% variant frequency and the *KRAS* mutation c.A>C/p.Gly12Val in exon 2 was revealed with 33% variant frequency in patient #4 (Table 2). As a control, patient #4 (*KRAS* p.Gly12Val) was successfully verified using Sanger sequencing.

These results indicate that tumor specific mutations can be detected in cfDNA derived from plasma samples in colon cancer patients below the detection limit of Sanger sequencing (10% variant allele frequency, internal communication) using our NGS workflow presented here.

3.3. ctDNA detection in renal cancer xenografts

A second proof-of-concept study was started to test whether renal cancer cells shed ctDNA per-se and whether mutations in *VHL* may be detected in vivo. Therefore, SCID-beige mice (10 weeks old) were subcutaneously injected with the renal cancer A-498 cell line (5×10^6 cells) in BD Matrigel GFR. One mouse (A2) obtained one injection and another (A3) two injections into each flank. When the tumor size reached 1 cm^3 (approx. after 7 weeks) around 800 μl of blood was collected from each mouse and ~300 μl of plasma was obtained it. As a control, blood was collected from a non-xenografted SCID-beige mouse littermate (C2). After the collection of the blood, xenograft tumors were excised (Fig. S2) and part of the tumor tissue was used for histological preparation and evaluation and part was used for DNA isolation.

Table 1
Tumor mutation detection on DNA extracted from FFPE.

Patient	Mutation detected	Total reads	Reads for the wt	Reads for the variant	% wt	% variant
#68	c. 345insC p.Leu116ProfsX15 exon 2	9867	8355	1492	85%	15%
#69	1) c.354C>T p.wt	1) 22,664	1) 20,303	1) 2360	90%	10%
	2) c.388G>C p.Val130Leu exon 2	2) 22,778	2) 20,445	2) 2301		
#78	WT (by Sanger sequencing)	n.a.	n.a.	n.a.	n.a.	n.a.
#84	c.300_315del16 p.Leu101AlafsX26 exon 1	31	29	2	94%	6%
#115	c.345C>G p.His115Gln exon 2	11,058	8283	2748	75%	25%
#155	c.578insA p.Asp193LysfsX63 exon 3 (by Sanger sequencing)	n.a.	n.a.	n.a.	n.a.	n.a.
#159	c.488T>C p.Leu163Pro exon 3 (by Sanger sequencing)	n.a.	n.a.	n.a.	n.a.	n.a.
#163	WT (by Sanger sequencing)	n.a.	n.a.	n.a.	n.a.	n.a.
#172	WT (by Sanger sequencing)	n.a.	n.a.	n.a.	n.a.	n.a.

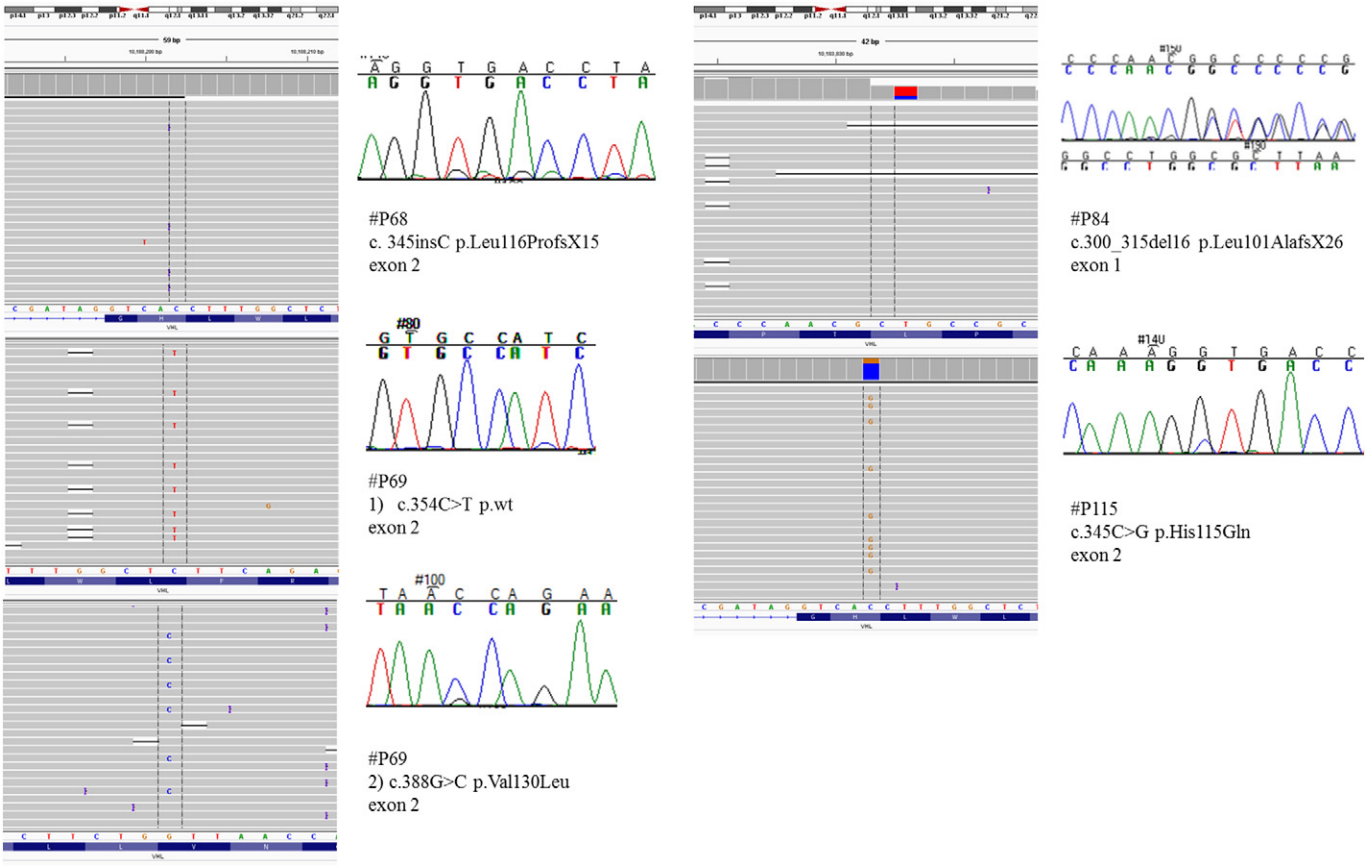

Fig. 1. *VHL* next generation sequencing vs Sanger sequencing. Output data for deep sequencing of DNA derived from primary tumor tissue of five ccRCC patients. The electropherogram highlights the same mutation identified by Sanger sequencing.

Subsequently, cfDNA was isolated and its concentration was measured (Table S7). The total cfDNA extracted ranged from 8 to 12.1 ng with a concentration of 0.266–0.402 ng/μl. Interestingly, no differences were observed in cfDNA amount between control and xenograft mice when normalized to the amount of plasma used as input.

cfDNA and DNA derived from xenografted tumor tissue were extracted and then amplified using the human specific gene target set from theCHP2 which includes *VHL*. Subsequently, the amplicons were enriched and sequenced on the PGM platform. As a control, DNA derived from the A-498 cell line, which was used for injection, was amplified with the CHP2 and sequenced in parallel. We successfully identified the *VHL* mutation (c.426_429delTGCA/p.Val142fsX14located in exon 2) in the cfDNA of mice (Fig. 2a), in the DNA derived from the corresponding xenograft tumors (Fig. 2b), and in the A-498 cell line (Fig. 2a). The sequencing metrics are summarized in the supplementary Table S8.

NGS of the xenografted tumor tissues revealed the presence of the mutation of interest with >98% frequency, whereas in the cfDNA the mutation was detected with 100% frequency in the mouse A2 and in the mouse A3 with 3.5% variant frequency (Table 3).

These results indicate that the subcutaneously growing renal cancer A-498 cell line can release its DNA in the tumor microenvironment and in the blood circulation in mice and that our NGS approach delivers reliable results using *VHL* mutations as a biomarker.

3.4. Mutation specific qPCR

Since our concept studies have validated and proven that ctDNA with *VHL* mutations from renal cancer cells may be used as biomarker, we tested whether the ctDNA detection in our renal cancer patient cohort was missed due to the sensitivity of our NGS workflow. Therefore, a mutation specific qPCR was performed which has a detection limit of <1%. For this experiment, patient #69 was selected because of the point mutation c.388G>C/p.Val130Leu in *VHL* for which a commercial kit was available. In this kit a *VHL* wild-type (wt) assay was included as control.

To determine assay specificity and sensitivity, DNA extracted from HEK293 (wt at location c.388G) was first tested using different amounts of DNA input concentration (1.25 ng, 5 ng, 10 ng, 20 ng). The ct values ranged from 38.5–35.7 for the mutation specific assay and from 26.0–21.7 for the wt assay with $R^2 = 0.95$ and $R^2 = 0.99$, respectively (Fig. 3a). The limit of detection (LOD) of a real mutation with the mutation specific probe was therefore set to ct = 38.49 when using 1.25 ng as input for the mutation and ct = 25.06 for the reference. As additional controls,

Table 2
Circulating tumor DNA detection in colon cancer patients.

Patient	Mutation detected	Total reads	Reads for the wt	Reads for the variant	% wt	% variant
#1	*KRAS* c.T>C/p.Ala146Thr exon 4	2666	2437	227	91.4%	8.5%
#2	No mutation was detected	/	/	/		/
#3	*KRAS* c.G>T/p.Gln61His exon 3	4876	4267	601	87.5%	12.3%
#4	*KRAS* c.A>C/p.Gly12Val exon 2	3490	2344	1144	67%	33%

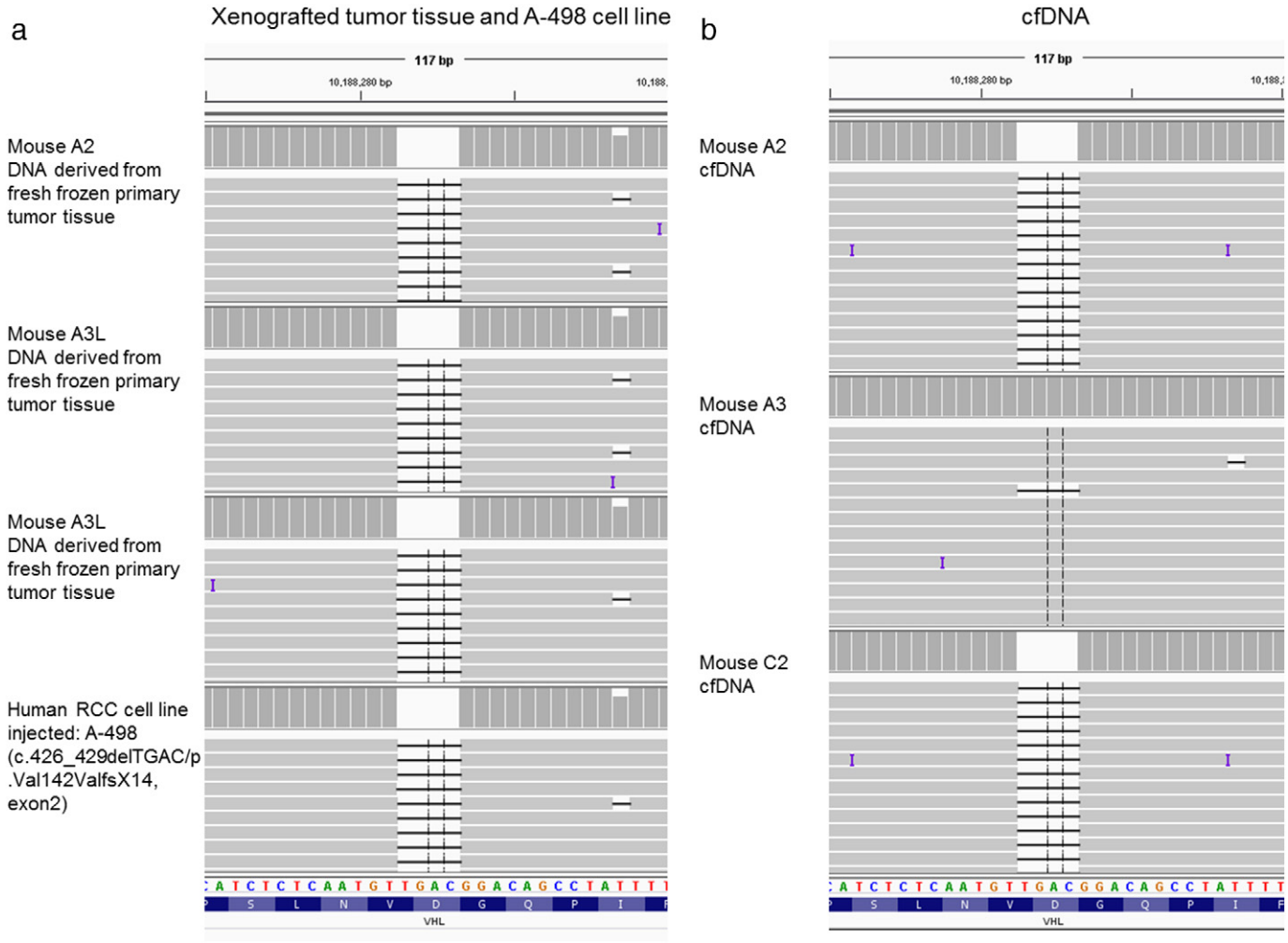

Fig. 2. Next generation sequencing of the xenografts. a) Output data for sequencing of DNA derived from xenografted tumor tissue and DNA derived directly from A-498 cell line. b) Output data for sequencing of cfDNA isolated from plasma of corresponding xenograft mice.

the SLR26 cell line (*VHL*c.389T>A/p.V130A), and T138 tissue (*VHL* c.388G>T/p.V130F) were included as negative controls whereas DNA derived from the patient's primary tumor was added as positive control.

We could successfully identify the mutation in 1.25 ng input DNA derived from the primary tumor tissue ($2^{-dct} = 0.3$; *p*-value: 0.0001; Fig. 3b) and the cfDNA (3.8×10^{-4}; *p*-value: 0.04). Moreover, we could discriminate between the specific mutation (c.388G>C:3.8×10^{-4}) and another mutation (c.389T>A: 2.3×10^{-6}; *p*-value: 0.004) in the adjacent nucleotide after normalization. Additionally, we could discriminate between the specific mutation (c.388G>C: 3.8×10^{-4}) and another mutation (c.388G>T: 8.4×10^{-5}; *p*-value: 0.009)at the same position but involving another nucleotide.

These results show the higher sensitivity of the mutation specific qPCR compared to our NGS approach, which is, however, only possible with prior knowledge of a specific mutation.

4. Discussion

In this study, we could not detect *VHL* mutations in plasma or serum samples derived from nine ccRCC patients using next-generation sequencing, whereas we identified four specific *KRAS* mutations in cfDNA derived from four colon cancer patients. Importantly, we confirmed that renal cancer is capable to shed ctDNA into the blood circulation by detection of specific *VHL* mutations in cfDNA derived from RCC

Table 3
Circulating tumor DNA detection in xenografted mice.

ID	Mutation detected	Total reads	Reads for the wt	Reads for the variant	% wt	% variant
Tumor tissue						
A-498 cell pellet	c.426_429delTGCA p.Val142fsX14 exon 2	2593	22	2571	0.85%	99.25%
A2	c.426_429delTGCA p.Val142fsX14 exon 2	2808	36	2772	1.28%	98.72%
A3L	c.426_429delTGCA p.Val142fsX14 exon 2	1624	30	1594	1.84%	98.16%
A3R	c.426_429delTGCA p.Val142fsX14 exon 2	1547	8	1539	0.51%	99.49%
cfDNA						
C2	/	1839	1839	/	100%	/
A2	c.426_429delTGCA p.Val142fsX14 exon 2	97	/	97	/	100%
A3	c.426_429delTGCA p.Val142fsX14 exon 2	9600	9266	334	96.5%	3.5%

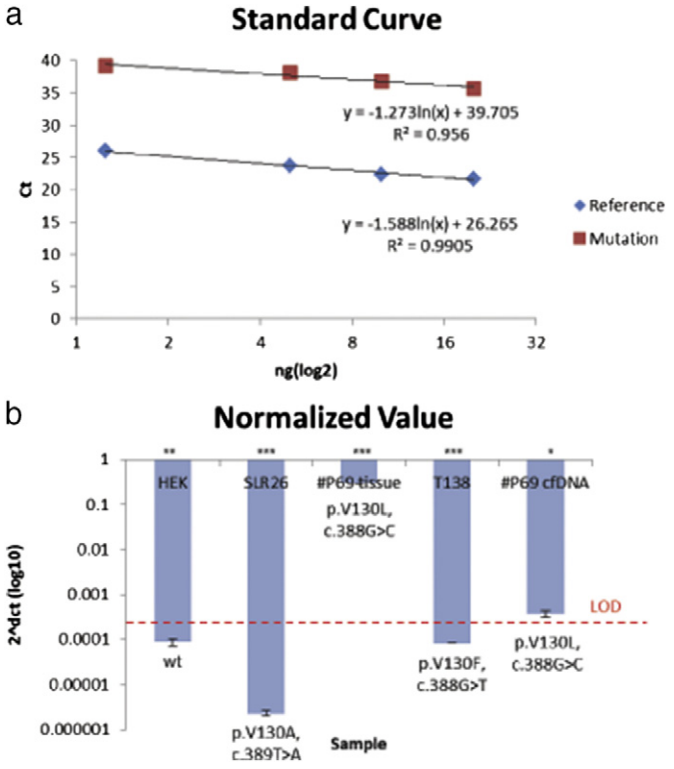

Fig. 3. Mutation specific qPCR. a) The HEK293 cell line (wt at location c.388G) was used as negative control in order to determine the sensitivity and specificity of the assay. Different concentrations of DNA (1.25 ng, 5 ng, 10 ng, 20 ng) were tested. The ct values ranged from 38.5–35.7 for the mutation specific assay and from 26.0–21.7 for the wt assay with $R^2 = 0.95$ and $R^2 = 0.99$, respectively. b) Normalized values for all the five samples in 1.25 ng input DNA are reported in the figure which shows the detection of the mutation of interest in the DNA derived from tumor tissue in #P69. The limit of detection (LOD) calculated in Fig. 3a for 1.25 ng input DNA is highlighted in red.

xenografts. We successfully identified such a specific *VHL* mutation in the plasma sample of one ccRCC patient using a highly sensitive Taqman mutation detection assay.

The physiological role of kidneys and the high vascularization of ccRCC suggest a high likelihood to release ctDNA from the cancer cells into the blood circulation. However, Bettegowda and co-workers (Bettegowda et al., 2014) have shown that renal cancer represents one of the tumor types with the lowest ctDNA shedding. ctDNA was found in only two out of five patients (40%). In their study, cfDNA was extracted from 5 ml of plasma derived from five metastatic RCC patients. In three out of five cases (60%), *VHL* mutations were present in prior analyzed tumor tissue. Only one *VHL* mutation was detected subsequently in cfDNA using a highly sensitive PCR-ligation approach (Bettegowda et al., 2014). In our analysis, no mutation in ctDNA derived from nine ccRCC patients was detected by NGS.

Several other studies have tried to correlate the presence and the amount of cfDNA to tumor stage and grade in renal cancer with discordant results (de Martino et al., 2012; Feng et al., 2013; Perego et al., 2008; Jung et al., 2010). However, none of them investigated the presence of *VHL* mutations in cfDNA. In these studies, cfDNA values were determined using housekeeping genes in qRT-PCR. RCC patients showed significantly higher cfDNA concentrations compared to healthy donors. Feng and co-workers analyzed 18 metastatic ccRCC patients showing that plasma cfDNA levels were significantly decreased upon sorafenib treatment and these levels positively correlate with TNM stage and Fuhrman grade (5). Further, cfDNA concentrations after eight to 24 weeks of treatment were able to predict remission, stable disease or progression (5). On the contrary, de Martino et al. and Perego et al. did not find any significant association between these parameters after having analyzed serum and plasma samples derived from 112 and 39 ccRCC patients, respectively (4,6). These groups also observed decreased cfDNA levels after nephrectomy (4,6). In our study, cfDNA levels were determined using a fluorometric assay (Qubit) and no correlation was found between cfDNA levels and tumor stage, presence of metastases and necrosis.

In contrast to RCC, ctDNA is readily detectable in colon cancer patients. ctDNA was found in >50% of the cases (Diehl et al., 2008; Schwarzenbach et al., 2008; Bettegowda et al., 2014; Frattini et al., 2006; Diehl et al., 2005), suggesting that the release of DNA into blood is common among colon cancer patients. The concept of liquid biopsies is therefore a very promising clinical tool for patients with colorectal cancer. Our findings are in line with these results, as we also detected *KRAS* mutations in three out of four patients (75%). Importantly, *KRAS* mutations in colon cancer were reported by our NGS analysis workflow without knowing the mutation status i.e., to be present in the primary tumor. Thus, our workflow allows the identification of unknown mutations presenting 'de novo'. This could be especially important after targeted therapy, because this approach is not restricted to monitor known mutations from primary tumor tissues.

In order to investigate the capability of RCC tumors to release ctDNA in the blood, the RCC cell line A-498 was subcutaneously injected into SCID mice. The analysis of the ctDNA release in vivo confirmed the possibility to detect specific RCC mutations in heterotopic xenografts. These results confirmed that RCC cells are able to release ctDNA into tumor microenvironment and blood circulation. Interestingly, a specific *VHL* mutation was found in the ctDNA of one RCC patient by mutation specific PCR (qPCR), indicating that this method has higher sensitivity than NGS. The patient with this *VHL* mutation had low tumor stage and no tumor necrosis, suggesting that qPCR could be applied also in patients with low tumor burden. Unfortunately, mutation-specific PCR does not allow a broad mutation screening since each PCR has to be designed for a specific location and nucleotide change. The same is true when applying BEAMing or ddPCR technologies which are methods that have even higher detection sensitivities. The detection limit of these techniques lies below 1% allele count (Kukita et al., 2013; Diehl et al., 2005; Kinde et al., 2011). Bettegowda and co-workers used plasma volumes five times greater than in our approach in combination with a highly sensitive detection method, which requires a known mutation status of the patient's tumor tissue (PCR-ligation). This underscores the limitations of liquid biopsies in clinical settings for renal cancer patients because this approach is limited to patients with known mutation status from primary tumor tissue.

It is tempting to speculate that ccRCC might have lower tumor shedding in general compared to other tumor types i.e., colon cancer. One could argue that specific mutations were detected in the RCC xenografts because ctDNA was isolated after collection of blood samples by complete bleeding of the animal. Further, RCC tumor cells were growing subcutaneously at the injection side which is not the physiological location of this tumor type. In addition, ctDNA is usually subjected to a high clearance and the half-life of ctDNA has been shown to be from few minutes to some hours (Fleischhacker and Schmidt, 2007). This could be even more pronounced in renal cancers where ctDNA might be easily excreted into the urine without entering the blood circulation. In summary, highly sensitive detection methods and prior knowledge of the mutation are required for liquid biopsies in renal cancer, limiting their applicability in the clinics.

Supplementary data to this article can be found online at http://dx.doi.org/10.1016/j.yexmp.2017.02.009.

Conflict of interest statement

The authors declare no conflicts of interest regarding this manuscript.

Acknowledgments

The authors thank Peter Schraml (PhD), director of tissue biobank at the Institute of Surgical Pathology, University Hospital Zurich; and Alexandra Veloudios (Department of Urology, University Hospital Zurich) for her support in collecting blood samples from RCC patients. This study was supported by the Swiss National Cancer Foundation to H.M. (3238BO-10314).

References

Baldewijns, M.M., van Vlodrop, I.J., Schouten, L.J., Soetekouw, P.M., de Bruine, A.P., van Engeland, M., 2008. Genetics and epigenetics of renal cell cancer. Biochim. Biophys. Acta 1785 (2):133–155. http://dx.doi.org/10.1016/j.bbcan.2007.12.002 (PubMed PMID: 18187049).

Beroukhim, R., Brunet, J.P., Di Napoli, A., Mertz, K.D., Seeley, A., Pires, M.M., et al., 2009. Patterns of gene expression and copy-number alterations in von Hippel-Lindau disease-associated and sporadic clear cell carcinoma of the kidney. Cancer Res. 69 (11):4674–4681. http://dx.doi.org/10.1158/0008-5472.CAN-09-0146 (PubMed PMID: 19470766; PubMed Central PMCID: PMC2745239).

Bettegowda, C., Sausen, M., Leary, R.J., Kinde, I., Wang, Y., Agrawal, N., et al., 2014. Detection of circulating tumor DNA in early- and late-stage human malignancies. Sci. Transl. Med. 6 (224), 224ra24 Epub 2014/02/21. 10.1126/scitranslmed.3007094 (6/224/224ra24 [pii]. PubMed PMID: 24553385).

Brugarolas, J., 2014. Molecular genetics of clear-cell renal cell carcinoma. J. Clin. Oncol. 32 (18):1968–1976. http://dx.doi.org/10.1200/JCO.2012.45.2003 (PubMed PMID: 24821879; PubMed Central PMCID: PMC4050206).

de Martino, M., Klatte, T., Haitel, A., Marberger, M., 2012. Serum cell-free DNA in renal cell carcinoma: a diagnostic and prognostic marker. Cancer 118 (1):82–90. http://dx.doi.org/10.1002/cncr.26254 (PubMed PMID: 21713763).

Diehl, F., Li, M., Dressman, D., He, Y., Shen, D., Szabo, S., et al., 2005. Detection and quantification of mutations in the plasma of patients with colorectal tumors. Proc. Natl. Acad. Sci. U. S. A. 102 (45):16368–16373. http://dx.doi.org/10.1073/pnas.0507904102 (PubMed PMID: 16258065; PubMed Central PMCID: PMC1283450).

Diehl, F., Schmidt, K., Choti, M.A., Romans, K., Goodman, S., Li, M., et al., 2008. Circulating mutant DNA to assess tumor dynamics. Nat. Med. 14 (9):985–990. http://dx.doi.org/10.1038/nm.1789 (PubMed PMID: 18670422; PubMed Central PMCID: PMC2820391).

Esposito, A., Bardelli, A., Criscitiello, C., Colombo, N., Gelao, L., Fumagalli, L., et al., 2014. Monitoring tumor-derived cell-free DNA in patients with solid tumors: clinical perspectives and research opportunities. Cancer Treat. Rev. 40 (5):648–655. http://dx.doi.org/10.1016/j.ctrv.2013.10.003 (PubMed PMID: 24184333).

Feng, G., Ye, X., Fang, F., Pu, C., Huang, H., Li, G., 2013. Quantification of plasma cell-free DNA in predicting therapeutic efficacy of sorafenib on metastatic clear cell renal cell carcinoma. Dis. Markers 34 (2):105–111. http://dx.doi.org/10.3233/DMA-120950 (PubMed PMID: 23324577; PubMed Central PMCID: PMC3810240).

Fleischhacker, M., Schmidt, B., 2007. Circulating nucleic acids (CNAs) and cancer—a survey. Biochim. Biophys. Acta 1775 (1):181–232. http://dx.doi.org/10.1016/j.bbcan.2006.10.001 (PubMed PMID: 17137717).

Forshew, T., Murtaza, M., Parkinson, C., Gale, D., Tsui, D.W., Kaper, F., et al., 2012. Noninvasive identification and monitoring of cancer mutations by targeted deep sequencing of plasma DNA. Sci. Transl. Med. 4 (136), 136ra68. http://dx.doi.org/10.1126/scitranslmed.3003726 (PubMed PMID: 22649089).

Frattini, M., Gallino, G., Signoroni, S., Balestra, D., Battaglia, L., Sozzi, G., et al., 2006. Quantitative analysis of plasma DNA in colorectal cancer patients: a novel prognostic tool. Ann. N. Y. Acad. Sci. 1075:185–190. http://dx.doi.org/10.1196/annals.1368.025 (PubMed PMID: 17108210).

Gnarra, J.R., Tory, K., Weng, Y., Schmidt, L., Wei, M.H., Li, H., et al., 1994. Mutations of the VHL tumour suppressor gene in renal carcinoma. Nat. Genet. 7 (1):85–90. http://dx.doi.org/10.1038/ng0594-85 (PubMed PMID: 7915601).

Hashad, D., Sorour, A., Ghazal, A., Talaat, I., 2012. Free circulating tumor DNA as a diagnostic marker for breast cancer. J. Clin. Lab. Anal. 26 (6):467–472. http://dx.doi.org/10.1002/jcla.21548 (PubMed PMID: 23143630).

Jung, K., Fleischhacker, M., Rabien, A., 2010. Cell-free DNA in the blood as a solid tumor biomarker—a critical appraisal of the literature. Clin. Chim. Acta 411 (21–22):1611–1624. http://dx.doi.org/10.1016/j.cca.2010.07.032 (PubMed PMID: 20688053).

Kinde, I., Wu, J., Papadopoulos, N., Kinzler, K.W., Vogelstein, B., 2011. Detection and quantification of rare mutations with massively parallel sequencing. Proc. Natl. Acad. Sci. U. S. A. 108 (23):9530–9535. http://dx.doi.org/10.1073/pnas.1105422108 (PubMed PMID: 21586637; PubMed Central PMCID: PMC3111315).

Kukita, Y., Uchida, J., Oba, S., Nishino, K., Kumagai, T., Taniguchi, K., et al., 2013. Quantitative identification of mutant alleles derived from lung cancer in plasma cell-free DNA via anomaly detection using deep sequencing data. PLoS One 8 (11), e81468. http://dx.doi.org/10.1371/journal.pone.0081468 (PubMed PMID: 24278442; PubMed Central PMCID: PMC3836767).

Latif, F., Tory, K., Gnarra, J., Yao, M., Duh, F.M., Orcutt, M.L., et al., 1993. Identification of the von Hippel-Lindau disease tumor suppressor gene. Science 260 (5112), 1317–1320 (PubMed PMID: 8493574).

Mandel, P., Metais, P., 1948. C. R. Seances Soc. Biol. Fil. 142 (3–4), 241–243 (PubMed PMID: 18875018).

Moch, H., Gasser, T., Amin, M.B., Torhorst, J., Sauter, G., Mihatsch, M.J., 2000. Prognostic utility of the recently recommended histologic classification and revised TNM staging system of renal cell carcinoma: a Swiss experience with 588 tumors. Cancer 89 (3), 604–614 (PubMed PMID: 10931460).

Moch, H., Humphrey, P.A., Ulbright, T.M., Reuter, V.E., 2016. WHO Classification of Tumors of the Urinary System and Male Genital Organs. 8(8) p. 400.

Nickerson, M.L., Jaeger, E., Shi, Y., Durocher, J.A., Mahurkar, S., Zaridze, D., et al., 2008. Improved identification of von Hippel-Lindau gene alterations in clear cell renal tumors. Clin. Cancer Res. 14 (15):4726–4734. http://dx.doi.org/10.1158/1078-0432.CCR-07-4921 (PubMed PMID: 18676741; PubMed Central PMCID: PMC2629664).

Perego, R.A., Corizzato, M., Brambilla, P., Ferrero, S., Bianchi, C., Fasoli, E., et al., 2008. Concentration and microsatellite status of plasma DNA for monitoring patients with renal carcinoma. Eur. J. Cancer 44 (7):1039–1047. http://dx.doi.org/10.1016/j.ejca.2008.03.008 (PubMed PMID: 18397824).

Rechsteiner, M.P., von Teichman, A., Nowicka, A., Sulser, T., Schraml, P., Moch, H., 2011. VHL gene mutations and their effects on hypoxia inducible factor HIFalpha: identification of potential driver and passenger mutations. Cancer Res. 71 (16):5500–5511. http://dx.doi.org/10.1158/0008-5472.CAN-11-0757 (PubMed PMID: 21715564).

Rechsteiner, M., von Teichman, A., Ruschoff, J.H., Fankhauser, N., Pestalozzi, B., Schraml, P., et al., 2013. KRAS, BRAF, and TP53 deep sequencing for colorectal carcinoma patient diagnostics. J. Mol. Diagn. 15 (3):299–311. http://dx.doi.org/10.1016/j.jmoldx.2013.02.001 (PubMed PMID: 23531339).

Sato, Y., Yoshizato, T., Shiraishi, Y., Maekawa, S., Okuno, Y., Kamura, T., et al., 2013. Integrated molecular analysis of clear-cell renal cell carcinoma. Nat. Genet. 45 (8):860–867. http://dx.doi.org/10.1038/ng.2699 (PubMed PMID: 23797736).

Schwarzenbach, H., Stoehlmacher, J., Pantel, K., Goekkurt, E., 2008. Detection and monitoring of cell-free DNA in blood of patients with colorectal cancer. Ann. N. Y. Acad. Sci. 1137:190–196. http://dx.doi.org/10.1196/annals.1448.025 (PubMed PMID: 18837946).

Schwarzenbach, H., Hoon, D.S., Pantel, K., 2011. Cell-free nucleic acids as biomarkers in cancer patients. Nat. Rev. Cancer 11 (6):426–437. http://dx.doi.org/10.1038/nrc3066 (PubMed PMID: 21562580).

Siegel, R., DeSantis, C., Virgo, K., Stein, K., Mariotto, A., Smith, T., et al., 2012. Cancer treatment and survivorship statistics, 2012. CA Cancer J. Clin. 62 (4):220–241. http://dx.doi.org/10.3322/caac.21149 (PubMed PMID: 22700443).

Zhang, Q., Yang, H., 2012. The roles of VHL-dependent ubiquitination in signaling and cancer. Front. Oncol. 2:35. http://dx.doi.org/10.3389/fonc.2012.00035 (PubMed PMID: 22649785; PubMed Central PMCID: PMC3355907).

Supplementary table S1: ccRCC patient characteristics.

Patient	Tumor Grade	Tumor Stage	Presence of metastasis and tumor necrosis	Tumor Dimension (cm)	*VHL* Mutation Status
#68	4	pT3a	Yes necrosis	8.5	c.345insC/p.Leu116ProfsX15 exon 2
#69	3	pT1b	No	6.7	c.354C>T/p.wt c.388G>C/p.Val130Leu exon 2
#78	1	pT3a	No	6.0	wt
#84	3	pT2b	Yes necrosis	10.5	c.300_315del16/p.Leu101AlafsX26 exon 1
#115	4	pT3a	No	10.5	c.345C>G/p.His115Gln exon 2
#155	3	pT3a	No	9.5	c.578insA/p.Asp193LysfsX63 exon 3
#159	3	pT1b	No	0.55	c.488T>C/p.Leu163Pro exon 3
#163	3	pT3a, V1	No	8	wt
#172	4	pT3a	Yes	9.5	wt

Supplementary table S2: cfDNA isolation from serum and plasma samples derived from ccRCC patients.

Patient	Serum	[cfDNA] ng/µl	Total [cfDNA] ng
#68	1 ml	0.950	28.5
#69	1 ml	0.633	19.0
#78	1 ml	1.07	32.2
#84	1 ml	0.967	29.0
#115	1 ml	1.62	48.6
	Plasma EDTA		
#155	1 ml	0.310	9.3

#159	1 ml	0.420	12.6
#163	1 ml	0.482	14.5
#172	1 ml	0.394	11.8

Supplementary table S3: Sequencing metrics from the PGM platform in ccRCC patients.

Patient	Mapped Reads	On Target	Mean Depth	Uniformity
Primary Tumor Tissue				
#68	1,933,729	98.22%	8,465	94.08%
#69	1,612,613	92.98%	6,555	97.63%
#78	n.a.	n.a.	n.a.	n.a.
#84	64,119	90.77%	254.4	98.65%
#115	2,252,690	96.70%	10,895	99.73%
cfDNA				
#68	n.a.	n.a.	n.a.	n.a.
#69	2,270,554	83.89%	8,408	99.99%
#78	n.a.	n.a.	n.a.	n.a.
#84	2,709,445	84.51%	10,164	99.58%
#115	1,880,043	93.41%	7,880	99.41%
#155	n.a.	n.a.	n.a.	n.a.
#159	n.a.	n.a.	n.a.	n.a.
#163	n.a.	n.a.	n.a.	n.a.
#172	n.a.	n.a.	n.a.	n.a.

Supplementary table S4: Sequencing metrics from the PROTON platform in ccRCC patients.

Patient	Mapped Reads	On Target	Mean Depth	Uniformity
cfDNA				
#68	17,749,598	87.20%	847	71.00%
#69	69,658,394	84.10%	245,786	95.48%
#78	39,884,838	95.34%	2,252	87.79%
#84	n.a.	n.a.	n.a.	n.a.
#115	84,252,873	93.34%	334,688	96.44%
#155	5,806,973	94.69%	338	93.57%
#159	5,117,607	91.67%	277	91.39%
#163	32,682,145	93.00%	1,864	91.01%
#172	34,848,264	95.76%	2,091	91.47%

Supplementary table S5: cfDNA isolation from plasma samples derived from colon cancer patients.

Patient	Plasma EDTA	[cfDNA] ng/µl	Total [cfDNA] ng
#1	1 ml	0.410	12.3
#2	1 ml	0.656	19.7
#3	1 ml	0.887	26.6
#4	1 ml	2.9	87

Supplementary table S6: Sequencing metrics from the PGM platform in colon cancer patients.

Patient	Mapped Reads	On Target	Mean Depth	Uniformity
#1	1,325,090	85.67%	4,983	99.90%
#2	743,225	92.94%	3,067	99.99%
#3	912,307	89.64%	3,700	99.79%
#4	1,748,642	79.75%	6,079	99.05%

Supplementary table S7: cfDNA isolation from plasma samples derived from heterotopic xenografts.

ID	Tumor Volume	Blood Volume	Plasma EDTA	[cfDNA] ng/µl	Total [cfDNA] ng
C2	No tumor	700 µl	280 µl	0.266	8.00
A2	1 cm^3	800 µl	400 µl	0.402	12.1
A3	L: 1 cm^3 R: 0.5 cm^3	800 µl	350 µl	0.352	10.6

Supplementary table S8: Sequencing metrics from the PGM platform in RCC xenografts.

ID	Mapped Reads	On Target	Mean Depth	Uniformity
Tumor Tissue				
A-498 cell pellet	668,443	97.43%	3,001	97.14%
A2	771,817	97.43%	3,435	97.36%
A3L	494,383	97.52%	2,193	98.74%
A3R	464,635	97.60%	2,074	97.56%
cfDNA				
C2	374,999	48.44%	151.2	9.48%
A2	103,009	53.52%	663.8	27.9%
A3	950,057	69.08%	2,365	50.3%

Supplementary table S9: Sanger sequencing primer characteristics.

Exon	1	2	3
Primer forward	5′-cgagcgcgcgcgaagactac-3′	5′-accggtgtggctctttaaca-3′	5′-gagaccctagtctgtcactgag-3′
Primer Reverse	5′-gaccgtgctatcgtccctgc-3′	5′-tcctgtacttaccacaacaacctt-3′	5′-tcatcagtaccatcaaaagctg-3′
Size	267bp	215bp	277bp

6.1.2 The dual function of exosomes in modulating cancer stem cell activities and improving the clinical applicability of liquid biopsies.

In our study, exosomes were isolated from seven RCC cultures under normoxia and hypoxia conditions (48 and 72 h) by differential ultracentrifugation. For hypoxic treatment, cells were cultured at 0.2 % of oxygen in an INVIVO2 hypoxia workstation 300 (Ruskin Technology, Bridgend, UK). As expected, isolated exosomes ranged between 40 and 100 nm in size (Fig. 6.1.2A). Normal kidney epithelial HK2 cell line was used as a control to compare tumor-derived RCC cultures with. Whereas, Burkitt's lymphoma cell line Raji was used as internal positive control as it was previously shown secreting high levels of exosomes (255).

Enhanced exosome secretion was observed under hypoxia condition in A498, 786O, 769P, ACHN, RCC4, Raji, SLR21 and SLR23 cell lines (Fig. 6.1.2B), indicating that environmental stress induces exosome release by cancer cells to communicate with neighboring cells. As proof of principle, protein expression of HIFs and HIF-target genes was evaluated in Raji cell line by Western blot. High expression of HIF1α was observed upon hypoxia induction at 48 and 72h (Fig. 6.1.2C). At the same time, enhanced levels of CAIX and Glut1 were also observed (Fig. 6.1.2C). Considering that, exosomes contain functional nucleic acids (mRNAs, microRNAs and DNA), proteins and lipids (200,203); the exosome content was determined by exosomal protein quantification using BCA protein assay and Qubit protein assay. Protein content ranged between 14.6 µg/ml and 45.2 µg/ml under normoxia, whereas under hypoxia between 22.2 µg/ml and 70.7 µg/ml. Subsequently, exo-DNA quantity and quality was determined using Bioanalyzer and the fluorimetric Qubit dsDNA high sensitivity assay. Exosomes contained DNA fragments of about 300 bp in size, meaning no further processing (i.e. fragmentation) should be generated prior NGS (Fig. 6.1.2D). Moreover, no sign of DNA degradation or contamination by other nucleic acids was observed upon DNA extraction (Fig. 6.1.2D). In order to isolate exoDNA, the exosome suspension was treated with DNAse1 which digests cfDNA or DNA bound to the cell membrane. Afterwards, DNAse1 activity has been inactivated by adding EDTA and heating up to 70 °C for 10 minutes. Exosome membranes were digested by proteinase K and exoDNA extracted using the QIAamp

Circulating free DNA Kit. The DNA content in the exosomes ranged between 0.4 ng/µl and 0.5ng/µl (Fig. 6.1.2E), indicating it can be used for NGS analysis of the genomic content.

As a next step, exoDNA will be exploited as a potential diagnostic and prognostic biomarker in the liquid biopsy setting next to the cfDNA, and as a tool to investigate tumor heterogeneity and RCC pathogenesis by genomic, transcriptomic, and proteomic analysis of the exosome content derived from *in vitro* cultures of RCC tumor cells (cell lines and primary cultures), and CSC subpopulations, as well as, *in vivo* tumor xenografts during tumor progression and upon therapeutic intervention. Ultimately, the information retained by the *in vitro* and *in vivo* tumor modelling will reflect and correlate to the clinicopathological features of the ccRCC patients.

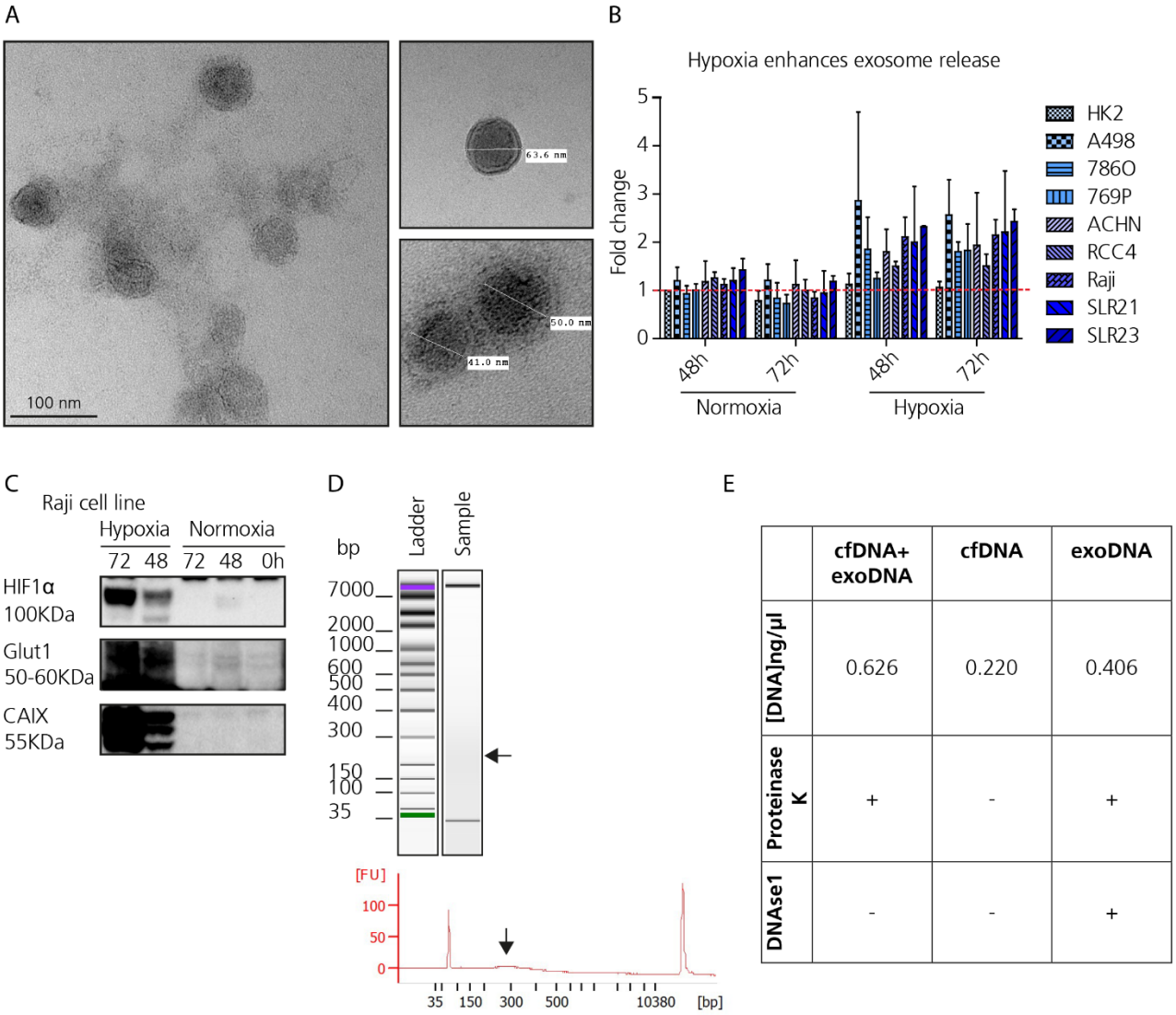

	cfDNA+ exoDNA	cfDNA	exoDNA
[DNA]ng/µl	0.626	0.220	0.406
Proteinase K	+	-	+
DNAse1	-	-	+

Figure 6.1.2 A) Representative transmission electron microscopy (TEM) showing exosomes isolated from RCC cultures. The exosome size ranged between 40 and 100 nm. **B)** Hypoxia induces exosome release in all the cell line analyzed except for the normal kidney epithelial cell line HK2. An increased in the exosome content up to three fold was observed. No further enhancement in the exosome secretion was observed over 48h hypoxia incubation. **C)** As expected, western blot analysis of HIF1α and HIF-target genes CAIX and Glut1, revealed increased expression levels upon hypoxia incubation at 48h and 72h. **D)** exoDNA was successfully extracted from the exosomes without degradation or contamination by other nucleic acids as shown by the elecropherogram. ExoDNA exhibited a molecular size of around 300 bp (gel-like image), meaning no further processing (i.e. fragmentation) should be generated prior NGS.

6.2 Dissecting tumor heterogeneity and personalized medicine using primary cultures.

6.2.1 Cancer tissue biobanking at the next level: Establishing patient-derived renal cancer cell cultures as a resource for research and precision medicine

Author contributions

H.M. and **P.S.** together with **H.A.B.** and **C.C.** conceived the original idea. **H.A.B.** and **C.C.** developed necessary methodology, generated 2D and 3D PDC models and designed and performed experiments on them. They were responsible for all data acquisition, analysis and interpretation. **H.A.B.** wrote the manuscript and **C.C.** assisted in drafting and editing of the manuscript. **A.v.T.** collected and processed tumor specimens, established culture protocols and performed Sanger sequencing. **C.P.** reviewed cytopathological smears and cases used for the T/CMA and supported the generation of tumor organoids and drug screening. **F.C.** generated 3D cancer microtissues with the hanging drop technology and performed drug testing on them. **N.C.T.** analyzed the NGS data. **S.D.** and **F.P.** provided administrative support and generated the T/CMA. **W.M.** and **M.R.** provided critical support during experimental design. **H.M.** reviewed all renal tumor specimens and neoplasms. Finally, **H.M.** and **P.S.** established the tissue biobank, provided conceptual support, assisted in the manuscript writing and supervised the study. All authors discussed the results and commented on the manuscript.

Cancer tissue biobanking at the next level: Patient-derived renal cancer cell models as a resource for research and precision medicine

Hella A. Bolck[1†], Claudia Corrò[1†], Adriana von Teichman[1], Chantal Pauli[1], Francesca Chiovaro[2], Nora C. Toussaint[3], Susanne Dettwiler[1], Fabiola Prutek[1], Wolfgang Moritz[2], Markus Rechsteiner[1], Holger Moch[1] and Peter Schraml[1*]

[1]Department of Pathology and Molecular Pathology, University Hospital Zurich, 8091 Zurich, Switzerland.

[2]InSphero AG, Schlieren, Switzerland.

[3]NEXUS Personalized Health Technologies, ETH Zurich, Zurich, Switzerland and SIB Swiss Institute of Bioinformatics, Zurich, Switzerland.

† These authors contributed equally to this work.

* To whom correspondence should be addressed: Dr. Peter Schraml Peter.Schraml@usz.ch;

One sentence summary:

Generation of patient-derived 2D and 3D renal cancer cell models as an integrative addition to routine tissue biobanking has the potential to provide more relevant tools for cancer research and ultimately advance precision medicine.

Abstract

Drug discovery screens and applied cancer studies often fail to translate into new cancer therapies because they rely on the use of immortalized cell lines that inadequately represent fundamental biological aspects of primary tumors. In order to provide more accurate renal cancer models for research and personalized medicine, we have extended routine tissue biobanking with patient-derived cancer cell cultures from tumor nephrectomies sent to pathology for diagnostic purposes. We generated 2D and 3D cell cultures from renal cell carcinoma (RCC) surgical specimens and employed targeted sequencing, fluorescence *in situ* hybridization (FISH), cytology and immunohistochemistry (IHC) profiling to validate resemblance of these cell models to their respective primary tumors. Analysis of the mutational landscapes of four RCC-derived monolayer cell cultures over several passages revealed that genetically distinct subclones of the primary tumor were retained in the corresponding cell culture but were subject to clonal selection. We further explored the benefits of RCC cell models by comparative drug screening across different cell models. To conclude our findings, we suggest a general workflow for living cell biobanking from cancer tissue. The integration of 2D and 3D cell models into a comprehensive tissue biobank platform has the potential to satisfy the growing need for more relevant cancer models. It will provide a resource for scientists aiming to generate *in vitro* cell models that more closely resemble human cancers and are therefore suitable tools to advance pre-clinical drug development and precision cancer treatment.

Introduction

Despite the significant progress made in understanding and treating cancer in the last decades, this disease is still one of the leading causes of mortality worldwide accounting for 8.8 million deaths in 2015 (WHO Cancer Fact Sheet February 2017). At this scale, cancer-associated mortality is not only a health-related issue but also has significant economic impact. Consequently, the identification of novel therapeutic strategies and predictive biomarkers is still one of the most crucial aspects of pre-clinical and translational cancer research. Recent advances in sequencing technologies and the increasing feasibility of genomic tumor profiling have triggered a substantial rise in the development of anti-cancer compounds targeting specific genomic alterations. Yet, the average number of new drugs approved for cancer therapy has declined at the same time (*1, 2*). A major reason for the failure to translate promising drug candidates from the bench to the bedside can certainly be attributed to the inadequate use of model systems for human cancer research. Particularly *in vitro* cancer drug discovery screens have largely relied on monolayer cultures of immortalized cell lines, which often fail to recapitulate fundamental biological features of human tumors (*3*). Establishing patient-derived cell (PDC) cultures is one of the most promising strategies to overcome many of the disadvantages of using transformed cell lines. PDC models are potentially more accurate in reflecting patient-specific molecular features and are amenable to a variety of experimental applications making them essential tools for translational studies. Recently, three-dimensional (3D) cell culture formats have gained attention in disease modelling (*4, 5*). They are considered superior in retaining cell-cell and cell-matrix interactions, which more closely mirrors the architecture of human tissues and impacts on cellular behavior and drug response (*6*). However, a better understanding about phenotypic and molecular features of different PDC models and to what extend these represent the original human tumor is required to determine their optimal applications.

As human PDC models will constitute important tools for predicting clinical treatment outcome and allow for individualized drug testing, they hold a particular promise for cancer patients with an unfavorable prognosis and a limited number of treatment options. Renal cell carcinoma (RCC) is a one of the cancer types that is associated with very high mortality and even novel treatment modalities using targeted therapy have failed to deliver a cure (*7, 8*). One reason for this shortcoming may stem from the fact that RCC is a diverse disease with significant pathophysiological and molecular heterogeneity (*9, 10*). The most frequent histologic subtype of RCC is the clear cell variant, accounting for about 70 - 80 % of adult RCCs (*11, 12*). Clear cell RCC (ccRCC) is characterized by the biallelic loss of the von Hippel Lindau (*VHL*) gene (*13*). To date, pre-clinical studies and screening programs of potential anti-cancer drugs have usually employed immortalized ccRCC cell lines, which represent inadequate platforms for drug discovery (*3, 14, 15*). Therefore, ccRCC patients may particularly benefit from the development of biologically relevant *in vitro* tumor models for the assessment of therapeutic alternatives.

Here we describe the development of a comprehensive biobanking platform that has evolved from our extensive routine sample collection of biospecimens from human tumors. We outline a protocol for processing human surgical specimens and explore the feasibility of growing patient-derived 2D and 3D tumor cell models generated as an integrative addition to human tissue biobanking and patient care. We illustrate how PDC models can be validated in terms of their resemblance to the primary tumor and how comprehensive tissue biobanking can be utilized as a tool to bridge the gap between successful pre-clinical studies and success in clinical trials. Moreover, we also highlight challenges and pitfalls that may hamper the implementation of patient-derived cancer cell models. Our findings will serve as a resource for scientists aiming to overcome many of the disadvantages of using transformed cell lines for cancer research thus significantly advancing pre-clinical disease modelling and early stage drug development.

Results

Generation of a living biobank of PDC cultures from RCC

The macroscopic and microscopic examination of surgical specimens and biopsies is the core of the diagnostic workflow carried out by pathologists. Tissue specimens are routinely archived as FFPE blocks, the gold standard material for histological and immunohistochemistry analysis (*16-18*). With the advent of molecular pathology, we have established a complementing collection of fresh frozen cancer and adjacent normal tissue, which is a valuable asset for the use of –omics technologies (e.g. genomics, transcriptomics, epigenomics, metabolomics and proteomics) on human tissues. Recently, we have further extended our tumor tissue biobanking strategy by establishing primary cell cultures derived from surgical specimens of malignant human tumors (Figure 1). Such PDC models are amenable to a wide variety of molecular biology assays including high-throughput -omics and drug screens as well as the generation of PDX- and immune-oncology models. Even though our cell culture biobank receives a wide variety of tumors, our initial study focused on RCC. Surplus fresh RCC tumor tissue from human surgical specimens was sent to the cell culture biobank subsequent to pathological review. Frequently, the majority of the resected tissue was required for diagnostic procedures, which have priority over biobanking and research (Figure 1). Only for a subset of the renal tumor cases, we were able to obtain enough tumor material that allowed for the generation of PDC cultures. Over a period of three years, we acquired 62 renal tumor samples. In 69.4 % (43/62 cases) we successfully established PDC cultures and expanded them to confluence for at least three passages. Upon entering the biobank workflow, primary tumor tissue was mechanically disaggregated and enzymatically digested with Collagenase A in order to obtain single cell suspensions (Suppl. Figure 1A). The size of tumor pieces we received ranged from approximately 0.5 - 8 cm^3 yielding 100 000 to several millions of single cells (Suppl. Figure 1B). Dissociated cells were plated into Collagen I-coated cell culture dishes and maintained in K1 medium supplemented with 0.5 % fetal calf serum and Epinephrine which sustained primary cell viability (*19, 20*). In some instances, single cell suspensions of tumor

cells were directly used for the formation of 3D PDC models or subjected to functional assays. Dissociated primary cancer cells were cryopreserved whenever enough material was available.

Validation of PDC monolayer cultures from RCC

From our initial cohort, we expanded 36 RCC PDC monolayer cultures to yield cell pellets suitable for formalin-fixation, paraffin-embedding (FFPE) and *in situ* analysis. We used these samples to construct a tissue and cell culture microarray (T/CMA), in which cylinders from surgical tumor samples were placed side-by-side to the corresponding cell cultures (Figure 2A and B). Using the T/CMA, we assessed whether PDC cultures resembled the corresponding patients' primary tumors. When evaluating haematoxylin and eosin (HE)-stained sections, we found that histological features were rarely retained during FFPE-processing of cultured cells (Figure 2B). We therefore performed immunohistochemical analyses using eight markers commonly used in RCC diagnostics (Table 1 and Suppl. Table 1). Pax8 (Paired box 8) is a transcription factor expressed only in epithelial cells of the adult kidney (glomerular parietal epithelial cells, renal collecting ductal cells, atrophic renal tubular epithelial cells) and in about 90 % of renal cell neoplasms (*21, 22*). Indeed, 94 % (33/35) of cell cultures we derived from renal tumors were positive for Pax8 thereby recapitulating the positive staining of the primary tumors (Table 1 and Suppl. Table 2). Pax8 was not expressed in the primary angiomyolipoma, but was present in the corresponding PDC culture indicating that incongruity existed in some cases. Regardless of the passage number, all RCC-derived cultures retained high expression of cytokeratins confirming their epithelial nature. Cytokeratin 7 (CK7), which has proven useful in the diagnosis of chromophobe and papillary RCCs (*23, 24*), displayed positivity in both the primary tumor and the corresponding PDC cultures in four out of five papillary RCC and in one chromophobe RCCs. In several PDC cultures, CK7 appeared to be upregulated while the corresponding primary tumor showed only little or no CK7 expression indicating that CK7 may be expressed during *in vitro* cell growth. Vimentin, a marker often observed in clear cell and papillary RCCs but rarely in chromophobe RCC and oncocytoma (*25*),

stained positive in 11 of the 25 primary ccRCC and all papillary RCC cases on the T/CMA. Interestingly, Vimentin was positive in all but one PDC cultures, independent of the expression in the primary tumor, suggesting differential regulation during cell culturing similarly to CK7. All primary ccRCCs, one clear cell papillary RCC and two of five papillary RCCs showed positive immunostaining for CD10, a protein strongly expressed in podocytes and proximal tubular cell brush borders of the healthy kidney as well as in clear cell and papillary RCCs (*25*). Positive CD10-staining was retained by 81 % (21/26) of the ccRCC- and clear cell papillary RCC-derived cell cultures. Interestingly, CD10 was slightly upregulated in all papillary RCC-derived cell cultures regardless of its expression status in the primary tumor. PDC cultures were further analyzed for the expression of Carboanhydrase 9 (CAIX), which is known to be expressed in the majority of ccRCCs and in a subset of papillary RCCs but not in normal renal cells (*26*). Of the 25 primary ccRCC and one clear cell papillary RCC samples displaying positive CAIX staining, 72 % of the corresponding cell cultures retained the immunophenotype (18/26). It is important to note that the two PDC cultures that did not retain Pax8 expression also failed to display matching CAIX staining when compared to the primary tumor. Only one primary papillary RCC showed expression of CAIX, which was not recapitulated by the corresponding cell culture. The RCC antibody generated against a crude microsomal fraction of proximal tubules from the normal human kidney (*27*) showed positive IHC staining in all but one ccRCCs and all papillary RCC but was negative in chromophobe RCCs and other neoplasms of the kidney. However, none of the PDC cultures displayed RCC positivity indicating that this marker was not suitable for cell culture validation. The c-kit proto-oncogene (CD117) was expressed in both primary chromophobe RCCs of the T/CMA as well as in the oncocytoma. None of the corresponding cell cultures retained CD117 expression casting doubt on the resemblance of the cultures to the primary tumors. Notably, for one patient of our cohort, papillary RCC type I with overexpression of c-Met was diagnosed as part of the clinical workflow. Our subsequent analysis confirmed that c-Met overexpression was preserved in

the corresponding cell culture (Suppl. Figure 2A) verifying the resemblance between primary tumor and the cell culture derived thereof.

Taken together, the analysis of Pax8, and Cytokeratin expression by IHC proved most useful in validating the renal epithelial origin of PDC cultures. CK7, Vimentin and in some instances even CD10 were found to be upregulated in the PDC culture regardless of their expression status in the primary tumor. Therefore, we found them of limited value for the validation of patient-derived cell cultures. In a number of cases, kidney cancer-specific markers such as CAIX or c-Met could confirm that the neoplastic phenotype of the tumor cells was retained during culturing. Our results suggest that IHC analysis can be a suitable tool to verify the origin of cell types, although frequently it did not provide sufficient information to distinguish renal cancer cells from normal epithelial kidney cells.

Genotypic validation of known driver mutations is a more reliable method to exclude that PDC cultures contain predominantly benign epithelial cells. The most frequent histologic subtype of RCC, the clear cell variant, is characterized by a biallelic loss of the von Hippel Lindau (VHL) gene, which can occur by mutation, deletion or promotor methylation (*13*). We screened the primary ccRCC tumor samples of our cohort by targeted sequencing and found that 19 of the 25 ccRCCs carried a mutation in *VHL* (exons 1-3) (Table 1). Targeted sequencing of *VHL* in the corresponding cell cultures revealed that 68 % of samples (13/19) harbored the same *VHL* mutations as the primary tumor at various passage numbers. The remaining six PDC cultures (Patients 10, 12, 14, 15, 19 and 20) displayed no *VHL* mutation within the detection limit of Sanger sequencing (10 % of mutated alleles in a heterogeneous population, (*28*)) thus revealing incongruity with the genotype of the primary tumor. Interestingly, both *VHL* mutations present in the clear cell papillary RCC primary tumor could be verified in the cell culture derived thereof. Somatic copy number alterations, particularly deletions affecting chromosome 3, are another hallmark of ccRCC that can be exploited for the comparison between primary tumors and corresponding cell cultures (*29, 30*).

In the six *VHL*-wildtype ccRCC cases (Patients 3, 4, 16, 18, 22 and 24), we analyzed cytogenetic abnormalities on chromosome 3 by FISH (Figure 2C and Suppl. Figure 2B). Our results revealed that in all six cases 60 – 80 % of the tumor cells displayed either loss of the entire chromosome 3 or deletion of the short arm of chromosome 3 (3p loss). These cytogenetic aberrations were recapitulated by each of the cell cultures derived from those tumors indicating their resemblance to the original tumors.

As a result, using *VHL* sequencing and FISH analysis of chromosome 3 in primary tumors and PDC cultures, we could verify that 77% (20/26) of clear cell and clear cell papillary RCC-derived cell cultures matched the primary tumor on the genetic level. Interestingly, our IHC results indicated that from the six PDC cultures for which the *VHL* mutation could not be confirmed, one also did not display Pax8 expression (Patient 12) and four did not retain CAIX and/or CD10 expression (Patients 12, 14, 15 and 19). This implies that these markers are the most useful for the validation of the neoplastic properties of ccRCC-derived cell cultures.

Characterization of mutation spectra during ccRCC-PDC culturing

For our subsequent analysis, we focused on three representative ccRCC-derived cultures and one that was generated from a ccRCC metastasis of the adrenal gland (Figure 3A). Cellular morphologies of the cultures established from fresh tumor tissue are depicted in Figure 3B. Importantly, *VHL* mutations of the primary tumors and the metastasis were retained in all cultures, as were the IHC profiles (Figure 3B and Suppl. Figure 3A, B, C and D). It is worth noting that unlike the other patient-derived cell cultures, cells obtained from the ccRCC metastasis (Patient A) have not undergone senescence to date and keep proliferating past passage 25.

To gain insights into genotypic changes associated with culturing of PDCs, we assessed the mutation spectra of primary ccRCCs and cell cultures by next generation sequencing (NGS). We successfully obtained tumor specific genomic profiles for the complete coding sequence of 409 cancer genes using the Ion Ampliseq Comprehensive Cancer Panel (CCP) for primary tumors as

well as from the PDC cultures at different passages for each of the four patients described. Genomic alterations were highly concordant between primary patient samples and the corresponding cell cultures (Suppl. Figure 3E). Notably, concordance was higher between samples originating from the same patient than between cell cultures derived from different patients excluding genetic adaptation due to culture techniques. Besides the *VHL* driver mutations identified by targeted Sanger sequencing, primary tumors and corresponding cell cultures exhibited non-silent somatic mutations in well-known ccRCC-associated genes like *PBRM1*, *SETD2* and *BAP1* (*13*). Additionally, we identified several mutations in the primary tumor that were not only retained but enriched during PDC serial passaging (Figure 3C). Genes we found to be mutated in that manner included *FLT3, ERBB3, ERCC2, PAX3, DST, KMT2D* and *SRC.* However, the overall diversity of mutations present in the primary ccRCCs and the ccRCC metastasis diminished during *in vitro* cell growth. A significant number of mutations observed in the primary tumor were not detected in the corresponding cell cultures or were only present in early passages. Loss of tumor-specific variants appeared lower when comparing patient-derived cell cultures to dissociated fresh primary tumor cells (patients B and C). When FFPE tissue of the original tumors was used as a reference (patients A and D), the apparent loss of variants observed during serial cell culture was higher. This was likely due to formalin-induced sequencing artefacts or sampling discrepancies (*31*). Genetic adaptation of the cell cultures seemed limited and often variants that appeared after passaging of patient-derived cells were categorized as “low confidence” during the analysis. We therefore concluded that subclones with distinct mutational profiles coexisted within the tumor and were subject to clonal selection during cell culture of the primary material.

Drug profiling in patient-derived 2D and 3D cancer models

Human PDC models can be utilized to predict clinical treatment outcomes by individualized drug testing. In ccRCC patients with low grade or localized disease, targeted therapy is administered only when the tumor relapses and metastasizes. To preserve PDCs until patients require drug

treatment, we stored them in liquid nitrogen. Importantly, none of the four patients described here (Figure 3A) have received systemic therapy and none of them have experienced a relapse yet. Nevertheless, we reactivated a subset of their samples for a proof-of-principle study. Cryopreserved dissociated and passaged cells were thawed and put into culture. Some samples failed to regrow due to reduced cell viability upon thawing illustrating the inherent risk associated with cryopreservation. We successfully regenerated PDC cultures from frozen cells for patient A and confirmed the *VHL* mutation. Consequently, we determined a cell doubling time of approximately four days (Suppl. Figure 4A). For cells derived from patient B, the culture we reconstituted from frozen dissociated or passaged cells did not recapitulate the *VHL* mutation of the original tumor and the cell culture established from fresh cells.

Three-dimensional cancer cell models are considered to more accurately mirror the complex spatial organization of tumor tissue *in vivo* (*6*). Here, we used cells cryopreserved after tissue dissociation or 2D growth to test their capacity of forming microtissues using the hanging drop technology (hereafter referred to as “microtissues”) (*32*). Dissociated primary as well as passaged frozen cells developed stable aggregates within three days under the condition that exogenous normal human dermal fibroblasts (nHDF) were supplied at a ratio of 1:20 (Figure 4A). Microtissues reached a final size of about 100-200 µm in diameter. Characterization by IHC revealed that expression of cytokeratins, Pax8 and CAIX was retained in the microtissues derived from patient A but only in a small subset of cells from patient B (Figure 4A). Likewise, we used cryopreserved dissociated primary and passaged cells to establish tumor organoids grown in matrigel (hereafter referred to as “organoids”) using a workflow that has been described previously (*33*). Overall, we noted that proliferation of ccRCC cells in matrigel was slow and required supplementing the cell culture medium with additional growth factors and epinephrine (refer to Material and Methods). Cells derived from the ccRCC of patient A formed only small organoids consisting of few cells (Figure 4B). Organoids generated from dissociated ccRCC cells from patient B developed readily but contained a mixture of morphologically distinct entities. Further characterization of cells from

organoids by cytology revealed the presence of multiple nuclei, large nucleoli and clear vacuoles all of which are suggestive of malignancy (Figure 4B). A detailed summary of benefits and limitations of the 2D and 3D cell models used in this study is given in table 2.

As cell models derived from cells of patient A best represented the primary tumor, we utilized these to examine drug responses to a panel of agents used to treat locally advanced and metastatic ccRCC (*34*). Overall, the correlation between drug sensitivity was high across different PDC models (Figure 4C). Three-dimensional PDC models showed a slightly higher sensitivity towards the targeted agents than the monolayer culture. Remarkably, 2D and 3D models derived from this particular patient responded only modestly to any of the therapeutics. Severe cytotoxicity was only induced by high doses of sunitinib, albeit in all PDC models. Treatment with high doses of everolimus caused significant cell death in microtissues and was reflected by changes in their morphology (Suppl. Figure 4 B). Similarly, treatment with high doses of sunitinib caused extensive disruption of microtissue morphology. A decrease of microtissue size was also detected after treatment with pazopanib and carbozantinib but failed to translate into a perceivable reduction of signal in the cell viability assay (Figure 4C).

Discussion

The increasing understanding of the remarkable complexity of human malignant tumors has triggered the emergence of a new paradigm for medical care in which treatment is tailored to patient-specific cancer subtypes. Part of this development has been the growing interest in using biospecimen collections and ultimately PDCs as model systems for translational research and drug profiling (*5, 33, 35*). In this article, we focused on renal cancers describing a platform enabling us to generate and incorporate patient-derived cancer cell models into a comprehensive tissue biobanking strategy as an integrative addition to patient care.

While primary tumor cells isolated from surgical RCC specimens represent the most relevant *in vitro* disease model, their direct use presents several challenges: With early detection and permanently optimized surgical interventions, the availability of such specimens becomes increasingly limited. Due to the priority of diagnostic procedures, relinquishing sufficient amounts of primary tissue for research purposes is restricted. The expansion of cells derived from primary RCC tissue by culturing techniques can circumvent this problem but requires stringent validation in order to ensure that the cultures are viable, retain important molecular features of the primary tumor and are not contaminated with non-tumor or stromal cells that can outcompete the cancer cells during growth (*36, 37*). Targeted sequencing of the *VHL* driver mutation and analysis of chromosome 3 by FISH enabled us to confirm the resemblance of 20 out of 26 patient-derived ccRCC and clear cell papillary RCC cell cultures to their respective primary tumors resulting in a validation success rate of 77 %. Since such characteristic molecular features are relatively rare or yet unknown in the remaining RCC subtypes, we evaluated the expression of a RCC-specific panel of IHC markers for all cases (*38*). We concluded that contamination of mesenchymal cells was not a primary concern but in accordance with previous reports, we observed that benign epithelial kidney cells could efficiently grow under cell culture conditions (*5, 37*). According to our results, IHC alone was often not reliable in confirming the malignant phenotype of the cultured cells.

One of the main advantages of PDC cultures may be its ability to more adequately represent the mixed heterogeneous cell populations of the primary tumor. In PDC cultures, non-silent, somatic variants were highly correlated with those found in the original tissue. The *VHL* driver mutations as well as subsets of mutations commonly found in ccRCC were not only maintained but also enriched during serial passaging of cell cultures. In contrast to data reported for xeno-transplantation of human tumor cells into immunodeficient mice, PDC *in vitro* cultures were hardly permissive for new variants to arise (*39*). Our findings therefore reflect the capacity of PDC cultures to capture a subset of sub-clonal populations. As our data also indicates that clonal selection is an ongoing process during *in vitro* cell growth, early passages should resemble the original tumor more closely in terms of genetic cellular heterogeneity. In order to preserve the original, most heterogeneous populations of tumor and associated cells, we cryopreserve dissociated tumor cells before culturing whenever possible. We perceive that PDC models will be utilized for various translational cancer studies in the context of personalized medicine. Since primary cell cultures usually become senescent after a few passages, both applications may require temporary storage of early-passage cells for later use (i.e. biobanking). However, cultures generated from frozen cells did not always display the VHL driver mutation of the primary tumor and the original cell culture making it essential to validate newly established cultures again.

Lastly, we sought to explore the utility of patient-derived ccRCC models for sensitivity testing against a number of clinically approved drugs. Two-dimensional cell culture models are sometimes considered too simplistic for such experiments because they fail to recapitulate important aspects of spatial interactions and structural organization of human tumors (*32, 33, 40, 41*). As drug responses may ultimately vary depending on the cell culture assay conditions, we additionally generated 3D microtissues and multicellular spheroid models from PDCs. Success rates for the generation of 2D and 3D cultures varied greatly with no one model being more effective for the majority of the cases. The efficacy of a panel of targeted drugs used to treat metastatic ccRCC was comparable across 2D and 3D RCC cell culture models. In contrast to a study carried out with

breast cancer cell models, we did not observe increased drug resistance in 3D models (*42*). Treatment with the targeted agents used in this study rather resulted in a slightly higher cytotoxicity in the 3D cell models compared to the monolayer cell culture. Taken together, patient-derived short-term 2D cell cultures represented the original ccRCC and allowed for *in vitro* screening at a reasonably large scale and moderate cost. Patient-derived 3D cell models were associated with considerably higher costs and their inherent complexity presented additional experimental challenges. Importantly, RCC microtissues and 2D cell cultures required only a few weeks while 3D organoid cultures needed approximately two to three months of propagation to produce drug-sensitivity data. Microtissues were unsuitable for expanding the limited amount of primary cell material whereas monolayer cell cultures and organoids could be cultured for several passages to facilitate biobanking of PDCs. Additional advantages and disadvantages of the cell culture models used in this study are summarized in table 2.

A biobank should potentially fulfill requirements for a variety of research questions of the biomedical community. Provided that sufficient primary tumor tissue is available, it is advisable to: (i) cryopreserve dissociated tumor cells, (ii) generate 2D and 3D models for propagation of limited primary cell material, (iii) preserve and store living passaged cells for later use, and (iv) implement stringent, tumor type specific validation criteria (Figure 5). This demonstrates that collecting a well-characterized cohort of representative PDC samples must be a collaborative effort and will require significant resources. In conclusion, our results indicate that RCC-derived cell models, validated and characterized in the context of diagnostic tissue collections, can be employed for drug profiling and might provide important information to direct ccRCC treatment decisions. Even though, more thorough analysis may be required before such cell models can be implemented in routine clinical procedures, PDC cultures represent a valuable resource for translational cancer studies and can provide key rationales for designing clinical trials in order to identify novel therapeutic options.

Materials and Methods

Ethics Statement

All tissue samples were made available by the Tissue Biobank of the Institute of Pathology and Molecular Pathology, University Hospital of Zurich, Switzerland. The local ethics commission approved this study (KEK-ZH-Nr. 2011-0072 and KEK-ZH-Nr. 2014-0614) and all patients gave written consent.

Specimen Procurement and tissue processing

Renal tumors and neoplasms were surgically resected and underwent routine tissue processing and rapid sectioning for diagnostic purposes and biobanking (including formalin fixation and paraffin embedding, snap freezing of fresh tumor and normal tissue). A pathologist with specialization in uropathology (H. Moch) reviewed all tissue specimens. Tumors were histologically classified and graded according to the WHO classification (*43*). If available, additional fresh tissue samples macroscopically identified as cancer from adjacent areas were placed into sterile 50-ml conical tubes containing transport media (RPMI (Gibco) with 10 % FCS (Gibco) and Antibiotic-Antimycotic® (Gibco)) and stored at 4 °C. Tissue samples were further processed within 24 hrs.

Tissue specimens were rinsed with PBS and finely cut into small fragments using a scalpel. Consequently, samples were enzymatically digested in a TBS/Collagenase A-mix containing a surplus of Ca^{2+} for 2-3 hrs at 37 °C. The slurry was passed through a 70 µm cell strainer to remove large fragments and centrifuged at 1000 rpm for 5 min. The Collagenase A digestion was stopped by incubating the pellet in 1 ml Stop solution (50 mM Tris, 150 mM NaCl, 10 mM EDTA) for 5 min at room temperature. Cells were washed once with PBS and erythrocytes were lysed by incubating the cells in ACK buffer (150 mM NH_4Cl, 10 mM $KHCO_3$, 100 mM EDTA) for 2 min. After a final wash with PBS, the viability of the dissociated cells was evaluated by trypan blue dye exclusion.

Appropriate amounts of cell suspension were resuspended in freezing medium (FCS containing 10 % DMSO) for long-term storage in liquid nitrogen.

Generation of monolayer primary cell cultures

Dissociated cells (fresh or frozen) were resuspended in K1n medium (Dulbecco's Modified Eagle Medium: Nutrient Mixture F-12 (DMEM:F12, Gibco) with 0.5 % FCS (Gibco), Antibiotic-Antimycotic® (Gibco), 2.5 μg/ml insulin (Sigma), 0.625 ng/ml Prostaglandin E_1 (PGE1, Cayman Chmical), 26 pM 3,3,5, Triiodthyronine (T3, Sigma), 2.5 μg/ml transferrin (TF, Sigma), 50 pM sodium selenite (SS, Sigma), 25 nM Hydrocortisone (HC, Sigma), 10 μg/ml EGF (Thermo Fisher) and 0.5 μg/ml epinephrine (Sigma)) and transferred into collagen I-coated cell culture dishes (Corning) for culture in a humidified incubator at 37 °C with 5% CO_2. The medium was replaced no earlier than 5 days after initial plating and subsequently every three to four days. Cells were expanded by passaging and aliquots were regularly frozen in liquid nitrogen for biobanking purposes.

Generation of 3D tumor organoids

Generation of tumor organoids was performed as described previously (*33*). In brief, an appropriate amount of dissociated cells was resuspended in a small volume of 3D media (Advanced Dulbecco's modified Eagle medium (Gibco) with 1X Glutamax (Gibco), B27 supplement (Gibco), Antibiotic-Antimycotic (Gibco), 1.25 mM N-Acetylcysteine (Sigma), 50 ng/mL Mouse Recombinant EGF (Thermo Fisher), 20 ng/mL Human Recombinant FGF-10 (Thermo Fisher), 1 ng/mL Recombinant Human FGF-basic (Thermo Fisher), 10 μM Rock inhibitor Y-27632 (Selleck Chemical Inc), 500 nM A-83-01 (Tocris Bioscience), 10 μM SB202190 (Selleck Chemical Inc), 10 mM Nicotinamide (Sigma), 1 μM PGE2 (Sigma), 2.5 μg/ml insulin (Sigma), 0.625 ng/ml Prostaglandin E_1 (PGE1, Cayman Chmical), 26 pM 3,3,5, Triiodthyronine (T3, Sigma), 2.5 μg/ml transferrin (TF, Sigma), 50 pM sodium selenite (SS, Sigma), 25 nM Hydrocortisone (HC, Sigma),

0.5 μg/ml epinephrine (Sigma), Noggin and RSpondin (conditioned media, self-made) and mixed with a 1:1 - 1:2 volume of growth factor reduced Matrigel (Corning). Drops of cell suspension/Matrigel were distributed in a cell culture plate and allowed to solidify for 30 min at 37°C, upon which 3D media was added to cover the drops. The media was replaced every five to seven days. Organoids at approximately 300 to 500 μm were passaged by incubation with TrypLE Express (Gibco) for up to 30 min in a water bath at 37°C. The trypsin was then inactivated by adding at least three volumes of DMEM containing 10 % FBS and the cells were pelleted by centrifugation at 1000 rpm for 5 min. Cell pellets were washed once with 3D media to remove residual FBS. Single cells and small cell clusters were re-plated according to the procedure described above.

Generation of 3D tumor microtissues

3D culture by microtissue formation was performed in hanging drop cultures using GravityPLUS™ plates (InSphero) as described previously (*32*). Cells were seeded at a density of 1000-2000 cells per drop and co-cultured with normal human dermal fibroblasts (nHDF) at a ratio of nHDF to primary tumor cells of 1:20. After successful spheroid formation, microtissues were transferred into GravityTrap™ ULA plates (InSphero) for further processing.

Histological and Immunohistochemistry (IHC) analysis

Formalin-fixed paraffin-embedded (FFPE) cell pellets from 2D cell cultures were prepared as previously described (*44*). FFPE cell pellets and corresponding FFPE primary RCC specimens were used to construct T/CMA according to the procedure described in (*17*). Microtissues were collected in 1.5 ml tubes and washed once with PBS. Consequently, they were fixed in 4 % para-formaldehyde for 1 hr at 4 °C. Fixed microtissues were collected in the tip of a 1.5 ml microtube, embedded in 2 % agarose (Amresco®, Solon) and covered with PBS. For paraffin-embedding, the agarose plugs were taken out of the microtubes and the tip containing the microtissues was

cut and placed in formalin for 12-14 hrs, followed by gradual dehydration. Finally, the plugs were embedded in paraffin (microtissues facing downwards) in order to facilitate sectioning. Cytological smears of 3D organoid cultures were prepared as previously described (*45*) and immediately wet-fixed in *Delaney* solution. The Papanicolaou (Pap) stain was performed for cytopathological evaluation. Sections (2 µm) were prepared from FFPE specimens and were stained with haematoxylin and eosin (HE) for histological evaluation. For IHC, sections (2 µm) were transferred to glass slides followed by antigen retrieval. Antibodies used for IHC are summarized in supplementary table 1. IHC was performed using the Ventana Benchmark automated system (Ventana Medical Systems, USA) and Ventana reagents. The Optiview DAB IHC detection kit was used to stain with the antibodies against CKpanB, CK7, Pax8, CD10, CD117, Vimentin, RCC and cMet. The staining procedure for CAIX was carried out with the automated Leica BOND system using the Bond Polymer Refine Detection Kit (Leica Biosystems) and HMB45 IHC was conducted using the UltraView AP detection kit.

VHL mutation analysis

Sanger sequencing was employed to assess the mutation status of the *VHL* gene for all ccRCC primary tumors and the corresponding monolayer cell cultures. A pathologist reviewed HE-stained sections of FFPE or fresh frozen tissue for tumor cell content and the tumor area was marked. DNA was isolated from FFPE punches (3 cylinders with a diameter of 0.6 mm), sections of fresh-frozen tissue (5 sections à 30 µm) or a minimum of 10000 cultured cells using the Maxwell® 16 DNA Purification Kits (Promega). PCR and sequencing of *VHL* was performed as previously described (*46*). For DNA extracted from fresh-frozen tissue and cultured cells, we amplified the complete Exon 1 by using the following alternative forward primer: 5’-CGAGCGCGCGCGAAGACTAC-3’.

Fluorescence In Situ Hybridization (FISH)

FISH analysis of chromosome 3p was carried out using the ZytoLight SPEC VHL/CEN 3 Dual-color Probe (ZytoVision). HE-stained slides were examined to identify areas containing tumor cells. Consecutive unstained sections (4 µm) of FFPE tissue and cell blocks were prepared and deparaffinized. FISH probes were denatured on the tissue slides at 75 °C for 10 min followed by hybridization at 37 °C for at least 20 hrs in a ThermoBrite hybridization oven (Abbott). Subsequently, slides were washed (2X SSC, 0.3% NP40) and nuclei were counterstained with DAPI. Slides were examined on a fluorescence microscope (Leica, 63X objective and appropriate filter sets) and images were acquired. Using ImageJ (*47*), a minimum of fifty non-overlapping nuclei from different areas were analyzed, and the number of VHL and CEN3 signals was recorded for each nucleus. The total number of VHL and CEN3 signals as well as the percentage of cells with less VHL than CEN3 signals (3p loss) and loss of chromosome 3 (monosomy) were calculated.

Next-Generation Sequencing (NGS)

DNA was extracted from the primary tumor, adjacent normal tissue and from cultured cells as described above. Barcoded libraries were generated from 40 ng of total genomic DNA per sample using the Ion AmpliSeq Comprehensive Cancer Panel (Life Technologies) and the Ion Ampliseq library kit 2.0 (Life Technologies) according to the manufacturer's instructions. Libraries were quantified by qPCR with the Ion Library Quantitation kit (Life Technologies) and amplicon distribution was analysed using the 2100 Bioanalyzer (Agilent). Subsequently, libraries were diluted to 12 pM, mixed and used for template preparation, loaded on a Proton chip and sequenced on the Proton platform (Ion Proton Sequencing 200 Kit v3 or Ion Pi Hi-Q Sequencing 200 Kit; Life Technologies) according to the manufacturer's instructions. Signal processing, base calling, alignment, and variant calling was carried out using the AmpliSeq CCP - Proton - w1.1 - Single Sample and AmpliSeq CCP w1.1 - Tumor-Normal pair workflows to identify germline and somatic

mutations in the Ion Reporter Software version 5.4 (Life Technologies). Sample concordance was determined based on a subset of Ion AmpliSeq CCP Hotspots (5.4), for which at least two different genotypes could be observed across all samples (46 diverse hotspot positions). A potential somatic variant was included in our analysis for the respective patient when the following criteria were met: (i) a minimum coverage depth of 50 reads in the normal sample, (ii) a minimum variant allele frequency of 10 % and a minimum of 10 reads supporting the variant in at least one of the non-normal samples of a patient. Non-synonymous coding variants passing these criteria were manually reviewed using the Integrative Genomics Viewer (IGV, Broad Institute, Boston, MA). For a small number of these variants, the Ion Reporter Software could not reliably determine the normal genotype, which could result in a false positive somatic variant call. We manually inspected the reported reference and alternate allele observations at these positions and found sufficient evidence to include the corresponding tumor-specific somatic calls for further analysis.

Analysis of cell proliferation

Cell proliferation was characterized in patient-derived monolayer cell cultures. Cells were plated in 100 µl K1n medium at a density of approximately 500 cells per well in collagen I-coated 96-well plates (Corning) and allowed to attach for 4 hrs. Subsequently, the baseline level of living cells (day 0) was determined by adding PrestoBlue® Cell Viability Reagent (Invitrogen) according to manufacturer's instructions. Fluorescence (535/590 nm) was recorded using a plate reader (Tecan infinite 200). Measurements were taken every 48 hrs for 14 days and normalized to the baseline value on day 0. Data normalization and analysis was performed using Graph Pad Prism 6 (GraphPad Software, Inc.).

Drug Profiling in PDC models

For 2D drug profiling, white clear-bottom 96-well plates (Corning) were coated with 0.01 % collagen (Sigma) prior to plating 1000 cells per well in K1n medium. For 3D organoid drug profiling,

1000 cells per well were plated in a 10 µl cell culture media- and Matrigel-mix (v/v 1:1) in white clear-bottom 96-well plates (Corning). Plates were incubated for 30 min at 37°C to solidify the cell–matrix mix; 80 µl of 3D media was added to each well. For drug profiling of the microtissues, 2000 cells were plated in the hanging drop plates and allowed to form microtissues for 72 hrs. Twenty-four hours after plating (2D and 3D organoid cultures) or upon formation of microtissues (72 hrs post cell seeding), drugs were administered in technical duplicates (3D cultures) or triplicates (2D cultures). Cell viability was measured either at 6 days (2D drug profiling), 9 days (hanging drop) or 14 days (3D matrigel) following drug treatment. A re-dosing of the drugs was undertaken on day 7 of the 3D assays. For all drug screens, viability assays were performed using CellTiter-Glo® Reagent (Promega). 2D assays were processed according to manufacturer's guidelines. In brief, a volume of CellTiter-Glo® Reagent equal to the volume of cell culture medium present in each well was added and the content was incubated on a shaker for 30 min to induce cell lysis. Luminescence was recorded using a plate reader (Tecan infinite 200) with 1 sec of integration time. For 3 D drug organoid assays, the media was replaced with 60 µL CellTiter-Glo® Reagent and plates were incubated for 90 min in a cell culture incubator (37 °C, 5 % CO_2) to ensure tumor organoid lysis. Luminescence was read as described above. To measure the cell viability of microtissues cultured in 96-well GravityTRAP™ ULA Plates, CellTiter-Glo® Reagent was added at a volume of 1:1 to the culture supernatant and the content was transferred into a white, opaque 96-well microplate (Corning). Complete lysis of the microtissues was ensured by incubating the plates on an orbital shaker for 20 min at room temperature before recording the luminescence intensity as described above. Analysis of drug sensitivity was performed Graph Pad Prism 6 (GraphPad Software, Inc.).

References:

1. M. Hay, D. W. Thomas, J. L. Craighead, C. Economides, J. Rosenthal, Clinical development success rates for investigational drugs. *Nat Biotech* **32**, 40-51 (2014).
2. D. M. Hyman, B. S. Taylor, J. Baselga, Implementing Genome-Driven Oncology. *Cell* **168**, 584-599 (2017).
3. P. Horvath, N. Aulner, M. Bickle, A. M. Davies, E. D. Nery, D. Ebner, M. C. Montoya, P. Ostling, V. Pietiainen, L. S. Price, S. L. Shorte, G. Turcatti, C. von Schantz, N. O. Carragher, Screening out irrelevant cell-based models of disease. *Nat Rev Drug Discov* **15**, 751-769 (2016).
4. H. Clevers, Modeling Development and Disease with Organoids. *Cell* **165**, 1586-1597 (2016).
5. M. van de Wetering, Hayley E. Francies, Joshua M. Francis, G. Bounova, F. Iorio, A. Pronk, W. van Houdt, J. van Gorp, A. Taylor-Weiner, L. Kester, A. McLaren-Douglas, J. Blokker, S. Jaksani, S. Bartfeld, R. Volckman, P. van Sluis, Vivian S. W. Li, S. Seepo, C. Sekhar Pedamallu, K. Cibulskis, Scott L. Carter, A. McKenna, Michael S. Lawrence, L. Lichtenstein, C. Stewart, J. Koster, R. Versteeg, A. van Oudenaarden, J. Saez-Rodriguez, Robert G. J. Vries, G. Getz, L. Wessels, Michael R. Stratton, U. McDermott, M. Meyerson, Mathew J. Garnett, H. Clevers, Prospective Derivation of a Living Organoid Biobank of Colorectal Cancer Patients. *Cell* **161**, 933-945.
6. O. I. Hoffmann, C. Ilmberger, S. Magosch, M. Joka, K. W. Jauch, B. Mayer, Impact of the spheroid model complexity on drug response. *Journal of biotechnology* **205**, 14-23 (2015).
7. R. Fisher, M. Gore, J. Larkin, Current and future systemic treatments for renal cell carcinoma. *Semin Cancer Biol* **23**, 38-45 (2013).
8. R. L. Siegel, K. D. Miller, A. Jemal, Cancer statistics, 2016. *CA: a cancer journal for clinicians* **66**, 7-30 (2016).
9. M. Gerlinger , A. J. Rowan , S. Horswell , J. Larkin , D. Endesfelder , E. Gronroos , P. Martinez , N. Matthews , A. Stewart , P. Tarpey , I. Varela , B. Phillimore , S. Begum , N. Q. McDonald , A. Butler , D. Jones , K. Raine , C. Latimer , C. R. Santos , M. Nohadani , A. C. Eklund , B. Spencer-Dene , G. Clark , L. Pickering , G. Stamp , M. Gore , Z. Szallasi , J. Downward , P. A. Futreal , C. Swanton Intratumor Heterogeneity and Branched Evolution Revealed by Multiregion Sequencing. *New England Journal of Medicine* **366**, 883-892 (2012).
10. J. I. Lopez, Intratumor heterogeneity in clear cell renal cell carcinoma: a review for the practicing pathologist. *APMIS : acta pathologica, microbiologica, et immunologica Scandinavica* **124**, 153-159 (2016).
11. H. Moch, T. Gasser, M. B. Amin, J. Torhorst, G. Sauter, M. J. Mihatsch, Prognostic utility of the recently recommended histologic classification and revised TNM staging system of renal cell carcinoma: a Swiss experience with 588 tumors. *Cancer* **89**, 604-614 (2000).
12. B. Shuch, A. Amin, A. J. Armstrong, J. N. Eble, V. Ficarra, A. Lopez-Beltran, G. Martignoni, B. I. Rini, A. Kutikov, Understanding Pathologic Variants of Renal Cell Carcinoma: Distilling Therapeutic Opportunities from Biologic Complexity. *European urology* **67**, 85-97 (2015).
13. Comprehensive molecular characterization of clear cell renal cell carcinoma. *Nature* **499**, 43-49 (2013).
14. R. Beroukhim, J. P. Brunet, A. Di Napoli, K. D. Mertz, A. Seeley, M. M. Pires, D. Linhart, R. A. Worrell, H. Moch, M. A. Rubin, W. R. Sellers, M. Meyerson, W. M. Linehan, W. G. Kaelin, Jr., S. Signoretti, Patterns of gene expression and copy-number alterations in von-hippel lindau disease-associated and sporadic clear cell carcinoma of the kidney. *Cancer Res* **69**, 4674-4681 (2009).
15. K. K. Brodaczewska, C. Szczylik, M. Fiedorowicz, C. Porta, A. M. Czarnecka, Choosing the right cell line for renal cell cancer research. *Molecular Cancer* **15**, 83 (2016).
16. L. Bubendorf, A. Nocito, H. Moch, G. Sauter, Tissue microarray (TMA) technology: miniaturized pathology archives for high-throughput in situ studies. *J Pathol* **195**, 72-79 (2001).
17. H. Moch, P. Schraml, L. Bubendorf, M. Mirlacher, J. Kononen, T. Gasser, M. J. Mihatsch, O. P. Kallioniemi, G. Sauter, High-Throughput Tissue Microarray Analysis to Evaluate Genes Uncovered by cDNA Microarray Screening in Renal Cell Carcinoma. *The American Journal of Pathology* **154**, 981-986 (1999).
18. P. Schraml, J. Kononen, L. Bubendorf, H. Moch, H. Bissig, A. Nocito, M. J. Mihatsch, O. P. Kallioniemi, G. Sauter, Tissue microarrays for gene amplification surveys in many different tumor types. *Clin Cancer Res* **5**, 1966-1975 (1999).

19. Y. Zhao, H. Zhao, Y. Zhang, T. Tsatralis, Q. Cao, Y. Wang, Y. Wang, Y. M. Wang, S. I. Alexander, D. C. Harris, G. Zheng, Isolation and epithelial co-culture of mouse renal peritubular endothelial cells. *BMC Cell Biology* **15**, 40 (2014).
20. M. Taub, B. U, L. Chuman, M. J. Rindler, M. H. Saier, Jr., G. Sato, Alterations in growth requirements of kidney epithelial cells in defined medium associated with malignant transformation. *Journal of supramolecular structure and cellular biochemistry* **15**, 63-72 (1981).
21. G. X. Tong, W. M. Yu, N. T. Beaubier, E. M. Weeden, D. Hamele-Bena, M. M. Mansukhani, K. M. O'Toole, Expression of PAX8 in normal and neoplastic renal tissues: an immunohistochemical study. *Modern pathology : an official journal of the United States and Canadian Academy of Pathology, Inc* **22**, 1218-1227 (2009).
22. A. Ozcan, S. S. Shen, C. Hamilton, K. Anjana, D. Coffey, B. Krishnan, L. D. Truong, PAX 8 expression in non-neoplastic tissues, primary tumors, and metastatic tumors: a comprehensive immunohistochemical study. *Modern pathology : an official journal of the United States and Canadian Academy of Pathology, Inc* **24**, 751-764 (2011).
23. M. E. Mathers, A. M. Pollock, C. Marsh, M. O'Donnell, Cytokeratin 7: a useful adjunct in the diagnosis of chromophobe renal cell carcinoma. *Histopathology* **40**, 563-567 (2002).
24. B. Delahunt, J. N. Eble, Papillary renal cell carcinoma: a clinicopathologic and immunohistochemical study of 105 tumors. *Modern pathology : an official journal of the United States and Canadian Academy of Pathology, Inc* **10**, 537-544 (1997).
25. L. D. Truong, S. S. Shen, Immunohistochemical diagnosis of renal neoplasms. *Archives of pathology & laboratory medicine* **135**, 92-109 (2011).
26. G. Li, M. Cuilleron, M. Cottier, A. Gentil-Perret, C. Lambert, C. Genin, J. Tostain, The use of MN/CA9 gene expression in identifying malignant solid renal tumors. *European urology* **49**, 401-405 (2006).
27. D. K. McGregor, K. K. Khurana, C. Cao, C. C. Tsao, G. Ayala, B. Krishnan, J. Y. Ro, J. Lechago, L. D. Truong, Diagnosing primary and metastatic renal cell carcinoma: the use of the monoclonal antibody 'Renal Cell Carcinoma Marker'. *The American journal of surgical pathology* **25**, 1485-1492 (2001).
28. C. Corro, T. Hejhal, C. Poyet, T. Sulser, T. Hermanns, T. Winder, G. Prager, P. J. Wild, I. Frew, H. Moch, M. Rechsteiner, Detecting circulating tumor DNA in renal cancer: An open challenge. *Exp Mol Pathol* **102**, 255-261 (2017).
29. J. Dagher, S.-F. Kammerer-Jacquet, A. Brunot, A. Pladys, J.-J. Patard, K. Bensalah, C. Perrin, G. Verhoest, J. Mosser, A. Lespagnol, C. Vigneau, F. Dugay, M.-A. Belaud-Rotureau, N. Rioux-Leclercq, Wild-type VHL Clear Cell Renal Cell Carcinomas Are a Distinct Clinical and Histologic Entity: A 10-Year Follow-up. *European Urology Focus* **1**, 284-290 (2016).
30. H. Moch, P. Schraml, L. Bubendorf, J. Richter, T. C. Gasser, M. J. Mihatsch, G. Sauter, Intratumoral Heterogeneity of Von Hippel-Lindau Gene Deletions in Renal Cell Carcinoma Detected by Fluorescence in Situ Hybridization. *Cancer Research* **58**, 2304-2309 (1998).
31. S. Q. Wong, J. Li, A. Y.-C. Tan, R. Vedururu, J.-M. B. Pang, H. Do, J. Ellul, K. Doig, A. Bell, G. A. McArthur, S. B. Fox, D. M. Thomas, A. Fellowes, J. P. Parisot, A. Dobrovic, Sequence artefacts in a prospective series of formalin-fixed tumours tested for mutations in hotspot regions by massively parallel sequencing. *BMC Medical Genomics* **7**, 23 (2014).
32. C. R. Thoma, M. Zimmermann, I. Agarkova, J. M. Kelm, W. Krek, 3D cell culture systems modeling tumor growth determinants in cancer target discovery. *Advanced drug delivery reviews* **69-70**, 29-41 (2014).
33. C. Pauli, B. D. Hopkins, D. Prandi, R. Shaw, T. Fedrizzi, A. Sboner, V. Sailer, M. Augello, L. Puca, R. Rosati, T. J. McNary, Y. Churakova, C. Cheung, J. Triscott, D. Pisapia, R. Rao, J. M. Mosquera, B. Robinson, B. M. Faltas, B. E. Emerling, V. K. Gadi, B. Bernard, O. Elemento, H. Beltran, F. Demichelis, C. J. Kemp, C. Grandori, L. C. Cantley, M. A. Rubin, Personalized In Vitro and In Vivo Cancer Models to Guide Precision Medicine. *Cancer Discovery*, (2017).
34. B. Escudier, C. Porta, M. Schmidinger, F. Algaba, J. J. Patard, V. Khoo, T. Eisen, A. Horwich, Renal cell carcinoma: ESMO Clinical Practice Guidelines for diagnosis, treatment and follow-up. *Annals of oncology : official journal of the European Society for Medical Oncology* **25 Suppl 3**, iii49-56 (2014).

35. J. Y. Lee, S. Y. Kim, C. Park, N. K. D. Kim, J. Jang, K. Park, J. H. Yi, M. Hong, T. Ahn, O. Rath, J. Schueler, S. T. Kim, I.-G. Do, S. Lee, S. H. Park, Y. I. Ji, D. Kim, J. O. Park, Y. S. Park, W. K. Kang, K.-M. Kim, W.-Y. Park, H. Y. Lim, J. Lee, Patient-derived cell models as preclinical tools for genome-directed targeted therapy. *Oncotarget* **6**, 25619-25630 (2015).
36. A. Mitra, L. Mishra, S. Li, Technologies for deriving primary tumor cells for use in personalized cancer therapy. *Trends in biotechnology* **31**, 347-354 (2013).
37. N. C. Lobo, C. Gedye, A. J. Apostoli, K. R. Brown, J. Paterson, N. Stickle, M. Robinette, N. Fleshner, R. J. Hamilton, G. Kulkarni, A. Zlotta, A. Evans, A. Finelli, J. Moffat, M. A. S. Jewett, L. Ailles, Efficient generation of patient-matched malignant and normal primary cell cultures from clear cell renal cell carcinoma patients: clinically relevant models for research and personalized medicine. *BMC Cancer* **16**, 485 (2016).
38. P. H. Tan, L. Cheng, N. Rioux-Leclercq, M. J. Merino, G. Netto, V. E. Reuter, S. S. Shen, D. J. Grignon, R. Montironi, L. Egevad, J. R. Srigley, B. Delahunt, H. Moch, Renal tumors: diagnostic and prognostic biomarkers. *The American journal of surgical pathology* **37**, 1518-1531 (2013).
39. P. Eirew, A. Steif, J. Khattra, G. Ha, D. Yap, H. Farahani, K. Gelmon, S. Chia, C. Mar, A. Wan, E. Laks, J. Biele, K. Shumansky, J. Rosner, A. McPherson, C. Nielsen, A. J. Roth, C. Lefebvre, A. Bashashati, C. de Souza, C. Siu, R. Aniba, J. Brimhall, A. Oloumi, T. Osako, A. Bruna, J. L. Sandoval, T. Algara, W. Greenwood, K. Leung, H. Cheng, H. Xue, Y. Wang, D. Lin, A. J. Mungall, R. Moore, Y. Zhao, J. Lorette, L. Nguyen, D. Huntsman, C. J. Eaves, C. Hansen, M. A. Marra, C. Caldas, S. P. Shah, S. Aparicio, Dynamics of genomic clones in breast cancer patient xenografts at single-cell resolution. *Nature* **518**, 422-426 (2015).
40. F. Pampaloni, E. G. Reynaud, E. H. Stelzer, The third dimension bridges the gap between cell culture and live tissue. *Nature reviews. Molecular cell biology* **8**, 839-845 (2007).
41. M. Pickl, C. H. Ries, Comparison of 3D and 2D tumor models reveals enhanced HER2 activation in 3D associated with an increased response to trastuzumab. *Oncogene* **28**, 461-468 (2009).
42. S. Breslin, L. O'Driscoll, The relevance of using 3D cell cultures, in addition to 2D monolayer cultures, when evaluating breast cancer drug sensitivity and resistance. *Oncotarget* **7**, 45745-45756 (2016).
43. P. A. Humphrey, H. Moch, A. L. Cubilla, T. M. Ulbright, V. E. Reuter, The 2016 WHO Classification of Tumours of the Urinary System and Male Genital Organs-Part B: Prostate and Bladder Tumours. *Eur Urol* **70**, 106-119 (2016).
44. K. Struckmann, K. D. Mertz, S. Steu, M. Storz, P. Staller, W. Krek, P. Schraml, H. Moch, pVHL co-ordinately regulates CXCR4/CXCL12 and MMP2/MMP9 expression in human clear-cell renal cell carcinoma. *The Journal of Pathology* **214**, 464-471 (2008).
45. C. Pauli, L. Puca, J. M. Mosquera, B. D. Robinson, H. Beltran, M. A. Rubin, R. A. Rao, An emerging role for cytopathology in precision oncology. *Cancer cytopathology* **124**, 167-173 (2016).
46. M. P. Rechsteiner, A. von Teichman, A. Nowicka, T. Sulser, P. Schraml, H. Moch, VHL gene mutations and their effects on hypoxia inducible factor HIFalpha: identification of potential driver and passenger mutations. *Cancer Res* **71**, 5500-5511 (2011).
47. C. A. Schneider, W. S. Rasband, K. W. Eliceiri, NIH Image to ImageJ: 25 years of image analysis. *Nat Meth* **9**, 671-675 (2012).

Acknowledgement

The authors thank André Fitsche and colleagues from the *in situ* laboratory, Raquel Herrador and Katharina Mühlbauer for technical assistance. We are grateful to Peter Bode for cytopathological review, to Axel Mischo and Sumeer Dhar for valuable suggestions and to Abdullah Kahraman and Aashil Batavia for critical reading. All authors have no conflict of interest to declare.

This study was supported by the Swiss Commission for Technology and Innovation CTI (CTI grant no. 18547.1 PFLS-LS), the University Research Priority Program (URPP) in Translational Cancer Research (University of Zurich, Switzerland) and the local government of the Canton Zurich (Project in Highly Specialized Medicine (HSM II)). C.C. was supported by the Swiss National Science Foundation (SNSF grant number S-87701-03-01).

Table 1: Analysis of the cases of the T/CMA.

Comparison of FFPE-primary tumor tissue (PT) and the corresponding cell culture (CC) using IHC with the indicated antibodies and sequencing of the VHL gene.

Patient	Subtype	Pax8		CkpanB		CK7		Vim		CD10		CAIX		RCC		CD117		VHL mutation status	
		PT	CC	PT	CC	PT	CC	PT	CC	PT	CC	PT	CC	PT	CC	PT	CC	PT	CC (Passage)
1	chromophobe																	/	/
2	chromophobe					NA												/	/
3	clear cell																	WT	/
4	clear cell																	WT	/
5	clear cell																	c.579insA/p.Asp193LysfsX63	retained (P3)
6	clear cell																	c.464-6_482delinsG	retained (P3)
7	clear cell																	c.488T>C/p.Leu163Pro	retained (P4)
8	clear cell																	c.201delC/p.Asn67AsnfsX91	retained (P7)
9	clear cell																	c.556G>T/p.Glu186X	retained (P3)
10	clear cell																	c.444delT/p.Phe148LeufsX11	not retained (P5)
11	clear cell																	c.158_164del/p.Glu53GlyfsX12	retained (P5)
12	Clear cell																	c.IVS1+2T>A(c.340+2T>A)	not retained (P5)
13	clear cell						NA				NA							c.IVS1+1G>A (c.340+1G>A)	retained (P3)
14	clear cell																	c.419_420delTC/p.Leu140GlnfsX3	not retained (P4)
15	clear cell																	c.194C>G/Ser65Trp	not retained (P5)
16	clear cell																	WT	/
17	clear cell																	c.74C>T/p.Pro25Leu	retained (P2)
18	clear cell																	WT	/
19	clear cell																	c.234insA/p.Asn78ArgfsX54	not retained (P3)
20	clear cell																	c.228insT/p.Phe76PhefsX55	not retained (P2)
21	clear cell																	c.493delG/p.Val165LeufsX5	retained (P2)
22	clear cell																	WT	/
23	clear cell																	c.390delT/p.Val130ValfsX28	retained (P2)
24	clear cell																	WT	/
25	clear cell																	c.533_537del/p.Leu178HisfsX76	retained (P3)
26	clear cell																	c.230insT/p.Phe77LeufsX55	retained (P3)
27	clear cell																	c.231C>A/p.Cys77X	retained (P3)
28	clear cell/papillary																	c.269A>T/p.Asn90Ile; c.525C>G/p.Tyr175X	retained (P1)
29	papillary																	/	
30	papillary													NA				/	
31	papillary																	/	
32	papillary																	/	
33	papillary																	/	
34	unclassified																	WT	/
35	oncocytoma																	/	
36	angiomyolipoma																	/	

Table 2: Advantages and disadvantages of cell models used in this study

	Advantages	Disadvantages
Monolayer cultures	– represents the original tumor – can be cultured for several passages to facilitate biobanking – reasonable costs – simple to use, robust	– physiological less relevant due to limited spatial interactions between cells – cell growth on flat plastic surface may influence experimental outcomes
Microtissues	– simple and fast gravity- based method to generate 3D cancer models – more accurate representation of cell-cell interactions within the original tumor – formation of uniform 3D models facilitates high-throughput assays	– unsuitable for expanding primary cell material – cellular composition may be hampered due necessary addition of stromal component – interactions with the stromal compartment may influence experimental outcomes
Organoids	– more accurate representation of spatial (cell-cell and cell-matrix) interactions within the original tumor – can be cultured over long times to facilitate biobanking	– laborious culturing procedures – very slow proliferation of renal cancer cells – big variation of organoid sizes within one sample complicates high-throughput assays – matrigel scaffold may influence outcomes

Fig. 1: Workflow for collecting human tumor tissue for diagnostic purposes and biobanking

Surgical specimens and biopsies that enter the pathology department are sectioned and consequently processed into formalin-fixed and paraffin-embedded tissue blocks (1) or fresh frozen tissue samples (2) while the remainder is used to generate PDC models (3). The repository of biospecimens can be further extended, e.g. by collecting matched body fluids (e.g. blood or urine).

Fig. 2: Validation in a cohort of patient-derived monolayer cell cultures derived from neoplasms of the kidney

(A) Distribution of RCC subtypes and renal neoplasms arrayed on the T/CMA for validation of patient-derived monolayer cell cultures in comparison to the tumor of origin.

(B) H&E-stained section of the T/CMA. Each spot of FFPE-preserved primary tumor is followed by two spots from the FFPE cell pellet of the corresponding PDC culture. Primary tumor elements are circled and colors denote cases belonging to certain RCC subtypes as indicated in (A). Cases are numbered corresponding to table 1.

(C) FISH analysis of chromosome 3 in *VHL*-wildtype ccRCC cases using the ZytoLight ® SPEC VHL/CEN 3 Dual Color probe. Losses of whole chromosome 3 or of the short arm of chromosome 3 (3p) were determined in a minimum of 50 non-overlapping nuclei. Numbers denote patient cases and correspond to Figure 2B and table 1. PT – primary tumor, CC – corresponding cell culture.

Fig. 3: Characterization of ccRCC patient-derived monolayer cell cultures

(A) Clinical characteristics of donors for ccRCC-derived cell models. *VHL* driver mutations present in the primary tumors are stated.

(B) Monolayer ccRCC-derived cell culures grown on collagen I-coated dishes. Brightfield images (X10 objective) depict the morphology of the cultured cells at Passage 3 (Patient A) or Passage 1

(Patient B, C and D). Scale bar denotes 50 µm. *VHL* driver mutations shown in (A) were verified by targeted sequencing confirming resemblance of cultured cells to the primary tumor.

(C) High-confidence, non-silent somatic variants were identified by NGS. Tumor-specific mutation spectra were generated for FFPE-tissue (patient A and D) or dissociated primary cells of the original ccRCC (patients B and C) and compared to DNA extracted from cultures cells at the designated passage numbers (P1-8). Variant allele frequencies are indicated and correspond to the color scale.

Fig. 4: Generation of RCC patient-derived 3D models and comparative drug profiling in 2D and 3D cell models

(A) HE and IHC staining with the indicated antibodies on consecutive sections of primary tumors (FFPE) and corresponding FFPE-microtissues generated by the hanging drop technology (X20 objective, insets X40 objective). Cryopreserved cells from patient A (passage 9) and patient B (dissociated primary cancer cells) were used as input for microtissue formation. Brightfield images depict microtissue morphology (X10 objective), scale bar denotes 300 µm.

(B) Histopathological features of tumor organoids generated using matrigel. Cryopreserved cells from patient A (passage 9) and patient B (dissociated primary cancer cells) were used as input for organoid formation. Brightfield images (X20 objective) of tumor organoids, scale bar denotes 30 µm. Pap–stained smears (X40 objective) of tumor organoids showing criteria of malignancy (presence of multiple nuclei, large nucleoli, clear vacuoles).

(C) *In vitro* testing of selected drugs in ccRCC-derived cell models generated from patient A. Cryopreserved patient-derived cells (passage 9) were seeded into monolayer cell culture, 3D microtissues and 3D organoids and exposed to the indicated drugs for 6 days (monolayer), 9 days (microtissues) or 14 days (organoids). Re-dosing of the drugs was undertaken on day 7 in the 3D assays. Cell viability was measured to determine dose-responses. The means of at least two technical replicates are shown. For monolayer cultures, N = 2, data are presented as mean ± S.D.

Fig. 5: Optimal workflow for the implementation of patient-derived 2D and 3D cancer models

Fresh RCC tissue is reviewed by pathologists before processing into single cell suspensions. Ideally, 2D and 3D cell models should be generated in parallel, validated and assessed for growth characteristics. To facilitate biobanking, cells have to be cryopreserved for later use. Each culture that is established from frozen stocks must be characterized before being subjected to further analysis, e.g. *in vitro* drug profiling.

Figure 1.

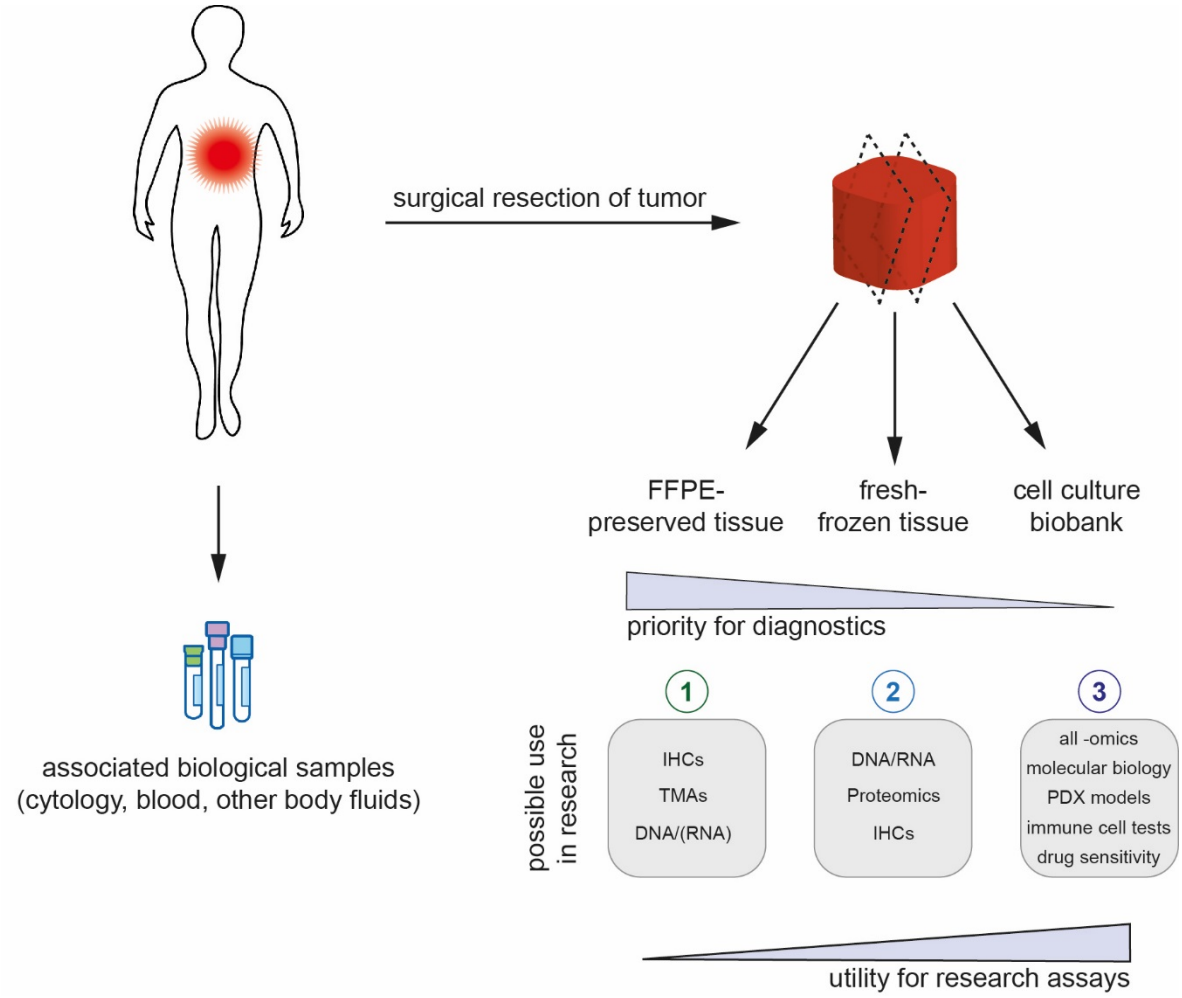
surgical resection of tumor
FFPE-
preserved tissue
fresh-
frozen tissue
cell culture
biobank
priority for diagnostics
associated biological samples
(cytology, blood, other body fluids)
possible use
in research
1
IHCs
TMAs
DNA/(RNA)
2
DNA/RNA
Proteomics
IHCs
3
all -omics
molecular biology
PDX models
immune cell tests
drug sensitivity
utility for research assays

Figure 2.

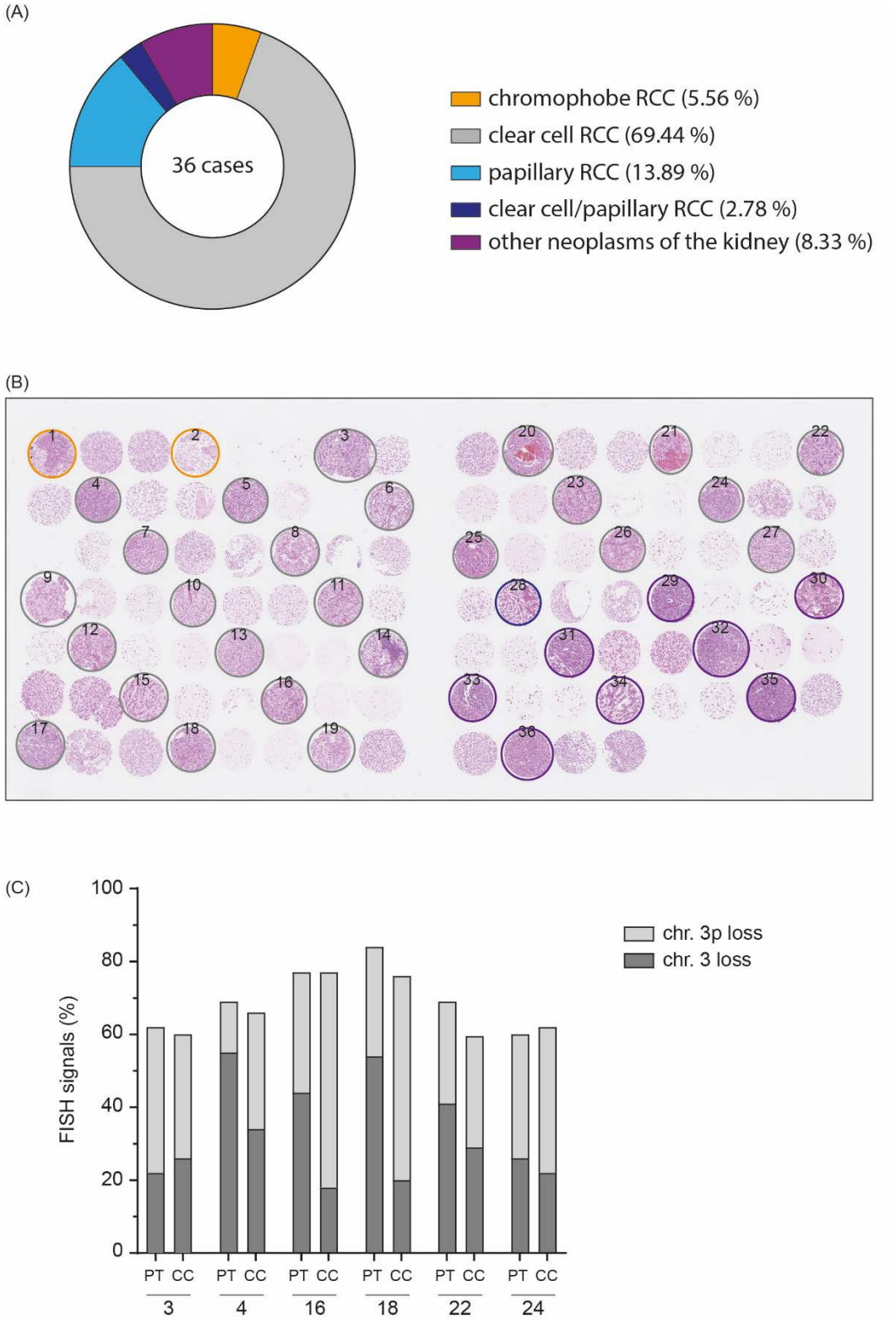
(A)
36 cases
chromophobe RCC (5.56 %)
clear cell RCC (69.44 %)
papillary RCC (13.89 %)
clear cell/papillary RCC (2.78 %)
other neoplasms of the kidney (8.33 %)
(B)
1
2
3
4
5
6
7
8
9
10
11
12
13
14
15
16
17
18
19
20
21
22
23
24
25
26
27
28
29
30
31
32
33
34
35
36
(C)
FISH signals (%)
100
80
60
40
20
0
chr. 3p loss
chr. 3 loss
PT CC
3
4
16
18
22
24

Figure 3.

(A)

Patient	Age	Gender	Type	Site of tumor	Tumor diameter (cm)	TNM	Grade (WHO 2016)	*VHL* mutation status
A	68	M	ccRCC Metastasis	Adrenal gland	1.6	pT3a	3	c.IVS1-1G>C(c.341-1G>C)
B	70	M	ccRCC	Kidney	5.0	pT3a	2	c.158_164del/p.Glu53GlyfsX12
C	71	M	ccRCC	Kidney	5.6	pT1b	2	c.533_537del/p.Leu178HisfsX76
D	49	M	ccRCC	Kidney	9.5	pT3a	3	c.579insA/p.Asp193LysfsX63

(B)

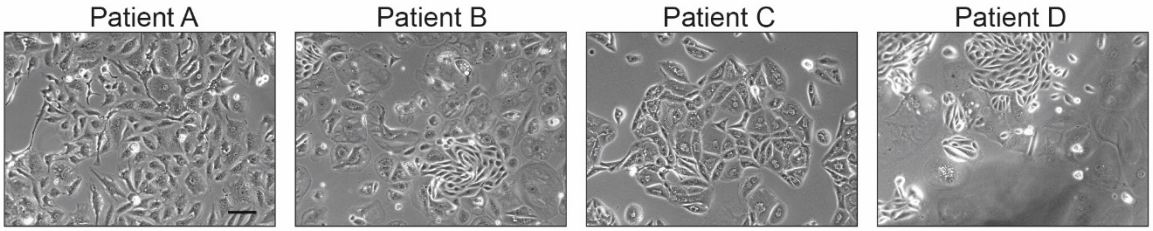

(C)

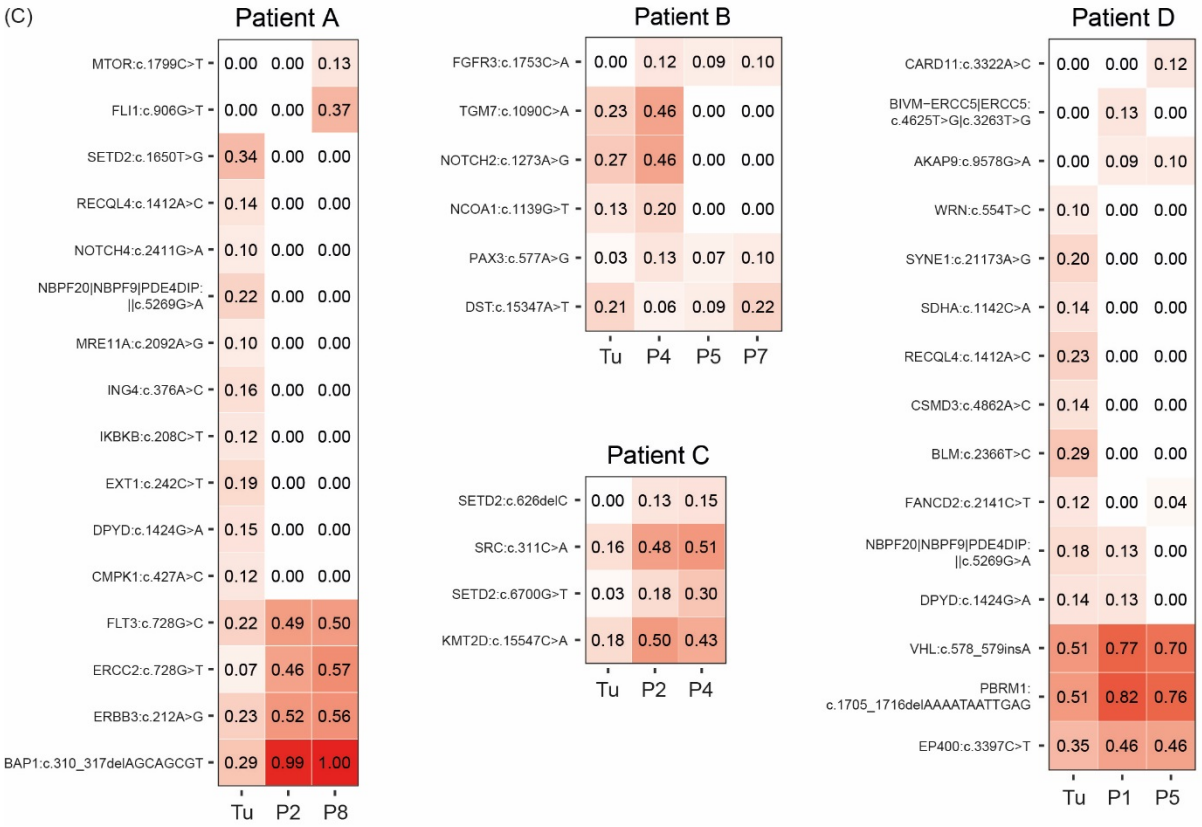

Figure 4.

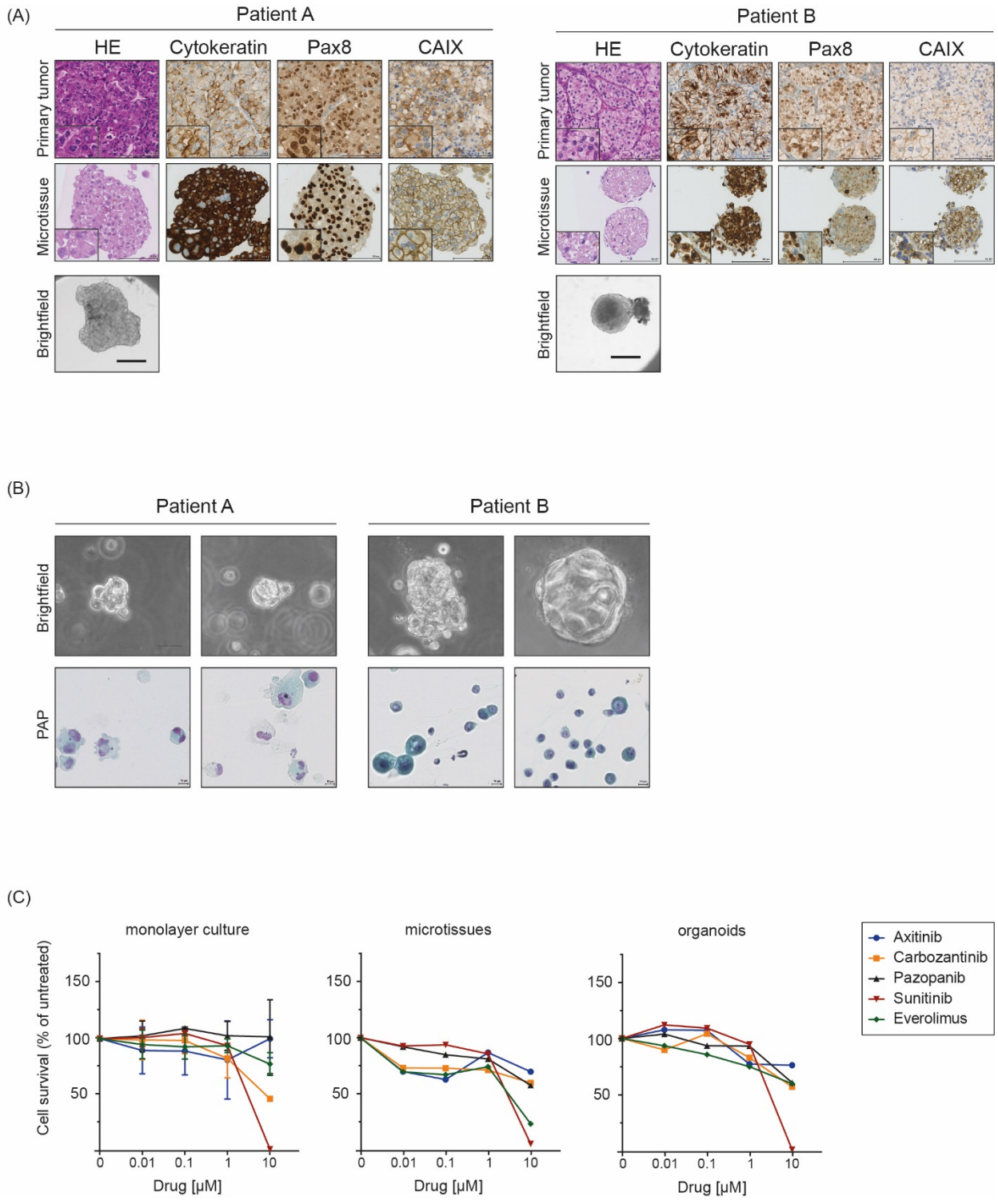
(A)
Patient A
HE
Cytokeratin
Pax8
CAIX
Primary tumor
Microtissue
Brightfield
Patient B
HE
Cytokeratin
Pax8
CAIX
Primary tumor
Microtissue
Brightfield
(B)
Patient A
Patient B
Brightfield
PAP
(C)
monolayer culture
microtissues
organoids
Cell survival (% of untreated)
150
100
50
0
0.01
0.1
1
10
Drug [µM]
Axitinib
Carbozantinib
Pazopanib
Sunitinib
Everolimus

Figure 5.

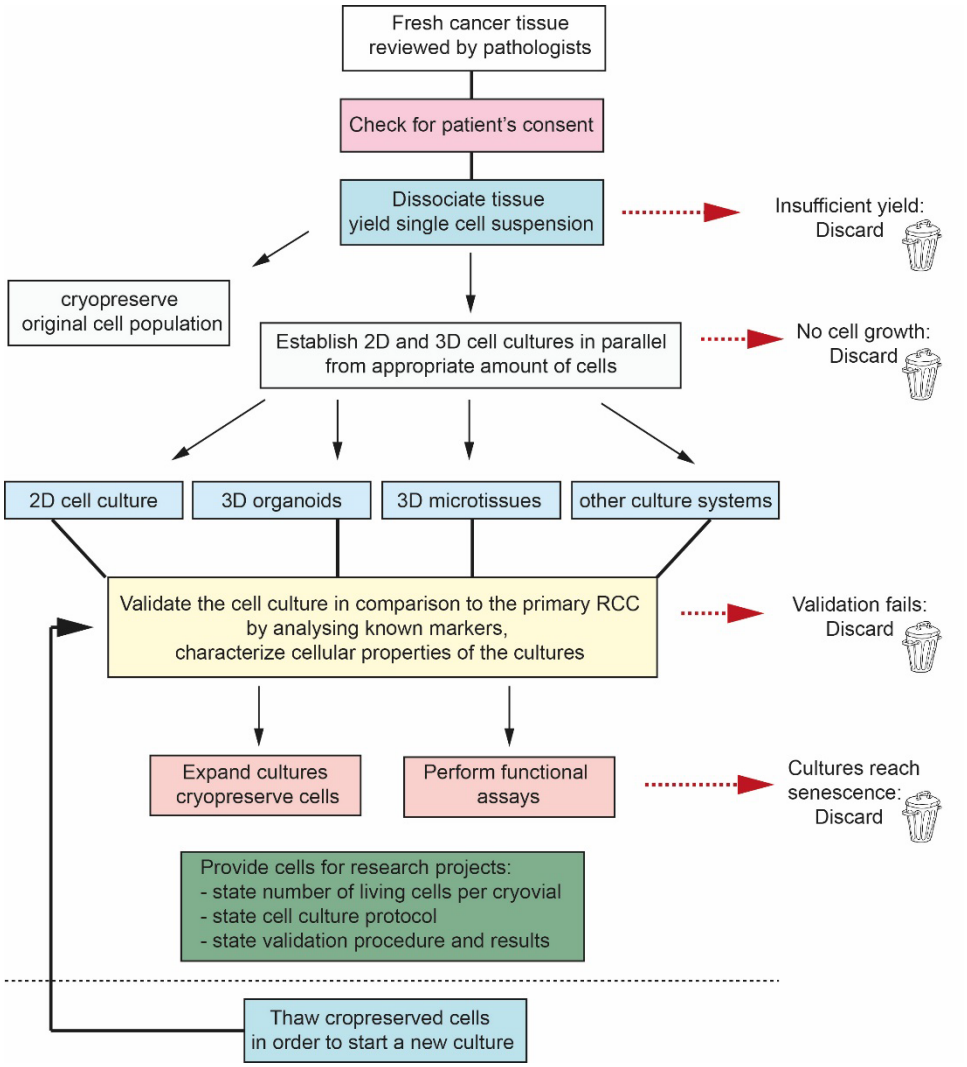
Fresh cancer tissue reviewed by pathologists
Check for patient's consent
Dissociate tissue yield single cell suspension
Insufficient yield: Discard
cryopreserve original cell population
Establish 2D and 3D cell cultures in parallel from appropriate amount of cells
No cell growth: Discard
2D cell culture
3D organoids
3D microtissues
other culture systems
Validate the cell culture in comparison to the primary RCC by analysing known markers, characterize cellular properties of the cultures
Validation fails: Discard
Expand cultures cryopreserve cells
Perform functional assays
Cultures reach senescence: Discard
Provide cells for research projects:
- state number of living cells per cryovial
- state cell culture protocol
- state validation procedure and results
Thaw cropreserved cells in order to start a new culture

Supplementary Materials

Supplementary Table 1: Antibodies used for IHC.

Antibody	Name/Clone	Dilution IHC	Supplier
CKpanB	Cytokeratin AE1/AE3	1:50	DAKO A/S
CK7	OV-TL 12/30	1:100	DAKO A/S
Pax8	Paired box 8	1:400	Protein Tech Group, Inc.
CA-IX	Carbonic Anhydrase IX polyclonal	1:6000	Abcam
CD10	56C6	1:25	Novocastra Laboratories Ltd
CD117	c-Kit Oncoprotein	1:200	Cell Marque Lifescreen Ltd.
HMB45	Melanosome	1:50	DAKO A/S
Vimentin	Vim3B4	1:800	Abcam
RCC	Renal Cell Carcinoma PN-15	1:250	Ventana-Cell Marque
cMet	c-Met (SP44)	1:100	Spring Bioscience

Supplementary Table 2: Links to HE- and IHC-images of the T/CMA

Link	ZTMA	alias	IHC stain
Schnitt-Link	240	cd117	c-Kit Oncoprotein CD117
Schnitt-Link	240	ck 7	Mouse anti-Human Cytokeratin 7
Schnitt-Link	240	ckpan b	Mouse anti-Human Cytokeratin AE1/AE3
Schnitt-Link	240	vim	Mouse anti-human Vimentin
Schnitt-Link	240	cd 10	Mouse monoclonal anti-CD10
Schnitt-Link	240	CA IX	Rabbit anti-Carbonic Anhydrase IX
Schnitt-Link	240	pax8	Rabbit anti-Paired Box 8, Pax8
Schnitt-Link	240	rcc	Renal Cell Carcinoma
Schnitt-Link	240	he	haematoxylin and eosin

Suppl. Fig. 1: Tissue processing within the living biobank

(A) Schematic representation of tissue processing workflow. Surgical specimens are dissociated into single cell suspensions by mechanical fragmentation and enzymatic digestion. These can be cryopreserved, utilized for the generation of patient-derived cancer models or subjected to further analysis.

(B) Representative images of surgical RCC specimens entering the living biobank workflow to generate RCC patient-derived tumor cell models.

Suppl. Fig. 2: Validation of representative PDC monolayer cultures from RCC

(A) IHC using a c-Met-antibody on FFPE-primary tumor tissue and the corresponding cell culture (X20 objective, insets X40 objective) for patient 33 (refer to table 1).

(B) The ZytoLight ® SPEC VHL/CEN 3 Dual Color Probe was used to assess aberrations on chromosome 3 (X60 objective). An orange fluorochrome-labeled probe is specific for the centromeric region of chromosome 3 (D3Z1) and a green fluorochrome-labeled SPEC VHL probe spans the *VHL* gene at 3p25.3. Representative images are shown for patient 4 (refer to table 1).

Suppl. Fig. 3: IHC characterization and concordance of representative PDC cultures from ccRCC

(A) to **(D)** For each patient A-D, consecutive sections of FFPE-pellets from monolayer cell cultures were characterized by HE staining and IHC with the indicated antibodies and compared to the corresponding primary tumors (X20 objective, insets X40 objective).

(E) Sample concordance of genomic alterations in patient tissue and corresponding ccRCC-derived cell cultures at the indicated passage numbers.

Suppl. Fig. 4: Proliferation and drug response in PDC models from patient A

(A) Cell proliferation of patient-derived 2D culture from patient A was analyzed using a plate-based cell viability assay. The relative number of living cells was determined every 48 hrs and normalized to the value measured on the day of seeding. N = 2, data are pesented as mean ± S.D.

(B) Bright-field images of ccRCC-derived 3D microtissues (X10 objective) from *in vitro* testing of selected drugs. Dissociated primary cancer cells were mixed with 5 % nHDFs and allowed to form microtissues for 72 hrs using GravityPLUS™ plates and then transferred to GravityTRAP™ ULA Plates. Drugs were administered 24 hrs after transfer and re-dosing was undertaken on day 7. Images of microtissues were taken 9 days after of drug exposure to illustrate dose-responses. The scale bar denotes 300 µm. Doxo – Doxorubcin (cytotoxic positive control).

Supplementary Figure 1.

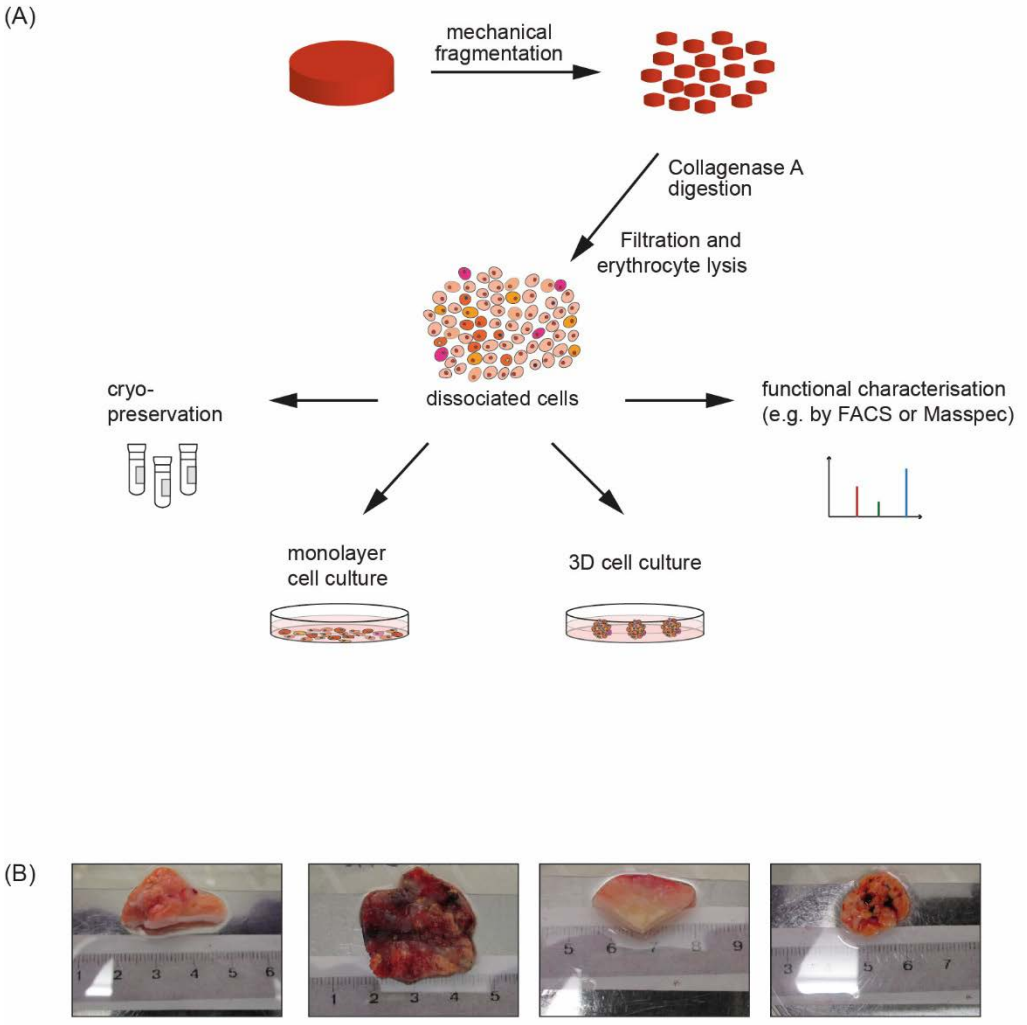

Supplementary Figure 2.

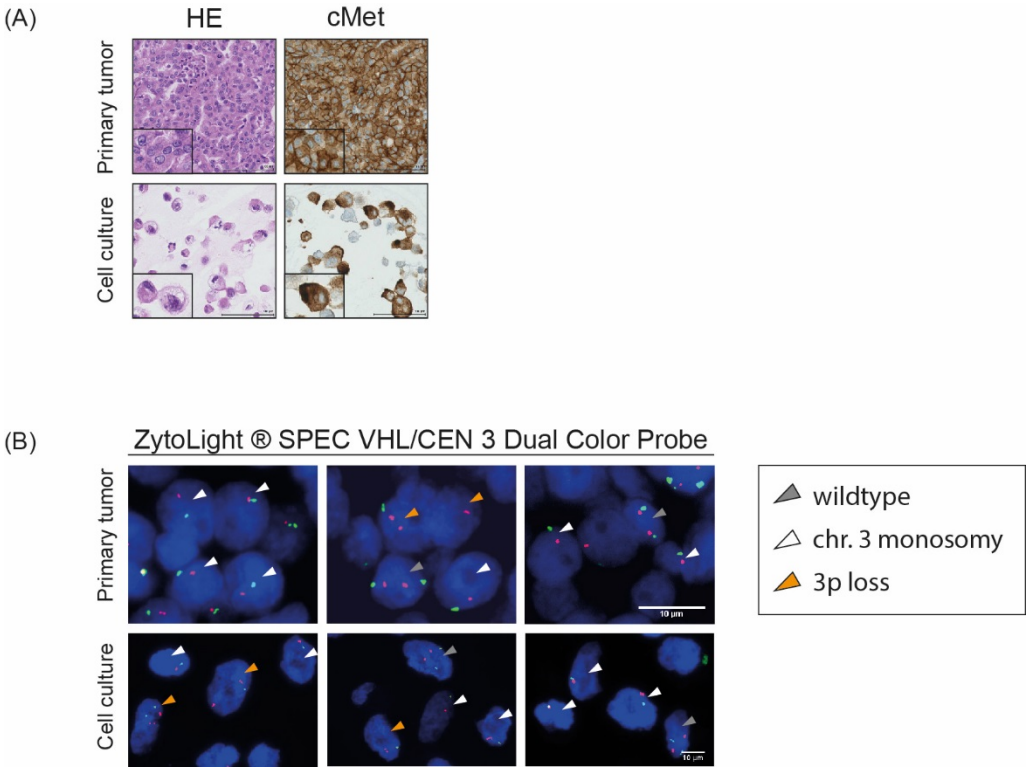

Supplementary Figure 3.

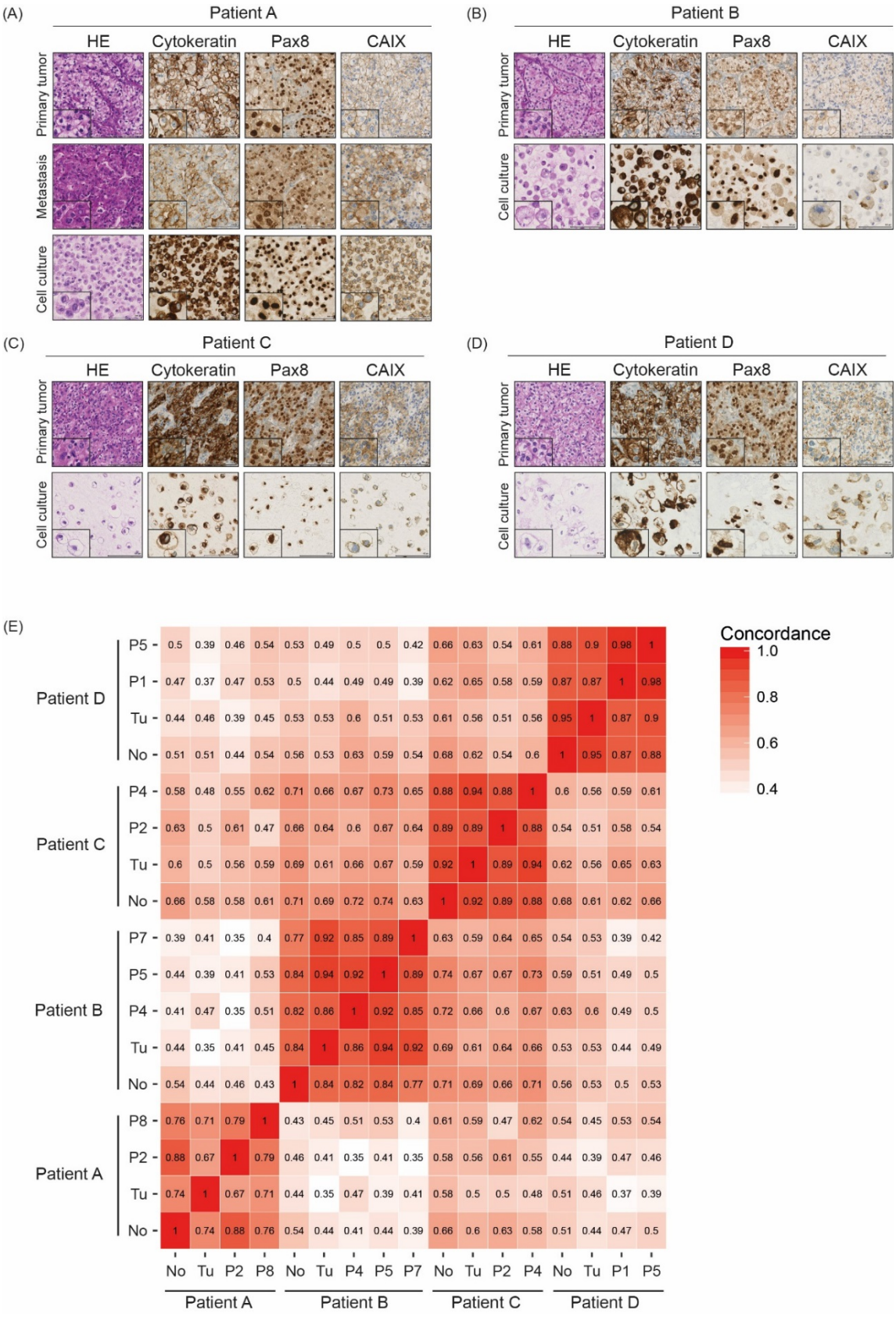

Supplementary Figure 4.

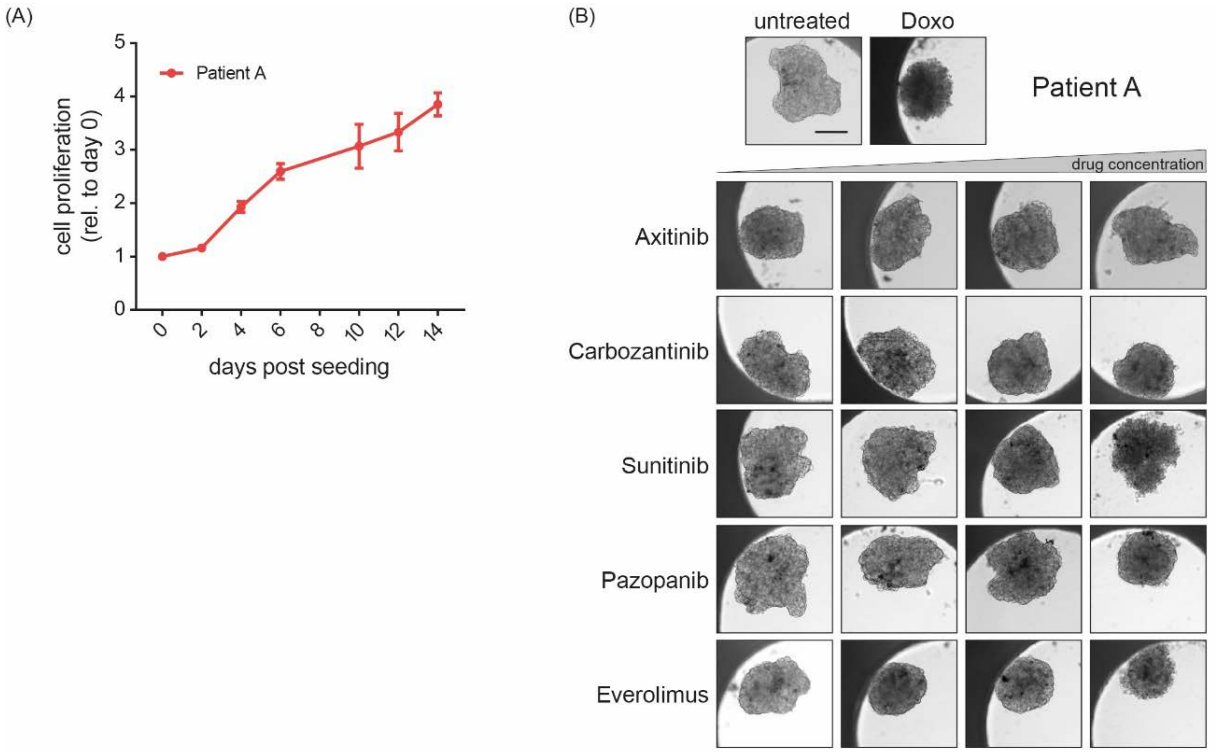

6.3 Identifying new biomarkers for renal cancer stem cells with potential therapeutic implications.

6.3.1 IL-8 and CXCR1 are associated with cancer stem cell-like properties in renal cancer and represent a potential therapeutic target for ccRCC patients.

Author contributions

C.C. and **M.R.** conceived the original idea. **C.C.** designed and performed the experiments such as western blots, gene expression arrays, cell proliferation, invasion and migration assays, tumorsphere generation, limiting dilution and clonogenic assays, adipogenesis, FACS and *in vivo* experiments. **C.C.** was also involved in the data acquisition, in the analysis and interpretation of the results as well as in the manuscript writing. **M.E.H** performed *in vivo* assays, revised the manuscript and provided critical suggestions during manuscript writing and project execution. **S.E.** and **B.B.** carried out mass spectrometry analysis of the samples. **P.S.** provided critical suggestions. **I.F** and **A.W.** revised the manuscript and provided with critical support during the conception of the animal experimentation. Finally, **H.M.** and **M.R.** assisted in the manuscript writing, provided administrative support, study supervision.

IL-8 and CXCR1 are associated with cancer stem cell-like properties in renal cancer and represent a potential therapeutic target for ccRCC patients.

Claudia Corrò[1,2], Marc Eammonn Healy[1], Stefanie Engler[3], Peter Schraml[1], Bernd Bodenmiller[3], Achim Weber[1], Ian Frew[4], Markus Rechsteiner[1], Holger Moch[1]

[1]Department of Pathology and Molecular Pathology, University Hospital Zurich, Switzerland; [2]Cancer Biology PhD Program, Life Science Zurich Graduate School, ETH and University of Zurich, Switzerland, [3]Institute of Molecular Life Sciences, University of Zurich, Switzerland; [4]Clinic of Internal Medicine I, University Medical Center Freiburg, Germany.

[*]Correspondence to Claudia Corrò, Department of Pathology and Molecular Pathology, University Hospital Zurich, Schmelzbergstrasse 12, 8091 Zurich, Switzerland, Phone: 41-44-2552537, Fax: 41-44-2554416, E-mail: Claudia.Corro@usz.ch;

Running title: IL-8/CXCR1 in renal cancer stem cells.

Keywords: IL-8, CXCL8, CXCR1, stem cells, renal cancer, repertaxin, spheres, xenografts, metastasis.

Conflict-of-interest statement: No.

ABSTRACT

Growing evidence suggests that clear cell renal cell carcinoma (ccRCC) as other solid tumors possess a rare population of cancer stem cells (CSCs) which contribute to metastasis and therapeutic resistance. In this study, we successfully isolate CSC populations from both human derived RCC cell lines as well as primary tissues. Interestingly, RCC-derived CSCs displayed high levels of the drug transporter ABCB5, the chemokine IL-8 and its receptor CXCR1. While the addition of recombinant IL-8 could significantly increase CSC number and properties *in vitro*, CXCR1 inhibition (CXCR1ab or repertaxin) significantly reduced these features. In addition, when injected into NSG mice, CSCs formed primary tumors capable of metastasizing to the lung and liver which expressed high levels of IL-8 and CXCR1. Furthermore, IL-8 expression correlated strongly with intratumoral lymphocytic infiltration and decreased overall survival in ccRCC patients. Taken together, these results suggest that the IL-8/CXCR1 axis is associated with cancer stem cell-like properties in renal cancer and represents a novel therapeutic target for ccRCC patients.

INTRODUCTION

Renal cell carcinoma (RCC), a malignant tumor affecting the adult kidney, is among the 10 most common cancers worldwide, affecting approximately 64'000 people every year with 5 % mortality (1,2). Clear cell renal cell carcinoma (ccRCC) is the most common type of RCC (3) and inactivation of the von Hippel-Lindau (*VHL*) tumor suppressor gene by mutation or promoter methylation has been found responsible for about 80 % of ccRCC cases (4-6).

Although therapeutic interventions that specifically target the VHL-HIF-VEGF pathway are routinely used for treating ccRCC, these treatment options have only moderately improved overall patient survival while also having significant side effects for patients (7,8).

There is growing evidence to suggest that renal cancer and other solid tumors possess a rare population of cancer stem cells (CSCs) that are capable of self-renewal and contribute to metastasis and resistance to therapy (9). CSCs are a small population of neoplastic cells within a tumor which present characteristics reminiscent of normal stem cells. CSCs are characterized by unlimited cell division, maintenance of the stem cell pool (self-renewal), give rise to all cell types within the tumor and contribute to metastasis *in vivo* (tumorigenicity), treatment resistance and recurrence (10-12). While conventional therapies, such as chemotherapy or irradiation, usually eliminate the majority of cells in the tumor bulk, the CSC pool is often unaffected (13).

CSCs were first identified in 1994 when Dick and colleagues isolated $CD34^+/CD38^-$ cells from acute myeloid leukemia (AML) patients and showed they could initiate AML *in vivo* upon re-transplantation into NOD/SCID mice (14). Subsequently, several others have showed the presence of CSCs in colorectal cancer, breast cancer, glioblastoma, melanoma, lung cancer, liver and prostate cancer (15-24). In addition, numerous studies have since tried to identify the CSC population from RCC (25-29), with CD105, ALDH1, OCT4, CD133 and CXCR4 reported as markers of CSC or CSC-like cells from RCC (30-32).

CD105 (endoglin) was expressed on a ccRCC subpopulation with potent capability to grow as spheres and initiate tumors and metastasis in mice (9,26). Additionally, immunohistochemistry (IHC) of tumoral CD105 has been found positively correlated to nuclear grade and tumor stage

(33). On the contrary, sorted $CD133^+$ cells from RCC patients did not show tumorigenic capability *in vivo* although they expressed stem cell markers such as CD44, CD29, Vimentin, and Pax2 (34). When co-transplanted with renal carcinoma cells, $CD133^+$ progenitors significantly enhanced tumor development and growth. The same result was obtained using $CD133^+$ cells derived from normal kidney tissue (35). $CD105^+$ cells did not express CD133 suggesting that $CD133^+$ cells may be renal resident adult progenitor cells.

However, none of these markers were shown to embody the entire tumor resident CSC pool and contrasting results are reported in the literature (36-39). Therefore, improving the identification of a specific subpopulation of cells within a tumor that either initiate or maintain tumorigenesis is of utmost importance for understanding tumor biology and in the development of novel therapies.

CXCL8 (C-X-C motif ligand 8 or IL-8), represents one of the major chemokines associated with the promotion of neutrophils and inflammatory response (40). It is induced in response to inflammatory cytokines, hypoxia and environmental stress (41,42). Previous studies have demonstrated that IL-8 is also involved in proliferation and survival of neoplastic cells. IL-8 acts through several signaling pathways associated with apoptosis, multidrug resistance, angiogenesis and metastasis-related tissue remodeling in a positive feedback loop (42-46). IL-8 interacts with both CXCR1 and CXCR2 with different affinities and potencies to mediate different cellular responses. CXCR1/2 have recently been demonstrated to be associated with CSC populations as well as proliferation, migration and invasion in certain type of human cancers such as breast, prostate, colon and pancreatic cancers (47-50).

In particular, a recent study on pancreatic cancer showed that positive CXCR1 expression correlates with metastasis and poor survival rate in patients (47). Furthermore, IL-8 increased sphere formation and invasion in pancreatic cancer, and these effects could be reversed by CXCR1 blockade (47). In addition, Ginestier et. al. developed a strategy to target breast cancer stem cells using either CXCR1-specific antibodies or repertaxin. Repertaxin, a small molecule blocking CXCR1/2, was able to specifically target breast cancer xenografts retarding tumor growth and reducing metastasis (49). Nevertheless, the role of the IL-8/CXCR1 axis in ccRCC

94 is currently unknown. In this study, we identify an essential role for IL-8/CXCR1 signaling in
95 the proliferation, migration and invasion, sphere formation and self-renewal capabilities of
96 RCC-derived tumor cells, and highlight the therapeutic potential of blocking IL-8/CXCR1
97 signaling during ccRCC.

MATERIALS AND METHODS

Ethics statement

The local ethics commission (KEK-ZH-Nr. 2011-0072 and KEK-ZH-Nr. 2014-0614) approved this study and all patients gave written consent (General Consent, Institute of Pathology and Molecular Pathology, University Hospital of Zurich, Switzerland). NOD.Cg-Prkdcscid Il2rgtm1Wjl/SzJ (NSG) mice were purchased from The Jackson Laboratory (Mouse strain #005557). Housing and experimental procedures of all animals were performed at the University of Zurich in accordance with the Cantonal Veterinary Office (Zurich, Switzerland) under the license number ZH104/2015. Animals were maintained under specific pathogen free (spf) conditions with a light/dark cycle of a 12 h/12 h cycle with artificial light of approximately 40 lux in the cage. The mean room temperature was 21 ± 1 °C, with a relative humidity of 50 ± 5 % and 15 complete changes of filtered air per hour (HEPA H14 filter); the air pressure was controlled at 50 Pa.

Specimen Procurement

Renal cell carcinomas (RCCs) were surgically resected and underwent routine tissue processing for diagnostic purposes. One pathologist (H.M.) evaluated all tissue specimens. Tumors were histologically classified and graded according to the World Health Organization classification (51), and tumour staging was performed according to the current TNM system. If available, additional fresh adjacent tissue samples from areas macroscopically identified as cancer were placed into sterile 50-ml conical tubes containing transport media (RPMI (Gibco, Thermo Fisher Scientific Inc., Zug, Switzerland) with 10 % vol/vol dialyzed fetal calf serum (FCS, Gibco) and Antibiotic-Antimycotic (Gibco)) and kept at 4 °C. Tissue samples were further processed within 24 h.

Tissue processing and generation of 2D primary cell cultures

RCC tumor specimens as well as xenograft tumors were rinsed with PBS and finely cut into small fragments using a scalpel. Consequently, samples were enzymatically digested in a

TBS/Collagenase A-mix containing a surplus of Ca^{2+} for 2-3 h at 37 °C. The slurry was passed through a 70 µm cell strainer to remove large fragments and centrifuged at 1'000 rpm for 5 minutes. The Collagenase A digestion was stopped by incubating the pellet in 1 ml Stop solution (50 mM Tris, 150 mM NaCl, 10 mM EDTA) for 5 minutes at room temperature. Cells were washed once with PBS and erythrocytes were lysed by incubating the cells for 2 minutes in ACK buffer (150 mM NH_4Cl, 10 mM $KHCO_3$, 100 mM EDTA). After a final wash with PBS, dissociated cells were evaluated for cell viability by trypan blue dye exclusion. Appropriate amounts of cell suspension were resuspended in K1n medium to be transferred to collagen I-coated cell culture dishes for culture in a humidified incubator at 37 °C with 5 % CO_2. The medium was replaced no earlier than after 5 days after initial plating and consecutively every three to four days.

Cell lines

The RCC cell lines 769P, A498, Caki1 and ACHN together with the lung cancer cell lines A549 and H460, were purchased from ATCC (Manassas, VA). These cell lines were additionally authenticated via STR-based DNA-profiling by IdentiCell (Department of Molecular Medicine, Aarhus University, Denmark). Cells were cultured using Dulbecco's Modified Eagle Medium (DMEM, Gibco) or RMPI medium containing 10 % FCS and 2 mM glutamine (Gibco). Cells were split when reaching 80 % confluence.

Immunohistochemistry (IHC)

Tissue and cell culture microarrays (T/CMAs) were constructed as described previously (52).

T/CMA, whole tumor and cell pellet sections (2 µm) were prepared from formalin-fixed, paraffin-embedded specimens and were stained with H&E for histological evaluation. For immunohistochemistry, sections (2 µm) were transferred to glass slides followed by antigen retrieval. IHC was performed using the Ventana Benchmark automated system (Ventana Medical Systems, United States) and Ventana reagents. The Optiview DAB IHC detection kit was used for staining with the antibodies against PanCKa, Pax8, E-cadherin, CD105, Snail/Slug, and CXCR1. The staining procedure for CA-IX, Vimentin, and CXCL8 was carried

out with the automated Leica BOND system using the Bond Polymer Refine Detection Kit (Leica Biosystems). Antibodies used for immunostains are listed in the supplementary table 1.

Sanger sequencing

In order to obtain DNA from the primary tumor, HE-stained sections of FFPE or fresh frozen tissue were reviewed by a pathologist for tumor content and the tumor area was marked. DNA was isolated from FFPE punches (3 cylinders with a diameter of 0.6 mm) or a minimum of 10'000 cultured cells using the Maxwell 16 DNA Purification Kit (Promega, Dübendorf, Switzerland). PCR and sequencing of VHL was performed as previously described (53) using primers for amplification of the *VHL* exons 1-3. For DNA extracted from FFPE tissue specimens only a section of Exon 1 was amplified using the primer Exon 1B forward. The same primers as described above were used for the exons 2 and 3. The RefSeq for *VHL* was NM198156.4. The following primers were used:

Exon 1 forward: 5'-CGAGCGCGCGCGAAGACTAC-3';
Exon 1 reverse: 5`-GACCGTGCTATCGTCCCTGC-3';
Exon 1B forward: 5'-AGAGTCCGGCCCGGAGGAACT-3';
Exon 2 forward: 5'-ACCGGTGTGGCTCTTTAACA-3';
Exon 2 reverse: 5'-TCCTGTACTTACCACAACAACC TT-3';
Exon 3 forward: 5'-GAGACCCTAGTCTGT CACTGAGG-3';
Exon 3 reverse: 5'-TCATCAGTAC CATCAAAAGCTGA-3'

Western blot

Cell and tissue lysates were prepared using NP-40 buffer (10 mM Tris pH 8, 1 mM EDTA pH 8, 400 nM NaCl, 0,1 % NP40, 1 mM DTT) containing complete protease and phosphatase inhibitor cocktail (Roche, Applied Science). Lysates were centrifuged for 15 minutes (16'000 rcf, 4 °C). Protein concentration of the supernatant was determined by the BCA Assay (Thermo Fisher Scientific Inc.) with bovine serum albumin (BSA) as a standard. Equal amounts of protein (40 ng) in NuPAGE LDS sample buffer (Thermo Fisher Scientific Inc.) and a size marker (MagicMark XP and SeeBlue Plus2, Thermo Fisher Scientific Inc.) were loaded on a 4

% to 12 % gradient Bis-Tris gel (Thermo Fisher Scientific Inc.) and transferred to PVDF membrane. The membrane was incubated for 1 h in 5 % milk and subsequently with primary antibody over night at 4 °C. As secondary antibodies anti-rabbit-HRP or anti-mouse-HRP (Thermo Fisher Scientific Inc., California, United States) were used. Proteins were detected by using the ClarityTM Western ECL Substrate Kit (Bio-Rad Laboratories Inc.). The following antibodies were employed: human CXCR1 ab (clone 42705, 5 µg/µl, R&D, Minneapolis, United States), human CXCL8 ab (clone 6217, 10 µg/µl, R&D), HIF1α (1:1'000, Novus Biologicals, Colorado, United States), HIF2α (1:500, Abnova, Taiwan), CAIX (clone M75, 1:1'000, J. Zavada, Prague, Czech Republic) and actin (1:2000, Chemicon International, California, United States).

Quantitative real-time PCR

Total RNA was purified using the Maxwell 16 RNA Purification Kit (Promega) and quantified using the Qubit Protein Assay Kit (Thermo Fisher Scientific Inc.). Total RNA (400 ng) was reverse-transcribed using the RT2 First Strand Kit (Qiagen, Hilden, Germany). A human CSC gene expression array (RT^2 Profiler PCR Array; Qiagen), which profiles 84 genes linked to CSCs, was employed. In addition, the expression of the three candidate genes was verified separately using the RT^2 qPCR Primer Assay for ABCB5, NM_001163941; CXCR1, NM_000634; and IL-8, NM_000584. Analysis was performed on qPCR machine (ViiATM7 Real-Time PCR System, Applied Biosystems, Thermo Fisher Scientific Inc.) in 10 µl of total volume.

Hypoxia

For hypoxic treatment, cells were cultured at 0.2 % of oxygen in an INVIVO2 hypoxia workstation 300 (Ruskin Technology, Bridgend, UK) for 48 h.

Cell invasion and migration

Migratory/invasive potential of RCC cell lines was measured in real-time using the xCELLigence RTCA DP System (ACEA Biosciences, San Diego, United States). This technique adapts the boyden chamber principle and combines it with impedance

measurements. Cells seeded in the upper chamber of a microplate containing “low chemoattractant (1 % FCS)” can migrate through the microporous membrane into the lower chamber being the “high chemoattractant (10 % FCS)” compartement. Migrated cells adhere to the gold micro-electrode sensor located at the lower side of the membrane and lead to an increase in impedance, which is measured by the RTCA DP instrument. Optimal cell seeding densities were determined in pre-experiments and 20’000 cells were found to be optimal. Impedance measurements were performed for 72-96 h. For invasion assays, the membrane was coated with Matrigel Basement Membrane Matrix (BD Biosciences, 400 µg/ml protein in 1 % FCS-containing medium).

Tumorsphere culture

Generation of tumorspheres was performed by resuspending $5x10^4$ cells into a special medium containing DMEM/F12 (Gibco), 2 % B27 supplement (Gibco), 20 ng/mL Human Recombinant EGF (Gibco), 10 ng/mL Recombinant Human FGF-basic (Thermo Fisher Scientific Inc.), 5 µg/ml Insulin (Sigma) and 10 % FCS. Cells were then plated into ultra-low attachment 10 cm^2 dishes (Corning, NY, United States) and the medium was refreshed every 4 days.

Tumorspheres at approximately 300 µm in size were collected by centrifugation (500 rpm, 5 minutes) into 50 ml Falcon tubes. Carefully the supernant was removed and spheres were washed using PBS. Spheres were passaged by incubation with 1 ml of TrypLE Express (Gibco) for 5 minutes in incubator at 37°C. Spheres were further dissociated by slowly pipetting up and down the cell suspension. The trypsin was then inactivated by adding at least three volumes of DMEM containing 10 % FCS and the cells were pelleted by centrifugation at 500 rpm for 5 minutes. Single cell suspension was re-plated according to the procedure described above.

Sphere formation assay

Tumor cells growing into adherent conditions were transferred into 6 well ultra-low attachment plates containing tumorsphere medium at $5x10^3$ cells/well. Spheres were grown for 15 days. In enrichment step, spheres were split and plate at the same initial cell density of $5x10^3$

cells/well every 15 days and counted at the end of each period. This step was repeated for at least five times.

When talking about spheres in this manuscript, we always refer to CSCs enriched in the sphere formation assay for at least three passages.

Limiting dilution assay

Sphere formation capability was evaluated by limiting dilution assay (LDA). Adherent tumor cells and sphere-derived cells were plated in triplicates into 96 well plates at 0.5 cell/well density in the tumorsphere medium. Only wells which contained 1 cell/well were marked and observed every day. 10 µl of fresh medium was added every 2 days. After a week, tumorsphere formation was evaluated in the marked wells using the formula: (n of positive wells/n of total marked wells) x 100.

Clonogenic assay

Cells were harvested, counted, and diluted in sterile tubes, in order to plate 200 cells/well into 6 well plates or 2'000 cells into 10 cm^2 dishes. Appropriate medium was used to grow cells over two-week time period. Fresh medium was added every 3 days to avoid cell death due to senescence. In the treatment experiment, cells were pretreated for 72 h before seeding them into the clonogenic assay. After two weeks, medium was removed and cells were rinsed carefully with PBS. Methanol was used to fix the cells for 10 min following staining with 0.5 % crystal violet for 15 minutes. The excessive dye was removed by rinsing each well with tap water. Dishes and plates were left to dry in normal air at RT. Colonies containing up to 50 cells were counted under the microscope.

Adipogenesis

Cells plated in triplicate in 48 well plates at 2'000 cells per well. Complete medium used to differentiate contained DMEM with 10 % FCS, L-glutamine and penicillin/streptomycin. Cells were induced for 3 days with 400 µl of complete medium supplemented with dexamethasone (1 µM, D4902, Sigma), insulin (10 µg/ml), indomethacin (120 µM, I7378, Sigma) and 3-Isobutyl-

1-methylxanthine (IBMX, 0.5 mM, I5879, Sigma). Further, cells were maintained for 15 days in complete medium added with dexamethasone, insulin and indomethacin. Medium was changed every 3 days.

Xenografts

Female NSG mice were subcutaneously injected with parental or sphere-derived cells from the RCC cell lines 769P and Caki1. 10^6 cells, 10^4 cells or 10^2 cells were injected into the left flank of each mouse in 50 % mixture of Matrigel (growth factor reduced 35623, Corning) and PBS in triplicates. Each group of three mice received either tumor cells or only matrigel and PBS. Mice were monitored daily in the first 10 days post-injection and when the tumor started to grow, otherwise every second day. Tumor size was measured using a caliper. When the tumor size reached 1 cm^3, mice were euthanized and the tumor was harvested. The tumor tissue was used for primary culture and FFPE tissue preparation. At the same time, mice were extensively inspected in order to determine the presence of macro-metastasis. Lungs, liver, heart, spleen, and kidneys were harvested and processed for paraffin embedding. These tissues were screened for micro-metastasis by IHC staining for H&E and Pax8.

Flow cytometry

Flow cytometry was performed on the LSR Fortessa instrument at the Flow cytometry Facility (University of Zurich, Switzerland). 10^6 tumor cells were resuspended into 1 ml of DMEM containing 2 % FCS and 10 mM HEPES (Thermo Fisher Scientific Inc.) together with Hoechst 33342 (H3570, Thermo Fisher Scientific Inc.) at the final concentration of 5 µg/ml. Cells were then incubated at 37 °C in the water bath for 90 minutes. To confirm that the correct cells are identified as SP on the flow cytometer, an aliquot of cells was treated using 50 µM verapamil (V4629, Sigma) which blocks the efflux of Hoechst in the SP before incubation in the Hoechst staining solution. Upon verapamil treatment, SP disappears from the plot. After 90 minutes, cells were centrifuged at 500 rpm and resuspended in ice-cold HBSS containing 2 % FCS and 10 mM HEPES. Samples were further stained with either CXCR1 (Alexa Fluor 700, FAB330N, R&D) or CXCR2 (PerCP, FAB3331C, R&D) antibody for 1hr at 4 °C and subsequently fixed in

1.6 % PFA (Thermo Fisher Scientific Inc.) for 10 minutes. 2 µg/ml propidium iodide (PI) was added right before flow cytometry for cell dead discrimination. Hoechst was excited at 405 nm and the blue signal was collected with a 450/40 nm band-pass filter, whereas the red fluorescence with a 610/20 nm filter. Due to the high capability to extrude Hoechst dye, side population can be defined as the negative population for Hoechst blue and Hoechst red. CXCR1 was detected by using the laser 640 nm and 730/45 nm filter, whereas for CXCR2 the laser 488 nm and 710/50 nm filter were applied.

cyTOF: Barcoding and Staining

Formalin-fixed cell lines (Caki1 and ACHN) and the corresponding spheres were resuspended with Cell Staining Medium (CSM) with 0.3 % Saponin (CSM-S) and loaded into a 96-well plate. Samples were washed with PBS-S and barcoded with barcoding reagent (^{104}Pd, ^{106}Pd, ^{108}Pd, ^{110}Pd, ^{113}In, ^{115}In) at a final concentration of 100 nM for 45 minutes at RT (54). Sample were washed three times in CSM-S. Afterwards barcoded cells and spheres were combined and stained with a metal-conjugated antibody mix (Suppl. Table 2) diluted in CSM-S for 1 h at 4 °C. Sample was washed three times with CSM-S and once with PBS with 0.03 % Saponin (PBS-S). Samples were intercalated and fixed using MaxPar Intercalator 500 µM (Fluidigm) diluted 1:10'000 in 1.6 % PFA in PBS over night at 4 °C. Samples were washed three times in PBS. Before analysis, the samples were washed once with ddH_2O and filtered through a 35 µm cell strainer.

Mass cytometry analysis

Samples were mixed 1:10 with EQTM Four Element Calibration Beads (Fluidigm) and then analyzed on a CyTOF2. Following the manufacturer's standard operation procedure, samples were acquired at a rate of ~500 cells per second. After acquisition all generated fcs files were concatenated (54), then data were normalized and bead events removed (55), followed by a debarcoding step (56). The data analysis was done using Cytobank (http://www.cytobank.org/). Therefore, cells were gated using ^{191}Ir and ^{193}Ir to remove doublets and debris.

Drug treatment

Different compounds were used in the treatment of cells in this study. Repertaxin (HY15251, Hycultec) is a small molecule with potent inhibitory activity on CXCR1/2. It was used at 100 nM concentration. Anti-CXCR1 antibody (clone 42705, R&D) was used at the concentration of 20 µg/ml, whereas to achieve CXCR1 activation the human recombinantug IL-8 (208-IL, R&D) was exploited at the concentration of 1 µg/ml. Sunitinib (S7781, Selleck) is a small molecule targeting the receptor tyrosine kinase (RTK). It is currently used as a first line treatment in ccRCC patients. Sunitinib was used at 2 µM.

Statistical and computational analyses

Analysis between groups was carried out with two-way ANOVA and Bonferroni multiple comparison. Student's *t* test, Kruscal-Wallis test associated with Dunn's multiple comparison, and Wilcoxon signed rank test were also employed. Survival curves were estimated with the Kaplan–Meier method and the log-rank test. All these analysis were performed using GraphPad Prism 5 (GraphPad Software) and the p-values < 0.05 were considered statistically significant and presented as follow: * p-value < 0.05; ** p-value < 0.02; *** p-value < 0.001; **** p-value < 0.0001.

RESULTS

CcRCC contains CSC populations capable of self-renewal

The presence of a cancer stem cell population in RCC was investigated first in nine RCC cell lines by sphere formation assay. Five out of nine RCC-derived cell lines (55 %) displayed sphere formation and self-renewal properties (Fig. 1A). Self-renewal properties were evaluated by enriching the CSC population over five passages. In particular, two metastasis-derived RCC cell lines (Caki1 and ACHN) showed significantly greater sphere formation capability and self-renewal features when compared to RCC cell lines derived from primary tumors (769P and A498) (Fig. 1B). In addition, spheres derived from Caki1 and ACHN were significantly bigger in size than the spheres formed by 769P and A498, ranging between 20 and 300 µm (Fig. 1C). Increased expression of EMT markers such as Vimentin, Snail/Slug and N-cadherin, and the cancer stem cell marker CD105 was found by IHC in the spheres compared to the corresponding mono-adherent cells, whereas a decreased expression of E-cadherin was observed (Fig. 1D).

The capability to revert the EMT phenotype was also investigated by seeding spheres into normal adherence tissue culture dishes. Spheres were able to attach again to the surface and propagate by dissolving the sphere structure (Suppl. Fig. 1A). The same markers where then investigated in these cells after attachment and the expression patter observed was comparable to the parental mono-adherent cells (data not shown). Additionally, sphere-derived cells were able to differentiate *in vitro* into adipocytes upon induction (Suppl. Fig. 1B).

By limiting dilution assay, Caki1 and ACHN further exhibited an improved sphere formation capability compared to 769P and A498 (Suppl. Fig. 1C). Moreover, Caki1 and ACHN also displayed enhanced clonogenic activity compared to primary tumor-derived cultures indicating increased self-renewal properties (Suppl. Fig. 1D and E).

Several recent studies have shown that hypoxic conditions enhanced stemness features (34,57,58). Therefore, sphere formation capability was investigated under hypoxia (48 h, 0.2 % O_2, 5 % CO_2). An increased sphere production was observed in parental cells upon hypoxia incubation, whereas sphere-derived cells did not further enhance sphere formation probably

due to the constitutive expression of HIFs under normoxia (Suppl. Fig. 1F). In fact, sphere-derived cells showed increased level of HIF1α and its downstream target CAIX compared to the corresponding parental cells. A498 and 769P did not show HIF1α expression due to homozygous deletion of HIF1α, instead they did express high levels of HIF2α (Suppl. Fig. 1G; (59)).

In accordance with the observations obtained from RCC cell lines, two metastatic primary cultures derived from ccRCC patients showed enhanced sphere formation capability compared to primary tumor-derived cultures, suggesting an increased CSC fraction in the metastatic sites compared to the primary tumors (Fig. 1A and E).

Identification of potential novel cancer stem cell markers

To identify potential novel CSC markers, a human cancer stem cell gene expression array (RT^2 Profiler PCR Array; Qiagen), which profiles 84 genes linked to cancer stem cells, was performed on 769P, A498, Caki1 and ACHN cells. Changes in the gene expression profile such as upregulation of EMT, stemness markers and genes involved in developmental pathways (e.g. NANOG, WNT and MYC), were observed in sphere-forming cells vs corresponding parental cells (Suppl. Fig. 2A). Moreover, potentially new and already described CSC markers being CD105, CD44, CXCR4, ALDH1A1 and CXCL8, were found highly expressed by the sphere population. The differentially expressed genes are summarized in the supplementary table 3.

These findings were supported by CYTOF data in which differential expression of these markers was found in sphere-derived cells compared to the corresponding mono-adherent cells (Fig. 2A). Spheres showed an increased expression of EMT and putative stem cell markers (CD24, Vim, CD44, and CXCR4) as well as a decreased expression of markers of cellular differentiation (CD13, CD10) (Fig. 2A).

Among all the candidates, we focused our attention on CXCL8, CXCR1, and ABCB5 since their role in ccRCC as potential CSC and chemoresistance markers is currently unknown.

The IL-8/CXCR1 axis is associated with cancer stem cell properties in ccRCC

In order to confirm the results obtained by the gene expression array, and to further dissect the role of IL-8/CXCR1 axis in RCC, qPCR for IL-8, CXCR1 and ABCB5 was performed. Enhanced expression of IL-8, CXCR1 and ABCB5 was observed in the sphere-derived cells compared to the parental cells in all the cell lines analyzed except for Caki1 cells (Fig. 2B). Western blot and immunohistochemical analysis showed an increased level of IL-8 and CXCR1 in the sphere-derived cells compared to the parental cells in all RCC-derived cell lines (Fig. 2C and D). Interestingly, Caki1 cells showed increased levels of IL-8 and CXCR1 on protein level which was not observed using qPCR. However, Caki1 cells had high basal IL-8 expression level on qPCR making any difference hard to detect. These results indicate that cancer stem-like cells express high contents of IL-8 and its receptor CXCR1. These results were also confirmed by Flow cytometry analysis. Two lung cancer cell lines (H460 and A549) were exploited to determine the gating strategy for CXCR1. As described by Zhu and co-authors, H460 cell line express CXCR1 at high levels, therefore it served as positive control (60). On the other hand, A549 showed low CXCR1 levels (Suppl. Fig. 2B).

The Hoechst side population (SP) analysis is one of the several strategies used to identify stem cell populations. The ability to discriminate the SP is based on the differential efflux of Hoechst 33342 by a multi-drug resistance transporter. Stem cells possess higher activity and/or higher amount of the multi-drug transporters. Therefore, SP stands out as the portion of cells able to extrude the dye against a concentration gradient when compared to cells not having stem cell features. Therefore, SP was identified as the portion of events that disappeared upon treatment with 100 µM verapamil which blocks the efflux of Hoechst in the CSCs (Fig. 3A). All parental RCC cell lines analyzed exhibited the presence of a CSC SP (3.85 % ± 1.6 %) expressing CXCR1 (6.9 % ± 1.6 %). Of note, sphere-derived SP increased by more than three times (14.6 % ± 0.7 %) compared to the parental cell lines and the total CXCR1 population increased twice (17.1 % ± 8.9 %; Fig. 3C; Suppl. Fig. 3A, B and C). For instance, spheres-derived from Caki1 cell line contained 16.3 % of $CXCR1^+$ cells, which mainly overlapped for 91.9 % with $CXCR1^+$ cells in the side population compartment (Fig. 3A). A

primary culture derived from patient primary tumor showed reduced CSC content represented by only 1.1 % SP. This population was mainly composed for 70 % of $CXCR1^+$ cells (Fig. 3B). In line with our previous results, spheres displayed increased content of CSCs, here depicted by the SP, and $CXCR1^+$ cells compared to parental samples. Surprisingly, SP values in the spheres and parental cells were very similar between metastasis-derived cultures and primary tumor-derived cultures suggesting that not all cells contained in the side population may have the ability to form spheres in culture. In addition, in some cases $CXCR1^+$ cells were more frequent than SP cells indicating that also non-CSCs may express CXCR1 (Fig. 3C).

As previously reported in the literature, IL-8 also interacts with CXCR2, and therefore we also investigated whether CXCR2 may play a role in promoting the cancer stem cell phenotype. Interestingly, preliminary data suggests that CXCR1 but not CXCR2 is involved in this process (Suppl. Fig. 3D). CXCR2 was found expressed by over 60 % of the cells including the CSC population by flow cytometry (Fig. 3C). Moreover, western blot analysis revealed no difference in the protein expression between sphere-derived cells and parental cells (Suppl. Fig. 3E). Therefore, from this point on we focused our attention on CXCR1.

CXCR1 blockage was achieved by either using anti-CXCR1 antibody (20 µg/ml) or the small molecule repertaxin (100 nM). Whereas the human recombinant IL-8 (1 µg/ml) was employed for IL-8 stimulation. Increased cell proliferation was observed after 72 h treatment using human recombinant IL-8, whereas the opposite was observed when adding anti-CXCR1 antibody (Suppl. Fig. 4A). Additionally, IL-8 treatment was found to enhance cell invasion and migration using the real time cell analyzer XCELLigence in all the cell lines tested, most pronounced for Caki1 and ACHN (Suppl. Fig. 4B). CXCR1 blockade showed opposite or no effect, whereas the combination of treatments showed intermediate increase of invasive and migratory properties indicating that IL-8 may also act through other signaling pathways (Suppl. Fig. 4B). To test the effect of IL-8/CXCR1 on tumorsphere formation, cells were incubated for 72 h in the sphere formation assay under anti-CXCR1ab, repertaxin or IL-8 treatment. Anti-CXCR1ab slightly decreased sphere formation, whereas IL-8 treatment increased sphere content by 1.5-fold in all the cell lines analyzed (Fig. 4A and B). Repertaxin alone or in combination with IL-8

did not show any major effect on sphere formation except for 769P where it significantly decreased sphere formation (Fig. 4A and B). Additionally, 20 % increase in the sphere number was observed over enrichment passages upon IL-8 treatment in Caki1 and 769P (data not shown). 72 h pre-treatment of cells prior sphere formation assay did not improve the effect observed previously.

Additionally, flow cytometry analysis revealed that 72 h treatment with repertaxin significantly decreased side population and $CXCR1^+$ cells in the spheres as well as in the parental samples (Supplementary Table 4; Suppl. Fig. 5 A, B, C and D). For instance, in Caki1 spheres, the $CXCR1^+$ side population decreased of about 50 % upon repertaxin treatment going from 84.8 % to 44.5 % $CXCR1^+$ cells (Fig. 4C and D). Surprisingly, repertaxin treatment alone as well as combined with sunitinib (standard of care in ccRCC patients) did not show any effect in the clonogenic assay (Suppl. Fig. 4C and D).

Taken together these results indicate that IL-8 stimulates cell proliferation and invasion as well as cancer stem cell formation and self-renewal. On the contrary, CXCR1 blockade decreases cell proliferation, cell invasion and cancer stem cell properties.

The IL-8/CXCR1 axis is essential for tumor development and metastasis formation in vivo

Sphere-derived cells as well as parental cells isolated from Caki1 were capable to give rise to tumors when injected into NSG mice at three different cell densities (10^6, 10^4, 10^2). However, in each case tumor formation and growth was enhanced when tumor cells derived from the spheres were injected compared to parental cells. For instance, Caki1 spheres injected at 10^6 cells reached the tumor size of 1 cm^3 after only 19 days, whereas mice injected with parental cells harbored less than half of the tumor size (358.1 ± 187.4 mm) after the same time period (Fig. 5A and B).

Mice injected with 10^2 parental cells did eventually develop tumors at the site of injection after 70 days post-injection, time point in which tumors derived from spheres were already harvested. Caki1 cell line is derived from a metastatic tumor; therefore, these cells are more

aggressive and prone to tumor formation. In fact, metastasis-derived cultures contained more stem cells than primary tumor-derived cell lines. In support of this, sphere-derived cells from 769P developed tumors when injected into NSG mice as low as 10^2 cells (Suppl. Fig. 6A and B). Whereas, no tumor formation was observed after over 130 days post-injection when parental cells were injected into NSG mice at the cell density of 10^6, 10^4, or 10^2.

Xenografted tumors histologically resembled the ccRCC subtype and were positive for the kidney marker Pax8 and the epithelial marker PanCKa (Fig. 5C; Suppl. Fig. 6C). Interestingly, tumors derived from spheres showed higher CXCR1 and IL-8 expression in IHC compared to tumors derived from parental cells (Fig. 5C; Suppl. Fig. 6C).

Mice injected with sphere-derived cells did harbor micrometastasis preferentially in lung and liver, whereas mice injected with parental cells did not show the presence of micrometastasis (Fig. 5D; Suppl. Fig. 6D and E). Interestingly, macrometastasis were identified when mice received sphere-derived cells at a density of 10^4 but not 10^6. This is most likely due to the much shorter time-span required for primary tumor to reach 1 cm^3 in mice which received 10^6 cells, at which point the mice were sacrificed (Suppl. Fig. 6F; Suppl. Table 5).

Xenografted primary tumors isolated from mice as soon as they had grown to 1 cm^3, were dissociated and re-injected into new NSG mice at a cell density of 10^4 cells. Xenografted primary tumors were re-transplanted for a further two generations. Strikingly, enhanced tumor growth was observed upon each re-transplantation (Fig. 5F). Each time the primary xenograft was harvested and dissociated, part of the single cell suspension generated was used to analyze the $CXCR1^+$ population by flow cytometry. Interestingly, $CXCR1^+$ cells also increased in number upon each re-transplantation. For instance, dissociated tumor cells derived from Caki1 sphere xenografts included 19.3 % of $CXCR1^+$ cells in the first round of transplants that increased to 23.4 % in the second round, and finally reached 34.4 % in the third round of transplantations (Fig. 5G). Unexpectedly, side populations used to identify CSCs *in vitro* were not found within the primary xenografted tumors. At the same time, another portion of the dissociated tumor tissue was plated into the sphere formation assay. As expected, tumor cells

were capable to reform spheres in culture indicating that they retain stem cell features (Fig. 5E; Suppl. Fig. 6G).

IL-8/CXCR1 expression correlates negatively with clinical prognosis in ccRCC patients

In order to investigated the translational relevance of the IL-8/CXCR1 axis to the clinic, IL-8 and CXCR1 protein expression was evaluated in 255 ccRCC patients using tissue microarrays and staining intensities were classified in absent, moderate and strong (Fig. 6A and C, Suppl. Fig. 7A). We found a striking negative correlation between IL-8 and CXCR1 with overall survival of ccRCC patients with a p-value of 0.004 and 0.027, respectively (Fig. 6B and D). In particular, the median survival for ccRCC patients expressing high IL-8 levels was 48 months, whereas patients expressing low IL-8 levels showed an improved median survival to 84 months. High CXCR1 levels showed a median survival of 57 months, whereas low CXCR1 showed an extension of the medium survival to 93 months.

Additionally, the RNA expression of IL-8 was investigated in 90 patients affected by ccRCC (61). The RNA expression was compared to normal kidney tissue (n = 5). Significantly higher IL-8 expression was found in metastatic ccRCC (n = 32; p-value: 0.0001; Fig. 6E) compared to normal tissue, and a positive trend was observed in relation to tumor grade and stage in ccRCC patients (Suppl. Fig. 7B). In addition, IL-8 was found positively correlated with tumor lymphocytes infiltration (p-value: 0.0125; Fig. 6F), and decreased overall survival (p-value: 0.009; Suppl. Fig. 7C and D).

Taken together, the IL-8/CXCR1 axis represents a prognostic factor as well as a novel therapeutic target for ccRCC patients.

DISCUSSION

Characterized by high intra- and inter-tumor heterogeneity renal cell carcinoma is resistant to chemo- and radiotherapy in metastatic stage. Growing evidence suggests that ccRCCs as other solid tumors possess a rare population of cells contributing to metastasis and resistance to therapy namely CSCs (9). Therefore, identifying CSCs and understanding the mechanism underlying self-renewal properties is essential for dissecting tumor heterogeneity and drug treatment efficiency. In our study, we isolated CSCs derived from RCC cell lines as well as primary tissues expressing high levels of the chemokine IL-8 and its receptor CXCR1. Interestingly, we found that IL-8/CXCR1 axis was associated with CSC-like properties *in vitro* and *in vivo*. Further, IL-8 expression correlated with intratumoral lymphocytic infiltration and decreased overall survival in ccRCC patients, indicating its prognostic and therapeutic implications for ccRCC patients.

Several markers were found specifically expressed in cancer stem cells and cancer-like stem cells derived from RCC such as CD105, ALDH1, OCT4, CD133 and CXCR4 (25-32). However, contrasting results on these markers are reported in the literature (36-39), increasing the need of new biomarkers. On the contrary to the majority of the studies whereby cancer stem cells were isolated by antigen-based techniques, in the present work, functional studies and *in vivo* models were used to identify a potential new biomarker for targeting renal CSCs. The sphere formation assay allowed us to isolate cancer stem cells from RCC cell lines and primary cultures. Interestingly, metastasis-derived cultures showed pronounced sphere formation efficiency and self-renewal properties compared to the primary tumor-derived cultures indicating an increased CSC fraction in the metastatic sites compared to primary tumors. For instance, the metastatic RCC cell line Caki1 showed 2 % sphere formation efficiency and 6 % of CSCs embodied by SP. Whereas primary culture derived RCC cell line 769P only 0.5 % sphere formation efficiency and 3.8 % CSCs by analysis of the SP in flow cytometry. Cancer cells isolated by the sphere formation assay displayed self-renewal properties, upregulation of EMT markers (Vimentin, Snail/Slug and N-cadherin), stemness and developmental genes

(CD105, CD44, CXCR4, ALDH1A1, Nanog, MYC and WNT). Spheres expressed low levels of E-cadherin and differentiation markers such as CD10 and CD13. Additionally, they were able to differentiate into adipocytes upon induction.

It has been previously reported that hypoxia and enhanced expression and activity of HIF1 and HIF2 in cancer stem/progenitor cells and their progeny frequently occur during disease progression and metastases, and may induce the expression of several genes involved in self-renewal, survival, metabolism, angiogenesis, invasion, migration and resistance to therapy (62,63). In our study, CSC properties were enhanced upon hypoxia incubation and higher expression of HIFs was observed in the spheres compared to parental cells. Moreover, higher levels of the drug transporter ABCB5 as well as the chemokine IL-8 and its receptor CXCR1 but not CXCR2 were found on RNA and protein level by Western blot, IHC and flow cytometry. Interestingly, the drug efflux transporter ABCB5 is functionally involved in the regulation of IL-8/CXCR1 signaling through IL1β in melanoma cells and has therefore been associated with cancer stem-like cells, clinical disease progression and tumor recurrence (40,45). Additionally, IL-8 and CXCR1/2 have recently been demonstrated to be associated with cancer stem cell populations in many tumor types such as breast, prostate, colon and pancreatic cancers (47-50). However, CXCR1 and CXCR2 were found expressed independently or together in different tumor types, indicating they may have different influence on CSC activity (47,50,64). In line with previous studies in HCC, breast and pancreatic cancers where anti-IL-8/CXCR1 impaired CSC features (40,47,49), ccRCC cultures treated with CXCR1 blocking agents (anti-CXCR1ab and repertaxin) showed reduced proliferation, migration and invasion, sphere formation and self-renewal properties, whereas IL-8 stimulation enhanced CSC properties. Moreover, flow cytometry analysis revealed that repertaxin treatment significantly decreased side population and $CXCR1^+$ cells in the spheres as well in the parental samples. Surprisingly, no effect in the clonogenic assay was observed after repertaxin treatment compared to the standard of care sunitinib. When injected subcutaneously into NSG mice, sphere-derived cells gave rise to tumors and metastasis in only 20 days. Whereas, parental cells derived exclusively from the metastatic ccRCC culture Caki1 were only able to form tumors after over 100 days.

This data also support the idea that metastasis-derived cultures possess an increased CSC content. Interestingly, high IL-8 and CXCR1 levels were found in the xenograft tumor tissue derived from spheres. In addition, CXCR1 expression as well as tumor development were enhanced upon tumor transplantation. These results suggest that transplantation fosters the expansion of CSCs, thus, $CXCR1^{+}$ populations may play a key role in tumor progression.

IL-8 represents one of the major chemokines associated with the promotion of neutrophils and inflammatory response (40). Increased expression of IL-8 is potentially an independent adverse prognostic biomarker for CSS and RFS in patients with ccRCC after nephrectomy (65).

In our study, significantly higher IL-8 levels were found in metastatic ccRCCs compared to normal tissue, and a positive trend was observed in relation to tumor grade and stage in ccRCC patients. Moreover, IL-8 was found to be positively correlated with tumor lymphocytes infiltration, poor prognosis and decreased overall survival. Interestingly, in ccRCC increased IL-8 expression were associated with sunitinib resistance *in vitro* and *in vivo* (66). Taken together, these results suggest that the IL-8/CXCR1 axis is associated with cancer stem cell-like properties in renal cancer and represents a potential therapeutic target for ccRCC patients. Targeting IL-8 in combination with conventional chemotherapy agents and/or immunotherapy would be the next step towards overcoming tumor recurrence.

REFERENCES

1. Moch H. Kidey Cancer. Lyon, Fr.: Int. Agency Res. Cancer/World Health Organ; 2014. 2-9 p.
2. Bhatt JR, Finelli A. Landmarks in the diagnosis and treatment of renal cell carcinoma. Nat Rev Urol **2014**;11(9):517-25 doi 10.1038/nrurol.2014.194.
3. Moch H. [The WHO/ISUP grading system for renal carcinoma]. Pathologe **2016**;37(4):355-60 doi 10.1007/s00292-016-0171-y.
4. Kaelin WG. Von Hippel-Lindau disease. Annu Rev Pathol **2007**;2:145-73 doi 10.1146/annurev.pathol.2.010506.092049.
5. Zhang Q, Yang H. The Roles of VHL-Dependent Ubiquitination in Signaling and Cancer. Frontiers in oncology **2012**;2:35 doi 10.3389/fonc.2012.00035.
6. Choueiri TK, Fay AP, Gagnon R, Lin Y, Bahamon B, Brown V*, et al.* The role of aberrant VHL/HIF pathway elements in predicting clinical outcome to pazopanib therapy in patients with metastatic clear-cell renal cell carcinoma. Clin Cancer Res **2013**;19(18):5218-26 doi 10.1158/1078-0432.CCR-13-0491.
7. Gossage L, Eisen T. Alterations in VHL as potential biomarkers in renal-cell carcinoma. Nat Rev Clin Oncol **2010**;7(5):277-88 doi nrclinonc.2010.42 [pii] 10.1038/nrclinonc.2010.42.
8. Clark PE. The role of VHL in clear-cell renal cell carcinoma and its relation to targeted therapy. Kidney Int **2009**;76(9):939-45 doi 10.1038/ki.2009.296.
9. Bussolati B, Bruno S, Grange C, Ferrando U, Camussi G. Identification of a tumor-initiating stem cell population in human renal carcinomas. FASEB journal : official publication of the Federation of American Societies for Experimental Biology **2008**;22(10):3696-705 doi 10.1096/fj.08-102590.
10. Shackleton M, Quintana E, Fearon ER, Morrison SJ. Heterogeneity in cancer: cancer stem cells versus clonal evolution. Cell **2009**;138(5):822-9 doi 10.1016/j.cell.2009.08.017.
11. Kreso A, Dick JE. Evolution of the cancer stem cell model. Cell stem cell **2014**;14(3):275-91 doi 10.1016/j.stem.2014.02.006.
12. Nguyen LV, Vanner R, Dirks P, Eaves CJ. Cancer stem cells: an evolving concept. Nature reviews Cancer **2012**;12(2):133-43 doi 10.1038/nrc3184.
13. Flemming A. Cancer stem cells: Targeting the root of cancer relapse. Nat Rev Drug Discov **2015**;14(3):165 doi 10.1038/nrd4560.
14. Bonnet D, Dick JE. Human acute myeloid leukemia is organized as a hierarchy that originates from a primitive hematopoietic cell. Nat Med **1997**;3(7):730-7.
15. Collins AT, Berry PA, Hyde C, Stower MJ, Maitland NJ. Prospective identification of tumorigenic prostate cancer stem cells. Cancer Res **2005**;65(23):10946-51 doi 10.1158/0008-5472.CAN-05-2018.
16. Fang D, Nguyen TK, Leishear K, Finko R, Kulp AN, Hotz S*, et al.* A tumorigenic subpopulation with stem cell properties in melanomas. Cancer Res **2005**;65(20):9328-37 doi 10.1158/0008-5472.CAN-05-1343.
17. Hermann PC, Bhaskar S, Cioffi M, Heeschen C. Cancer stem cells in solid tumors. Seminars in Cancer Biology **2010**;20(2):77-84 doi https://doi.org/10.1016/j.semcancer.2010.03.004.
18. Hermann PC, Bhaskar S, Cioffi M, Heeschen C. Cancer stem cells in solid tumors. Semin Cancer Biol **2010**;20(2):77-84 doi 10.1016/j.semcancer.2010.03.004.
19. Kim CF, Jackson EL, Woolfenden AE, Lawrence S, Babar I, Vogel S*, et al.* Identification of bronchioalveolar stem cells in normal lung and lung cancer. Cell **2005**;121(6):823-35 doi 10.1016/j.cell.2005.03.032.
20. Ma S, Chan KW, Hu L, Lee TK, Wo JY, Ng IO*, et al.* Identification and characterization of tumorigenic liver cancer stem/progenitor cells. Gastroenterology **2007**;132(7):2542-56 doi 10.1053/j.gastro.2007.04.025.

21. O'Brien CA, Pollett A, Gallinger S, Dick JE. A human colon cancer cell capable of initiating tumour growth in immunodeficient mice. Nature **2007**;445(7123):106-10 doi 10.1038/nature05372.
22. Ricci-Vitiani L, Lombardi DG, Pilozzi E, Biffoni M, Todaro M, Peschle C*, et al.* Identification and expansion of human colon-cancer-initiating cells. Nature **2007**;445(7123):111-5 doi 10.1038/nature05384.
23. Schatton T, Murphy GF, Frank NY, Yamaura K, Waaga-Gasser AM, Gasser M*, et al.* Identification of cells initiating human melanomas. Nature **2008**;451(7176):345-9 doi 10.1038/nature06489.
24. Singh SK, Hawkins C, Clarke ID, Squire JA, Bayani J, Hide T*, et al.* Identification of human brain tumour initiating cells. Nature **2004**;432(7015):396-401 doi 10.1038/nature03128.
25. Bussolati B, Brossa A, Camussi G. Resident stem cells and renal carcinoma. International journal of nephrology **2011**;2011:286985 doi 10.4061/2011/286985.
26. Grange C, Tapparo M, Collino F, Vitillo L, Damasco C, Deregibus MC*, et al.* Microvesicles released from human renal cancer stem cells stimulate angiogenesis and formation of lung premetastatic niche. Cancer Res **2011**;71(15):5346-56 doi 10.1158/0008-5472.CAN-11-0241.
27. Kim K, Ihm H, Ro JY, Cho YM. High-level expression of stem cell marker CD133 in clear cell renal cell carcinoma with favorable prognosis. Oncology letters **2011**;2(6):1095-100 doi 10.3892/ol.2011.365.
28. Ueda K, Ogasawara S, Akiba J, Nakayama M, Todoroki K, Ueda K*, et al.* Aldehyde dehydrogenase 1 identifies cells with cancer stem cell-like properties in a human renal cell carcinoma cell line. PLoS One **2013**;8(10):e75463 doi 10.1371/journal.pone.0075463.
29. Varna M, Gapihan G, Feugeas JP, Ratajczak P, Tan S, Ferreira I*, et al.* Stem cells increase in numbers in perinecrotic areas in human renal cancer. Clin Cancer Res **2015**;21(4):916-24 doi 10.1158/1078-0432.CCR-14-0666.
30. Struckmann K, Mertz K, Steu S, Storz M, Staller P, Krek W*, et al.* pVHL co-ordinately regulates CXCR4/CXCL12 and MMP2/MMP9 expression in human clear-cell renal cell carcinoma. J Pathol **2008**;214(4):464-71 doi 10.1002/path.2310.
31. Xiao W, Gao Z, Duan Y, Yuan W, Ke Y. Notch signaling plays a crucial role in cancer stem-like cells maintaining stemness and mediating chemotaxis in renal cell carcinoma. J Exp Clin Cancer Res **2017**;36(1):41 doi 10.1186/s13046-017-0507-3.
32. Baracca A, Sgarbi G, Solaini G, Lenaz G. Rhodamine 123 as a probe of mitochondrial membrane potential: evaluation of proton flux through F(0) during ATP synthesis. Biochimica et biophysica acta **2003**;1606(1-3):137-46.
33. Saroufim A, Messai Y, Hasmim M, Rioux N, Iacovelli R, Verhoest G*, et al.* Tumoral CD105 is a novel independent prognostic marker for prognosis in clear-cell renal cell carcinoma. Br J Cancer **2014**;110(7):1778-84 doi 10.1038/bjc.2014.71.
34. Myszczyszyn A, Czarnecka AM, Matak D, Szymanski L, Lian F, Kornakiewicz A*, et al.* The Role of Hypoxia and Cancer Stem Cells in Renal Cell Carcinoma Pathogenesis. Stem Cell Rev **2015**;11(6):919-43 doi 10.1007/s12015-015-9611-y.
35. Bruno S, Bussolati B, Grange C, Collino F, Graziano ME, Ferrando U*, et al.* CD133+ renal progenitor cells contribute to tumor angiogenesis. Am J Pathol **2006**;169(6):2223-35 doi 10.2353/ajpath.2006.060498.
36. Song L, Ye W, Cui Y, Lu J, Zhang Y, Ding N*, et al.* Ecto-5'-nucleotidase (CD73) is a biomarker for clear cell renal carcinoma stem-like cells. Oncotarget **2017** doi 10.18632/oncotarget.16667.
37. Peired AJ, Sisti A, Romagnani P. Mesenchymal Stem Cell-Based Therapy for Kidney Disease: A Review of Clinical Evidence. Stem Cells Int **2016**;2016:4798639 doi 10.1155/2016/4798639.
38. Zhang Y, Sun B, Zhao X, Liu Z, Wang X, Yao X*, et al.* Clinical significances and prognostic value of cancer stem-like cells markers and vasculogenic mimicry in renal cell carcinoma. J Surg Oncol **2013**;108(6):414-9 doi 10.1002/jso.23402.

39. Abourbih S, Sircar K, Tanguay S, Kassouf W, Aprikian A, Mansure J*, et al.* Aldehyde dehydrogenase 1 expression in primary and metastatic renal cell carcinoma: an immunohistochemistry study. World J Surg Oncol **2013**;11:298 doi 10.1186/1477-7819-11-298.
40. Park SY, Han J, Kim JB, Yang MG, Kim YJ, Lim HJ*, et al.* Interleukin-8 is related to poor chemotherapeutic response and tumourigenicity in hepatocellular carcinoma. Eur J Cancer **2014**;50(2):341-50 doi 10.1016/j.ejca.2013.09.021.
41. Liu Q, Li A, Tian Y, Wu JD, Liu Y, Li T*, et al.* The CXCL8-CXCR1/2 pathways in cancer. Cytokine Growth Factor Rev **2016**;31:61-71 doi 10.1016/j.cytogfr.2016.08.002.
42. Waugh DJ, Wilson C. The interleukin-8 pathway in cancer. Clin Cancer Res **2008**;14(21):6735-41 doi 10.1158/1078-0432.CCR-07-4843.
43. Lindoso RS, Collino F, Camussi G. Extracellular vesicles derived from renal cancer stem cells induce a pro-tumorigenic phenotype in mesenchymal stromal cells. Oncotarget **2015**;6(10):7959-69 doi 10.18632/oncotarget.3503.
44. Maxwell PJ, Gallagher R, Seaton A, Wilson C, Scullin P, Pettigrew J*, et al.* HIF-1 and NF-kappaB-mediated upregulation of CXCR1 and CXCR2 expression promotes cell survival in hypoxic prostate cancer cells. Oncogene **2007**;26(52):7333-45 doi 10.1038/sj.onc.1210536.
45. Wilson BJ, Saab KR, Ma J, Schatton T, Putz P, Zhan Q*, et al.* ABCB5 maintains melanoma-initiating cells through a proinflammatory cytokine signaling circuit. Cancer Res **2014**;74(15):4196-207 doi 10.1158/0008-5472.CAN-14-0582.
46. Chevrier S, Levine JH, Zanotelli VRT, Silina K, Schulz D, Bacac M*, et al.* An Immune Atlas of Clear Cell Renal Cell Carcinoma. Cell **2017**;169(4):736-49 e18 doi 10.1016/j.cell.2017.04.016.
47. Chen L, Fan J, Chen H, Meng Z, Chen Z, Wang P*, et al.* The IL-8/CXCR1 axis is associated with cancer stem cell-like properties and correlates with clinical prognosis in human pancreatic cancer cases. Sci Rep **2014**;4:5911 doi 10.1038/srep05911.
48. Chen Y, Shi M, Yu GZ, Qin XR, Jin G, Chen P*, et al.* Interleukin-8, a promising predictor for prognosis of pancreatic cancer. World J Gastroenterol **2012**;18(10):1123-9 doi 10.3748/wjg.v18.i10.1123.
49. Ginestier C, Liu S, Diebel ME, Korkaya H, Luo M, Brown M*, et al.* CXCR1 blockade selectively targets human breast cancer stem cells in vitro and in xenografts. J Clin Invest **2010**;120(2):485-97 doi 10.1172/JCI39397.
50. Lee YS, Choi I, Ning Y, Kim NY, Khatchadourian V, Yang D*, et al.* Interleukin-8 and its receptor CXCR2 in the tumour microenvironment promote colon cancer growth, progression and metastasis. Br J Cancer **2012**;106(11):1833-41 doi 10.1038/bjc.2012.177.
51. Humphrey PA, Moch H, Cubilla AL, Ulbright TM, Reuter VE. The 2016 WHO Classification of Tumours of the Urinary System and Male Genital Organs-Part B: Prostate and Bladder Tumours. Eur Urol **2016**;70(1):106-19 doi 10.1016/j.eururo.2016.02.028.
52. Moch H, Schraml P, Bubendorf L, Mirlacher M, Kononen J, Gasser T*, et al.* High-Throughput Tissue Microarray Analysis to Evaluate Genes Uncovered by cDNA Microarray Screening in Renal Cell Carcinoma. The American Journal of Pathology **1999**;154(4):981-6.
53. von Teichman A, Comperat E, Behnke S, Storz M, Moch H, Schraml P. VHL mutations and dysregulation of pVHL- and PTEN-controlled pathways in multilocular cystic renal cell carcinoma. Modern pathology : an official journal of the United States and Canadian Academy of Pathology, Inc **2011**;24(4):571-8 doi 10.1038/modpathol.2010.222.
54. Bodenmiller B, Zunder ER, Finck R, Chen TJ, Savig ES, Bruggner RV*, et al.* Multiplexed mass cytometry profiling of cellular states perturbed by small-molecule regulators. Nat Biotechnol **2012**;30(9):858-67 doi 10.1038/nbt.2317.

55. Finck R, Simonds EF, Jager A, Krishnaswamy S, Sachs K, Fantl W*, et al.* Normalization of mass cytometry data with bead standards. Cytometry A **2013**;83(5):483-94 doi 10.1002/cyto.a.22271.
56. Zunder ER, Finck R, Behbehani GK, Amir el AD, Krishnaswamy S, Gonzalez VD*, et al.* Palladium-based mass tag cell barcoding with a doublet-filtering scheme and single-cell deconvolution algorithm. Nat Protoc **2015**;10(2):316-33 doi 10.1038/nprot.2015.020.
57. Li Z, Rich JN. Hypoxia and hypoxia inducible factors in cancer stem cell maintenance. Current topics in microbiology and immunology **2010**;345:21-30 doi 10.1007/82_2010_75.
58. Heddleston JM, Li Z, McLendon RE, Hjelmeland AB, Rich JN. The hypoxic microenvironment maintains glioblastoma stem cells and promotes reprogramming towards a cancer stem cell phenotype. Cell Cycle **2009**;8(20):3274-84 doi 10.4161/cc.8.20.9701.
59. Shinojima T, Oya M, Takayanagi A, Mizuno R, Shimizu N, Murai M. Renal cancer cells lacking hypoxia inducible factor (HIF)-1alpha expression maintain vascular endothelial growth factor expression through HIF-2alpha. Carcinogenesis **2007**;28(3):529-36 doi 10.1093/carcin/bgl143.
60. Zhu YM, Webster SJ, Flower D, Woll PJ. Interleukin-8/CXCL8 is a growth factor for human lung cancer cells. Br J Cancer **2004**;91(11):1970-6 doi 10.1038/sj.bjc.6602227.
61. Beleut M, Zimmermann P, Baudis M, Bruni N, Buhlmann P, Laule O*, et al.* Integrative genome-wide expression profiling identifies three distinct molecular subgroups of renal cell carcinoma with different patient outcome. BMC Cancer **2012**;12:310 doi 10.1186/1471-2407-12-310.
62. Bae KM, Dai Y, Vieweg J, Siemann DW. Hypoxia regulates SOX2 expression to promote prostate cancer cell invasion and sphere formation. Am J Cancer Res **2016**;6(5):1078-88.
63. Mimeault M, Batra SK. Hypoxia-inducing factors as master regulators of stemness properties and altered metabolism of cancer- and metastasis-initiating cells. J Cell Mol Med **2013**;17(1):30-54 doi 10.1111/jcmm.12004.
64. Liu YN, Chang TH, Tsai MF, Wu SG, Tsai TH, Chen HY*, et al.* IL-8 confers resistance to EGFR inhibitors by inducing stem cell properties in lung cancer. Oncotarget **2015**;6(12):10415-31 doi 10.18632/oncotarget.3389.
65. An H, Zhu Y, Xie H, Liu Y, Liu W, Fu Q*, et al.* Increased expression of interleukin-8 is an independent indicator of poor prognosis in clear-cell renal cell carcinoma. Tumour Biol **2016**;37(4):4523-9 doi 10.1007/s13277-015-4158-8.
66. Huang D, Ding Y, Zhou M, Rini BI, Petillo D, Qian CN*, et al.* Interleukin-8 mediates resistance to antiangiogenic agent sunitinib in renal cell carcinoma. Cancer Res **2010**;70(3):1063-71 doi 10.1158/0008-5472.CAN-09-3965.

FIGURE LEGEND

Figure 1. A) Nine RCC cell lines named A498, 769P, 786O, RCC4wt, RCC4VHL, SLR21, SLR23, Caki1, and ACHN, were tested in the sphere formation assay. A498, 769P, 786O, Caki1 and ACHN were capable to form spheres, whereas RCC4wt, RCC4VHL, SLR21 and SLR23 did not harbor any sphere. Spheres formed at the first seeding step by primary tumor-derived cultures ranged between 10.2 and 12.4, whereas metastasis-derived cultures showed a more pronounced sphere formation capability, which ranged between 23.4 to 69.8 spheres formed. **B)** 769P, A498, Caki1 and ACHN displayed self-renewal properties by enriching CSCs in over five passages. Again, metastasis-derived RCC cultures (Caki1 and ACHN) showed improved sphere formation compared to primary tumor derived culture (769P and A498). **C)** Representative pictures of the spheres derived from ccRCC cell lines. **D)** Immunohistochemical stains showing enhanced protein expression of the mesenchymal markers Vimentin, N-cadherin and Snail/slug, and decreased expression of E-cadherin indicating EMT in the spheres from Caki1 (upper panel) compared to parental cells (lower panel). Moreover, the cancer stem cell marker CD105 was highly expressed in the spheres. Interestingly, a gel-based shell was found covering the spheres upon formation (arrow head). **E)** Representative pictures of primary culture-derived spheres.

Figure 2. A) CyTOF analysis revealed high expression of CD24, CD44 and CXCR4 in the spheres compared to parental cells where on the contrary CD13, CD10 and E-cadherin were found highly expressed. **B)** Gene expression data showing significantly enhanced expression of IL-8, ABCB5 and CXCR1 in spheres derived from 769P, A498 and ACHN. **C)** Spheres displayed high protein levels of CXCR1 and IL-8 in Western blot. **D)** Representative pictures of IL-8 and CXCR1 upregulation in Caki1 spheres compared to parental cells.

Figure 3. A) 13.1 % of CSCs represented here by the side population were found in Caki1 spheres. Moreover, SP was composed by 91.9 % of $CXCR1^{+}$ cells. SP as well as $CXCR1^{+}$ cells disappeared upon treatment with 100 µM verapamil (0.99 % and 4.55 %, respectively).

We can better appreciate the difference between before and after treatment in the overlaid panel, where the population of interest is highlighted in red and verapamil treatment in blue. **B)** One representative example of primary culture showing low CSC content. Nevertheless, SP was composed for 68.4 % of $CXCR1^+$ cells. Blue: verapamil treatment. Red: population of interest. **C)** High levels of CSCs and $CXCR1^+$ cells were found in the spheres compared to parental cells. $CXCR2^+$ was extremely abundant and not specifically expressed by SP. Therefore, it was not considered as potential CSC marker.

Figure 4. A) Caki1 cells treated in the sphere formation assay with anti-CXCR1ab slightly decreased sphere formation. The opposite effect was observed upon IL-8 treatment. Treatment with repertaxin did not show any significant effect. Combination of treatment using CXCR1 blocking agents together with IL-8 did not show any significant effect. **B)** 769P cells treated in the sphere formation assay with anti-CXCR1ab or repertaxin slightly decreased sphere formation. The opposite effect was observed upon IL-8 treatment. Combination of treatment using CXCR1 blocking agents together with IL-8 did not show any effect compared with anti-CXCR1 treatment alone. **C)** A 3% reduction in the CSC content was observed upon repertaxin treatment by flow cytometry in Caki1 cell line (11.4 % - 7.4 %). Moreover, the whole $CXCR1^+$ population as well as $CXCR1^+$ SP was impaired. **D)** Histograms showing decreased SP and $CXCR1^+$ cells upon repertaxin treatment. The yellow area indicates the number of events for the two specific populations upon verapamil treatment. As expected, no SP and $CXCR1^+$ cells were found after verapamil treatment (internal control). The red area shows the CSC and $CXCR1^+$ populations in the sample. Whereas, the blue area displays the remainder number of events after repertaxin treatment. In this example, we can clearly appreciate the reduction in the CSC population expressing CXCR1 before (red) and after (blue) repertaxin treatment.

Figure 5. A) Tumor growth over time for Caki1 cell line. 10^6 sphere-derived cells injected subcutaneously into NSG mice formed tumors in less than 20 days, whereas parental cells

took around 30 days. **B)** Representative pictures of NSG mice at 19 days post-injection with either parental or sphere cells. Mice that received 10^6 parental cells displayed half of the tumor size compared to mice injected with spheres. **C)** Immunohistochemical stains of the xenografted tumors derived from Caki1 showing the histological subtype by H&E, and the epithelial and kidney nature by PanCKa and Pax8 positivity. CXCR1 and IL-8 were found highly expressed by tumors derived from the spheres compared to tumors derived from parental cells. **D)** Metastasis in lungs and liver were found in mice injected with sphere-derived cells. In this figure micrometastasis derived from Caki1 spheres are depicted. In the H&E images we can appreciate the normal histological structure of the tissue interrupted by clusters of larger cells. Moreover, these cells expressed Pax8 which is a specific kidney marker indicating the renal origin of the cells. **E)** Xenografted tumors were dissociated into single cell suspension and cells were plated into sphere formation assay. Tumor cells derived from both Caki1 xenografts, parental cells and spheres, retained the capability to form spheres *in vitro*. **F)** Three transplantation rounds were performed for those tumors where 10^4 cells were initially injected. The same cell density was used over the passages. Enhanced tumor progression was observed upon transplantation reaching the size of 1 cm^3 after 50 days in the first round, 40 days during the second, and less than 30 days in the third. **G)** $CXCR1^+$ cells increased in number upon transplantation. In yellow are depicted $CXCR1^+$ cells in the first round (19.3 %), in blue the second round (23.4 %), whereas CXCR1+ cells from the third round are shown here in red (34.4 %).

Figure 6. A) IL-8 protein expression on tissue microarrays. Strong IL-8 expression was observed in ccRCC and met. ccRCC compared to normal kidney tissue. **B)** Kaplan-Meier survival curve developed according to the mean IL-8 expression from tissue microarrays showing poor prognosis for patients expressing high IL-8 levels. **C)** CXCR1 protein expression on tissue microarrays. Strong CXCR1 expression was observed in ccRCC and met. ccRCC compared to normal kidney tissue. **D)** Kaplan-Meier survival curve developed according to the mean CXCR1 expression from tissue microarrays showing poor prognosis for patients

881 expressing high CXCR1 levels. **E)** Elevated IL-8 expression on RNA level correlated with the
882 presence of metastasis in ccRCC. **F)** High I-L8 expression on RNA level correlated with tumor
883 lymphocyte infiltration.
884

Figure 1

A

ccRCC cell line	769P	A498	Caki1	ACHN	**ccRCC primary culture**	Primary cells (n=8)	Primary cells (n=2)
Isolation site	Primary tumor	Primary tumor	Metastasis	Metastasis		Primary tumor	Metastasis
Sphere formation	10.2±0.7	12.4±3.0	23.4±2.2	69.8±19.2		11.5±3.3	28.8±4.1

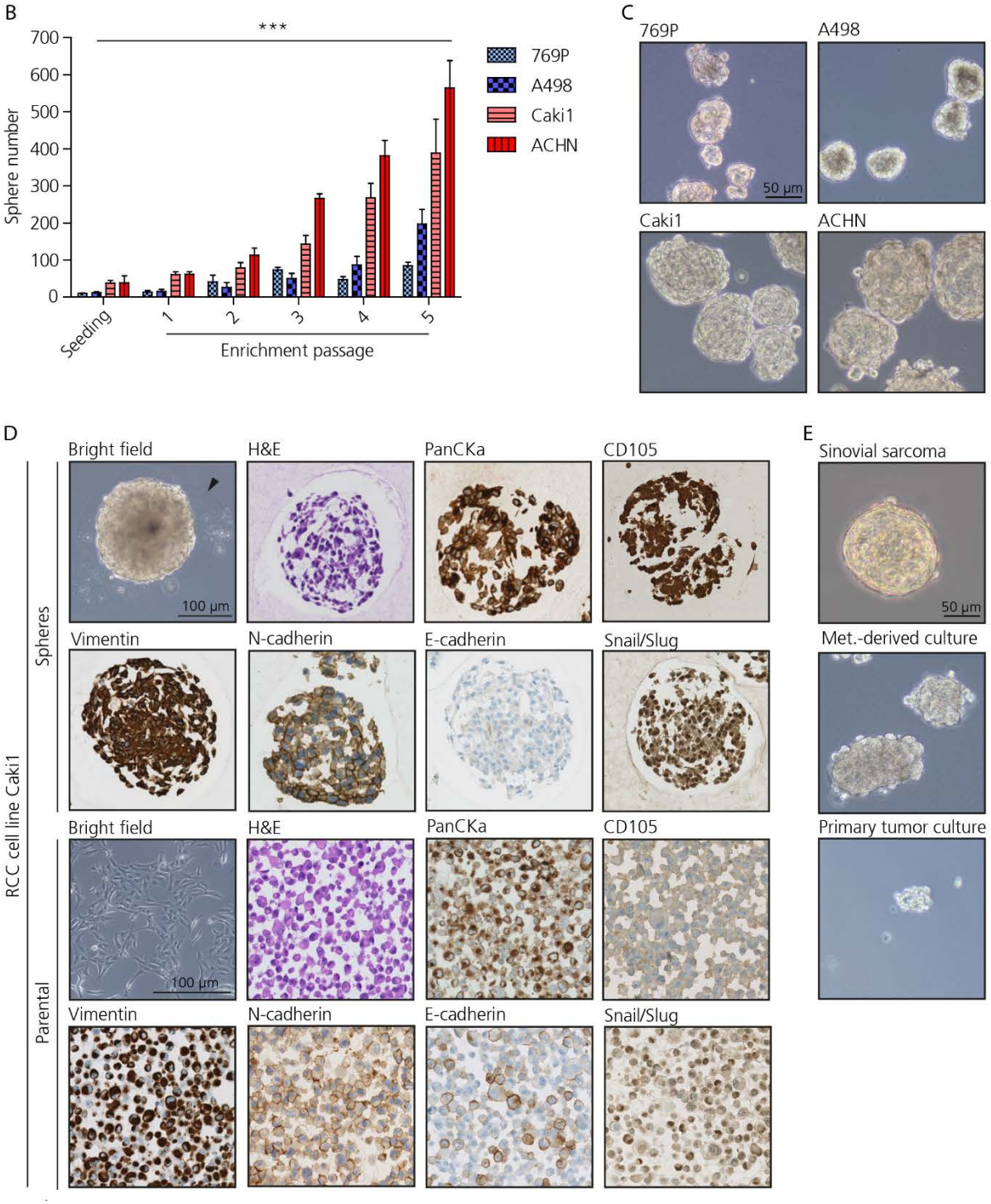

Figure 2

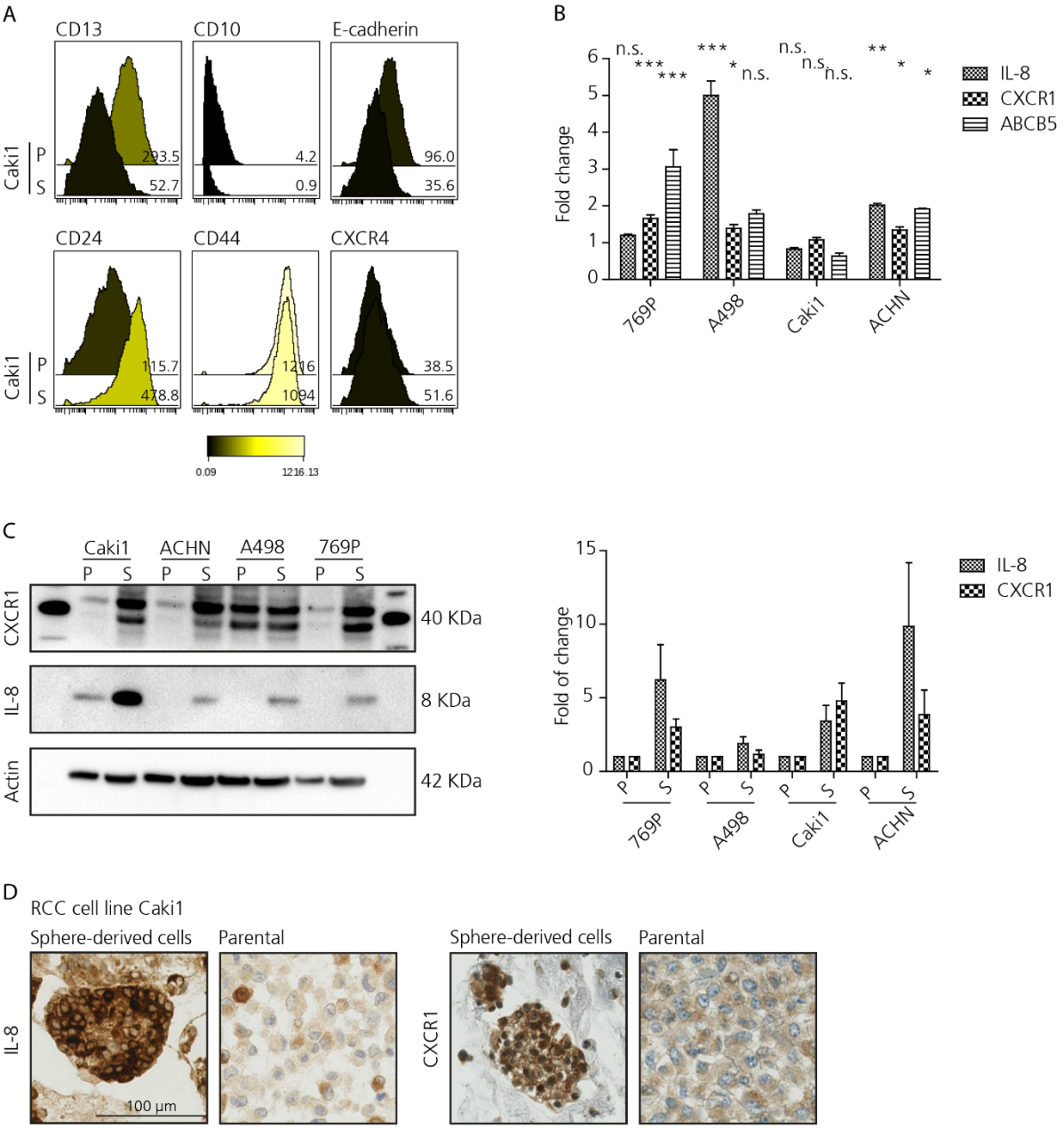
A
CD13
CD10
E-cadherin
Caki1
P
S
293.5
52.7
4.2
0.9
96.0
35.6
CD24
CD44
CXCR4
115.7
478.8
1216
1094
38.5
51.6
0.09
1216.13
B
n.s.
***
***
***
*
n.s.
n.s.
n.s.
**
*
*
Fold change
IL-8
CXCR1
ABCB5
769P
A498
Caki1
ACHN
C
Caki1
ACHN
A498
769P
CXCR1
IL-8
Actin
40 KDa
8 KDa
42 KDa
Fold of change
D
RCC cell line Caki1
Sphere-derived cells
Parental
IL-8
100 µm
CXCR1

Figure 3

A

RCC cell line Caki1, sphere cells

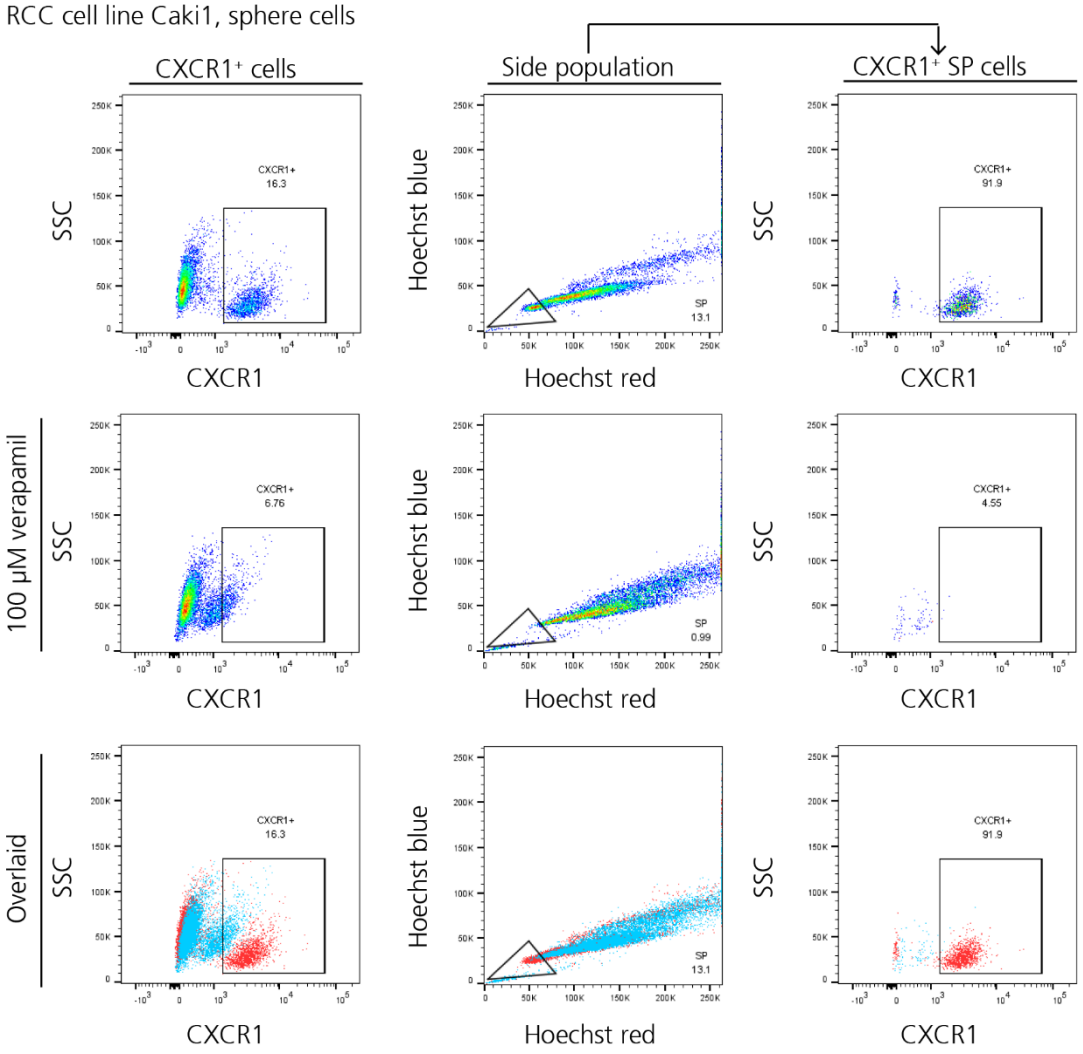

B

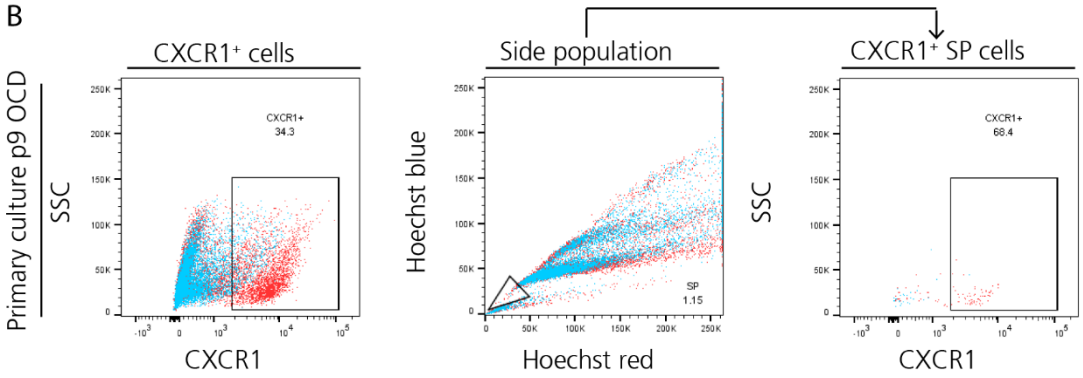

C

	769P		**A498**		**Caki1**		**ACHN**	
	parental	spheres	parental	spheres	parental	spheres	parental	spheres
SP	3.8±0.6	14.6±1.8	3.5±1.9	14.8±2.9	6±0.68	15.3±3.8	2.1±0.7	13.6±7.6
CXCR1	4.7±0.6	9.1±3.3	8.2±0.7	29.9±5	6.6±0.9	15±0.6	8±0.2	14.7±6
CXCR2		72±1.48				64.7±0.2		63±5.2

Figure 4

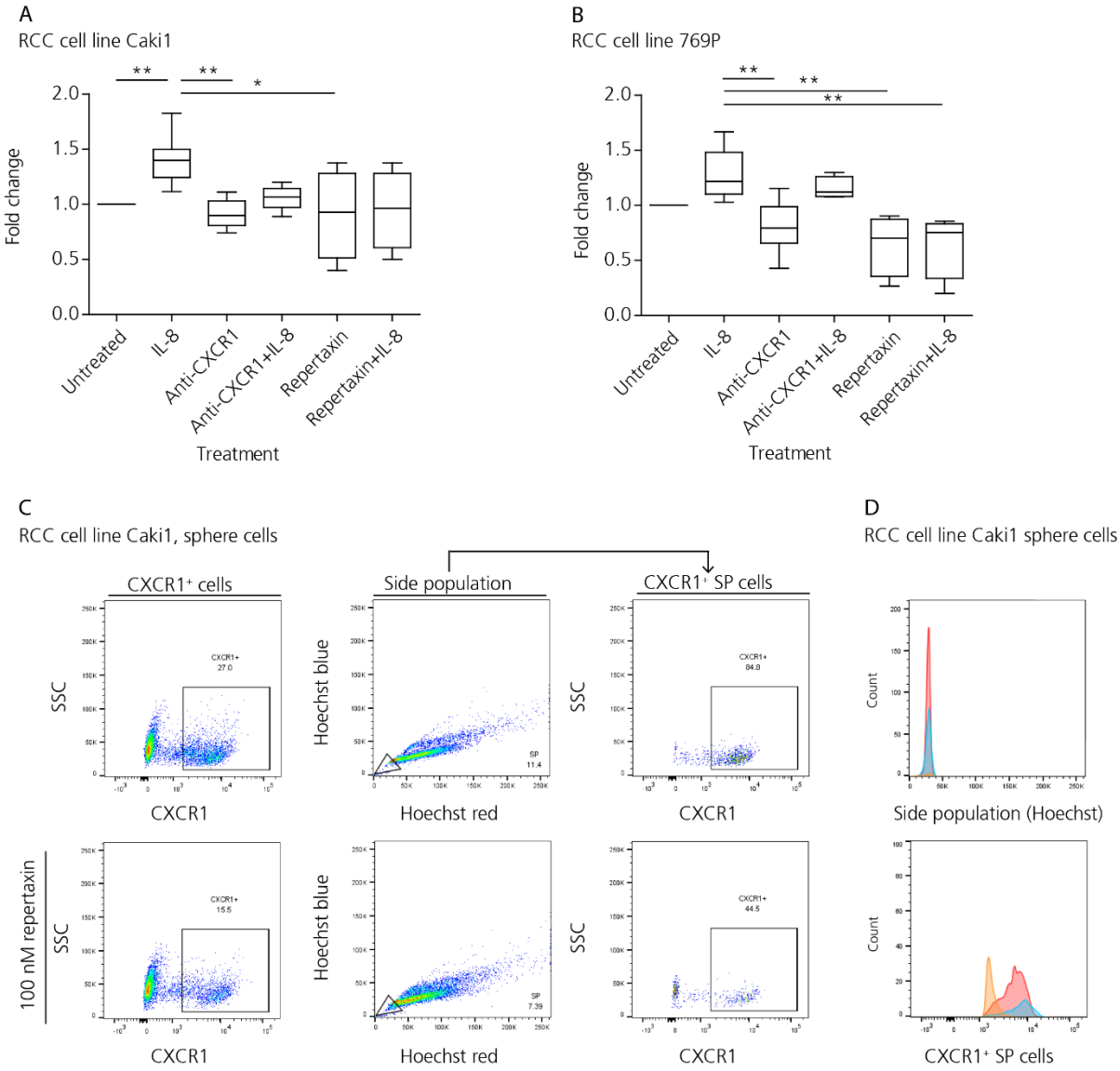
A
RCC cell line Caki1
Fold change
2.0
1.5
1.0
0.5
0.0
**
**
*
Untreated
IL-8
Anti-CXCR1
Anti-CXCR1+IL-8
Repertaxin
Repertaxin+IL-8
Treatment
B
RCC cell line 769P
Fold change
2.0
1.5
1.0
0.5
0.0
**
**
**
Untreated
IL-8
Anti-CXCR1
Anti-CXCR1+IL-8
Repertaxin
Repertaxin+IL-8
Treatment
C
RCC cell line Caki1, sphere cells
CXCR1⁺ cells
Side population
CXCR1⁺ SP cells
SSC
CXCR1
Hoechst blue
Hoechst red
SSC
CXCR1
100 nM repertaxin
SSC
CXCR1
Hoechst blue
Hoechst red
SSC
CXCR1
D
RCC cell line Caki1 sphere cells
Count
Side population (Hoechst)
Count
CXCR1⁺ SP cells

Figure 5

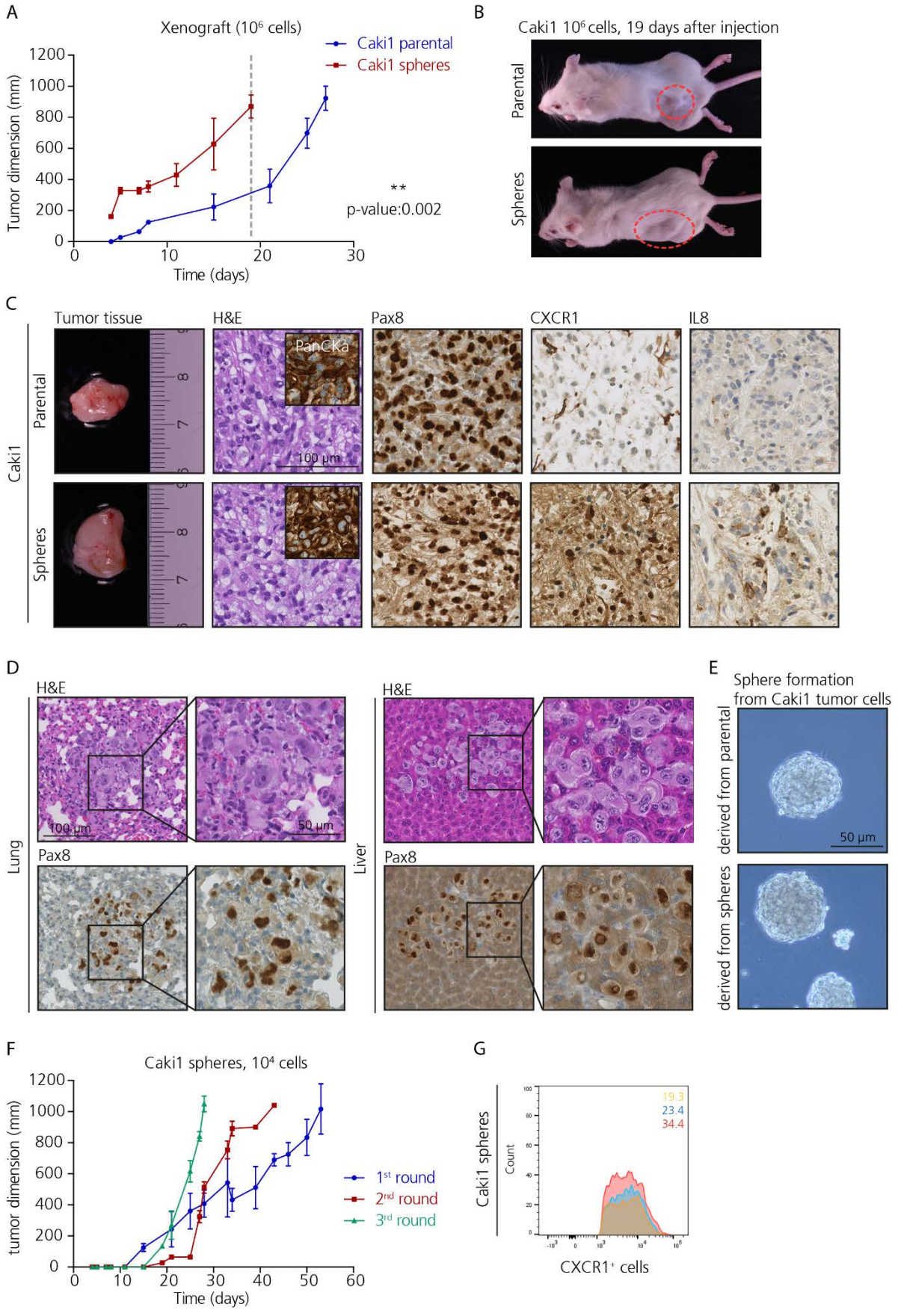
A
Xenograft (10⁶ cells)
Caki1 parental
Caki1 spheres
Tumor dimension (mm)
Time (days)
**
p-value:0.002
B
Caki1 10⁶ cells, 19 days after injection
Parental
Spheres
C
Tumor tissue
H&E
Pax8
CXCR1
IL8
Caki1
Parental
Spheres
PanCKa
100 µm
D
H&E
Pax8
Lung
Liver
100 µm
50 µm
E
Sphere formation from Caki1 tumor cells
derived from parental
derived from spheres
50 µm
F
Caki1 spheres, 10⁴ cells
tumor dimension (mm)
Time (days)
1st round
2nd round
3rd round
G
Caki1 spheres
Count
19.3
23.4
34.4
CXCR1⁺ cells

Figure 6

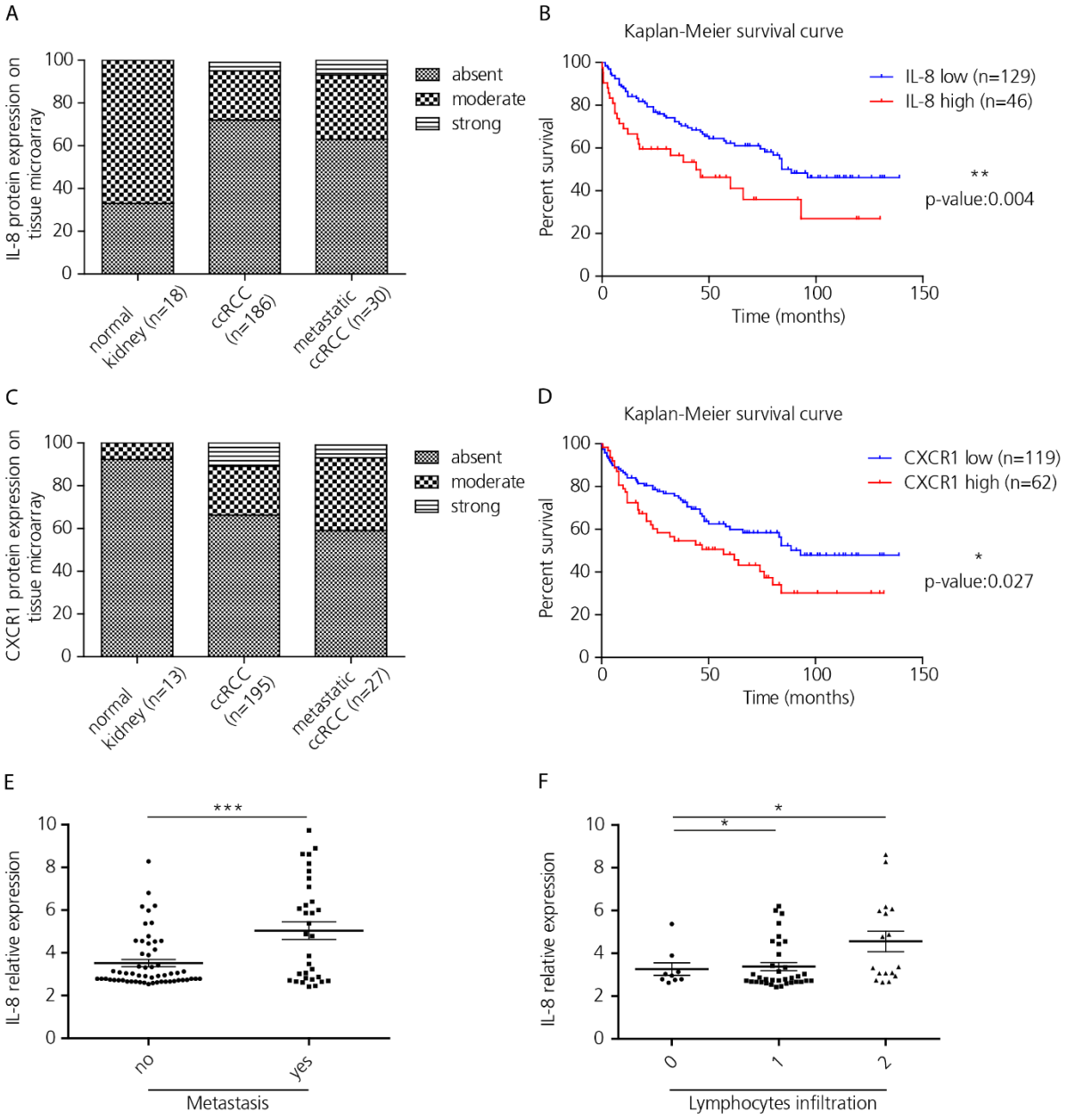
A
IL-8 protein expression on tissue microarray
100
80
60
40
20
0
absent
moderate
strong
normal kidney (n=18)
ccRCC (n=186)
metastatic ccRCC (n=30)
B
Kaplan-Meier survival curve
Percent survival
IL-8 low (n=129)
IL-8 high (n=46)
**
p-value:0.004
0
50
100
150
Time (months)
C
CXCR1 protein expression on tissue microarray
absent
moderate
strong
normal kidney (n=13)
ccRCC (n=195)
metastatic ccRCC (n=27)
D
Kaplan-Meier survival curve
Percent survival
CXCR1 low (n=119)
CXCR1 high (n=62)
*
p-value:0.027
Time (months)
E
IL-8 relative expression
***
10
8
6
4
2
0
no
yes
Metastasis
F
IL-8 relative expression
*
*
0
1
2
Lymphocytes infiltration

885 **SUPPLEMENTARY MATERIAL**

886 **Supplementary Table 1.**

Antibody	Name/ clone	Dilution	Supplier	IHC system	Reagents	Protocol/ detection
PanCKa	LU-5	1:50	DAKO A/S	Ventana Benchmark Ultra	OptiViewKit	Pretreatment: Protease1 4min
CK7	OV-TL 12/30	1:100	DAKO A/S	Ventana Benchmark Ultra	OptiViewKit	Pretreatment: Protease1 4min
Pax8	Paired box 8	1:400	Protein Tech Group, Inc.	Ventana Benchmark Ultra	OptiViewKit	Pretreatment: Tris-EDTA-Borat Buffer 80min
CAIX	Carbonic Anhydrase IX polyclonal	1:6000	Abcam	Leica Bond	Bond Polymer Refine Kit	Pretreatment: Tris-EDTA-Borat Buffer 30min
Vimentin	Vim3B4	1:800	Abcam	Leica Bond	Bond Polymer Refine Kit	Pretreatment: Tris-EDTA-Borat Buffer 60min
E-cadherin	EP700Y	1:200	CellMarque	Ventana Benchmark Ultra	OptiViewKit	Pretreatment: Tris-EDTA-Borat Buffer 40min
Snail/Slug		1:200	Abcam	Ventana DiscoveryUltra	ChromoMapKit	Pretreatment: Tris-EDTA-Borat Buffer 30min
CXCR1	42705	1:2000	R&D	Ventana DiscoveryUltra	ChromoMapKit	Pretreatment: Protease1 4min
CXCL8	6217	1:100	R&D	Leica Bond	Bond Polymer Refine Kit	Pretreatment: Tris-EDTA-Borat Buffer 90min
CD105	3A9	1:400	Novus Biologicals	Ventana Benchmark Ultra	OptiViewKit	Pretreatment: Tris-EDTA-Borat Buffer 60min

887

888

889

Supplementary Table 2.

Antibody	Clone	Concentration	Supplier
CD13	WM15	2µg/ml	Biolegend
CD24	32D12	2µg/ml	Miltenyi
CD44	IM7	0.5µg/ml	BectionDickinson
CD10	HI10a	2µg/ml	Biolegend
CXCR4	12G5	4µg/ml	Biolegend
Vimentin	RV202	0.1µg/ml	BectionDickinson
E-Cadherin	36/E-Cadherin	2µg/ml	BectionDickinson

Supplementary Table 3.

CSC Markers	Others	Stemness/Developmental pathways	Marker of interest
CD105	CD29	SNAIL	CXCL8
CD44	CD20	STAT3	
CD24	CD38	ZEB1/2	
ALDH1A1	BMP7	NANOG	
CXCR4	NOS2	WNT1	
		MYCN	
		TWIST1/2	

Supplementary Table 4.

	769P		**A498**		**Caki1**		**ACHN**	
	parental	spheres	parental	spheres	parental	spheres	parental	spheres
SP	8.45	4.64	3.91	4.06	10.6	11.4	19	4.98
CXCR1	31.6	20.5	4.19	6.06	23.2	27	16.9	18.2
SP CXCR1	1.6	19.6	20.2	13.9	29.3	85	24.9	64.4
+ Repertaxin								
SP	3.03	3.04	3.25	4.11	3.06	7.3	5.8	5.43
CXCR1	26.5	8.9	3.26	5.15	20	15.5	31.5	26.2
SP CXCR1	6.32	2.75	21.7	3.7	6.03	44	79.4	64

Supplementary Table 5.

Caki1 Parental				**Caki1 Spheres**			
Cell number	Tumor (1 cm^3)	Micro-metastasis	Macro-metastasis	Cell number	Tumor (1 cm^3)	Micro-metastasis	Macro-metastasis
10^6 cells	27 days	-	-	10^6 cells	19 days	+	-
10^4 cells	63 days	+	-	10^4 cells	53 days	+	+
10^2 cells	101days	-	-	10^2 cells	83 days	+	-

769P Parental				**769P Spheres**			
Cell number	Tumor (1 cm^3)	Micro-metastasis	Macro-metastasis	Cell number	Tumor (1 cm^3)	Micro-metastasis	Macro-metastasis
10^6 cells	-	n.a.	n.a.	10^6 cells	28 days	+	-
10^4 cells	-	n.a.	n.a.	10^4 cells	46 days	+	+
10^2 cells	-	n.a.	n.a.	10^2 cells	69 days	+	-

Supplementary Figure 1. A) Mesenchymal-epithelial transition (MET) of Caki1 spheres attached to the bottom of a plastic plate. **B)** Sphere-derived cells showing lipid islets due to differentiation into adipocytes upon induction. **C)** Caki1 and ACHN further proved a better sphere formation efficiency compared to 769P and A498 in the limiting dilution assay. **D)** Self-renewal properties were investigated by clonogenic assay. Again, metastasis-derived cultures showed pronounced CSC properties compared to primary-tumor derived cultures. **E)** Representative pictures of the colony formation assay. **F)** Incubation under hypoxia conditions improved sphere formation in parental cells compared to spheres. **G)** Spheres derived from Caki1 and ACHN showed high HIF1α levels, whereas 769P and A498 displayed HIF2α upregulation.

Supplementary Figure 2. A) Gene expression data of 84 genes linked to stemness for ACHN cell line. Significantly high IL-8 expression is highlighted. **B)** High CXCR4 expression was found correlated to ccRCC and met. ccRCC. **C)** ccRCC showed high MMP9 expression compared to normal kidney tissue. **D)** The lung cancer cell line H460 showing 28.2 % $CXCR1^+$ cells compared to A549 where only 2.6 % $CXCR1^+$ cells were found.

Supplementary Figure 3. A) Side population and corresponding $CXCR1^+$ cells in 769P spheres. Blue: verapamil treatment. Red: population of interest. **B)** Side population and corresponding $CXCR1^+$ cells in ACHN parental cells and spheres. Blue: verapamil treatment. Red: population of interest. **C)** Side population and corresponding $CXCR1^+$ cells in A498 parental cells and spheres. Blue: verapamil treatment. Red: population of interest. **D)** $CXCR2^+$

924 population (64.6 %) in Caki1 spheres. **E)** Western blot showing no differential expression in
925 the spheres compared to parental cells for CXCR2.
926
927 **Supplementary Figure 4. A)** Decreased cell proliferation was observed after 72h treatment
928 using anti-CXCR1ab, whereas the opposite was observed when adding human recombinant
929 IL-8. 769P cell line showed a more pronounced effect compare to Caki1. **B)** Caki1 showing
930 enhanced cell invasion and migration upon IL-8 treatment. Whereas, CXCR1 blockade showed
931 opposite effect. Interestingly, combination of treatments showed intermediate increase of
932 invasive and migratory properties. **C)** No effect was observed after repertaxin treatment in the
933 clonogenic assay. **D)** Representative picture of the colony formation assay for Caki1.
934
935 **Supplementary Figure 5. A)** Histograms showing decreased SP and $CXCR1^+$ cells upon
936 repertaxin treatment for Caki1 parental cells. The yellow area indicates the number of events
937 upon verapamil treatment. Whereas, the red and blue areas represent the population before
938 and after treatment, respectively. **B)** Histograms showing decreased SP and $CXCR1^+$ cells
939 upon repertaxin treatment for 769P parental cells and spheres. **C)** Histograms showing
940 decreased SP and $CXCR1^+$ cells upon repertaxin treatment for A498 parental cells and
941 spheres. **D)** Histograms showing decreased SP and $CXCR1^+$ cells upon repertaxin treatment
942 for ACHN parental cells and spheres.
943
944 **Supplementary Figure 6. A)** Tumor growth over time for 769P cell line. Sphere-derived cells
945 gave rise to tumors when injected subcutaneously into NSG mice at three different cell
946 densities (10^6, 10^4, 10^2). Whereas, parental cells did not. **B)** Representative pictures of NSG
947 mice injected with matrigel only (control), with 10^6 parental cells after 132 days, and with 10^6
948 sphere-derived cells after 28 days post-injection. Only spheres were capable to form tumors.
949 **C)** Immunohistochemical stains of the xenografted tumors derived from 769P spheres showing
950 the histological subtype by H&E, and the epithelial and kidney nature by PanCK and Pax8
951 positivity. CXCR1 and IL-8 were also found highly expressed. **D)** Metastasis in lungs and liver

were found in mice injected with sphere-derived cells. No positive staining for metastasis was observed in the control mice and mice that received parental cells. **E)** This figure shows a common process for tumor spreading and distal organ colonization which is the tumor cell extravasation. Tumor cells are here leaving the blood vessel and extravasating into the lung tissue to metastasize. **F)** Spheres were also capable to form macrometstasis when few tumor cells were injected, meaning they had enough time to grow bigger metastasis before the primary tumor could reach 1 cm^3 in size. Arrow heads and dashed lines indicate single tumor cells or clusters of cells in lung, liver, brain and lymph nodes for 769P spheres. **G)** Xenografted tumors were dissociated into single cell suspension and cells were plated into sphere formation assay. Tumor cells derived from 769P spheres retained the capability to form spheres *in vitro*.

Supplementary Figure 7. A) IL-8 and CXCR1 expression on tissue microarrays classified in absent, moderate and strong according to the staining intensity. **B)** Elevated IL-8 expression on RNA level correlated with the tumor grade in ccRCC. **C)** Kaplan-Meier survival curve developed according to the mean IL-8 expression on RNA showing poor prognosis for patients expressing high IL-8 levels. **D)** Enhanced IL-8 expression was found correlated with poor prognosis (five-year survival) in ccRCC patients.

Supplementary Figure 1

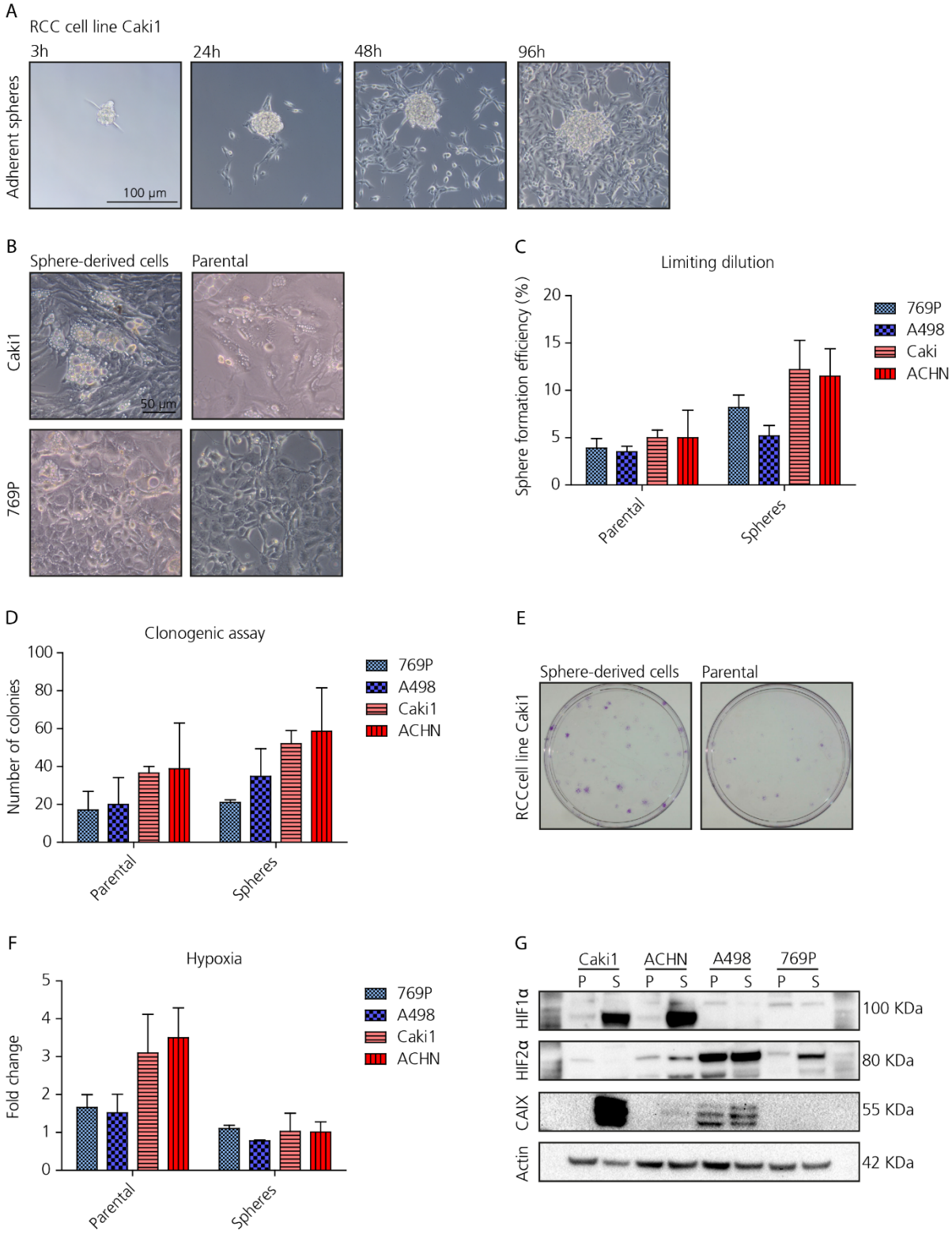

Supplementary Figure 2

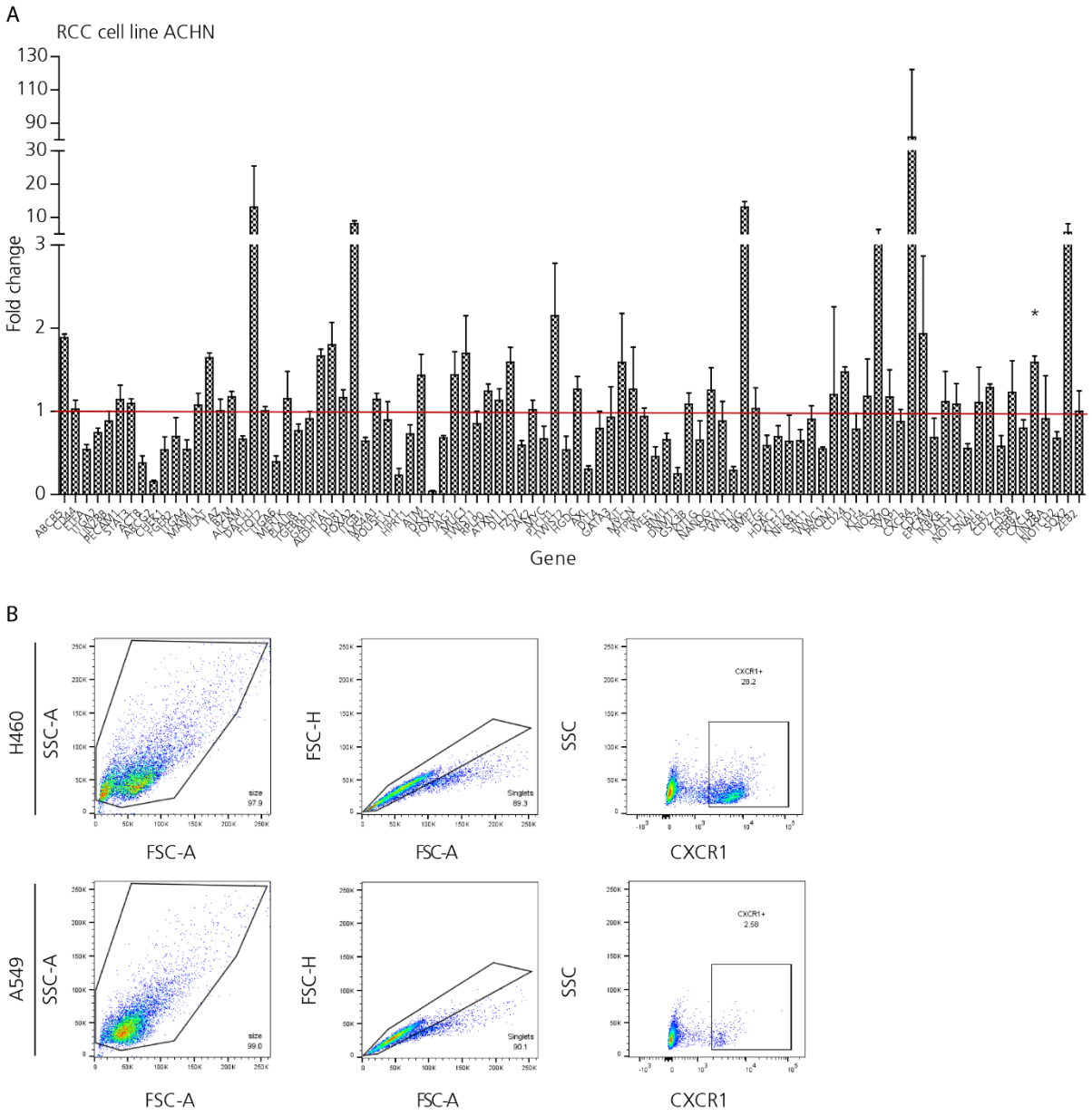

Supplementary Figure 3

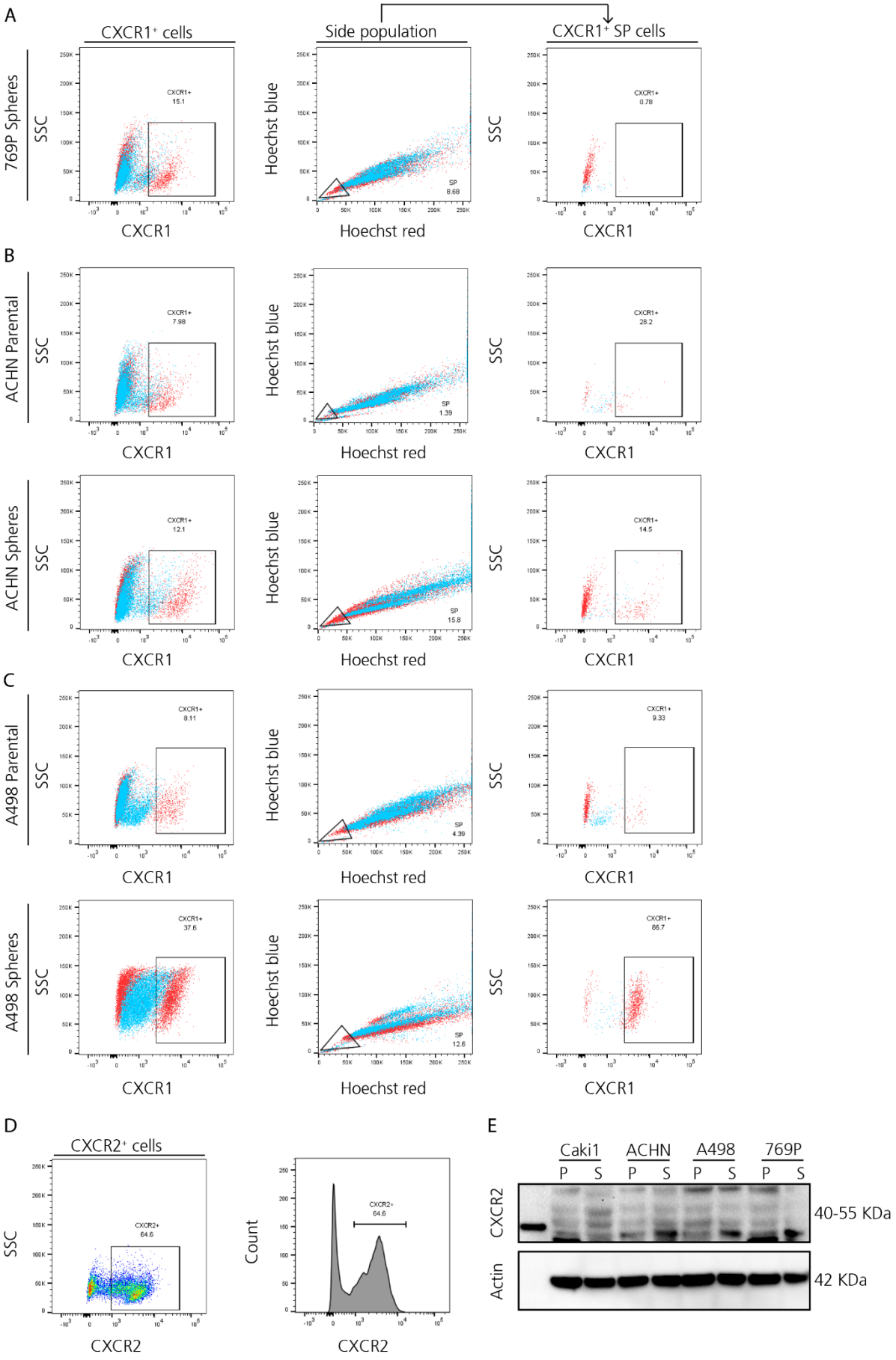

Supplementary Figure 4

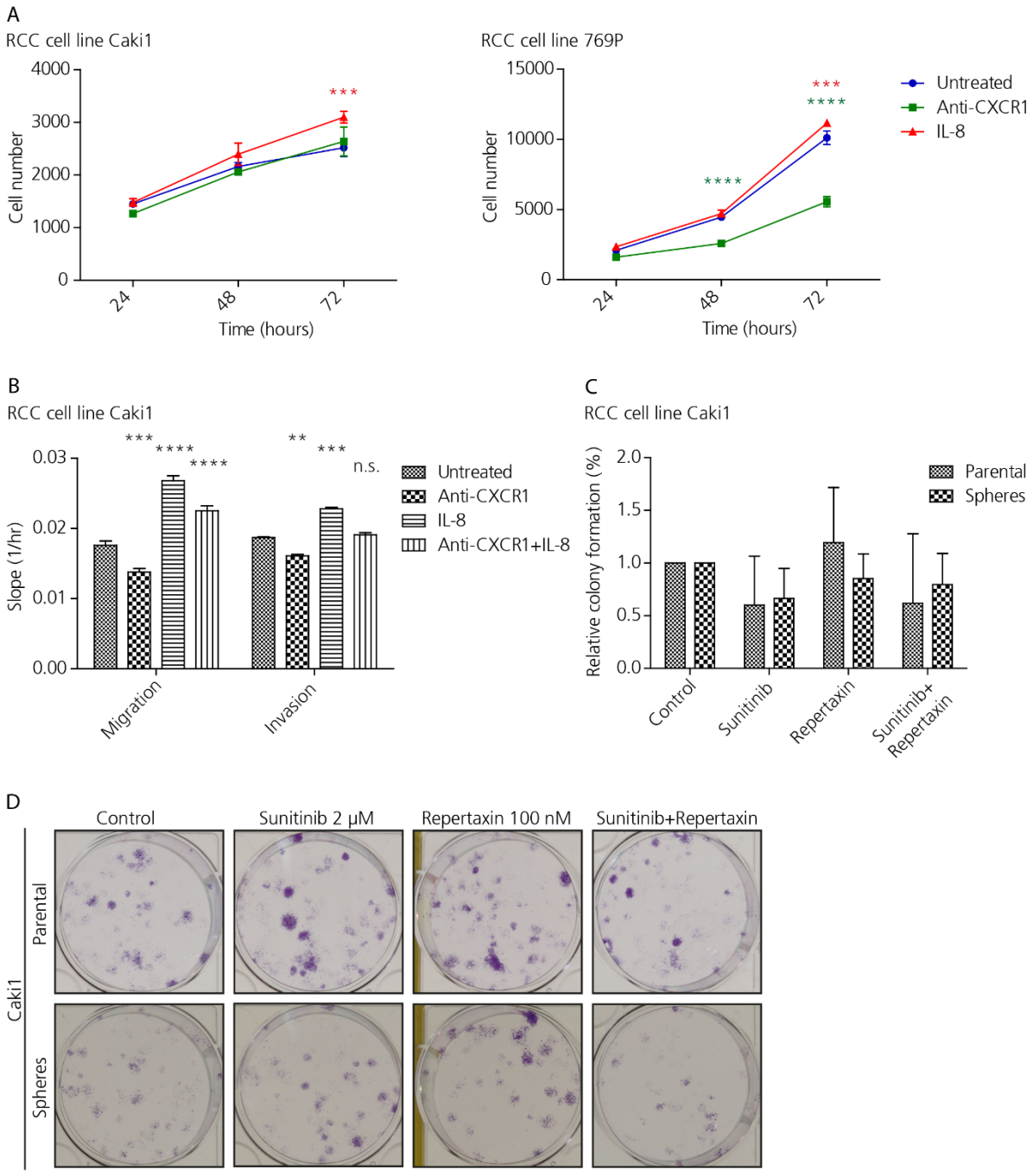

Supplementary Figure 5

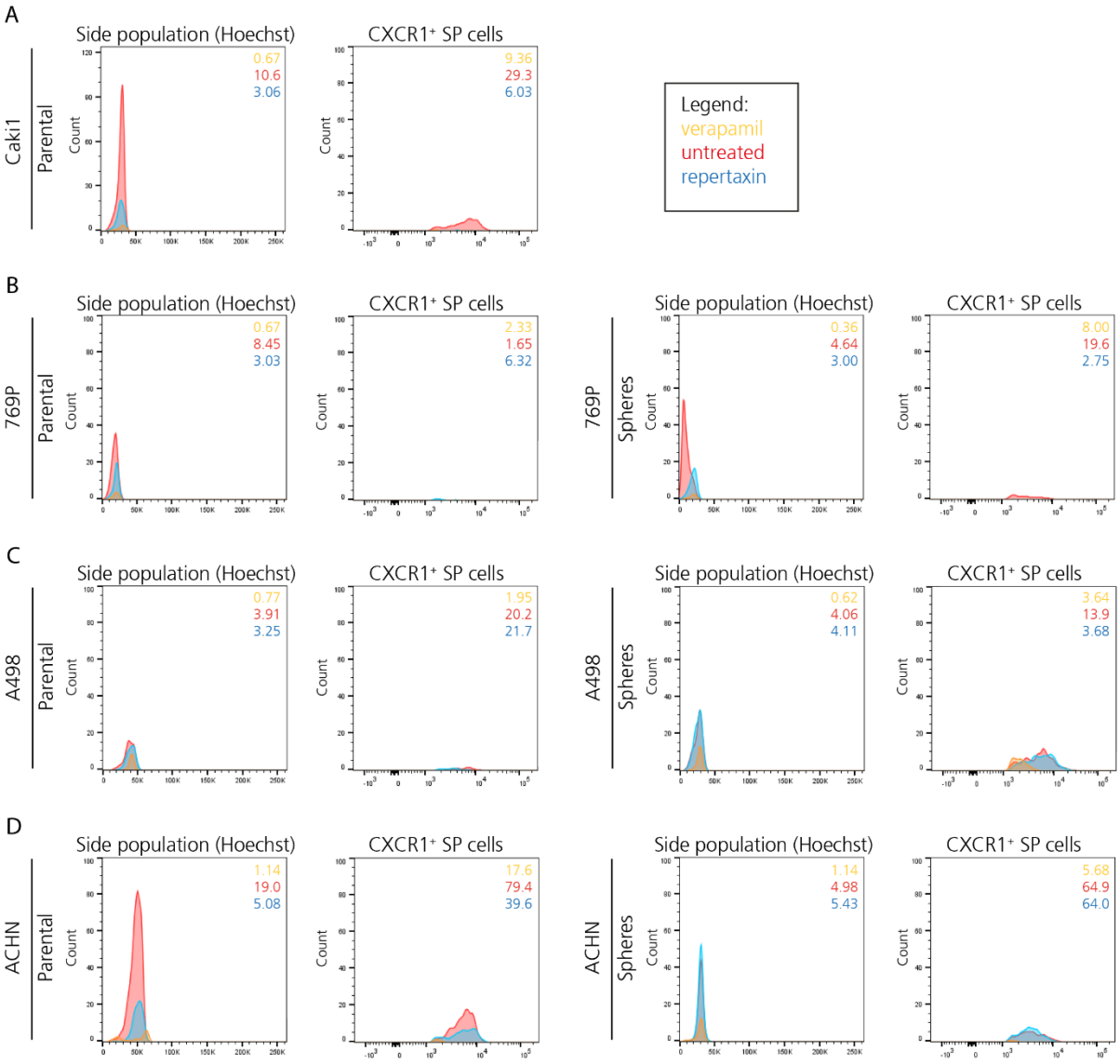

Supplementary Figure 6

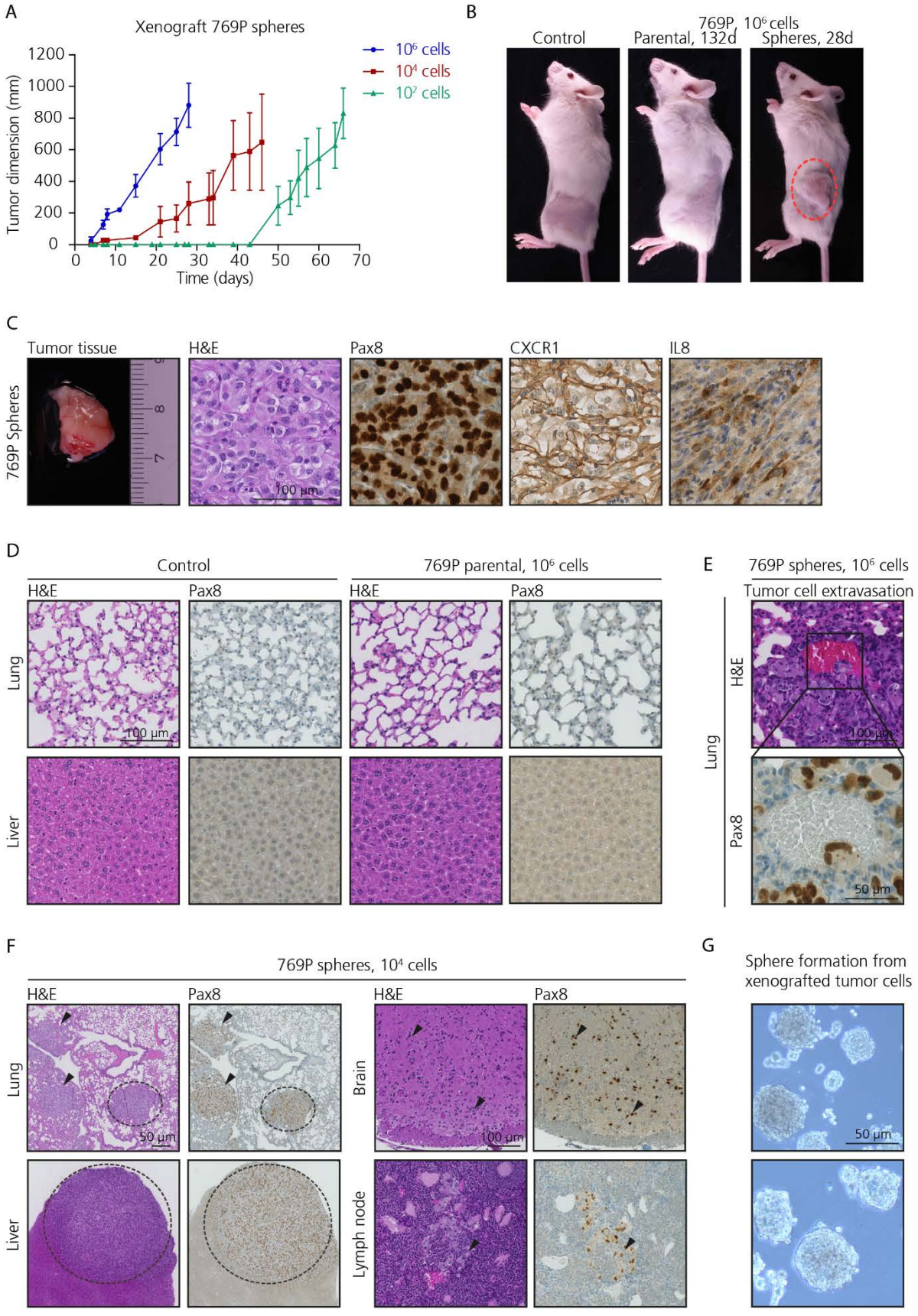

Supplementary Figure 7

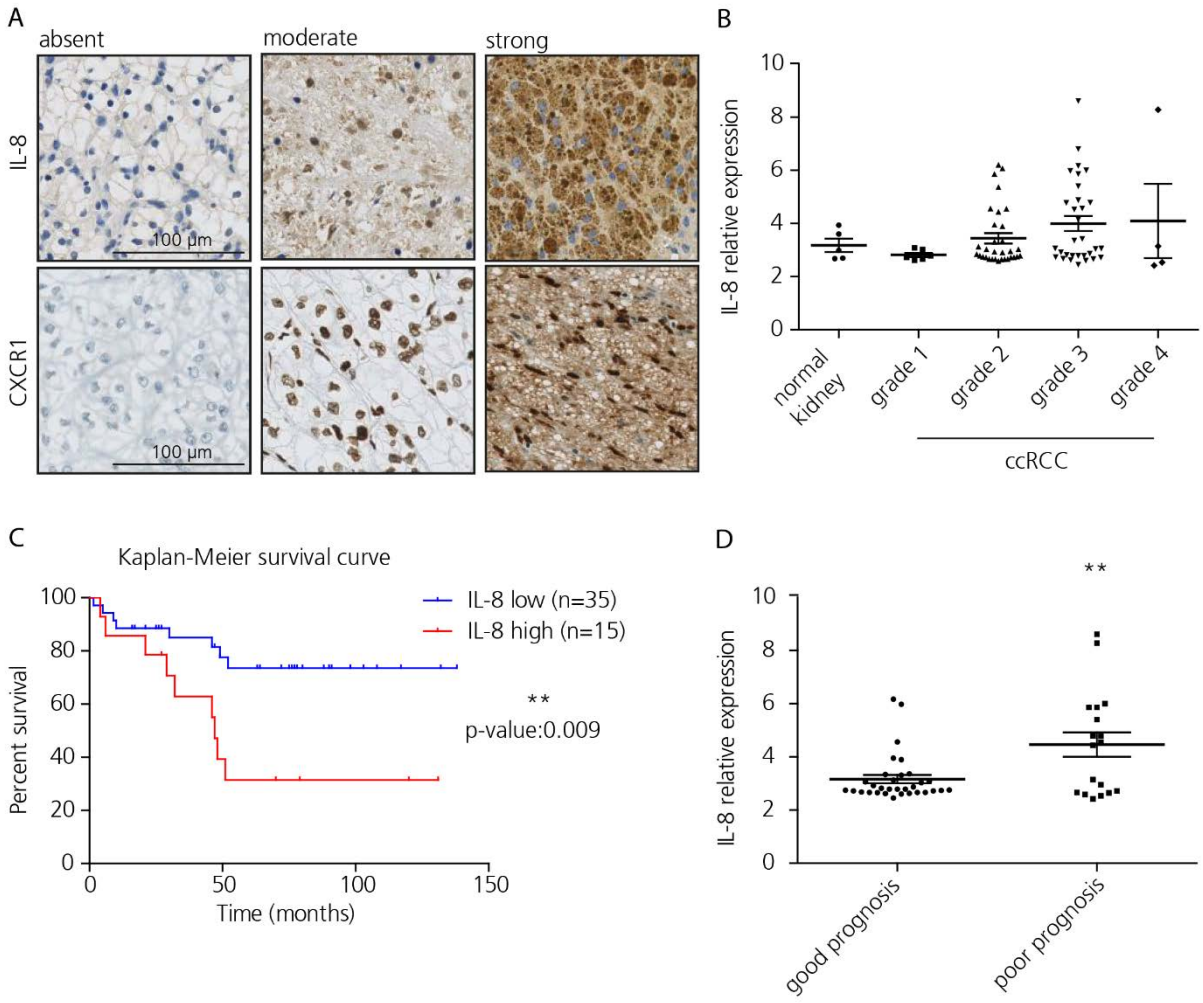

DISCUSSION

7. Discussion and future perspectives

Clear cell renal cell carcinoma is a very heterogeneous tumor, characterized by asymptomatic manifestation in early stage and a poor response to radiotherapy and chemotherapy in metastatic stage, making this tumor type very difficult to diagnose and treat (256,257). Therefore, new prognostic and predictive markers are needed. The possibility to dissect tumor heterogeneity and follow the evolution of tumor subpopulations during cancer progression and treatment is essential to overcome tumor recurrence.

The majority of biomarkers require invasive procedures such as biopsies and surgical intervention resulting in a static and rather simple modeling of the tumor disease, besides being an inadequate practice for the patient.

Blood and urine represent two valuable sources of cancer-derived molecules such as proteins, nucleic acids, extracellular vesicles and circulating tumor cells. Detection of changes in the level of these molecules in the body fluids have been associated with tumor load and malignant progression, proposing these liquid biopsies as a novel prognostic, diagnostic and predictive tool for cancer patients (63-65). Nevertheless, the development of non-invasive methods to detect de novo or to monitor already known tumor specific signatures continue to be a major challenge in renal cancer (75).

Detection of circulating tumor DNA in blood of cancer patients is regarded as an important step towards personalized medicine and treatment monitoring. Therefore, we investigated the clinical applicability of ctDNA as liquid biopsy in renal cancer. In our study, we confirmed the presence of specific *VHL* mutations in ctDNA derived from RCC xenografts indicating the capability of renal tumors to release DNA into the blood circulation. However, we could not detect any *VHL* mutation in plasma or serum samples derived from nine ccRCC patients, whereas a specific *VHL* mutation was successfully detected when using a highly sensitive Taqman assay. These data suggest a reduced tumor DNA shedding and an increased clearance of the tumor DNA from the circulation in renal cancer patients.

Therefore, highly sensitive detection methods and prior knowledge of the mutation are required for liquid biopsies in renal cancer, limiting their applicability in the clinics to tumor recurrence tracking.

Recently, the discovery of the presence of dsDNA in exosomes in different cell lines of pancreatic, breast and lung cancer has opened a new perspective in the cancer biomarkers field proposing exosomes as a novel biomarker in cancer detection (258).

Considering that not only wild-type DNA is packed in exosomes but tumor DNA as well, the mutational profile of the tumor might be assessed by isolating DNA contained in exosomes. Tumor cells can release EVs which may remain in close proximity to the place of origin or enter biological fluids and reach distant sites (208). Therefore, exoDNA derived from body fluids could be utilize as liquid biopsy to detect tumor-specific genetic mutations next to ctDNA improving the clinical applicability of ctDNA alone.

Moreover, an increased number of exosomes was detected in patients with poor prognosis and resistance to chemotherapy in many tumor types (208). Exosome secretion is promoted by different environmental stress signals (i.e. inflammation, hypoxia). Chemotherapy itself may trigger the release of EVs. Therefore, we could potentially take advantage of the enrichment of the exosome pool in the body fluids due to therapeutic intervention in order to successfully detect new mutations harboring in the context of a personalized medicine approach. In our study, we could identify the presence of dsDNA in the exosomes released by seven RCC cell lines. Our isolation technique provides a high quality samples which can be directly processed by NGS without further handling.

Interestingly, exosomes are involved in many different signaling processes related to intercellular communication, protein secretion pathways, immune system function, cancer progression (201,209).

Growing evidence suggests that renal cancer as other solid tumors possess a rare population of cells capable of self-renewal that contribute to metastasis and resistance to therapy namely cancer stem cells. CSCs have been found secreting higher amount of exosomes and CSC-derived exosomes have been found involved in promoting angiogenesis in xenograft mice with renal cancer (124), metastatic niche formation in lung carcinoma (221) as well as invasion, migration and tumor growth in many other tumor types (212,222-225).

In our study, we observed that hypoxia enhanced exosome secretion suggesting that environmental stress and stemness properties induce exosome release by cancer cells in order to communicate with neighboring cells and create a favorable niche to drive tumor progression.

Due to high tumor heterogeneity which tumor subpopulation, driver mutation, or stem cell like subpopulation, regulates tumor spreading and resistance to therapy in ccRCC remains unresolved. Therefore, besides the genomic investigation of exoDNA in blood of RCC patients as a potential diagnostic and prognostic biomarker, transcriptomic and proteomic analysis of the exosome content derived from *in vitro* cultures of RCC tumor cells and CSC subpopulations, as well as, *in vivo* tumor xenografts during tumor progression and upon therapeutic intervention, will help us understanding tumor heterogeneity and RCC pathogenesis.

In order to address these open questions, primary cultures derived from RCC patients were established, and *in vitro* 2D and 3D models were applied in the context of a personalized medicine approach. It has become increasingly clear that drug discovery screen and applied cancer studies often fail to translate into new cancer therapies because they largely relied on monolayer cultures of immortalized cell lines, which often fail to recapitulate fundamental biological features of human tumors such as, phenotypic and genetic heterogeneity, as well as, cell-cell interactions with the tumor microenvironment and in the spatial dimension (259).

Here, we proved that patient-derived cultures are more accurate in retaining patient-specific molecular features and, therefore, are a promising tool for translational cancer research studies. Indeed, primary cultures need validation and our study revealed that Pax8 and PanCK, together with *VHL*-targeted sequencing and fluorescence in situ hybridization are valuable in the characterization of ccRCC primary cultures. Mutational landscape analysis by next-generation sequencing of our primary cultures over several passages compared to the primary tumor they derived from, revealed that genetically distinct subpopulations are retained in the corresponding cell culture but that are subjected to clonal selection. Nevertheless, the genetic adaptation of the primary cultures was limited and often concerned variants considered of poor confidence

by the analysis. Therefore, primary cultures highly preserve the intra-tumor heterogeneity present in the corresponding primary tumor.

2D and 3D models were used to examine drug responses to a panel of agents used to treat locally advanced and metastatic RCCs. Taken together, our results indicate that drug profiling in patient-derived cell models can be a useful tool to direct ccRCC treatment decisions. Moreover, our drug profiling highlighted the intra-tumor heterogeneity inherent in ccRCCs. Analyzing a larger panel of approved and experimental drugs including combination therapy in a larger cohort of patient-derived cell models should be employed. In addition, single cell analysis of tumor heterogeneity with and within RCC patients, together with immune cell profiling of the tumor microenvironment (260) will be essential in order to discover more effective treatment strategies for ccRCC.

Importantly, one should consider that CSCs are recognized being the major cause of tumor recurrence and resistance to therapy. They are characterized by unlimited cell division, maintenance of the stem cell pool (self-renewal), capability to differentiate into several cell types and tumorigenicity (107-109). In our study, a subpopulation of cells retaining all these features was isolated from RCC cell lines and primary cultures. Interestingly, metastasis-derived cultures showed an increased CSC content and tumorigenic potential compared to primary tumor-derived cultures, indicating that, indeed, these cells were responsible for tumor progression and therapy failure in ccRCC. It is becoming increasingly clear that tumor microenvironment, stroma cells, soluble molecules and extracellular vesicles (i.e. exosomes) play an important role in modulating metastatic properties and sensitivity of tumor cells to therapy (192,260). Stemness traits can be acquired via genetic, epigenetic modification and interaction with tumor microenvironment. Processes like inflammation, hypoxia, angiogenesis and EMT contribute to maintenance of the CSC fate by acting on the most known pathways regulating CSCs and by maintaining the stem cell niche. Stem cell niches are often localized in hypoxic region where low O_2 levels induce slow cycle proliferation and minimize DNA damage due to ROS. Interestingly, Varna and co-authors showed that $CD133^+/CXCR4^+$ cells coexpressed HIF1α and were located in perinecrotic areas in RCCs (127,136). In our study, CSC properties were enhanced upon hypoxia incubation and high expression of HIFs and HIF-target genes were observed in renal CSCs.

Interestingly, our study also demonstrated that the IL-8/CXCR1 axis is associated with CSC-like properties *in vitro* and *in vivo* in renal cancer, and correlated with tumor lymphocytes infiltration, poor prognosis and decreased overall survival in ccRCC patients. CSCs derived from RCC cultures displayed self-renewal properties, enhanced expression of EMT and stemness markers, upregulation of genes involved in developmental pathways, capability differentiate into adipocytes and to give rise to tumors when injected into NSG mice. All these features were impaired when cells were treated with CXCR1 blocking agents such as anti-CXCR1 ab or repertaxin.

Additionally, CSCs expressed high levels of the multidrug ABC transporter. ABCB5 has been found functionally involved in the regulation of IL-8/CXCR1 signaling through IL1β in melanoma cells and has therefore been associated with cancer stem-like cells, clinical disease progression, tumor recurrence and therapy failure (176,228). An increased IL-8 expression was found associated with sunitinib resistance *in vitro* and *in vivo* in ccRCC (61). Conventional chemo- and radio-therapy usually eliminates the majority of cells present in the tumor bulk while sparing the CSC pool. Therefore, it is necessary to develop new approaches aimed to targeting CSCs. To date, several therapeutic agents targeting IL-8/CXCR1-2 are currently being tested in colon, bladder, ovarian and breast cancers (230,238,251,253). However, none of these treatments have been proposed for renal cancer. Investigating the effect of CXCR1 blockade on tumor progression and aggressiveness *in vivo* would further prove that targeting IL-8/CXCR1 axis is paramount to overcome therapy failure.

The management of ccRCC patients has dramatically changed in the last years (38). Poor response is observed upon chemotherapy and radiotherapy, whereas targeted therapies such as TKI are only palliative. Nevertheless, novel immunotherapies (i.e. checkpoint inhibitors) are demonstrating impressive activity across an increasing number of tumor types, including ccRCC patients (38,254,260). To date, nivolumab (monoclonal antibody against PD-1) has been approved in the second line setting for RCC patients (261,262). Moreover, increased levels of the chemokine CXCL9 and CXCL10 in peripheral blood was found predicting immunotherapy response (263). Of note, IL-8 represents one of the major chemokines associated with the

promotion of neutrophils and inflammatory response (228). IL-8 promotes the recruitment of bone marrow-derived MSCs to the tumor region, which support angiogenesis and tumor aggressiveness (231). Serum IL-8 levels correlated tumor burden and clinical stage in patients with melanoma, RCC, NSCLC and HCC (234,264). In a recent investigation, it was shown that treatment with anti-CXCR2 antibody along with anti-PD-1 antibody improved survival and delay in tumor growth in vivo in rhabdomyosarcoma (234,265). For this reason, targeting CSCs through IL-8/CXCR1 in combination with conventional chemotherapy agents and/or immunotherapy would be the next step towards overcoming tumor recurrence.

In conclusion, understanding the mechanisms underlying tumor heterogeneity and cancer stem cell contribution to tumor progression, metastasis formation and therapy failure, together with the use of primary cell cultures, may ultimately promote the discovery of more accurate and reliable diagnostic and prognostic tools as well as provide the instruments for precise and patient-oriented therapeutic intervention.

REFERENCES

1. Siegel RL, Miller KD, Jemal A. Cancer statistics, 2016. CA Cancer J Clin **2016**;66(1):7-30 doi 10.3322/caac.21332.
2. Hanahan D, Weinberg RA. The hallmarks of cancer. Cell **2000**;100(1):57-70.
3. Hanahan D, Weinberg RA. Hallmarks of cancer: the next generation. Cell **2011**;144(5):646-74 doi 10.1016/j.cell.2011.02.013.
4. Moch H. Kidey Cancer. Lyon, Fr.: Int. Agency Res. Cancer/World Health Organ; 2014. 2-9 p.
5. Bhatt JR, Finelli A. Landmarks in the diagnosis and treatment of renal cell carcinoma. Nat Rev Urol **2014**;11(9):517-25 doi 10.1038/nrurol.2014.194.
6. Znaor A, Lortet-Tieulent J, Laversanne M, Jemal A, Bray F. International variations and trends in renal cell carcinoma incidence and mortality. Eur Urol **2015**;67(3):519-30 doi 10.1016/j.eururo.2014.10.002.
7. Young AN, Master VA, Amin MB. Current trends in the molecular classification of renal neoplasms. ScientificWorldJournal **2006**;6:2505-18 doi 10.1100/tsw.2006.390.
8. Moch H. An overview of renal cell cancer: pathology and genetics. Semin Cancer Biol **2013**;23(1):3-9 doi 10.1016/j.semcancer.2012.06.006.
9. Siegel RL, Miller KD, Jemal A. Cancer statistics, 2015. CA Cancer J Clin **2015**;65(1):5-29 doi 10.3322/caac.21254.
10. Linehan WM, Srinivasan R, Schmidt LS. The genetic basis of kidney cancer: a metabolic disease. Nat Rev Urol **2010**;7(5):277-85 doi 10.1038/nrurol.2010.47.
11. Linehan WM, Ricketts CJ. The metabolic basis of kidney cancer. Semin Cancer Biol **2013**;23(1):46-55 doi 10.1016/j.semcancer.2012.06.002.
12. Frew IJ, Moch H. A clearer view of the molecular complexity of clear cell renal cell carcinoma. Annu Rev Pathol **2015**;10:263-89 doi 10.1146/annurev-pathol-012414-040306.
13. Campbell SCR, B.I. Renal cell carcinoma: clinical management. Klein EA, editor: Springer; 2013.
14. Vikram R, Ng CS, Tamboli P, Tannir NM, Jonasch E, Matin SF*, et al.* Papillary renal cell carcinoma: radiologic-pathologic correlation and spectrum of disease. Radiographics **2009**;29(3):741-54; discussion 55-7 doi 10.1148/rg.293085190.
15. Messer J, Drabick J, Kaag M. Rational therapy for renal cell carcinoma based on its genetic targets. Adv Exp Med Biol **2013**;779:291-308 doi 10.1007/978-1-4614-6176-0_13.
16. Delahunt B, Eble JN, McCredie MR, Bethwaite PB, Stewart JH, Bilous AM. Morphologic typing of papillary renal cell carcinoma: comparison of growth kinetics and patient survival in 66 cases. Hum Pathol **2001**;32(6):590-5 doi 10.1053/hupa.2001.24984.
17. Speicher MR, Schoell B, du Manoir S, Schrock E, Ried T, Cremer T*, et al.* Specific loss of chromosomes 1, 2, 6, 10, 13, 17, and 21 in chromophobe renal cell carcinomas revealed by comparative genomic hybridization. Am J Pathol **1994**;145(2):356-64.
18. Moch H, Montironi R, Lopez-Beltran A, Cheng L, Mischo A. Oncotargets in different renal cancer subtypes. Current drug targets **2015**;16(2):125-35.
19. Organization WH. Classification of Tumours. **2013**.
20. Ng CS, Wood CG, Silverman PM, Tannir NM, Tamboli P, Sandler CM. Renal cell carcinoma: diagnosis, staging, and surveillance. AJR Am J Roentgenol **2008**;191(4):1220-32 doi 10.2214/AJR.07.3568.
21. Fuhrman SA, Lasky LC, Limas C. Prognostic significance of morphologic parameters in renal cell carcinoma. Am J Surg Pathol **1982**;6(7):655-63.
22. Qayyum T, McArdle P, Orange C, Seywright M, Horgan P, Oades G*, et al.* Reclassification of the Fuhrman grading system in renal cell carcinoma-does it make a difference? Springerplus **2013**;2:378 doi 10.1186/2193-1801-2-378.
23. Delahunt B, Sika-Paotonu D, Bethwaite PB, McCredie MR, Martignoni G, Eble JN*, et al.* Fuhrman grading is not appropriate for chromophobe renal cell carcinoma. Am J Surg Pathol **2007**;31(6):957-60 doi 10.1097/01.pas.0000249446.28713.53.

24. Delahunt B, Cheville JC, Martignoni G, Humphrey PA, Magi-Galluzzi C, McKenney J*, et al.* The International Society of Urological Pathology (ISUP) grading system for renal cell carcinoma and other prognostic parameters. Am J Surg Pathol **2013**;37(10):1490-504 doi 10.1097/PAS.0b013e318299f0fb.
25. Humphrey PA, Moch H, Cubilla AL, Ulbright TM, Reuter VE. The 2016 WHO Classification of Tumours of the Urinary System and Male Genital Organs-Part B: Prostate and Bladder Tumours. Eur Urol **2016**;70(1):106-19 doi 10.1016/j.eururo.2016.02.028.
26. Bensalah K, Patard JJ. Kidney cancer in 2010: drugs, surgery and survival in RCC. Nat Rev Urol **2011**;8(2):66-8 doi 10.1038/nrurol.2010.228.
27. Cohen HT, McGovern FJ. Renal-cell carcinoma. N Engl J Med **2005**;353(23):2477-90 doi 10.1056/NEJMra043172.
28. Arora A, Scholar EM. Role of tyrosine kinase inhibitors in cancer therapy. J Pharmacol Exp Ther **2005**;315(3):971-9 doi 10.1124/jpet.105.084145.
29. Escudier B, Eisen T, Stadler WM, Szczylik C, Oudard S, Siebels M*, et al.* Sorafenib in advanced clear-cell renal-cell carcinoma. N Engl J Med **2007**;356(2):125-34 doi 10.1056/NEJMoa060655.
30. Sternberg CN, Davis ID, Mardiak J, Szczylik C, Lee E, Wagstaff J*, et al.* Pazopanib in locally advanced or metastatic renal cell carcinoma: results of a randomized phase III trial. J Clin Oncol **2010**;28(6):1061-8 doi 10.1200/JCO.2009.23.9764.
31. Motzer RJ, Hutson TE, Cella D, Reeves J, Hawkins R, Guo J*, et al.* Pazopanib versus sunitinib in metastatic renal-cell carcinoma. N Engl J Med **2013**;369(8):722-31 doi 10.1056/NEJMoa1303989.
32. Motzer RJ, Hutson TE, McCann L, Deen K, Choueiri TK. Overall survival in renal-cell carcinoma with pazopanib versus sunitinib. N Engl J Med **2014**;370(18):1769-70 doi 10.1056/NEJMc1400731.
33. Motzer RJ, McCann L, Deen K. Pazopanib versus sunitinib in renal cancer. N Engl J Med **2013**;369(20):1970 doi 10.1056/NEJMc1311795.
34. Hutson TE. Targeted therapy for renal cell carcinoma: a new treatment paradigm. Proc (Bayl Univ Med Cent) **2007**;20(3):244-8.
35. Clark PE. The role of VHL in clear-cell renal cell carcinoma and its relation to targeted therapy. Kidney Int **2009**;76(9):939-45 doi 10.1038/ki.2009.296.
36. Rini BI, Escudier B, Tomczak P, Kaprin A, Szczylik C, Hutson TE*, et al.* Comparative effectiveness of axitinib versus sorafenib in advanced renal cell carcinoma (AXIS): a randomised phase 3 trial. Lancet **2011**;378(9807):1931-9 doi 10.1016/S0140-6736(11)61613-9.
37. Escudier B. Emerging immunotherapies for renal cell carcinoma. Ann Oncol **2012**;23 Suppl 8:viii35-40 doi 10.1093/annonc/mds261.
38. Carlo MI, Voss MH, Motzer RJ. Checkpoint inhibitors and other novel immunotherapies for advanced renal cell carcinoma. Nat Rev Urol **2016**;13(7):420-31 doi 10.1038/nrurol.2016.103.
39. Bukowski RM, Yasothan U, Kirkpatrick P. Pazopanib. Nat Rev Drug Discov **2010**;9(1):17-8 doi 10.1038/nrd3073.
40. Eichelberg C, Junker K, Ljungberg B, Moch H. Diagnostic and prognostic molecular markers for renal cell carcinoma: a critical appraisal of the current state of research and clinical applicability. Eur Urol **2009**;55(4):851-63 doi 10.1016/j.eururo.2009.01.003.
41. Tan PH, Cheng L, Rioux-Leclercq N, Merino MJ, Netto G, Reuter VE*, et al.* Renal tumors: diagnostic and prognostic biomarkers. Am J Surg Pathol **2013**;37(10):1518-31 doi 10.1097/PAS.0b013e318299f12e.
42. Pflueger D, Sboner A, Storz M, Roth J, Comperat E, Bruder E*, et al.* Identification of molecular tumor markers in renal cell carcinomas with TFE3 protein expression by RNA sequencing. Neoplasia **2013**;15(11):1231-40.
43. Swanton C, Larkin JM, Gerlinger M, Eklund AC, Howell M, Stamp G*, et al.* Predictive biomarker discovery through the parallel integration of clinical trial and functional genomics datasets. Genome Med **2010**;2(8):53 doi 10.1186/gm174.
44. Zhao H, Ljungberg B, Grankvist K, Rasmuson T, Tibshirani R, Brooks JD. Gene expression profiling predicts survival in conventional renal cell carcinoma. PLoS Med **2006**;3(1):e13 doi 10.1371/journal.pmed.0030013.

45. Hirota E, Yan L, Tsunoda T, Ashida S, Fujime M, Shuin T*, et al.* Genome-wide gene expression profiles of clear cell renal cell carcinoma: identification of molecular targets for treatment of renal cell carcinoma. Int J Oncol **2006**;29(4):799-827.
46. Lambrechts D, Claes B, Delmar P, Reumers J, Mazzone M, Yesilyurt BT*, et al.* VEGF pathway genetic variants as biomarkers of treatment outcome with bevacizumab: an analysis of data from the AViTA and AVOREN randomised trials. Lancet Oncol **2012**;13(7):724-33 doi 10.1016/S1470-2045(12)70231-0.
47. Xu CF, Johnson T, Garcia-Donas J, Choueiri TK, Sternberg CN, Davis ID*, et al.* IL8 polymorphisms and overall survival in pazopanib- or sunitinib-treated patients with renal cell carcinoma. Br J Cancer **2015**;112(7):1190-8 doi 10.1038/bjc.2015.64.
48. Lasseigne BN, Burwell TC, Patil MA, Absher DM, Brooks JD, Myers RM. DNA methylation profiling reveals novel diagnostic biomarkers in renal cell carcinoma. BMC Med **2014**;12:235 doi 10.1186/s12916-014-0235-x.
49. Schraml P, Struckmann K, Hatz F, Sonnet S, Kully C, Gasser T*, et al.* VHL mutations and their correlation with tumour cell proliferation, microvessel density, and patient prognosis in clear cell renal cell carcinoma. J Pathol **2002**;196(2):186-93 doi 10.1002/path.1034.
50. Cowey CL, Rathmell WK. VHL gene mutations in renal cell carcinoma: role as a biomarker of disease outcome and drug efficacy. Curr Oncol Rep **2009**;11(2):94-101.
51. Lidgren A, Hedberg Y, Grankvist K, Rasmuson T, Vasko J, Ljungberg B. The expression of hypoxia-inducible factor 1alpha is a favorable independent prognostic factor in renal cell carcinoma. Clin Cancer Res **2005**;11(3):1129-35.
52. Kitamura H, Tsukamoto T. Prognostic biomarkers of renal cell carcinoma: Recent advances. Indian J Urol **2008**;24(1):10-5 doi 10.4103/0970-1591.38596.
53. Bui MH, Seligson D, Han KR, Pantuck AJ, Dorey FJ, Huang Y*, et al.* Carbonic anhydrase IX is an independent predictor of survival in advanced renal clear cell carcinoma: implications for prognosis and therapy. Clin Cancer Res **2003**;9(2):802-11.
54. Byun SS, Yeo WG, Lee SE, Lee E. Expression of survivin in renal cell carcinomas: association with pathologic features and clinical outcome. Urology **2007**;69(1):34-7 doi 10.1016/j.urology.2006.09.024.
55. Bui MH, Visapaa H, Seligson D, Kim H, Han KR, Huang Y*, et al.* Prognostic value of carbonic anhydrase IX and KI67 as predictors of survival for renal clear cell carcinoma. J Urol **2004**;171(6 Pt 1):2461-6.
56. Zigeuner R, Droschl N, Tauber V, Rehak P, Langner C. Biologic significance of fascin expression in clear cell renal cell carcinoma: systematic analysis of primary and metastatic tumor tissues using a tissue microarray technique. Urology **2006**;68(3):518-22 doi 10.1016/j.urology.2006.03.032.
57. Gibney GT, Aziz SA, Camp RL, Conrad P, Schwartz BE, Chen CR*, et al.* c-Met is a prognostic marker and potential therapeutic target in clear cell renal cell carcinoma. Ann Oncol **2013**;24(2):343-9 doi 10.1093/annonc/mds463.
58. Thompson RH, Kuntz SM, Leibovich BC, Dong H, Lohse CM, Webster WS*, et al.* Tumor B7-H1 is associated with poor prognosis in renal cell carcinoma patients with long-term follow-up. Cancer Res **2006**;66(7):3381-5 doi 10.1158/0008-5472.CAN-05-4303.
59. Krambeck AE, Thompson RH, Dong H, Lohse CM, Park ES, Kuntz SM*, et al.* B7-H4 expression in renal cell carcinoma and tumor vasculature: associations with cancer progression and survival. Proc Natl Acad Sci U S A **2006**;103(27):10391-6 doi 10.1073/pnas.0600937103.
60. Jacobsen J, Rasmuson T, Grankvist K, Ljungberg B. Vascular endothelial growth factor as prognostic factor in renal cell carcinoma. J Urol **2000**;163(1):343-7.
61. Huang D, Ding Y, Zhou M, Rini BI, Petillo D, Qian CN*, et al.* Interleukin-8 mediates resistance to antiangiogenic agent sunitinib in renal cell carcinoma. Cancer Res **2010**;70(3):1063-71 doi 10.1158/0008-5472.CAN-09-3965.
62. Mandel P, Metais P. [Not Available]. Comptes rendus des seances de la Societe de biologie et de ses filiales **1948**;142(3-4):241-3.

63. Esposito A, Bardelli A, Criscitiello C, Colombo N, Gelao L, Fumagalli L*, et al.* Monitoring tumor-derived cell-free DNA in patients with solid tumors: clinical perspectives and research opportunities. Cancer treatment reviews **2014**;40(5):648-55 doi 10.1016/j.ctrv.2013.10.003.
64. Fleischhacker M, Schmidt B. Circulating nucleic acids (CNAs) and cancer--a survey. Biochimica et biophysica acta **2007**;1775(1):181-232 doi 10.1016/j.bbcan.2006.10.001.
65. de Martino M, Klatte T, Haitel A, Marberger M. Serum cell-free DNA in renal cell carcinoma: a diagnostic and prognostic marker. Cancer **2012**;118(1):82-90 doi 10.1002/cncr.26254.
66. Feng G, Ye X, Fang F, Pu C, Huang H, Li G. Quantification of plasma cell-free DNA in predicting therapeutic efficacy of sorafenib on metastatic clear cell renal cell carcinoma. Dis Markers **2013**;34(2):105-11 doi 10.3233/DMA-120950.
67. Perego RA, Corizzato M, Brambilla P, Ferrero S, Bianchi C, Fasoli E*, et al.* Concentration and microsatellite status of plasma DNA for monitoring patients with renal carcinoma. Eur J Cancer **2008**;44(7):1039-47 doi 10.1016/j.ejca.2008.03.008.
68. Jung K, Fleischhacker M, Rabien A. Cell-free DNA in the blood as a solid tumor biomarker--a critical appraisal of the literature. Clin Chim Acta **2010**;411(21-22):1611-24 doi 10.1016/j.cca.2010.07.032.
69. Schwarzenbach H, Hoon DS, Pantel K. Cell-free nucleic acids as biomarkers in cancer patients. Nature reviews Cancer **2011**;11(6):426-37 doi 10.1038/nrc3066.
70. Kukita Y, Uchida J, Oba S, Nishino K, Kumagai T, Taniguchi K*, et al.* Quantitative identification of mutant alleles derived from lung cancer in plasma cell-free DNA via anomaly detection using deep sequencing data. PLoS One **2013**;8(11):e81468 doi 10.1371/journal.pone.0081468.
71. Forshew T, Murtaza M, Parkinson C, Gale D, Tsui DW, Kaper F*, et al.* Noninvasive identification and monitoring of cancer mutations by targeted deep sequencing of plasma DNA. Sci Transl Med **2012**;4(136):136ra68 doi 10.1126/scitranslmed.3003726.
72. Diehl F, Schmidt K, Choti MA, Romans K, Goodman S, Li M*, et al.* Circulating mutant DNA to assess tumor dynamics. Nat Med **2008**;14(9):985-90 doi 10.1038/nm.1789.
73. Schwarzenbach H, Stoehlmacher J, Pantel K, Goekkurt E. Detection and monitoring of cell-free DNA in blood of patients with colorectal cancer. Ann N Y Acad Sci **2008**;1137:190-6 doi 10.1196/annals.1448.025.
74. Hashad D, Sorour A, Ghazal A, Talaat I. Free circulating tumor DNA as a diagnostic marker for breast cancer. Journal of clinical laboratory analysis **2012**;26(6):467-72 doi 10.1002/jcla.21548.
75. Bettegowda C, Sausen M, Leary RJ, Kinde I, Wang Y, Agrawal N*, et al.* Detection of circulating tumor DNA in early- and late-stage human malignancies. Sci Transl Med **2014**;6(224):224ra24 doi 10.1126/scitranslmed.3007094.
76. Zhang Q, Yang H. The Roles of VHL-Dependent Ubiquitination in Signaling and Cancer. Frontiers in oncology **2012**;2:35 doi 10.3389/fonc.2012.00035.
77. Rechsteiner MP, von Teichman A, Nowicka A, Sulser T, Schraml P, Moch H. VHL gene mutations and their effects on hypoxia inducible factor HIFalpha: identification of potential driver and passenger mutations. Cancer Res **2011**;71(16):5500-11 doi 10.1158/0008-5472.CAN-11-0757.
78. Cancer Genome Atlas Research N. Comprehensive molecular characterization of clear cell renal cell carcinoma. Nature **2013**;499(7456):43-9 doi 10.1038/nature12222.
79. Brugarolas J. Molecular Genetics of Clear-Cell Renal Cell Carcinoma. J Clin Oncol **2014** doi 10.1200/JCO.2012.45.2003.
80. Gossage L, Murtaza M, Slatter AF, Lichtenstein CP, Warren A, Haynes B*, et al.* Clinical and pathological impact of VHL, PBRM1, BAP1, SETD2, KDM6A, and JARID1c in clear cell renal cell carcinoma. Genes, chromosomes & cancer **2014**;53(1):38-51 doi 10.1002/gcc.22116.
81. Ricketts CJ, Linehan WM. Intratumoral heterogeneity in kidney cancer. Nature genetics **2014**;46(3):214-5 doi 10.1038/ng.2904.
82. Kapur P, Pena-Llopis S, Christie A, Zhrebker L, Pavia-Jimenez A, Rathmell WK*, et al.* Effects on survival of BAP1 and PBRM1 mutations in sporadic clear-cell renal-cell carcinoma: a retrospective analysis with independent validation. Lancet Oncol **2013**;14(2):159-67 doi 10.1016/S1470-2045(12)70584-3.

83. Pena-Llopis S, Vega-Rubin-de-Celis S, Liao A, Leng N, Pavia-Jimenez A, Wang S*, et al.* BAP1 loss defines a new class of renal cell carcinoma. Nature genetics **2012**;44(7):751-9 doi 10.1038/ng.2323.
84. Shen C, Kaelin WG, Jr. The VHL/HIF axis in clear cell renal carcinoma. Semin Cancer Biol **2013**;23(1):18-25 doi 10.1016/j.semcancer.2012.06.001.
85. Hakimi AA, Ostrovnaya I, Reva B, Schultz N, Chen YB, Gonen M*, et al.* Adverse outcomes in clear cell renal cell carcinoma with mutations of 3p21 epigenetic regulators BAP1 and SETD2: a report by MSKCC and the KIRC TCGA research network. Clin Cancer Res **2013**;19(12):3259-67 doi 10.1158/1078-0432.CCR-12-3886.
86. Kapur P, Christie A, Raman JD, Then MT, Nuhn P, Buchner A*, et al.* BAP1 immunohistochemistry predicts outcomes in a multi-institutional cohort with clear cell renal cell carcinoma. J Urol **2014**;191(3):603-10 doi 10.1016/j.juro.2013.09.041.
87. Pawlowski R, Muhl SM, Sulser T, Krek W, Moch H, Schraml P. Loss of PBRM1 expression is associated with renal cell carcinoma progression. Int J Cancer **2013**;132(2):E11-7 doi 10.1002/ijc.27822.
88. Liu W, Fu Q, An H, Chang Y, Zhang W, Zhu Y*, et al.* Decreased Expression of SETD2 Predicts Unfavorable Prognosis in Patients With Nonmetastatic Clear-Cell Renal Cell Carcinoma. Medicine (Baltimore) **2015**;94(45):e2004 doi 10.1097/MD.0000000000002004.
89. Wang J, Liu L, Qu Y, Xi W, Xia Y, Bai Q*, et al.* Prognostic Value of SETD2 Expression in Patients with Metastatic Renal Cell Carcinoma Treated with Tyrosine Kinase Inhibitors. J Urol **2016**;196(5):1363-70 doi 10.1016/j.juro.2016.06.010.
90. Vogelstein B, Papadopoulos N, Velculescu VE, Zhou S, Diaz LA, Jr., Kinzler KW. Cancer genome landscapes. Science **2013**;339(6127):1546-58 doi 10.1126/science.1235122.
91. Gerlinger M, Horswell S, Larkin J, Rowan AJ, Salm MP, Varela I*, et al.* Genomic architecture and evolution of clear cell renal cell carcinomas defined by multiregion sequencing. Nature genetics **2014**;46(3):225-33 doi 10.1038/ng.2891.
92. Martinez P, Birkbak NJ, Gerlinger M, McGranahan N, Burrell RA, Rowan AJ*, et al.* Parallel evolution of tumour subclones mimics diversity between tumours. J Pathol **2013**;230(4):356-64 doi 10.1002/path.4214.
93. Gossage L, Eisen T. Alterations in VHL as potential biomarkers in renal-cell carcinoma. Nat Rev Clin Oncol **2010**;7(5):277-88 doi nrclinonc.2010.42 [pii]

10.1038/nrclinonc.2010.42.
94. Kaelin WG. Von Hippel-Lindau disease. Annu Rev Pathol **2007**;2:145-73 doi 10.1146/annurev.pathol.2.010506.092049.
95. Choueiri TK, Fay AP, Gagnon R, Lin Y, Bahamon B, Brown V*, et al.* The role of aberrant VHL/HIF pathway elements in predicting clinical outcome to pazopanib therapy in patients with metastatic clear-cell renal cell carcinoma. Clin Cancer Res **2013**;19(18):5218-26 doi 10.1158/1078-0432.CCR-13-0491.
96. Mack FA, Rathmell WK, Arsham AM, Gnarra J, Keith B, Simon MC. Loss of pVHL is sufficient to cause HIF dysregulation in primary cells but does not promote tumor growth. Cancer Cell **2003**;3(1):75-88.
97. Vanharanta S, Shu W, Brenet F, Hakimi AA, Heguy A, Viale A*, et al.* Epigenetic expansion of VHL-HIF signal output drives multiorgan metastasis in renal cancer. Nat Med **2013**;19(1):50-6 doi 10.1038/nm.3029.
98. Choueiri TK, Vaziri SA, Jaeger E, Elson P, Wood L, Bhalla IP*, et al.* von Hippel-Lindau gene status and response to vascular endothelial growth factor targeted therapy for metastatic clear cell renal cell carcinoma. J Urol **2008**;180(3):860-5; discussion 5-6 doi 10.1016/j.juro.2008.05.015.
99. Rini BI, Jaeger E, Weinberg V, Sein N, Chew K, Fong K*, et al.* Clinical response to therapy targeted at vascular endothelial growth factor in metastatic renal cell carcinoma: impact of patient characteristics and Von Hippel-Lindau gene status. BJU Int **2006**;98(4):756-62 doi 10.1111/j.1464-410X.2006.06376.x.

100. Kim BJ, Kim JH, Kim HS, Zang DY. Prognostic and predictive value of VHL gene alteration in renal cell carcinoma: a meta-analysis and review. Oncotarget **2017**;8(8):13979-85 doi 10.18632/oncotarget.14704.
101. Keefe SM, Nathanson KL, Rathmell WK. The molecular biology of renal cell carcinoma. Semin Oncol **2013**;40(4):421-8 doi 10.1053/j.seminoncol.2013.05.006.
102. Mandriota SJ, Turner KJ, Davies DR, Murray PG, Morgan NV, Sowter HM*, et al.* HIF activation identifies early lesions in VHL kidneys: evidence for site-specific tumor suppressor function in the nephron. Cancer Cell **2002**;1(5):459-68.
103. Yang H, Minamishima YA, Yan Q, Schlisio S, Ebert BL, Zhang X*, et al.* pVHL acts as an adaptor to promote the inhibitory phosphorylation of the NF-kappaB agonist Card9 by CK2. Mol Cell **2007**;28(1):15-27 doi 10.1016/j.molcel.2007.09.010.
104. Thoma CR, Toso A, Gutbrodt KL, Reggi SP, Frew IJ, Schraml P*, et al.* VHL loss causes spindle misorientation and chromosome instability. Nat Cell Biol **2009**;11(8):994-1001 doi 10.1038/ncb1912.
105. Davidowitz EJ, Schoenfeld AR, Burk RD. VHL induces renal cell differentiation and growth arrest through integration of cell-cell and cell-extracellular matrix signaling. Mol Cell Biol **2001**;21(3):865-74 doi 10.1128/MCB.21.3.865-874.2001.
106. Rycaj K, Tang DG. Cell-of-Origin of Cancer versus Cancer Stem Cells: Assays and Interpretations. Cancer Res **2015**;75(19):4003-11 doi 10.1158/0008-5472.CAN-15-0798.
107. Shackleton M, Quintana E, Fearon ER, Morrison SJ. Heterogeneity in cancer: cancer stem cells versus clonal evolution. Cell **2009**;138(5):822-9 doi 10.1016/j.cell.2009.08.017.
108. Kreso A, Dick JE. Evolution of the cancer stem cell model. Cell stem cell **2014**;14(3):275-91 doi 10.1016/j.stem.2014.02.006.
109. Nguyen LV, Vanner R, Dirks P, Eaves CJ. Cancer stem cells: an evolving concept. Nature reviews Cancer **2012**;12(2):133-43 doi 10.1038/nrc3184.
110. Gerstung M, Beisel C, Rechsteiner M, Wild P, Schraml P, Moch H*, et al.* Reliable detection of subclonal single-nucleotide variants in tumour cell populations. Nature communications **2012**;3:811 doi 10.1038/ncomms1814.
111. Prasetyanti PR, Medema JP. Intra-tumor heterogeneity from a cancer stem cell perspective. Mol Cancer **2017**;16(1):41 doi 10.1186/s12943-017-0600-4.
112. Bonnet D, Dick JE. Human acute myeloid leukemia is organized as a hierarchy that originates from a primitive hematopoietic cell. Nat Med **1997**;3(7):730-7.
113. Collins AT, Berry PA, Hyde C, Stower MJ, Maitland NJ. Prospective identification of tumorigenic prostate cancer stem cells. Cancer Res **2005**;65(23):10946-51 doi 10.1158/0008-5472.CAN-05-2018.
114. Fang D, Nguyen TK, Leishear K, Finko R, Kulp AN, Hotz S*, et al.* A tumorigenic subpopulation with stem cell properties in melanomas. Cancer Res **2005**;65(20):9328-37 doi 10.1158/0008-5472.CAN-05-1343.
115. Hermann PC, Bhaskar S, Cioffi M, Heeschen C. Cancer stem cells in solid tumors. Seminars in Cancer Biology **2010**;20(2):77-84 doi https://doi.org/10.1016/j.semcancer.2010.03.004.
116. Hermann PC, Bhaskar S, Cioffi M, Heeschen C. Cancer stem cells in solid tumors. Semin Cancer Biol **2010**;20(2):77-84 doi 10.1016/j.semcancer.2010.03.004.
117. Kim CF, Jackson EL, Woolfenden AE, Lawrence S, Babar I, Vogel S*, et al.* Identification of bronchioalveolar stem cells in normal lung and lung cancer. Cell **2005**;121(6):823-35 doi 10.1016/j.cell.2005.03.032.
118. Ma S, Chan KW, Hu L, Lee TK, Wo JY, Ng IO*, et al.* Identification and characterization of tumorigenic liver cancer stem/progenitor cells. Gastroenterology **2007**;132(7):2542-56 doi 10.1053/j.gastro.2007.04.025.
119. O'Brien CA, Pollett A, Gallinger S, Dick JE. A human colon cancer cell capable of initiating tumour growth in immunodeficient mice. Nature **2007**;445(7123):106-10 doi 10.1038/nature05372.
120. Ricci-Vitiani L, Lombardi DG, Pilozzi E, Biffoni M, Todaro M, Peschle C*, et al.* Identification and expansion of human colon-cancer-initiating cells. Nature **2007**;445(7123):111-5 doi 10.1038/nature05384.

121. Schatton T, Murphy GF, Frank NY, Yamaura K, Waaga-Gasser AM, Gasser M*, et al.* Identification of cells initiating human melanomas. Nature **2008**;451(7176):345-9 doi 10.1038/nature06489.
122. Singh SK, Hawkins C, Clarke ID, Squire JA, Bayani J, Hide T*, et al.* Identification of human brain tumour initiating cells. Nature **2004**;432(7015):396-401 doi 10.1038/nature03128.
123. Bussolati B, Brossa A, Camussi G. Resident stem cells and renal carcinoma. International journal of nephrology **2011**;2011:286985 doi 10.4061/2011/286985.
124. Grange C, Tapparo M, Collino F, Vitillo L, Damasco C, Deregibus MC*, et al.* Microvesicles released from human renal cancer stem cells stimulate angiogenesis and formation of lung premetastatic niche. Cancer Res **2011**;71(15):5346-56 doi 10.1158/0008-5472.CAN-11-0241.
125. Kim K, Ihm H, Ro JY, Cho YM. High-level expression of stem cell marker CD133 in clear cell renal cell carcinoma with favorable prognosis. Oncology letters **2011**;2(6):1095-100 doi 10.3892/ol.2011.365.
126. Ueda K, Ogasawara S, Akiba J, Nakayama M, Todoroki K, Ueda K*, et al.* Aldehyde dehydrogenase 1 identifies cells with cancer stem cell-like properties in a human renal cell carcinoma cell line. PLoS One **2013**;8(10):e75463 doi 10.1371/journal.pone.0075463.
127. Varna M, Gapihan G, Feugeas JP, Ratajczak P, Tan S, Ferreira I*, et al.* Stem cells increase in numbers in perinecrotic areas in human renal cancer. Clin Cancer Res **2015**;21(4):916-24 doi 10.1158/1078-0432.CCR-14-0666.
128. Huang B, Huang YJ, Yao ZJ, Chen X, Guo SJ, Mao XP*, et al.* Cancer stem cell-like side population cells in clear cell renal cell carcinoma cell line 769P. PLoS One **2013**;8(7):e68293 doi 10.1371/journal.pone.0068293.
129. Song L, Ye W, Cui Y, Lu J, Zhang Y, Ding N*, et al.* Ecto-5'-nucleotidase (CD73) is a biomarker for clear cell renal carcinoma stem-like cells. Oncotarget **2017** doi 10.18632/oncotarget.16667.
130. Lu J, Cui Y, Zhu J, He J, Zhou G, Yue Z. Biological characteristics of Rh123high stem-like cells in a side population of 786-O renal carcinoma cells. Oncology letters **2013**;5(6):1903-8 doi 10.3892/ol.2013.1270.
131. Peng L, Hu Y, Chen D, Jiao S, Sun S. Ubiquitin specific peptidase 21 regulates interleukin-8 expression, stem-cell like property of human renal cell carcinoma. Oncotarget **2016**;7(27):42007-16 doi 10.18632/oncotarget.9751.
132. Lichner Z, Saleh C, Subramaniam V, Seivwright A, Prud'homme GJ, Yousef GM. miR-17 inhibition enhances the formation of kidney cancer spheres with stem cell/ tumor initiating cell properties. Oncotarget **2015**;6(8):5567-81 doi 10.18632/oncotarget.1901.
133. Khan MI, Czarnecka AM, Lewicki S, Helbrecht I, Brodaczewska K, Koch I*, et al.* Comparative Gene Expression Profiling of Primary and Metastatic Renal Cell Carcinoma Stem Cell-Like Cancer Cells. PLoS One **2016**;11(11):e0165718 doi 10.1371/journal.pone.0165718.
134. Xiao W, Gao Z, Duan Y, Yuan W, Ke Y. Notch signaling plays a crucial role in cancer stem-like cells maintaining stemness and mediating chemotaxis in renal cell carcinoma. J Exp Clin Cancer Res **2017**;36(1):41 doi 10.1186/s13046-017-0507-3.
135. Nishizawa S, Hirohashi Y, Torigoe T, Takahashi A, Tamura Y, Mori T*, et al.* HSP DNAJB8 controls tumor-initiating ability in renal cancer stem-like cells. Cancer Res **2012**;72(11):2844-54 doi 10.1158/0008-5472.CAN-11-3062.
136. Micucci C, Matacchione G, Valli D, Orciari S, Catalano A. HIF2alpha is involved in the expansion of CXCR4-positive cancer stem-like cells in renal cell carcinoma. Br J Cancer **2015**;113(8):1178-85 doi 10.1038/bjc.2015.338.
137. Debeb BG, Zhang X, Krishnamurthy S, Gao H, Cohen E, Li L*, et al.* Characterizing cancer cells with cancer stem cell-like features in 293T human embryonic kidney cells. Mol Cancer **2010**;9:180 doi 10.1186/1476-4598-9-180.
138. Gassenmaier M, Chen D, Buchner A, Henkel L, Schiemann M, Mack B*, et al.* CXC chemokine receptor 4 is essential for maintenance of renal cell carcinoma-initiating cells and predicts metastasis. Stem Cells **2013**;31(8):1467-76 doi 10.1002/stem.1407.

139. Bussolati B, Bruno S, Grange C, Ferrando U, Camussi G. Identification of a tumor-initiating stem cell population in human renal carcinomas. FASEB journal : official publication of the Federation of American Societies for Experimental Biology **2008**;22(10):3696-705 doi 10.1096/fj.08-102590.
140. Bruno S, Bussolati B, Grange C, Collino F, Graziano ME, Ferrando U*, et al.* CD133+ renal progenitor cells contribute to tumor angiogenesis. Am J Pathol **2006**;169(6):2223-35 doi 10.2353/ajpath.2006.060498.
141. Galleggiante V, Rutigliano M, Sallustio F, Ribatti D, Ditonno P, Bettocchi C*, et al.* CTR2 identifies a population of cancer cells with stem cell-like features in patients with clear cell renal cell carcinoma. J Urol **2014**;192(6):1831-41 doi 10.1016/j.juro.2014.06.070.
142. Addla SK, Brown MD, Hart CA, Ramani VA, Clarke NW. Characterization of the Hoechst 33342 side population from normal and malignant human renal epithelial cells. Am J Physiol Renal Physiol **2008**;295(3):F680-7 doi 10.1152/ajprenal.90286.2008.
143. Yamashita M, Hirohashi Y, Torigoe T, Kusumoto H, Murai A, Imagawa T*, et al.* Dnajb8, a Member of the Heat Shock Protein 40 Family Has a Role in the Tumor Initiation and Resistance to Docetaxel but Is Dispensable for Stress Response. PLoS One **2016**;11(1):e0146501 doi 10.1371/journal.pone.0146501.
144. Zhong Y, Guan K, Guo S, Zhou C, Wang D, Ma W*, et al.* Spheres derived from the human SK-RC-42 renal cell carcinoma cell line are enriched in cancer stem cells. Cancer Lett **2010**;299(2):150-60 doi 10.1016/j.canlet.2010.08.013.
145. Dallas NA, Samuel S, Xia L, Fan F, Gray MJ, Lim SJ*, et al.* Endoglin (CD105): a marker of tumor vasculature and potential target for therapy. Clin Cancer Res **2008**;14(7):1931-7 doi 10.1158/1078-0432.CCR-07-4478.
146. Peired AJ, Sisti A, Romagnani P. Mesenchymal Stem Cell-Based Therapy for Kidney Disease: A Review of Clinical Evidence. Stem Cells Int **2016**;2016:4798639 doi 10.1155/2016/4798639.
147. Fonsatti E, Maio M. Highlights on endoglin (CD105): from basic findings towards clinical applications in human cancer. J Transl Med **2004**;2(1):18 doi 10.1186/1479-5876-2-18.
148. Myszczyszyn A, Czarnecka AM, Matak D, Szymanski L, Lian F, Kornakiewicz A*, et al.* The Role of Hypoxia and Cancer Stem Cells in Renal Cell Carcinoma Pathogenesis. Stem Cell Rev **2015**;11(6):919-43 doi 10.1007/s12015-015-9611-y.
149. Saroufim A, Messai Y, Hasmim M, Rioux N, Iacovelli R, Verhoest G*, et al.* Tumoral CD105 is a novel independent prognostic marker for prognosis in clear-cell renal cell carcinoma. Br J Cancer **2014**;110(7):1778-84 doi 10.1038/bjc.2014.71.
150. Grange C, Tapparo M, Tritta S, Deregibus MC, Battaglia A, Gontero P*, et al.* Role of HLA-G and extracellular vesicles in renal cancer stem cell-induced inhibition of dendritic cell differentiation. BMC Cancer **2015**;15:1009 doi 10.1186/s12885-015-2025-z.
151. Li Z. CD133: a stem cell biomarker and beyond. Exp Hematol Oncol **2013**;2(1):17 doi 10.1186/2162-3619-2-17.
152. Zhong LY, Du X, Geng SX, Weng JY, Zheng HT, Wu SJ*, et al.* [Expression of CD133 in the bone marrow of patients with myelodysplastic syndrome and its clinical significance]. Nan Fang Yi Ke Da Xue Xue Bao **2011**;31(5):854-5.
153. Sahlberg SH, Spiegelberg D, Glimelius B, Stenerlow B, Nestor M. Evaluation of cancer stem cell markers CD133, CD44, CD24: association with AKT isoforms and radiation resistance in colon cancer cells. PLoS One **2014**;9(4):e94621 doi 10.1371/journal.pone.0094621.
154. Park EK, Lee JC, Park JW, Bang SY, Yi SA, Kim BK*, et al.* Transcriptional repression of cancer stem cell marker CD133 by tumor suppressor p53. Cell Death Dis **2015**;6:e1964 doi 10.1038/cddis.2015.313.
155. Sun C, Song H, Zhang H, Hou C, Zhai T, Huang L*, et al.* CD133 expression in renal cell carcinoma (RCC) is correlated with nuclear hypoxia-inducing factor 1alpha (HIF-1alpha). J Cancer Res Clin Oncol **2012**;138(10):1619-24 doi 10.1007/s00432-012-1237-8.
156. Maeda K, Ding Q, Yoshimitsu M, Kuwahata T, Miyazaki Y, Tsukasa K*, et al.* CD133 Modulate HIF-1alpha Expression under Hypoxia in EMT Phenotype Pancreatic Cancer Stem-Like Cells. Int J Mol Sci **2016**;17(7) doi 10.3390/ijms17071025.

157. Feng G, Jiang F, Pan C, Pu C, Huang H, Li G. Quantification of peripheral blood CD133 mRNA in identifying metastasis and in predicting recurrence of patients with clear cell renal cell carcinoma. Urol Oncol **2014**;32(1):44 e9-14 doi 10.1016/j.urolonc.2013.06.003.
158. Zhang Y, Sun B, Zhao X, Liu Z, Wang X, Yao X*, et al.* Clinical significances and prognostic value of cancer stem-like cells markers and vasculogenic mimicry in renal cell carcinoma. J Surg Oncol **2013**;108(6):414-9 doi 10.1002/jso.23402.
159. Basakran NS. CD44 as a potential diagnostic tumor marker. Saudi Med J **2015**;36(3):273-9 doi 10.15537/smj.2015.3.9622.
160. Ma C, Komohara Y, Ohnishi K, Shimoji T, Kuwahara N, Sakumura Y*, et al.* Infiltration of tumor-associated macrophages is involved in CD44 expression in clear cell renal cell carcinoma. Cancer Sci **2016**;107(5):700-7 doi 10.1111/cas.12917.
161. Mikami S, Mizuno R, Kosaka T, Saya H, Oya M, Okada Y. Expression of TNF-alpha and CD44 is implicated in poor prognosis, cancer cell invasion, metastasis and resistance to the sunitinib treatment in clear cell renal cell carcinomas. Int J Cancer **2015**;136(7):1504-14 doi 10.1002/ijc.29137.
162. Li X, Ma X, Chen L, Gu L, Zhang Y, Zhang F*, et al.* Prognostic value of CD44 expression in renal cell carcinoma: a systematic review and meta-analysis. Sci Rep **2015**;5:13157 doi 10.1038/srep13157.
163. Fang X, Zheng P, Tang J, Liu Y. CD24: from A to Z. Cell Mol Immunol **2010**;7(2):100-3 doi 10.1038/cmi.2009.119.
164. Arik D, Can C, Dundar E, Kabukcuoglu S, Pasaoglu O. Prognostic Significance of CD24 in Clear Cell Renal Cell Carcinoma. Pathol Oncol Res **2017**;23(2):409-16 doi 10.1007/s12253-016-0128-8.
165. Jaggupilli A, Elkord E. Significance of CD44 and CD24 as cancer stem cell markers: an enduring ambiguity. Clin Dev Immunol **2012**;2012:708036 doi 10.1155/2012/708036.
166. Busillo JM, Benovic JL. Regulation of CXCR4 signaling. Biochimica et biophysica acta **2007**;1768(4):952-63 doi 10.1016/j.bbamem.2006.11.002.
167. Balkwill F. The significance of cancer cell expression of the chemokine receptor CXCR4. Semin Cancer Biol **2004**;14(3):171-9 doi 10.1016/j.semcancer.2003.10.003.
168. Balkwill F. Cancer and the chemokine network. Nature reviews Cancer **2004**;4(7):540-50 doi 10.1038/nrc1388.
169. Struckmann K, Mertz K, Steu S, Storz M, Staller P, Krek W*, et al.* pVHL co-ordinately regulates CXCR4/CXCL12 and MMP2/MMP9 expression in human clear-cell renal cell carcinoma. J Pathol **2008**;214(4):464-71 doi 10.1002/path.2310.
170. Cheng B, Yang G, Jiang R, Cheng Y, Yang H, Pei L*, et al.* Cancer stem cell markers predict a poor prognosis in renal cell carcinoma: a meta-analysis. Oncotarget **2016**;7(40):65862-75 doi 10.18632/oncotarget.11672.
171. Marcato P, Dean CA, Giacomantonio CA, Lee PW. Aldehyde dehydrogenase: its role as a cancer stem cell marker comes down to the specific isoform. Cell Cycle **2011**;10(9):1378-84 doi 10.4161/cc.10.9.15486.
172. Resetkova E, Reis-Filho JS, Jain RK, Mehta R, Thorat MA, Nakshatri H*, et al.* Prognostic impact of ALDH1 in breast cancer: a story of stem cells and tumor microenvironment. Breast Cancer Res Treat **2010**;123(1):97-108 doi 10.1007/s10549-009-0619-3.
173. Abourbih S, Sircar K, Tanguay S, Kassouf W, Aprikian A, Mansure J*, et al.* Aldehyde dehydrogenase 1 expression in primary and metastatic renal cell carcinoma: an immunohistochemistry study. World J Surg Oncol **2013**;11:298 doi 10.1186/1477-7819-11-298.
174. Ozbek E, Calik G, Otunctemur A, Aliskan T, Cakir S, Dursun M*, et al.* Stem cell markers aldehyde dehydrogenase type 1 and nestin expressions in renal cell cancer. Arch Ital Urol Androl **2012**;84(1):7-11.
175. Chen KG, Szakacs G, Annereau JP, Rouzaud F, Liang XJ, Valencia JC*, et al.* Principal expression of two mRNA isoforms (ABCB 5alpha and ABCB 5beta) of the ATP-binding cassette transporter gene ABCB 5 in melanoma cells and melanocytes. Pigment Cell Res **2005**;18(2):102-12 doi 10.1111/j.1600-0749.2005.00214.x.

176. Wilson BJ, Saab KR, Ma J, Schatton T, Putz P, Zhan Q*, et al.* ABCB5 maintains melanoma-initiating cells through a proinflammatory cytokine signaling circuit. Cancer Res **2014**;74(15):4196-207 doi 10.1158/0008-5472.CAN-14-0582.
177. Liu C, Tang DG. MicroRNA regulation of cancer stem cells. Cancer Res **2011**;71(18):5950-4 doi 10.1158/0008-5472.CAN-11-1035.
178. Baracca A, Sgarbi G, Solaini G, Lenaz G. Rhodamine 123 as a probe of mitochondrial membrane potential: evaluation of proton flux through F(0) during ATP synthesis. Biochimica et biophysica acta **2003**;1606(1-3):137-46.
179. Miltenyi S, Muller W, Weichel W, Radbruch A. High gradient magnetic cell separation with MACS. Cytometry **1990**;11(2):231-8 doi 10.1002/cyto.990110203.
180. Hu P, Zhang W, Xin H, Deng G. Single Cell Isolation and Analysis. Front Cell Dev Biol **2016**;4:116 doi 10.3389/fcell.2016.00116.
181. Moghbeli M, Moghbeli F, Forghanifard MM, Abbaszadegan MR. Cancer stem cell detection and isolation. Med Oncol **2014**;31(9):69 doi 10.1007/s12032-014-0069-6.
182. Khan MI, Czarnecka AM, Helbrecht I, Bartnik E, Lian F, Szczylik C. Current approaches in identification and isolation of human renal cell carcinoma cancer stem cells. Stem Cell Res Ther **2015**;6:178 doi 10.1186/s13287-015-0177-z.
183. Abbaszadegan MR, Bagheri V, Razavi MS, Momtazi AA, Sahebkar A, Gholamin M. Isolation, identification, and characterization of cancer stem cells: A review. J Cell Physiol **2017**;232(8):2008-18 doi 10.1002/jcp.25759.
184. Goodell MA. Stem cell identification and sorting using the Hoechst 33342 side population (SP). Curr Protoc Cytom **2005**;Chapter 9:Unit9 18 doi 10.1002/0471142956.cy0918s34.
185. Yuhas JM, Li AP, Martinez AO, Ladman AJ. A simplified method for production and growth of multicellular tumor spheroids. Cancer Res **1977**;37(10):3639-43.
186. Weiswald LB, Bellet D, Dangles-Marie V. Spherical cancer models in tumor biology. Neoplasia **2015**;17(1):1-15 doi 10.1016/j.neo.2014.12.004.
187. Clevers H. Modeling Development and Disease with Organoids. Cell **2016**;165(7):1586-97 doi 10.1016/j.cell.2016.05.082.
188. Drost J, Karthaus WR, Gao D, Driehuis E, Sawyers CL, Chen Y*, et al.* Organoid culture systems for prostate epithelial and cancer tissue. Nat Protoc **2016**;11(2):347-58 doi 10.1038/nprot.2016.006.
189. Pauli C, Hopkins BD, Prandi D, Shaw R, Fedrizzi T, Sboner A*, et al.* Personalized In Vitro and In Vivo Cancer Models to Guide Precision Medicine. Cancer Discov **2017**;7(5):462-77 doi 10.1158/2159-8290.CD-16-1154.
190. Kurosawa H. Methods for inducing embryoid body formation: in vitro differentiation system of embryonic stem cells. J Biosci Bioeng **2007**;103(5):389-98 doi 10.1263/jbb.103.389.
191. Thoma CR, Zimmermann M, Agarkova I, Kelm JM, Krek W. 3D cell culture systems modeling tumor growth determinants in cancer target discovery. Adv Drug Deliv Rev **2014**;69-70:29-41 doi 10.1016/j.addr.2014.03.001.
192. Atay S, Godwin AK. Tumor-derived exosomes: A message delivery system for tumor progression. Commun Integr Biol **2014**;7(1):e28231 doi 10.4161/cib.28231.
193. Plaks V, Kong N, Werb Z. The cancer stem cell niche: how essential is the niche in regulating stemness of tumor cells? Cell stem cell **2015**;16(3):225-38 doi 10.1016/j.stem.2015.02.015.
194. Kessenbrock K, Dijkgraaf GJ, Lawson DA, Littlepage LE, Shahi P, Pieper U*, et al.* A role for matrix metalloproteinases in regulating mammary stem cell function via the Wnt signaling pathway. Cell stem cell **2013**;13(3):300-13 doi 10.1016/j.stem.2013.06.005.
195. Wu J, Qu Z, Fei ZW, Wu JH, Jiang CP. Role of stem cell-derived exosomes in cancer. Oncology letters **2017**;13(5):2855-66 doi 10.3892/ol.2017.5824.
196. Cabarcas SM, Mathews LA, Farrar WL. The cancer stem cell niche--there goes the neighborhood? Int J Cancer **2011**;129(10):2315-27 doi 10.1002/ijc.26312.
197. Kalluri R, Weinberg RA. The basics of epithelial-mesenchymal transition. J Clin Invest **2009**;119(6):1420-8 doi 10.1172/JCI39104.

198. Yang C, Robbins PD. The roles of tumor-derived exosomes in cancer pathogenesis. Clin Dev Immunol **2011**;2011:842849 doi 10.1155/2011/842849.
199. Henderson MC, Azorsa DO. The genomic and proteomic content of cancer cell-derived exosomes. Frontiers in oncology **2012**;2:38 doi 10.3389/fonc.2012.00038.
200. Thakur BK, Zhang H, Becker A, Matei I, Huang Y, Costa-Silva B*, et al.* Double-stranded DNA in exosomes: a novel biomarker in cancer detection. Cell Res **2014**;24(6):766-9 doi 10.1038/cr.2014.44.
201. Fang DY, King HW, Li JY, Gleadle JM. Exosomes and the kidney: blaming the messenger. Nephrology **2013**;18(1):1-10 doi 10.1111/nep.12005.
202. Peinado H, Aleckovic M, Lavotshkin S, Matei I, Costa-Silva B, Moreno-Bueno G*, et al.* Melanoma exosomes educate bone marrow progenitor cells toward a pro-metastatic phenotype through MET. Nat Med **2012**;18(6):883-91 doi 10.1038/nm.2753.
203. Valadi H, Ekstrom K, Bossios A, Sjostrand M, Lee JJ, Lotvall JO. Exosome-mediated transfer of mRNAs and microRNAs is a novel mechanism of genetic exchange between cells. Nat Cell Biol **2007**;9(6):654-9 doi 10.1038/ncb1596.
204. Clayton A, Mason MD. Exosomes in tumour immunity. Curr Oncol **2009**;16(3):46-9.
205. Thery C, Amigorena S, Raposo G, Clayton A. Isolation and characterization of exosomes from cell culture supernatants and biological fluids. Curr Protoc Cell Biol **2006**;Chapter 3:Unit 3 22 doi 10.1002/0471143030.cb0322s30.
206. Matsuo H, Chevallier J, Mayran N, Le Blanc I, Ferguson C, Faure J*, et al.* Role of LBPA and Alix in multivesicular liposome formation and endosome organization. Science **2004**;303(5657):531-4 doi 10.1126/science.1092425.
207. Thery C, Ostrowski M, Segura E. Membrane vesicles as conveyors of immune responses. Nat Rev Immunol **2009**;9(8):581-93 doi 10.1038/nri2567.
208. Camussi G, Deregibus MC, Bruno S, Cantaluppi V, Biancone L. Exosomes/microvesicles as a mechanism of cell-to-cell communication. Kidney Int **2010**;78(9):838-48 doi 10.1038/ki.2010.278.
209. Borges FT, Reis LA, Schor N. Extracellular vesicles: structure, function, and potential clinical uses in renal diseases. Brazilian journal of medical and biological research = Revista brasileira de pesquisas medicas e biologicas / Sociedade Brasileira de Biofisica [et al] **2013**;46(10):824-30 doi 10.1590/1414-431X20132964.
210. Soekmadji C, Russell PJ, Nelson CC. Exosomes in prostate cancer: putting together the pieces of a puzzle. Cancers (Basel) **2013**;5(4):1522-44 doi 10.3390/cancers5041522.
211. Nilsson J, Skog J, Nordstrand A, Baranov V, Mincheva-Nilsson L, Breakefield XO*, et al.* Prostate cancer-derived urine exosomes: a novel approach to biomarkers for prostate cancer. Br J Cancer **2009**;100(10):1603-7 doi 10.1038/sj.bjc.6605058.
212. Kumar D, Gupta D, Shankar S, Srivastava RK. Biomolecular characterization of exosomes released from cancer stem cells: Possible implications for biomarker and treatment of cancer. Oncotarget **2015**;6(5):3280-91 doi 10.18632/oncotarget.2462.
213. Taylor DD, Zacharias W, Gercel-Taylor C. Exosome isolation for proteomic analyses and RNA profiling. Methods Mol Biol **2011**;728:235-46 doi 10.1007/978-1-61779-068-3_15.
214. Rajendran L, Honsho M, Zahn TR, Keller P, Geiger KD, Verkade P*, et al.* Alzheimer's disease beta-amyloid peptides are released in association with exosomes. Proc Natl Acad Sci U S A **2006**;103(30):11172-7 doi 10.1073/pnas.0603838103.
215. Lin LY, Du LM, Cao K, Huang Y, Yu PF, Zhang LY*, et al.* Tumour cell-derived exosomes endow mesenchymal stromal cells with tumour-promotion capabilities. Oncogene **2016**;35(46):6038-42 doi 10.1038/onc.2016.131.
216. Silva AM, Almeida MI, Teixeira JH, Maia AF, Calin GA, Barbosa MA*, et al.* Dendritic Cell-derived Extracellular Vesicles mediate Mesenchymal Stem/Stromal Cell recruitment. Sci Rep **2017**;7(1):1667 doi 10.1038/s41598-017-01809-x.
217. Hood JL, San RS, Wickline SA. Exosomes released by melanoma cells prepare sentinel lymph nodes for tumor metastasis. Cancer Res **2011**;71(11):3792-801 doi 10.1158/0008-5472.CAN-10-4455.

218. Paggetti J, Haderk F, Seiffert M, Janji B, Distler U, Ammerlaan W*, et al.* Exosomes released by chronic lymphocytic leukemia cells induce the transition of stromal cells into cancer-associated fibroblasts. Blood **2015**;126(9):1106-17 doi 10.1182/blood-2014-12-618025.
219. Riches A, Campbell E, Borger E, Powis S. Regulation of exosome release from mammary epithelial and breast cancer cells - a new regulatory pathway. Eur J Cancer **2014**;50(5):1025-34 doi 10.1016/j.ejca.2013.12.019.
220. Nazarenko I, Rana S, Baumann A, McAlear J, Hellwig A, Trendelenburg M*, et al.* Cell surface tetraspanin Tspan8 contributes to molecular pathways of exosome-induced endothelial cell activation. Cancer Res **2010**;70(4):1668-78 doi 10.1158/0008-5472.CAN-09-2470.
221. Jung T, Castellana D, Klingbeil P, Cuesta Hernandez I, Vitacolonna M, Orlicky DJ*, et al.* CD44v6 dependence of premetastatic niche preparation by exosomes. Neoplasia **2009**;11(10):1093-105.
222. Hu Y, Yan C, Mu L, Huang K, Li X, Tao D*, et al.* Fibroblast-Derived Exosomes Contribute to Chemoresistance through Priming Cancer Stem Cells in Colorectal Cancer. PLoS One **2015**;10(5):e0125625 doi 10.1371/journal.pone.0125625.
223. Bourkoula E, Mangoni D, Ius T, Pucer A, Isola M, Musiello D*, et al.* Glioma-associated stem cells: a novel class of tumor-supporting cells able to predict prognosis of human low-grade gliomas. Stem Cells **2014**;32(5):1239-53 doi 10.1002/stem.1605.
224. Wang M, Zhao C, Shi H, Zhang B, Zhang L, Zhang X*, et al.* Deregulated microRNAs in gastric cancer tissue-derived mesenchymal stem cells: novel biomarkers and a mechanism for gastric cancer. Br J Cancer **2014**;110(5):1199-210 doi 10.1038/bjc.2014.14.
225. Lin R, Wang S, Zhao RC. Exosomes from human adipose-derived mesenchymal stem cells promote migration through Wnt signaling pathway in a breast cancer cell model. Mol Cell Biochem **2013**;383(1-2):13-20 doi 10.1007/s11010-013-1746-z.
226. Hannafon BN, Ding WQ. Cancer stem cells and exosome signaling. Stem Cell Investig **2015**;2:11 doi 10.3978/j.issn.2306-9759.2015.05.02.
227. Ji R, Zhang B, Zhang X, Xue J, Yuan X, Yan Y*, et al.* Exosomes derived from human mesenchymal stem cells confer drug resistance in gastric cancer. Cell Cycle **2015**;14(15):2473-83 doi 10.1080/15384101.2015.1005530.
228. Park SY, Han J, Kim JB, Yang MG, Kim YJ, Lim HJ*, et al.* Interleukin-8 is related to poor chemotherapeutic response and tumourigenicity in hepatocellular carcinoma. Eur J Cancer **2014**;50(2):341-50 doi 10.1016/j.ejca.2013.09.021.
229. Liu Q, Li A, Tian Y, Wu JD, Liu Y, Li T*, et al.* The CXCL8-CXCR1/2 pathways in cancer. Cytokine Growth Factor Rev **2016**;31:61-71 doi 10.1016/j.cytogfr.2016.08.002.
230. Waugh DJ, Wilson C. The interleukin-8 pathway in cancer. Clin Cancer Res **2008**;14(21):6735-41 doi 10.1158/1078-0432.CCR-07-4843.
231. Lindoso RS, Collino F, Camussi G. Extracellular vesicles derived from renal cancer stem cells induce a pro-tumorigenic phenotype in mesenchymal stromal cells. Oncotarget **2015**;6(10):7959-69 doi 10.18632/oncotarget.3503.
232. Bi LK, Zhou N, Liu C, Lu FD, Lin TX, Xuan XJ*, et al.* Kidney cancer cells secrete IL-8 to activate Akt and promote migration of mesenchymal stem cells. Urol Oncol **2014**;32(5):607-12 doi 10.1016/j.urolonc.2013.10.018.
233. Yu PF, Huang Y, Han YY, Lin LY, Sun WH, Rabson AB*, et al.* TNFalpha-activated mesenchymal stromal cells promote breast cancer metastasis by recruiting CXCR2+ neutrophils. Oncogene **2017**;36(4):482-90 doi 10.1038/onc.2016.217.
234. Alfaro C, Sanmamed MF, Rodriguez-Ruiz ME, Teijeira A, Onate C, Gonzalez A*, et al.* Interleukin-8 in cancer pathogenesis, treatment and follow-up. Cancer treatment reviews **2017**;60:24-31 doi 10.1016/j.ctrv.2017.08.004.
235. Yang Z, Xie H, He D, Li L. Infiltrating macrophages increase RCC epithelial mesenchymal transition (EMT) and stem cell-like populations via AKT and mTOR signaling. Oncotarget **2016**;7(28):44478-91 doi 10.18632/oncotarget.9873.

236. Chen L, Fan J, Chen H, Meng Z, Chen Z, Wang P*, et al.* The IL-8/CXCR1 axis is associated with cancer stem cell-like properties and correlates with clinical prognosis in human pancreatic cancer cases. Sci Rep **2014**;4:5911 doi 10.1038/srep05911.
237. Chen Y, Shi M, Yu GZ, Qin XR, Jin G, Chen P*, et al.* Interleukin-8, a promising predictor for prognosis of pancreatic cancer. World J Gastroenterol **2012**;18(10):1123-9 doi 10.3748/wjg.v18.i10.1123.
238. Ginestier C, Liu S, Diebel ME, Korkaya H, Luo M, Brown M*, et al.* CXCR1 blockade selectively targets human breast cancer stem cells in vitro and in xenografts. J Clin Invest **2010**;120(2):485-97 doi 10.1172/JCI39397.
239. Lee YS, Choi I, Ning Y, Kim NY, Khatchadourian V, Yang D*, et al.* Interleukin-8 and its receptor CXCR2 in the tumour microenvironment promote colon cancer growth, progression and metastasis. Br J Cancer **2012**;106(11):1833-41 doi 10.1038/bjc.2012.177.
240. Mian BM, Dinney CP, Bermejo CE, Sweeney P, Tellez C, Yang XD*, et al.* Fully human anti-interleukin 8 antibody inhibits tumor growth in orthotopic bladder cancer xenografts via down-regulation of matrix metalloproteases and nuclear factor-kappaB. Clin Cancer Res **2003**;9(8):3167-75.
241. Knall C, Young S, Nick JA, Buhl AM, Worthen GS, Johnson GL. Interleukin-8 regulation of the Ras/Raf/mitogen-activated protein kinase pathway in human neutrophils. J Biol Chem **1996**;271(5):2832-8.
242. Luppi F, Longo AM, de Boer WI, Rabe KF, Hiemstra PS. Interleukin-8 stimulates cell proliferation in non-small cell lung cancer through epidermal growth factor receptor transactivation. Lung Cancer **2007**;56(1):25-33 doi 10.1016/j.lungcan.2006.11.014.
243. Venkatakrishnan G, Salgia R, Groopman JE. Chemokine receptors CXCR-1/2 activate mitogen-activated protein kinase via the epidermal growth factor receptor in ovarian cancer cells. J Biol Chem **2000**;275(10):6868-75.
244. Maxwell PJ, Gallagher R, Seaton A, Wilson C, Scullin P, Pettigrew J*, et al.* HIF-1 and NF-kappaB-mediated upregulation of CXCR1 and CXCR2 expression promotes cell survival in hypoxic prostate cancer cells. Oncogene **2007**;26(52):7333-45 doi 10.1038/sj.onc.1210536.
245. Liu YN, Chang TH, Tsai MF, Wu SG, Tsai TH, Chen HY*, et al.* IL-8 confers resistance to EGFR inhibitors by inducing stem cell properties in lung cancer. Oncotarget **2015**;6(12):10415-31 doi 10.18632/oncotarget.3389.
246. An H, Zhu Y, Xie H, Liu Y, Liu W, Fu Q*, et al.* Increased expression of interleukin-8 is an independent indicator of poor prognosis in clear-cell renal cell carcinoma. Tumour Biol **2016**;37(4):4523-9 doi 10.1007/s13277-015-4158-8.
247. Azzi S, Bruno S, Giron-Michel J, Clay D, Devocelle A, Croce M*, et al.* Differentiation therapy: targeting human renal cancer stem cells with interleukin 15. J Natl Cancer Inst **2011**;103(24):1884-98 doi 10.1093/jnci/djr451.
248. Giron-Michel J, Azzi S, Ferrini S, Chouaib S, Camussi G, Eid P*, et al.* Interleukin-15 is a major regulator of the cell-microenvironment interactions in human renal homeostasis. Cytokine Growth Factor Rev **2013**;24(1):13-22 doi 10.1016/j.cytogfr.2012.08.006.
249. Giron-Michel J, Azzi S, Khawam K, Caignard A, Devocelle A, Perrier A*, et al.* Interleukin-15 is a major regulator of the cell-microenvironment interactions in human renal cancer. Bull Cancer **2011**;98(5):32-9 doi 10.1684/bdc.2011.1359.
250. Wang L, Park P, La Marca F, Than KD, Lin CY. BMP-2 inhibits tumor-initiating ability in human renal cancer stem cells and induces bone formation. J Cancer Res Clin Oncol **2015**;141(6):1013-24 doi 10.1007/s00432-014-1883-0.
251. Varney ML, Singh S, Li A, Mayer-Ezell R, Bond R, Singh RK. Small molecule antagonists for CXCR2 and CXCR1 inhibit human colon cancer liver metastases. Cancer Lett **2011**;300(2):180-8 doi 10.1016/j.canlet.2010.10.004.
252. Singh S, Sadanandam A, Nannuru KC, Varney ML, Mayer-Ezell R, Bond R*, et al.* Small-molecule antagonists for CXCR2 and CXCR1 inhibit human melanoma growth by decreasing tumor cell proliferation, survival, and angiogenesis. Clin Cancer Res **2009**;15(7):2380-6 doi 10.1158/1078-0432.CCR-08-2387.

253. Merritt WM, Lin YG, Spannuth WA, Fletcher MS, Kamat AA, Han LY*, et al.* Effect of interleukin-8 gene silencing with liposome-encapsulated small interfering RNA on ovarian cancer cell growth. J Natl Cancer Inst **2008**;100(5):359-72 doi 10.1093/jnci/djn024.
254. Giesen C, Wang HA, Schapiro D, Zivanovic N, Jacobs A, Hattendorf B*, et al.* Highly multiplexed imaging of tumor tissues with subcellular resolution by mass cytometry. Nat Methods **2014**;11(4):417-22 doi 10.1038/nmeth.2869.
255. Mittelbrunn M, Gutierrez-Vazquez C, Villarroya-Beltri C, Gonzalez S, Sanchez-Cabo F, Gonzalez MA*, et al.* Unidirectional transfer of microRNA-loaded exosomes from T cells to antigen-presenting cells. Nature communications **2011**;2:282 doi 10.1038/ncomms1285.
256. Baldewijns MM, van Vlodrop IJ, Schouten LJ, Soetekouw PM, de Bruine AP, van Engeland M. Genetics and epigenetics of renal cell cancer. Biochimica et biophysica acta **2008**;1785(2):133-55 doi 10.1016/j.bbcan.2007.12.002.
257. Moch H. [The WHO/ISUP grading system for renal carcinoma]. Pathologe **2016**;37(4):355-60 doi 10.1007/s00292-016-0171-y.
258. Thakur BK, Zhang H, Becker A, Matei I, Huang Y, Costa-Silva B*, et al.* Double-stranded DNA in exosomes: a novel biomarker in cancer detection. Cell research **2014** doi 10.1038/cr.2014.44.
259. Horvath P, Aulner N, Bickle M, Davies AM, Nery ED, Ebner D*, et al.* Screening out irrelevant cell-based models of disease. Nat Rev Drug Discov **2016**;15(11):751-69 doi 10.1038/nrd.2016.175.
260. Chevrier S, Levine JH, Zanotelli VRT, Silina K, Schulz D, Bacac M*, et al.* An Immune Atlas of Clear Cell Renal Cell Carcinoma. Cell **2017**;169(4):736-49 e18 doi 10.1016/j.cell.2017.04.016.
261. Motzer RJ, Escudier B, McDermott DF, George S, Hammers HJ, Srinivas S*, et al.* Nivolumab versus Everolimus in Advanced Renal-Cell Carcinoma. N Engl J Med **2015**;373(19):1803-13 doi 10.1056/NEJMoa1510665.
262. Motzer RJ, Rini BI, McDermott DF, Redman BG, Kuzel TM, Harrison MR*, et al.* Nivolumab for Metastatic Renal Cell Carcinoma: Results of a Randomized Phase II Trial. J Clin Oncol **2015**;33(13):1430-7 doi 10.1200/JCO.2014.59.0703.
263. Choueiri TK, Fishman MN, Escudier B, McDermott DF, Drake CG, Kluger H*, et al.* Immunomodulatory Activity of Nivolumab in Metastatic Renal Cell Carcinoma. Clin Cancer Res **2016**;22(22):5461-71 doi 10.1158/1078-0432.CCR-15-2839.
264. Sanmamed MF, Carranza-Rua O, Alfaro C, Onate C, Martin-Algarra S, Perez G*, et al.* Serum interleukin-8 reflects tumor burden and treatment response across malignancies of multiple tissue origins. Clin Cancer Res **2014**;20(22):5697-707 doi 10.1158/1078-0432.CCR-13-3203.
265. Highfill SL, Cui Y, Giles AJ, Smith JP, Zhang H, Morse E*, et al.* Disruption of CXCR2-mediated MDSC tumor trafficking enhances anti-PD1 efficacy. Sci Transl Med **2014**;6(237):237ra67 doi 10.1126/scitranslmed.3007974.

ANNEX

8. Current updates in biomarker discovery for renal cancer stem cells

Author contributions

C.C. conceived and designed the manuscript. **C.C.** and **H.M.** acquired and interpreted literature data. **C.C.** wrote the manuscript, whereas **H.M.** assisted in the manuscript drafting and revision.

Current updates in biomarker discovery for renal cancer stem cells.

Journal:	*The Journal of Pathology: Clinical Research*
Manuscript ID	CJP-2017-09-0038.R1
Wiley - Manuscript type:	Invited Review
Date Submitted by the Author:	n/a
Complete List of Authors:	Corro, Claudia; UniversitatsSpital Zurich Institut fur klinische Pathologie, Department of Pathology Moch, Holger; Institute of Surgical Pathology , Department Pathology
Abstract:	Characterized by high intra- and inter-tumor heterogeneity renal cell carcinoma is resistant to chemo- and radiotherapy in metastatic stage. Therefore, development of new prognostic and diagnostic markers for RCC patients are needed. Cancer stem cells are a small population of neoplastic cells within a tumor presenting characteristics reminiscent of normal stem cells. In particular, they are capable to give rise to all the cell types present in the tumor tissue which they derive from (differentiation). They are characterized by unlimited cell division, maintenance of the stem cell pool (self-renewal), give rise to tumor and metastasis in vivo (tumorigenicity), and they are responsible for resistance to therapies and tumor recurrence. So far, many studies tried to establish unique biomarkers to identify cancer stem cell populations in RCC. At the same time, different approaches were developed with the aim to isolate cancer stem cells. Several markers were found specifically expressed in cancer stem cells and cancer-like stem cells derived from RCC such as CD105, ALDH1, OCT4, CD133, CXCR4 and Rh123. However, genetic and epigenetic mechanisms and tumor microenvironment contributing to cellular plasticity make the discovery of unique biomarkers a very difficult task. Therefore, a better understanding of the mechanism underlying CSC may help dissecting tumor heterogeneity and drug treatment efficiency.

Biomarker discovery for renal cancer stem cells.

Claudia Corrò[1] **and Holger Moch**[1]

[1]Department of Pathology and Molecular Pathology, University Hospital Zurich, Switzerland

[*]Correspondence to Claudia Corrò, Department of Pathology and Molecular Pathology, University Hospital Zurich, Schmelzbergstrasse 12, 8091 Zurich, Switzerland, Phone: 41-44-255-2537, Fax: 41-44-255-4440, E-mail: Claudia.Corro@usz.ch;

Running title: CSCs in RCC.

Conflict-of-interest statement: None.

Article category: Review.

Author contribution:

C.C. conceived and designed the manuscript. **C.C.** and **H.M.** acquired and interpreted literature data. **C.C.** wrote the manuscript, whereas **H.M.** assisted in the manuscript drafting and revision.

Abstract

Characterized by high intra- and inter-tumor heterogeneity, renal cell carcinoma (RCC) is resistant to chemo- and radiotherapy in metastatic stage. Therefore, the development of new prognostic and diagnostic markers for RCC patients is needed. Cancer stem cells (CSCs) are a small population of neoplastic cells within a tumor which present characteristics reminiscent of normal stem cells (NSCs). CSCs are characterized by unlimited cell division, maintenance of the stem cell pool (self-renewal), capability to give rise to all cell types within a tumor and contribute to metastasis *in vivo* (tumorigenicity), treatment resistance and recurrence. So far, many studies have tried to establish unique biomarkers to identify CSC populations in RCC. At the same time, different approaches were developed with the aim to isolate CSCs. Consequently, several markers were found specifically expressed in CSCs and cancer stem-like cells derived from RCC such as CD105, ALDH1, OCT4, CD133, and CXCR4. However, genetic and epigenetic mechanisms and tumor microenvironment contributing to cellular plasticity made the discovery of unique biomarkers a very difficult task. In fact, contrasting results regarding the applicability of such markers in the isolation of renal CSCs have been reported in the literature. Therefore, a better understanding of the mechanism underlying CSC may help dissecting tumor heterogeneity and drug treatment efficiency.

Keywords: cancer stem cells, tumor-initiating cells, renal cell carcinoma, biomarkers.

Introduction

Renal cell carcinoma (RCC), a malignant tumor affecting the adult kidney, accounts for 2 % of all cancers. Affecting 64'000 people every year with 20 % death incidence, RCC is among the 10 most common cancer worldwide [1]. Arising from the renal tubular epithelial cell, RCC is the most frequent malignancy affecting the adult kidney (87 %) [2].

RCCs are a very heterogeneous class of tumors [3]. According to the classification proposed by the World Health Organization in 2016, which combines histological and genetic characteristics and clinical implications, RCC can be subdivided into three different entities [3,4]. Clear cell renal cell carcinoma (ccRCC) is the most common subtype of RCC and represents up to 80 % of all RCCs [5,6], papillary renal cell carcinoma (pRCC) accounts for 10-15 % of all RCCs [7-9], whereas chromophobe RCC (chRCC) embodies only the remainder 5 % [10].

RCC is characterized by asymptomatic manifestation in early stage and a poor response to radiotherapy and chemotherapy in metastatic stage, making this tumor type very difficult to diagnose and treat [11]. Due to the much higher prevalence of ccRCCs, very few clinical trials have been carried out considering other histological RCC subtypes. Therefore, most of the drugs have been developed based on ccRCC, and they are currently applied to all RCC patients. Treatment of advanced or metastatic RCC patients is achieved primarily by targeted therapies (TKIs) and five-year survival for these patients is 12 % [12]. Despite all the progress made in the development of novel anti-cancer compounds, the management and treatment of RCC patients still remains a crucial aspect in the clinics.

In particular, intra-tumor and inter-tumor heterogeneity is one of the major limitation in the treatment of epithelial tumors [13]. Two different tumor models were proposed playing a role in tumor development, progression and tumor heterogeneity. The clonal evolution model or stochastic model implies the presence of a tumor cell population carrying different mutations

which were accumulated during time and then selected under different selective pressure [14]. Every cell within a tumor has potentially the same likelihood to facilitate tumor formation and progression. Selection, clonal expansion and genetic instability are the key elements driving the stochastic approach [15]. The cancer stem cell (CSC) model or hierarchical model, instead, proposes that tumor growth and propagation is driven by a small phenotypically distinct subset of cells within the total cancer cell population with pluriproliferative features [16,17]. According to this model, the tumor bulk is established by a pool of CSCs that have both stem cell potential and the ability to give rise to progeny with self-limited proliferative capacity [18]. As result of this model the elimination of the entire CSC population will result in the tumor eradication, whereas leaving even only one cell behind will end up in tumor recurrence [15,19].

Nevertheless, it is becoming increasingly clear that genetic and epigenetic factors are not just the only two factors contributing to tumor heterogeneity. The tumor microenvironment (TME), stroma cells, soluble molecules and extracellular vesicles (i.e. exosomes) play an important role in modulating metastatic properties and sensitivity of tumor cells to therapy [20,21]. Therapy itself may act as selection mechanism that shapes tumor evolution. More recently, a unifying model of clonal evolution applied to CSCs was proposed by Kreso et al., whereby CSCs can acquire mutations and generate new stem cell branches, and at the same time, tumor cells in the non-CSC subpopulation can undergo epithelial-mesenchymal transition (EMT) and acquire CSC-like features contributing to tumor heterogeneity [17] (Fig. 1). Processes like inflammation, hypoxia, angiogenesis and EMT undergoing in the TME contribute to maintenance of the CSC fate. Due to cellular plasticity, it is important to note that the cell of origin -the normal cell that acquires the first genetic hit(s) that culminate in the initiation of cancer- is not necessarily referred to the CSC population as the hierarchical model would suggest instead. CSCs are the cellular subset within the

tumor that uniquely sustains malignant growth. Cells-of-origin and CSCs refer to tumor-initiating cells (TICs) and cancer-propagating cells, respectively [22].

CSCs are a small population of neoplastic cells within a tumor presenting characteristics reminiscent of normal stem cells. In particular, they are capable to give rise to all the cell types present in the tumor tissue which they derive from (differentiation). They are characterized by unlimited cell division and maintenance of the stem cell pool (self-renewal). They can give rise to tumor and contribute to metastasis formation *in vivo* (tumorigenicity). Moreover, CSCs are recognized being the major cause of tumor recurrence and resistance to therapy.

Dick and co-authors performed the first experimental study on CSCs in 1994. They isolated $CD34^+/CD38^-$ cells from acute myeloid leukemia (AML) patients and showed they could initiate AML *in vivo* upon transplantation into NOD/SCID mice [23,24]. Subsequently, several others have showed the presence of CSCs in colorectal cancer, breast cancer, glioblastoma, melanoma, lung cancer, liver and prostate cancer [25-34]. Growing evidence suggests that renal cancer, as many other solid tumors, possesses a rare population of cells capable of self-renewal that contribute to metastasis and resistance to therapy [35]. Therefore, the identification of a specific subpopulation of cells within a tumor that either initiate or maintain tumorigenesis is of utmost importance for understanding tumor biology and in the development of novel therapies. In this review, we outline potential CSC markers in RCC as well as advantages and pitfalls in the identification of these tumor-propagating cells.

Cancer stem cell biomarkers

To date, several markers were found specifically expressed in CSCs and cancer stem-like cells derived from RCC. A summary of these putative CSC markers is listed in table 1.

CD105

Among those, CD105 (endoglin) is a transmembrane glycoprotein encoded by the *endoglin* gene located on chromosome 9q34. This protein is composed of two constitutively phosphorylated subunits of 95 KDa each, forming a 180 KDa homodimeric mature protein [36]. CD105 is an accessory protein of the TGFβ complex. Upon activation of the TGFβ complex, the binding of endoglin results in the activation of Smad proteins leading to the regulation of various cellular processes such as cell proliferation, migration, differentiation and angiogenesis [37]. Endoglin is predominantly expressed in endothelial cells where it is activated by hypoxia and TGFβ stimulation, whereas it is decreased by tumor necrosis factor α (TNFα) [38].

Interestingly, in breast, prostate and gastric cancer, CD105 was found present in endothelial cells forming immature tumor vasculature. In ccRCC, a subpopulation of cells representing <10 % of the tumor mass showed CD105 upregulation. $CD105^+$ cells isolated by magnetic sorting displayed potent capability to grow as spheres and initiate tumors and metastasis recapitulating the clear cell histological pattern in mice [39,40]. These cells also expressed mesenchymal markers CD44, CD90, CD29, CD73 and Vimentin; embryonic stem cell markers Oct3/4, Nanog and Nestin and the embryonic renal marker Pax2 [39]. However, they did not express CD133 also known as human tubular progenitor cell marker [41]. $CD105^+$ CSCs were able to differentiate into epithelial and endothelial cells and generate $CD105^-$ cells. Additionally, immunohistochemical analysis of tumoral CD105 was found positively correlated to nuclear grade and tumor stage, whereas endothelial expression negatively correlates with clinicopathological features [42]. Thus, CD105 has been proposed as the main marker for CSC identification in RCC.

CSCs have been found secreting higher amount of exosomes and CSC-derived exosomes have been found involved in promoting angiogenesis in xenograft mice with renal cancer [40],

metastatic niche formation in lung carcinoma [43] as well as invasion, migration and tumor growth in many other tumor types [44-48]. Interestingly, $CD105^+$ CSCs can release microvesicles and exosomes containing pro-angiogenic mRNAs (VEGF, FGF, MMP2 and 9) that trigger angiogenesis and promote the formation of a premetastatic niche *in vivo* [40]. Extracellular vesicles (EVs) derived from renal CSCs impaired T cell activation and dendritic cell differentiation by HLA-G promoting escape from the immune system [49].

Nevertheless, the use of CD105 as a renal CSCs marker was questioned in many studies where $CD105^-$ cells also showed CSC-like features [50].

CD133

Prominin-1 (CD133) is a transmembrane glycoprotein of 865 amino acids (120 KDa) encoded by the gene *PROM1* on chromosome 4p15 [51]. This protein exists in different isoforms and its regulation is quite complex [52,53]. Expressed by almost all cell types, CD133 localizes in the plasma membrane suggesting its involvement in membrane remodeling and signal transduction [52]. Phosphorylation of CD133 results in the activation of PI3K/AKT signaling pathway [54,55]. Hypoxia, mTOR inhibition, TGFβ1 increased CD133 expression in lung cancer, pancreatic cancer and hepatocellular carcinoma (HCC). Oct4 and Sox2 have been found binding the promoter region of CD133 inducing its activation in lung cancer cell lines. Along with its expression in stem and progenitor cells within normal tissues, CD133 has been proposed as putative CSC marker across different tumor types [52].

$CD133^+$ cancer cells were able to form spheres, give rise to tumors *in vivo* and exhibit chemoresistance properties in colorectal carcinoma (CRC), HCC, lung cancer, glioblastoma, pancreatic cancer and ovarian cancer. On the contrary, sorted $CD133^+$ cells from RCC patients did not show tumorigenic capability *in vivo* although they expressed stem cell markers such as CD44,

CD29, Vimentin, and Pax2 [41]. When co-transplanted with renal carcinoma cells, $CD133^+$ progenitors significantly enhanced tumor development and growth. The same result was obtain using $CD133^+$ cells derived from normal kidney tissue [56]. Of note, $CD105^+$ cells did not express CD133, suggesting that $CD133^+$ cells may represent renal resident adult progenitor cells rather than CSCs.

Interestingly, $CD133^+/CD24^+$ cells derived from RCC cell lines ACHN and Caki1 displayed sphere formation capability, enhanced invasion and migration properties, high colony formation efficiency in soft agar, and resistance to sorafenib and cisplatin [57].

Another interesting publication identified CD133 and CXCR4 coexpressing CSCs in spheres derived from RCC xenografts and tumor tissues. Increased expression of these markers was found in RCC patients after sunitinib treatment [58]. Nevertheless, whether the CD133 and CXCR4 positive or negative cells had detectable levels of CD105 was not assessed. Additionally, the gene expression profile as well as the tumorigenic potential of the spheres was not deciphered. Moreover, $CD133^-$ cells were also able to give riese to tumors in immunodeficient mice in glioblastoma and CRC [59,60].

Lastly, CD133 expression was found strongly correlated with nuclear HIF1α in RCC patients [61,62]. CD133 mRNA levels in blood can be useful for identifying metastasis, predicting recurrence, and stratifying the patients into different risk groups for possible adjuvant treatment [63]. However, CD133 expression analyzed by IHC in RCC patients was inconsistent and varied among different studies [37,64]. Because of the complex epigenetic and microenvironmental modulation together with higher protein processing and post-translation modifications, the applicability of CD133 as a CSC marker is limited [52].

CD44

CD44 is a transmembrane glycoprotein of 85 KDa (742 aa) encoded by the *CD44* gene located on chromosome 11. CD44 exists in more than 20 isoforms due to RNA alternative splicing, giving rise to different proteins in different cancer tissue subtypes. Due to the wide variety of isoforms, CD44 is involved in diverse biological processes such as cell-cell interaction, cell adhesion, migration, proliferation, differentiation and angiogenesis [65].

Although other extracellular matrix (ECM) components such as collagen, growth factors and metalloproteinases can interact with CD44, the extracellular glycosaminoglycan hyaluronan (HA) represent its primary ligand [66]. Binding of CD44 to HA promotes multiple signaling pathways including activation of receptor tyrosine kinases (RTK), TGFβ, MAPK, PI3K/AKT supporting cell proliferation, survival, invasion, and ultimately homing of CSCs in many tumor types [65,67]. In addition, CD44 has been found involved in the regulation of stem cell features via the Wnt/β-catenin signaling pathway and protein kinase C (PKC) [68]. Because of its tight interaction with the ECM, CD44 plays an essential role in the modulation of CSC niche. CSCs can synthetize HA to attract tumor-associated macrophages (TAMs) in the CSC niche. On the other hand, stromal cells will produce growth factors that regulate stem cell activity [65]. Enhanced CD44 expression was observed in RCC cell lines after co-culture with macrophages. This effect was the result of the activation of NFkβ pathway by the TNFα derived from TAMs [69]. TNF-α enhanced migration and invasion of ccRCC cells together with down-regulation of E-cadherin expression and up-regulation of matrix metalloproteinase 9 (MMP9) and CD44 expression [70]. Interestingly, spheres derived from HEK293T, ACHN, Caki-1 and 786O renal cancer cell lines as well as $CD105^{+}$ cells isolated from RCC specimens showed the presence of a $CD44^{+}$ population having self-renewal properties, sphere formation capability and resistance to therapy [71-73]. Moreover, CD44 expression was found associated with Fuhrman grade, primary tumor stage, histological subtype, and poor prognosis in

RCC patients [37,70,74]. Therefore, CD44 expression may serve as a prognostic and predictive as well as potential CSC marker for RCC [64].

Considering the involvement of CD44 in enhancing stem cell features in cancer cells and mediating the crosstalk with the TME, CD44-based therapeutic strategies have been developed [68]. Monoclonal antibodies against CD44 are now in clinical trial for patients affected by AML, whereas knockdown of CD44 has been shown to increase sensitivity to chemotherapy in cell cultures derived from HCC, lung, breast and pancreatic cancers [66,75].

CD24

CD24 is a small cell surface protein molecule composed by only 27 amino acids resulting in a molecular weight ranging between 20 and 70 KDa depending on the glycosylation status. It is encoded by the *CD24* gene located in the chromosome 6q21. CD24 is expressed in a wide variety of cell types, including hematopoietic cells [76]. Nevertheless, it is preferentially expressed in progenitor and stem cells. CD24 was shown to be an important maker for cancer diagnosis and prognosis in breast, non-small cell lung, colon, ovarian, and prostate cancer [76-78]. CD24 upregulation has been also found associated with CSCs and CSC features in many solid tumors, on the contrary breast cancer stem cells showed low CD24 levels, suggesting that the role of CD24 in stem cells may be tissue dependent [79-81]. Interestingly, high CD24 expression was observed in CSCs derived from the RCC cell line Caki2 [82], although contrasting results were reported when analyzing the expression of CD24 together with the CSC marker CD44. Nevertheless, CD24 expression was found correlated with tumor grade, overall survival and disease-free survival in RCCs suggesting its prognostic significance [77]. Lazzeri et al. identified a subpopulation of cells exhibiting self-renewal properties, expression of stem cell transcription factors, and the ability of regenerate kidney tissue upon injury. These cells derived from the human embryonic kidney

expressed both CD24 and CD133 indicating they may represent putative normal kidney stem cells [83].

Because of the very limited research studies conducted on CD24 in RCC, we can conclude that, to date, no clear observation that CD24 can be used as CSC marker in RCC has been made.

CXCR4

The CXC-chemokine receptor 4 (CXCR4 or CD184) is a seven transmembrane G protein-coupled receptor (GPCR) on the cell membrane. It is encoded by the *CXCR4* gene located on chromosome 2q22. CXCR4 selectively binds to the CXC chemokine stromal cell-derived factor 1 (SDF1 or CXCL12) leading to the activation of a variety of biological processes such as proliferation, survival, migration, stemness and angiogenesis [84]. A number of signaling pathways are involved in the signal transduction. For instance, PLC/MAPK, PI3K/AKT, JAK/STAT and the Ras/Raf pathway.

CXCR4 was found expressed in many different tumor tissues. It has been shown in breast, small cell lung cancer (SCLC), neuroblastoma and renal cancer that $CXCR4^+$ cells migrate towards tissues expressing high levels of SDF1 to metastasize [57,85,86]. Therefore, CXCR4/SDF1 is involved in cell-stroma interactions creating a permissive niche for metastasis [37]. Further, SDF1 stimulates adhesion of bone marrow progenitor/stem cells through CD44, demonstrating again a link between CD44 and CXCR4 signaling and TME [68].

Recent studies showed that $CXCR4^+$ cells derived from several RCC cell lines (RCC26 and RCC53; Caki1, Caki2, 786O and 769P) express high levels of stem cell-associated genes and exhibit resistance to therapy (TKIs) and enhanced capability to form spheres *in vitro* and tumors *in vivo* compared to $CXCR4^-$ cells [87,88]. Whereas, inhibition of CXCR4 by ADM3100 or small interfering RNA (siRNA) impaired tumor formation [87,88]. Interestingly, loss of pVHL in ccRCCs as well as

hypoxia showed increased CXCR4 and MMPs expression indicating HIF1α may be responsible for expansion of the CXCR4 population [89]. Supporting evidence showed that $CD133^+/CXCR4^+$ cells coexpressed HIF1α and were located in perinecrotic areas in RCCs [58]. Moreover, hypoxia promoted $CD133^+/CXCR4^+$ cells tumorigenicity, whereas HIF2α was shown to be involved in the expansion of $CXCR4^+$ CSCs in four RCC cell lines [88]. The translational relevance of CXCR4 expression in the clinic was investigated in 2'673 RCC patients by meta-analysis revealing a negative correlation with between CXCR4 expression and overall survival (OS), cancer free survival (CFS) and disease free survival (DFS) [90]. Taken together these results indicate that CXCR4 may be explored as a potential CSC marker in RCC perhaps in combination with a second marker. Nevertheless, care should be taken when choosing the appropriate marker for CSC isolation since a too restrictive selection may lead to a failure in targeting all the stem-like cells present in the tumor population.

ALDH1

Aldehyde dehydrogenase 1 (ALDH1) is a cytosolic enzyme involved in the dehydrogenation of aldehydes to their corresponding carboxylic acids [91]. It is encoded by the *ALDH1* gene located in the chromosome 9q21. ALDH1 plays an important role in cellular differentiation, proliferation, mobility, embryonic development and organ homeostasis [92].

ALDH1 has been initially proposed and used as a marker to isolate stem cells from normal tissues such as brain and bone marrow with potential applications in the area of regenerative medicine [93,94]. More recently, the activity of cytosolic ALDH1 has also been shown to be a reliable marker of CSCs in several types of solid tumors, including breast, colon, pancreas, lung, liver, prostate and bladder [95 {Resetkova, 2010 #204,96]. Nevertheless, its prognostic significance in RCC is still

unclear [97], although ALDH1 was found correlated with tumor grade in RCC by Ozbek and co-authors [98].

High expression of ALDH1 was found in the side population (SP) derived from the RCC cell line ACHN compared to the non-SP. Analysis of the $ALDH1^+$ cells revealed enhanced sphere formation capability, self-renewal properties, tumorigenicity and high expression of stemness genes in the $ALDH1^+$ cells compared to $ALDH1^-$ cells. Moreover, drug treatment and hypoxia conditions were showed to increase the $ALDH1^+$ cell population *in vitro* [92].

Interestingly, a recent study investigated ALDH1 expression patterns in 24 types of normal human tissues as well as primary epithelial tumor specimens and epithelial cancer cell lines showing that ALDH1 may not be a suitable CSC marker for all tumor types especially in tissues where ALDH1 is constitutively highly expressed such as in liver and pancreas [99]. Therefore, growing evidence suggests that ALDH1 is not only a putative stem cell marker, but may actually play multiple functional roles in regulating stem cell function [91].

ABCB5

The drug efflux transporter ABCB5 (ATP-binding cassette, sub-family B, member number 5), is an integral membrane glycoprotein encoded by the *ABCB5* gene located in the chromosome 7p21. It is composed of 812 amino acids for an overall molecular weight of 90 KDa. This protein is involved in the transport of small ions, sugar, peptides and organic molecules across the plasma membrane against a concentration gradient by hydrolysis of ATP [100]. Because of its function, ABCB5 has been considered responsible for mediating therapeutic resistance [101].

ABCB5 has been found overexpressed in CSCs derived from melanoma, liver and colorectal cancers. Moreover, it was found associated with tumor progression, chemotherapy resistance and

recurrence in many other tumor types [102]. For instance in renal cell cancer, *ABCB1* was found expressed in all cells and these tumors rarely respond to primary chemotherapy treatment [103]. Therefore, ABCB5 is exploited for distinguishing between stem cells (side population) and non-stem cells using flow cytometry.

Others

DNAJB8 is part of the heat shock family proteins (HSP40) that regulate chaperone activity. It is encoded by the *DNAJB8* gene located in chromosome 3q21. DNAJB8 is commonly expressed in the testis. Recently, Nishizawa et al., showed that DNAJB8 is expressed in different cancer cells including RCCs. In particular, the expression of DNAJB8 correlated with the SP compartment, and overexpression of the protein increased SP cells. Interestingly, DNAJB8 immunization completely abolished tumor formation in mice, indicating that DNAJB8 can be a target for immunotherapy [104].

MicroRNAs (miRNAs) are non-coding small RNA molecules (22 nucleotides) involved in regulation of gene expression by translational repression, mRNA cleavage, and deadenylation. The role of miRNAs in CSCs has been described for different tumor types [105]. Six miRNAs involved in TGFβ and Wnt signaling pathways showed the most significant variations in expression by RT-PCR between spheres and parental cells derived from two metastatic RCC cell lines, ACHN and Caki1. Among those, miR17 was significantly downregulated in Caki1 and ACHN spheres. Inhibition of miR17 resulted in enhanced sphere formation indicating that TGFβ signaling plays an important role in renal CSCs and that miR17 impair the signaling cascade by targeting TGFB signaling pathway [72].

Galleggiante et al. isolated a subpopulation of cancer cells expressing CD133 and CD24 from 40 RCC samples. This population showed stem cell properties such as self-renewal, differentiation,

tumorigenicity and expression of stemness-related transcription factors. $CD133^{+}/CD24^{+}$ cells appeared to be more undifferentiated compared to the corresponding tubular adult renal progenitor cells. Interestingly, these cells also expressed on the cell membrane the amino acid transporter CTR2 which was found involved in resistance to cisplatin [106].

Rhodamine 123 (Rh123) is a fluorescent dye that permeates the cell membrane and accumulates in the mitochondria proportionally to the mitochondrial membrane potential [107]. 786O cells were stained with Rh123 and sorted by flow cytometry into two population: $Rh123^{high}$ and $Rh123^{low}$. $Rh123^{high}$ exhibited high proliferative activity, differentiation, resistance to radiation, tumorigenic potential and spheroid formation in soft agar, indicating Rh123 as an alternative method to isolate CSCs [73].

Finally, high CD73 expression was observed in spheres derived from the 786O RCC cell line. Moreover, $CD73^{+}$ cells displayed high levels of stemness-related transcription factors, resistance to radiotherapy and tumorigenicity *in vivo* [50].

Isolation techniques

Different approaches for CSC isolation have been developed over the past years (Fig. 2).

Antigen-based methods require labelling of the cells based on the expression of specific markers. These include magnetic beads-conjugated antibodies (MACS) [108,109], fluorescent-activated cell sorting (FACS) [110,111], and in some extent side population (SP) analysis [112,113]. Antigen selection often relays on markers which have been found relevant in developmental biology, embryonic and hematopoietic stem cell studies. Nevertheless, dissociation of the tumor tissue into a single cell suspension may damage surface antigens limiting the efficiency of isolating CSCs using cellular marker-based methods [112]. Further, cells can lose viability upon enzyme treatment and

sorting procedure [114]. Cell sorting itself has proven to be imprecise with 1 - 3 % of tumorigenic cells that can contaminate the non-tumorigenic population [19]. In addition, no generally applicable markers are known so far, and excessively permissive or restrictive labelling may have meaningful implications when developing therapeutic strategies targeting CSCs based on the marker expression [19]. Thus, identification and characterization of putative CSC markers may also be achieved using functional assays [41]. In order to recreate the *in vivo* CSC niche using *in vitro* culture conditions, three-dimensional cell culture models were developed. Two different methods can be adopted for culturing CSCs in 3D: anchorage-independent and anchorage-dependent. While the anchorage-independent system takes advantage of the ability of CSCs to grow in suspension, the anchorage-dependent system uses scaffolds in order to enable cells to mimic their interaction with the ECM microenvironment and promote stemness features. These methods comprehend spheroid [115,116] and organoid cultures [117-119], and sphere formation assay [111,116,120] and hanging drops [121,122], respectively.

ECM plays crucial roles in establishing the CSC niche and in mediating tumor drug resistance. It is composed of collagens, laminins, fibronectin, proteoglycans and all the non-cellular components present in the tissues [123]. Different scaffolds can be used in these 3D CSC culture assays in order to mimic ECM. Natural scaffolds include collagen, gelatin, elastin, fibrinogen, agarose and alginate. Combinations of materials are also possible. Synthetic scaffolds can overcome the risk of contamination, degradation and batch-to-batch variations compared to natural scaffolds. These are mainly polymeric microparticles (i.e. hydrogels, PLGA and PLC) [124].

Antigen-based methods

Magnetic beads conjugated antibodies (MACS)

MACS allows the isolation and the enrichment of stem cells without further staining. Cells are labelled using antibodies conjugated to magnetic nanoparticles. Labelled cells are then transferred into a column placed in a strong magnetic field. During this step, cells expressing the antigen will end up being conjugated to the magnetic beads and will stay in the column, whereas all the other cells that are negative for the antigen will flow through [108,109]. The population of interest can be subsequently eluted from the column.

Fluorescent-activated cell sorting (FACS)

FACS is an alternative isolation method capable of sorting cells using fluorescently-labeled antibodies targeting selected surface proteins or intracellular markers via direct or indirect immune fluorescence staining. Flow cytometry allows a sample of cells or particles in suspension to be separated through a narrow liquid stream. As the sample pass through a laser it allows for detection of size, granularity, and fluorescent properties of individual cells/particles in the sample [125]. Generally, FACS separation uses fluorochromes directly conjugated with either primary or secondary antibodies with different emission wavelengths. Although MACS is simpler and requires less complicated equipment than FACS, it is monoparametric and cannot isolate cells via multiple markers simultaneously [110,111].

Side population (SP)

The Hoechst SP analysis is one of the several strategies used in the stem cell studies [126]. SP is defined as a small fraction of cancer cells within a tumor exhibiting stem-like properties. The ability to discriminate the SP is based on the differential efflux of Hoechst 33342 by the multi-drug resistance ABC transporters [127]. CSCs possess higher activity and/or higher amount of the ABC pumps, which are also responsible for the efflux of chemotherapeutic agents resulting in chemotherapy resistance of CSCs [101]. Therefore, SP stands out as the portion of cells able to

extrude the dye against a concentration gradient when compared to cells not having stem cell features [113].

Identification of CSCs is achieved by specifically inhibiting ABC pumps by verapamil (100 μM) or reserpine (5 μM). Hoechst is excited at 405 nm and the blue signal is collected with a 450/40 nm band-pass filter, whereas the red fluorescence with a 610/20 nm filter. Due to the high capability to extrude Hoechst dye, side population can be defined as the negative population for Hoechst blue and Hoechst red [112]. Nevertheless, analysis of the SP has risen many concerns due to the dynamic nature of the dye efflux property as well as toxicity of the Hoechst dye making this technique highly variable [114,126].

SP isolation can also be achieved by using rhodamine 123 (Rh123) [73,128,129]. Rh123 is a mitochondrial dye that stains mitochondria with increasing intensity as cells become activated [73]. Rh123 fluorescence intensity is an index of mitochondrial mass, number and activation state, and multidrug efflux pump activity [130]. Decreased intracellular accumulations of Rh123 result from the efflux of the dye. Because also non-stem cells may express some of the ABC transporters, the isolation of CSCs through SP analysis results imperfect. SP may contain some non-stem cells, as well as some stem cells may not be located in the SP fraction [101].

Functional assays

Sphere formation assay

The sphere formation assay exploits the capability of CSCs to grow *in vitro* in an anchorage-independent manner as spheroids due to the mesenchymal phenotype. Cells are plated onto ultra-low attachment plates under serum-free medium conditions. Recent studies demonstrated that CSC expansion requires medium lacking serum, which is believed to stimulated cellular

differentiation [111,116,120]. The medium composition may vary but it is generally composed of DMEM/F12 medium supplemented with stem cell growth factors and/or hormones (i.e. bFGF, EGF, HGF, insulin, androgen and progesterone). Therefore, cancer cells with stem cell-like features are capable to proliferate and form spherical structures, whereas all the others will die. Due to the asymmetrical cell division, each CSC is capable to form a sphere composed of both, cells that have stem cell features as well as more differentiated cells. By passaging the spheres, CSCs can be enriched [111,116,120]. This results in an increased sphere number from one passage to the other. Compared to MACS and FACS, the sphere formation assay may retain clonal variations within the CSC pool by avoiding marker selection. Nevertheless, several critical parameters can impair CSC isolation and investigation using the sphere formation assay. These are inappropriate seeding cell densities which can impact sphere formation and sphere clonality; presence of quiescent CSCs which cannot be expanded using this method; and finally, possible overestimation of the stem cell frequency [131].

Hanging drops

In the hanging drop system, droplets of cell suspension are deposited on a dish or into special plates (i.e. GravityPLUS™ Hanging Drop System and Perfecta3D® hanging drop plates). Upon inversion of the tray, cells accumulates and aggregates by gravity on the surface of the liquid drop. This method is mainly used in the study of embryonic stem cells [121,122]. The Hanging Drop system allows efficient formation of uniform-size spheroids in a relative short time proving to be a very useful tool for high-throughput screening studies.

Tumor spheroids

Incorporation of ECM proteins in serum-free medium may challenge CSC-ECM interactions, normoxic/hypoxic conditions, metabolic gradients, and cooperation with stromal cell components

by co-cultures [124]. In the tumor spheroid model, a defined amount of tumor cells are encapsulated into macro-beads derived from natural or synthetic scaffolds, and let them float into the medium until spheroids are formed. Another interesting version is based on plating tumor cell into soft agar [115,116]. An initial layer of agar composed of 0.6 % agarose is disposed on the bottom of the plate. Once it has settled, a second layer of 0.3 % agarose containing a tumor single cell suspension is placed onto the 0.6 % agarose. An additional feeder layer of 0.3 % agarose is added at the end. Agarose concentration may be adapted depending on the cancer type.

Tumor organoids

Organoids are formed by distributing dissociated tumor cells into Matrigel drops. Matrigel is a gel-based natural compound that consists of laminin, collagen IV and enactin. Matrigel drops containing tumor cells are disperse into normal tissue culture plates, and the cell-matrix mixture is incubated at 37 °C before adding the medium. Different ratio of cell suspension/matrigel can be used depending on tumor type. Organoid medium is composed of adDMEM/F12 supplemented with stem cell growth factors promoting Wnt signaling pathway (B27 supplement, N-acetyl-L-cysteine, EGF, A-83, Noggin and R-spondin 1)[117-119].

Transplantation assay

To finally evaluate the tumorigenic potential of a tumor cell population expressing CSC features, cancer cells are serially transplanted into immunocompromised mice (serial tumor transplantations) at low cell density (limiting dilution assay, LDA). Cancer cells capable to develop tumors repeatedly and to recapitulate the histological features and heterogeneity of the parental tumor are defined as TICs [13]. TICs and CSCs are often used interchangeably, although TIC more specifically refers to the cell-of-origin. Nevertheless, the capability of a cancer cell to form tumors *in vivo* and to recapitulate the tumor heterogeneity of the corresponding parental tumor is one of

the most known features of a CSC. Cancer cells capable to grow as 3D cultures but that do not have tumorigenic potential cannot be considered CSCs. Importantly, immune-deficient mice are not completely devoid of an immune system, and reactions involving host cytokines and immune cells may still take place when CSCs are transplanted into immunocompromised mice [19,132,133]. Additionally, cells need to adapt to the mouse milieu shaping CSC survival and properties. Therefore, optimization of the transplantation assay as well as critical interpretation of the results should be adopted when studying CSC properties *in vivo*.

Lineage tracing

To determine the cell(s) of origin of cancer, normal cells are labeled under cell-specific promoters followed by induction of genetic modifications. In this way, a single cell or a population of cells is marked and their signature is transmitted to all the progeny [134]. Investigation of the cellular source of a tumor can be achieved by identifying and tracing over time these transformed cells responsible for forming the tumor. In parallel, this technique can be adopted to resolve the cell fate of tumor subpopulations in established tumors or to determine how cells behave in the context of the intact tissue or organism [13]. More importantly, genetic lineage tracing allows *in vivo* visualization of stem cells [124].

Normal kidney stem cells

At the top of the cellular organization, normal adult stem cells matain tissues homeostasis and facilitate regeneration [135]. Kidneys carry out many different functions in the human body, including secreting hormones, absorbing minerals, filtering blood and producing urine. Hence, impaired kidney functions can ultimately lead to life threatening complications [136]. Tissue homeostasis in the kidney is limited and further diminished by age or disease [137]. This results in 20 million people worldwide suffering for chronic kidney disease (CKD) [138]. Therefore, identifying stem cell populations in the fetal and adult kidney is important for developing effective therapeutic applications and understanding stem cell biology within the kidney tissue.

Here, we briefly describe embryonic and adult renal stem cell markers with the aim to translate this knowledge to cancer stem cell biomarker discovery.

Wilms' tumors proved to be the best model system for studying embryonic renal stem cells. These tumors result from differentiation arrest of embryonic progenitor cells committed to the nephric lineage [139]. Comparative gene expression profiling of WT and fetal human kidneys showed high concordance in the expression of the following markers: Pax2, Six1/2, NCAM, Fzd7 and Fzd2 [140,141]. Nevertheless, embryonic renal stem cells are entirely exhausted during nephrogenesis and the expression of these genes is rapidly lost during differentiation [142], limiting their utility to uncover merely embryonic-specific renal stem cell markers.

Adult renal stem cells are investigated using BrdU staining [143]. BrdU is incorporated into dividing cells during the pulse phase, but further cell divisions will quickly dilute the stain leaving cells that divide infrequently like stem cells alone labeled with BrdU [144]. Nevertheless, some limitations must be considered such as adult stem cells divide infrequently and may not be labelled, and on the other hand, kidney has normally a limited mitotic index resulting in impaired signal dilution.

Following BrdU staining, a subset of cells expressing CD133 and CD24 were isolated from the urinary pole of the Bowman's capsule and from the proximal tubules, in particular in the S3 segment. These cells also expressed stemness markers (i.e. Sox2, CD44, Oct4 and Vimentin), and could be discriminated by CD106 differential expression [145,146]. Stem cells derived from the Bowman's capsule were shown to move and differentiate from the urinary pole to the vascular pole acquiring podocyte traits (PDX marker) and losing stem cell markers (CD133 and CD24), whereas stem cells from the distal end of the proximal tubules were able to migrate within this segment [145-147]. Renal papilla offers a perfect niche for stem cells due to its hypoxic and hyperosmotic microenvironment [148]. Interestingly, Nestin and CD133 have been found expressed in stem cells derived from papilla [149].

Several studies have demonstrated that resident adult kidney stem cells are not the major player involved in tissue repair in the proximal tubule [150]. While differentiated cells undergo EMT and proliferate to repopulate the damaged area, some investigators proposed that other non-resident stem cells such as bone marrow-derived stem cells or MSCs may be also involved in the process [142]. Nevertheless, these cells are defined as renal progenitor cells rather than renal stem cells due to their limited differentiation capability and lack of self-renewal properties.

Conclusions

Tumor relapse and metastasis are the primary causes of poor survival in ccRCC patients. CSCs are thought to be responsible for tumor propagation, metastasis formation and treatment failure in many solid tumors, including renal cancer [25-35]. According to the CSC hypothesis, conventional therapies (i.e. radiation and chemotherapy) usually eliminates the majority of cells present in the tumor bulk while sparing the CSC pool [18]. This results in tumor recurrence. Therefore, understanding of the mechanisms underlying metastasis and drug-resistance associated with CSCs may help identifying new therapeutic options.

Various approaches were developed with the aim to successfully isolate and characterize CSCs, leading to the identification of a variety of CSC markers [151]. However, contrasting results have been reported in the literature on the use of these biomarkers [50,59,60,99]. Several studies have shown that CSC markers are not unique across tumor types; therefore, knowledge on relevant markers for normal stem cells (NSCs) or CSCs from other tumor types may not be useful in renal cancer. Growing evidence suggests that distinct CSC subpopulations may coexist within a heterogeneous tumor and new CSC (sub-)clones can be generated, selected and compete with each other similarly to the stochastic model during tumor progression and treatment resulting in greater intra- and inter- CSC clone variability [135]. Therefore, some biomarkers can be relevant and applicable in certain phases during tumor development and progression, whereas they become obsolete in others.

Many scientists have raised their concerns about the stem cell hypothesis. In particular, the fact that CSCs are considered as a rare slow-cycling subpopulation of cells questioned the possibility of their involvement in treatment failure in support of mechanisms of acquired or intrinsic resistance [19]. Many studies demonstrate a higher CSC content than what one could expect under the

hypothesis of CSCs being a small subset, which can be explained by inefficient isolation methods affecting functional assays as well as xenograft rates [114]. Finally, if CSCs are slowly proliferating one could argue that CSCs are lost during *in vitro* manipulation, whereas these cells remain a constant fraction of the total population [101]. All these concerns finds their explanation in the plastic nature of CSCs as well as technical issues.

CSC traits are sustained by the interaction with the TME (niche) [21]. The CSC niche is an anatomical and distinct TME present within one tumor that support and sustain CSC properties [152,153]. It is composed of ECM, cancer-associated fibroblasts (CAFs), mesenchymal stem cells, endothelial and immune cells [132]. Stem cell niches are often localized in hypoxic region where low O_2 levels induce slow cycle proliferation and minimize DNA damage due to ROS [58,88]. Processes such as inflammation, hypoxia, angiogenesis and EMT taking place within the TME contribute to maintenance of the CSC fate by acting on the most known pathways regulating CSCs: Wnt, SHH, Notch, TGFβ, and growth factor-receptor tyrosine kinase (RTK) [112,132,153,154]. Interestingly, tumor cells in the non-CSC compartment can spontaneously undergo EMT changes and acquire CSC-like phenotype and surface marker expression [155]. At the same time, CSCs display different stemness features depending on the microenvironment, and these features may be transient [133,152]. The entire process has to be considered reversible, plastic and dynamic.

Therefore, understanding the mechanisms underlying CSC properties and the integration of genomic and functional assays exploiting such features may advance CSCs studies as well as promote the identification of new biomarkers for renal CSCs. CSC assays should take into consideration the niche contribution. Moreover, optimization of the transplantation assay using highly immune-deficient mice humanized with human TME and growth factors together with complementary lineage tracing analysis is of outmost importance for advancing CSC studies [132]. Lastly, combination of therapies specifically targeting CSCs by acting not only on CSC surface

555 markers but also inhibiting CSC-related signaling pathways, delivering CSC-specific therapeutics as
556 well as targeting the CSC niche together with conventional chemotherapy and radiotherapy may
557 ultimately lead to improving RCC patient survival [37,132].

558

Reference

1. Moch H. Kidey Cancer. (World Cancer Report 2014 ed). Int. Agency Res. Cancer/World Health Organ: Lyon, Fr., 2014.
2. Bhatt JR, Finelli A. Landmarks in the diagnosis and treatment of renal cell carcinoma. *Nat Rev Urol* 2014; **11**: 517-525.
3. Moch H. An overview of renal cell cancer: pathology and genetics. *Semin Cancer Biol* 2013; **23**: 3-9.
4. World Health Organization Classification of Tumours. Pathology and Genetics of Tumours of the Urinary System and Male Genital Organs. ed). IARCPress: Lyon, 2004.
5. Campbell SCR, B.I. Renal cell carcinoma: clinical management. ed). Springer, 2013.
6. Frew IJ, Moch H. A clearer view of the molecular complexity of clear cell renal cell carcinoma. *Annu Rev Pathol* 2015; **10**: 263-289.
7. Messer J, Drabick J, Kaag M. Rational therapy for renal cell carcinoma based on its genetic targets. *Adv Exp Med Biol* 2013; **779**: 291-308.
8. Vikram R, Ng CS, Tamboli P*, et al.* Papillary renal cell carcinoma: radiologic-pathologic correlation and spectrum of disease. *Radiographics* 2009; **29**: 741-754; discussion 755-747.
9. Delahunt B, Eble JN, McCredie MR*, et al.* Morphologic typing of papillary renal cell carcinoma: comparison of growth kinetics and patient survival in 66 cases. *Hum Pathol* 2001; **32**: 590-595.
10. Speicher MR, Schoell B, du Manoir S*, et al.* Specific loss of chromosomes 1, 2, 6, 10, 13, 17, and 21 in chromophobe renal cell carcinomas revealed by comparative genomic hybridization. *Am J Pathol* 1994; **145**: 356-364.
11. Moch H, Montironi R, Lopez-Beltran A*, et al.* Oncotargets in different renal cancer subtypes. *Current drug targets* 2015; **16**: 125-135.
12. Siegel RL, Miller KD, Jemal A. Cancer statistics, 2015. *CA Cancer J Clin* 2015; **65**: 5-29.
13. Rycaj K, Tang DG. Cell-of-Origin of Cancer versus Cancer Stem Cells: Assays and Interpretations. *Cancer Res* 2015; **75**: 4003-4011.
14. Gerstung M, Beisel C, Rechsteiner M*, et al.* Reliable detection of subclonal single-nucleotide variants in tumour cell populations. *Nature communications* 2012; **3**: 811.
15. Ashkenazi R, Gentry SN, Jackson TL. Pathways to tumorigenesis--modeling mutation acquisition in stem cells and their progeny. *Neoplasia* 2008; **10**: 1170-1182.
16. Shackleton M, Quintana E, Fearon ER*, et al.* Heterogeneity in cancer: cancer stem cells versus clonal evolution. *Cell* 2009; **138**: 822-829.
17. Kreso A, Dick JE. Evolution of the cancer stem cell model. *Cell stem cell* 2014; **14**: 275-291.
18. Nguyen LV, Vanner R, Dirks P*, et al.* Cancer stem cells: an evolving concept. *Nature reviews Cancer* 2012; **12**: 133-143.
19. Kern SE, Shibata D. The fuzzy math of solid tumor stem cells: a perspective. *Cancer Res* 2007; **67**: 8985-8988.
20. Prasetyanti PR, Medema JP. Intra-tumor heterogeneity from a cancer stem cell perspective. *Mol Cancer* 2017; **16**: 41.
21. Atay S, Godwin AK. Tumor-derived exosomes: A message delivery system for tumor progression. *Commun Integr Biol* 2014; **7**: e28231.
22. Visvader JE. Cells of origin in cancer. *Nature* 2011; **469**: 314-322.
23. Lapidot T, Sirard C, Vormoor J*, et al.* A cell initiating human acute myeloid leukaemia after transplantation into SCID mice. *Nature* 1994; **367**: 645-648.
24. Bonnet D, Dick JE. Human acute myeloid leukemia is organized as a hierarchy that originates from a primitive hematopoietic cell. *Nat Med* 1997; **3**: 730-737.
25. Collins AT, Berry PA, Hyde C*, et al.* Prospective identification of tumorigenic prostate cancer stem cells. *Cancer Res* 2005; **65**: 10946-10951.
26. Fang D, Nguyen TK, Leishear K*, et al.* A tumorigenic subpopulation with stem cell properties in melanomas. *Cancer Res* 2005; **65**: 9328-9337.
27. Hermann PC, Bhaskar S, Cioffi M*, et al.* Cancer stem cells in solid tumors. *Seminars in Cancer Biology* 2010; **20**: 77-84.

28. Hermann PC, Bhaskar S, Cioffi M*, et al.* Cancer stem cells in solid tumors. *Semin Cancer Biol* 2010; **20**: 77-84.
29. Kim CF, Jackson EL, Woolfenden AE*, et al.* Identification of bronchioalveolar stem cells in normal lung and lung cancer. *Cell* 2005; **121**: 823-835.
30. Ma S, Chan KW, Hu L*, et al.* Identification and characterization of tumorigenic liver cancer stem/progenitor cells. *Gastroenterology* 2007; **132**: 2542-2556.
31. O'Brien CA, Pollett A, Gallinger S*, et al.* A human colon cancer cell capable of initiating tumour growth in immunodeficient mice. *Nature* 2007; **445**: 106-110.
32. Ricci-Vitiani L, Lombardi DG, Pilozzi E*, et al.* Identification and expansion of human colon-cancer-initiating cells. *Nature* 2007; **445**: 111-115.
33. Schatton T, Murphy GF, Frank NY*, et al.* Identification of cells initiating human melanomas. *Nature* 2008; **451**: 345-349.
34. Singh SK, Hawkins C, Clarke ID*, et al.* Identification of human brain tumour initiating cells. *Nature* 2004; **432**: 396-401.
35. Bussolati B, Dekel B, Azzarone B*, et al.* Human renal cancer stem cells. *Cancer Lett* 2013; **338**: 141-146.
36. Dallas NA, Samuel S, Xia L*, et al.* Endoglin (CD105): a marker of tumor vasculature and potential target for therapy. *Clin Cancer Res* 2008; **14**: 1931-1937.
37. Peired AJ, Sisti A, Romagnani P. Mesenchymal Stem Cell-Based Therapy for Kidney Disease: A Review of Clinical Evidence. *Stem Cells Int* 2016; **2016**: 4798639.
38. Fonsatti E, Maio M. Highlights on endoglin (CD105): from basic findings towards clinical applications in human cancer. *J Transl Med* 2004; **2**: 18.
39. Bussolati B, Bruno S, Grange C*, et al.* Identification of a tumor-initiating stem cell population in human renal carcinomas. *FASEB journal : official publication of the Federation of American Societies for Experimental Biology* 2008; **22**: 3696-3705.
40. Grange C, Tapparo M, Collino F*, et al.* Microvesicles released from human renal cancer stem cells stimulate angiogenesis and formation of lung premetastatic niche. *Cancer Res* 2011; **71**: 5346-5356.
41. Myszczyszyn A, Czarnecka AM, Matak D*, et al.* The Role of Hypoxia and Cancer Stem Cells in Renal Cell Carcinoma Pathogenesis. *Stem Cell Rev* 2015; **11**: 919-943.
42. Saroufim A, Messai Y, Hasmim M*, et al.* Tumoral CD105 is a novel independent prognostic marker for prognosis in clear-cell renal cell carcinoma. *Br J Cancer* 2014; **110**: 1778-1784.
43. Jung T, Castellana D, Klingbeil P*, et al.* CD44v6 dependence of premetastatic niche preparation by exosomes. *Neoplasia* 2009; **11**: 1093-1105.
44. Hu Y, Yan C, Mu L*, et al.* Fibroblast-Derived Exosomes Contribute to Chemoresistance through Priming Cancer Stem Cells in Colorectal Cancer. *PLoS One* 2015; **10**: e0125625.
45. Kumar D, Gupta D, Shankar S*, et al.* Biomolecular characterization of exosomes released from cancer stem cells: Possible implications for biomarker and treatment of cancer. *Oncotarget* 2015; **6**: 3280-3291.
46. Bourkoula E, Mangoni D, Ius T*, et al.* Glioma-associated stem cells: a novel class of tumor-supporting cells able to predict prognosis of human low-grade gliomas. *Stem Cells* 2014; **32**: 1239-1253.
47. Wang M, Zhao C, Shi H*, et al.* Deregulated microRNAs in gastric cancer tissue-derived mesenchymal stem cells: novel biomarkers and a mechanism for gastric cancer. *Br J Cancer* 2014; **110**: 1199-1210.
48. Lin R, Wang S, Zhao RC. Exosomes from human adipose-derived mesenchymal stem cells promote migration through Wnt signaling pathway in a breast cancer cell model. *Mol Cell Biochem* 2013; **383**: 13-20.
49. Grange C, Tapparo M, Tritta S*, et al.* Role of HLA-G and extracellular vesicles in renal cancer stem cell-induced inhibition of dendritic cell differentiation. *BMC Cancer* 2015; **15**: 1009.
50. Song L, Ye W, Cui Y*, et al.* Ecto-5'-nucleotidase (CD73) is a biomarker for clear cell renal carcinoma stem-like cells. *Oncotarget* 2017.
51. Li Z. CD133: a stem cell biomarker and beyond. *Exp Hematol Oncol* 2013; **2**: 17.

52. Grosse-Gehling P, Fargeas CA, Dittfeld C*, et al.* CD133 as a biomarker for putative cancer stem cells in solid tumours: limitations, problems and challenges. *J Pathol* 2013; **229**: 355-378.
53. Zhong LY, Du X, Geng SX*, et al.* [Expression of CD133 in the bone marrow of patients with myelodysplastic syndrome and its clinical significance]. *Nan Fang Yi Ke Da Xue Xue Bao* 2011; **31**: 854-855.
54. Sahlberg SH, Spiegelberg D, Glimelius B*, et al.* Evaluation of cancer stem cell markers CD133, CD44, CD24: association with AKT isoforms and radiation resistance in colon cancer cells. *PLoS One* 2014; **9**: e94621.
55. Park EK, Lee JC, Park JW*, et al.* Transcriptional repression of cancer stem cell marker CD133 by tumor suppressor p53. *Cell Death Dis* 2015; **6**: e1964.
56. Bussolati B, Bruno S, Grange C*, et al.* Isolation of renal progenitor cells from adult human kidney. *Am J Pathol* 2005; **166**: 545-555.
57. Xiao W, Gao Z, Duan Y*, et al.* Notch signaling plays a crucial role in cancer stem-like cells maintaining stemness and mediating chemotaxis in renal cell carcinoma. *J Exp Clin Cancer Res* 2017; **36**: 41.
58. Varna M, Gapihan G, Feugeas JP*, et al.* Stem cells increase in numbers in perinecrotic areas in human renal cancer. *Clin Cancer Res* 2015; **21**: 916-924.
59. Shmelkov SV, Butler JM, Hooper AT*, et al.* CD133 expression is not restricted to stem cells, and both CD133+ and CD133- metastatic colon cancer cells initiate tumors. *J Clin Invest* 2008; **118**: 2111-2120.
60. Beier D, Hau P, Proescholdt M*, et al.* CD133(+) and CD133(-) glioblastoma-derived cancer stem cells show differential growth characteristics and molecular profiles. *Cancer Res* 2007; **67**: 4010-4015.
61. Sun C, Song H, Zhang H*, et al.* CD133 expression in renal cell carcinoma (RCC) is correlated with nuclear hypoxia-inducing factor 1alpha (HIF-1alpha). *J Cancer Res Clin Oncol* 2012; **138**: 1619-1624.
62. Maeda K, Ding Q, Yoshimitsu M*, et al.* CD133 Modulate HIF-1alpha Expression under Hypoxia in EMT Phenotype Pancreatic Cancer Stem-Like Cells. *Int J Mol Sci* 2016; **17**.
63. Feng G, Jiang F, Pan C*, et al.* Quantification of peripheral blood CD133 mRNA in identifying metastasis and in predicting recurrence of patients with clear cell renal cell carcinoma. *Urol Oncol* 2014; **32**: 44 e49-14.
64. Zhang Y, Sun B, Zhao X*, et al.* Clinical significances and prognostic value of cancer stem-like cells markers and vasculogenic mimicry in renal cell carcinoma. *J Surg Oncol* 2013; **108**: 414-419.
65. Basakran NS. CD44 as a potential diagnostic tumor marker. *Saudi Med J* 2015; **36**: 273-279.
66. Thapa R, Wilson GD. The Importance of CD44 as a Stem Cell Biomarker and Therapeutic Target in Cancer. *Stem Cells Int* 2016; **2016**: 2087204.
67. Ponta H, Sherman L, Herrlich PA. CD44: from adhesion molecules to signalling regulators. *Nat Rev Mol Cell Biol* 2003; **4**: 33-45.
68. Zoller M. CD44: can a cancer-initiating cell profit from an abundantly expressed molecule? *Nature reviews Cancer* 2011; **11**: 254-267.
69. Ma C, Komohara Y, Ohnishi K*, et al.* Infiltration of tumor-associated macrophages is involved in CD44 expression in clear cell renal cell carcinoma. *Cancer Sci* 2016; **107**: 700-707.
70. Mikami S, Mizuno R, Kosaka T*, et al.* Expression of TNF-alpha and CD44 is implicated in poor prognosis, cancer cell invasion, metastasis and resistance to the sunitinib treatment in clear cell renal cell carcinomas. *Int J Cancer* 2015; **136**: 1504-1514.
71. Debeb BG, Zhang X, Krishnamurthy S*, et al.* Characterizing cancer cells with cancer stem cell-like features in 293T human embryonic kidney cells. *Mol Cancer* 2010; **9**: 180.
72. Lichner Z, Saleh C, Subramaniam V*, et al.* miR-17 inhibition enhances the formation of kidney cancer spheres with stem cell/ tumor initiating cell properties. *Oncotarget* 2015; **6**: 5567-5581.
73. Lu J, Cui Y, Zhu J*, et al.* Biological characteristics of Rh123high stem-like cells in a side population of 786-O renal carcinoma cells. *Oncology letters* 2013; **5**: 1903-1908.
74. Li X, Ma X, Chen L*, et al.* Prognostic value of CD44 expression in renal cell carcinoma: a systematic review and meta-analysis. *Sci Rep* 2015; **5**: 13157.

75. Jin L, Hope KJ, Zhai Q, *et al.* Targeting of CD44 eradicates human acute myeloid leukemic stem cells. *Nat Med* 2006; **12**: 1167-1174.
76. Fang X, Zheng P, Tang J, *et al.* CD24: from A to Z. *Cell Mol Immunol* 2010; **7**: 100-103.
77. Arik D, Can C, Dundar E, *et al.* Prognostic Significance of CD24 in Clear Cell Renal Cell Carcinoma. *Pathol Oncol Res* 2017; **23**: 409-416.
78. Yun EJ, Zhou J, Lin CJ, *et al.* Targeting Cancer Stem Cells in Castration-Resistant Prostate Cancer. *Clin Cancer Res* 2016; **22**: 670-679.
79. Ricardo S, Vieira AF, Gerhard R, *et al.* Breast cancer stem cell markers CD44, CD24 and ALDH1: expression distribution within intrinsic molecular subtype. *J Clin Pathol* 2011; **64**: 937-946.
80. Gao MQ, Choi YP, Kang S, *et al.* CD24+ cells from hierarchically organized ovarian cancer are enriched in cancer stem cells. *Oncogene* 2010; **29**: 2672-2680.
81. Honeth G, Bendahl PO, Ringner M, *et al.* The CD44+/CD24- phenotype is enriched in basal-like breast tumors. *Breast Cancer Res* 2008; **10**: R53.
82. Jaggupilli A, Elkord E. Significance of CD44 and CD24 as cancer stem cell markers: an enduring ambiguity. *Clin Dev Immunol* 2012; **2012**: 708036.
83. Lazzeri E, Crescioli C, Ronconi E, *et al.* Regenerative potential of embryonic renal multipotent progenitors in acute renal failure. *J Am Soc Nephrol* 2007; **18**: 3128-3138.
84. Busillo JM, Benovic JL. Regulation of CXCR4 signaling. *Biochimica et biophysica acta* 2007; **1768**: 952-963.
85. Balkwill F. The significance of cancer cell expression of the chemokine receptor CXCR4. *Semin Cancer Biol* 2004; **14**: 171-179.
86. Balkwill F. Cancer and the chemokine network. *Nature reviews Cancer* 2004; **4**: 540-550.
87. Gassenmaier M, Chen D, Buchner A, *et al.* CXC chemokine receptor 4 is essential for maintenance of renal cell carcinoma-initiating cells and predicts metastasis. *Stem Cells* 2013; **31**: 1467-1476.
88. Micucci C, Matacchione G, Valli D, *et al.* HIF2alpha is involved in the expansion of CXCR4-positive cancer stem-like cells in renal cell carcinoma. *Br J Cancer* 2015; **113**: 1178-1185.
89. Struckmann K, Mertz K, Steu S, *et al.* pVHL co-ordinately regulates CXCR4/CXCL12 and MMP2/MMP9 expression in human clear-cell renal cell carcinoma. *J Pathol* 2008; **214**: 464-471.
90. Cheng B, Yang G, Jiang R, *et al.* Cancer stem cell markers predict a poor prognosis in renal cell carcinoma: a meta-analysis. *Oncotarget* 2016; **7**: 65862-65875.
91. Ma I, Allan AL. The role of human aldehyde dehydrogenase in normal and cancer stem cells. *Stem Cell Rev* 2011; **7**: 292-306.
92. Ueda K, Ogasawara S, Akiba J, *et al.* Aldehyde dehydrogenase 1 identifies cells with cancer stem cell-like properties in a human renal cell carcinoma cell line. *PLoS One* 2013; **8**: e75463.
93. Kastan MB, Schlaffer E, Russo JE, *et al.* Direct demonstration of elevated aldehyde dehydrogenase in human hematopoietic progenitor cells. *Blood* 1990; **75**: 1947-1950.
94. Corti S, Locatelli F, Papadimitriou D, *et al.* Identification of a primitive brain-derived neural stem cell population based on aldehyde dehydrogenase activity. *Stem Cells* 2006; **24**: 975-985.
95. Marcato P, Dean CA, Pan D, *et al.* Aldehyde dehydrogenase activity of breast cancer stem cells is primarily due to isoform ALDH1A3 and its expression is predictive of metastasis. *Stem Cells* 2011; **29**: 32-45.
96. Resetkova E, Reis-Filho JS, Jain RK, *et al.* Prognostic impact of ALDH1 in breast cancer: a story of stem cells and tumor microenvironment. *Breast Cancer Res Treat* 2010; **123**: 97-108.
97. Abourbih S, Sircar K, Tanguay S, *et al.* Aldehyde dehydrogenase 1 expression in primary and metastatic renal cell carcinoma: an immunohistochemistry study. *World J Surg Oncol* 2013; **11**: 298.
98. Ozbek E, Calik G, Otunctemur A, *et al.* Stem cell markers aldehyde dehydrogenase type 1 and nestin expressions in renal cell cancer. *Arch Ital Urol Androl* 2012; **84**: 7-11.
99. Deng S, Yang X, Lassus H, *et al.* Distinct expression levels and patterns of stem cell marker, aldehyde dehydrogenase isoform 1 (ALDH1), in human epithelial cancers. *PLoS One* 2010; **5**: e10277.
100. Chen KG, Szakacs G, Annereau JP, *et al.* Principal expression of two mRNA isoforms (ABCB 5alpha and ABCB 5beta) of the ATP-binding cassette transporter gene ABCB 5 in melanoma cells and melanocytes. *Pigment Cell Res* 2005; **18**: 102-112.

101. Dean M, Fojo T, Bates S. Tumour stem cells and drug resistance. *Nature reviews Cancer* 2005; **5**: 275-284.
102. Wilson BJ, Saab KR, Ma J*, et al.* ABCB5 maintains melanoma-initiating cells through a proinflammatory cytokine signaling circuit. *Cancer Res* 2014; **74**: 4196-4207.
103. Dean M. ABC transporters, drug resistance, and cancer stem cells. *J Mammary Gland Biol Neoplasia* 2009; **14**: 3-9.
104. Nishizawa S, Hirohashi Y, Torigoe T*, et al.* HSP DNAJB8 controls tumor-initiating ability in renal cancer stem-like cells. *Cancer Res* 2012; **72**: 2844-2854.
105. Liu C, Tang DG. MicroRNA regulation of cancer stem cells. *Cancer Res* 2011; **71**: 5950-5954.
106. Galleggiante V, Rutigliano M, Sallustio F*, et al.* CTR2 identifies a population of cancer cells with stem cell-like features in patients with clear cell renal cell carcinoma. *J Urol* 2014; **192**: 1831-1841.
107. Baracca A, Sgarbi G, Solaini G*, et al.* Rhodamine 123 as a probe of mitochondrial membrane potential: evaluation of proton flux through F(0) during ATP synthesis. *Biochimica et biophysica acta* 2003; **1606**: 137-146.
108. Miltenyi S, Muller W, Weichel W*, et al.* High gradient magnetic cell separation with MACS. *Cytometry* 1990; **11**: 231-238.
109. Hu P, Zhang W, Xin H*, et al.* Single Cell Isolation and Analysis. *Front Cell Dev Biol* 2016; **4**: 116.
110. Moghbeli M, Moghbeli F, Forghanifard MM*, et al.* Cancer stem cell detection and isolation. *Med Oncol* 2014; **31**: 69.
111. Khan MI, Czarnecka AM, Helbrecht I*, et al.* Current approaches in identification and isolation of human renal cell carcinoma cancer stem cells. *Stem Cell Res Ther* 2015; **6**: 178.
112. Abbaszadegan MR, Bagheri V, Razavi MS*, et al.* Isolation, identification, and characterization of cancer stem cells: A review. *J Cell Physiol* 2017; **232**: 2008-2018.
113. Goodell MA. Stem cell identification and sorting using the Hoechst 33342 side population (SP). *Curr Protoc Cytom* 2005; **Chapter 9**: Unit9 18.
114. Hill RP. Identifying cancer stem cells in solid tumors: case not proven. *Cancer Res* 2006; **66**: 1891-1895; discussion 1890.
115. Yuhas JM, Li AP, Martinez AO*, et al.* A simplified method for production and growth of multicellular tumor spheroids. *Cancer Res* 1977; **37**: 3639-3643.
116. Weiswald LB, Bellet D, Dangles-Marie V. Spherical cancer models in tumor biology. *Neoplasia* 2015; **17**: 1-15.
117. Clevers H. Modeling Development and Disease with Organoids. *Cell* 2016; **165**: 1586-1597.
118. Drost J, Karthaus WR, Gao D*, et al.* Organoid culture systems for prostate epithelial and cancer tissue. *Nat Protoc* 2016; **11**: 347-358.
119. Pauli C, Hopkins BD, Prandi D*, et al.* Personalized In Vitro and In Vivo Cancer Models to Guide Precision Medicine. *Cancer Discov* 2017; **7**: 462-477.
120. Zhong Y, Guan K, Guo S*, et al.* Spheres derived from the human SK-RC-42 renal cell carcinoma cell line are enriched in cancer stem cells. *Cancer Lett* 2010; **299**: 150-160.
121. Kurosawa H. Methods for inducing embryoid body formation: in vitro differentiation system of embryonic stem cells. *J Biosci Bioeng* 2007; **103**: 389-398.
122. Thoma CR, Zimmermann M, Agarkova I*, et al.* 3D cell culture systems modeling tumor growth determinants in cancer target discovery. *Adv Drug Deliv Rev* 2014; **69-70**: 29-41.
123. Egeblad M, Rasch MG, Weaver VM. Dynamic interplay between the collagen scaffold and tumor evolution. *Curr Opin Cell Biol* 2010; **22**: 697-706.
124. Bielecka ZF, Maliszewska-Olejniczak K, Safir IJ*, et al.* Three-dimensional cell culture model utilization in cancer stem cell research. *Biol Rev Camb Philos Soc* 2017; **92**: 1505-1520.
125. Kalisky T, Quake SR. Single-cell genomics. *Nat Methods* 2011; **8**: 311-314.
126. Golebiewska A, Brons NH, Bjerkvig R*, et al.* Critical appraisal of the side population assay in stem cell and cancer stem cell research. *Cell stem cell* 2011; **8**: 136-147.
127. Salcido CD, Larochelle A, Taylor BJ*, et al.* Molecular characterisation of side population cells with cancer stem cell-like characteristics in small-cell lung cancer. *Br J Cancer* 2010; **102**: 1636-1644.

128. Greve B, Kelsch R, Spaniol K*, et al.* Flow cytometry in cancer stem cell analysis and separation. *Cytometry A* 2012; **81**: 284-293.
129. Vieyra DS, Rosen A, Goodell MA. Identification and characterization of side population cells in embryonic stem cell cultures. *Stem Cells Dev* 2009; **18**: 1155-1166.
130. Bertoncello I, Williams B. Hematopoietic stem cell characterization by Hoechst 33342 and rhodamine 123 staining. *Methods Mol Biol* 2004; **263**: 181-200.
131. Pastrana E, Silva-Vargas V, Doetsch F. Eyes wide open: a critical review of sphere-formation as an assay for stem cells. *Cell stem cell* 2011; **8**: 486-498.
132. Plaks V, Kong N, Werb Z. The cancer stem cell niche: how essential is the niche in regulating stemness of tumor cells? *Cell stem cell* 2015; **16**: 225-238.
133. Oskarsson T, Batlle E, Massague J. Metastatic stem cells: sources, niches, and vital pathways. *Cell stem cell* 2014; **14**: 306-321.
134. Kretzschmar K, Watt FM. Lineage tracing. *Cell* 2012; **148**: 33-45.
135. Baccelli I, Trumpp A. The evolving concept of cancer and metastasis stem cells. *J Cell Biol* 2012; **198**: 281-293.
136. Rosenberg ME, Gupta S. Stem cells and the kidney: where do we go from here? *J Am Soc Nephrol* 2007; **18**: 3018-3020.
137. Pleniceanu O, Harari-Steinberg O, Dekel B. Concise review: Kidney stem/progenitor cells: differentiate, sort out, or reprogram? *Stem Cells* 2010; **28**: 1649-1660.
138. Breyer MD, Susztak K. The next generation of therapeutics for chronic kidney disease. *Nat Rev Drug Discov* 2016; **15**: 568-588.
139. Moch H, Humphrey PA, Ulbright TM*, et al.* WHO Classification of Tumors of the Urinary System and Male Genital Organs. 2016; **8**: 400.
140. Dekel B, Metsuyanim S, Schmidt-Ott KM*, et al.* Multiple imprinted and stemness genes provide a link between normal and tumor progenitor cells of the developing human kidney. *Cancer Res* 2006; **66**: 6040-6049.
141. Pode-Shakked N, Metsuyanim S, Rom-Gross E*, et al.* Developmental tumourigenesis: NCAM as a putative marker for the malignant renal stem/progenitor cell population. *J Cell Mol Med* 2009; **13**: 1792-1808.
142. Bussolati B, Camussi G. Therapeutic use of human renal progenitor cells for kidney regeneration. *Nat Rev Nephrol* 2015; **11**: 695-706.
143. Humphreys BD. Cutting to the chase: taking the pulse of label-retaining cells in kidney. *Am J Physiol Renal Physiol* 2015; **308**: F29-30.
144. Huling J, Yoo JJ. Comparing adult renal stem cell identification, characterization and applications. *J Biomed Sci* 2017; **24**: 32.
145. Ronconi E, Sagrinati C, Angelotti ML*, et al.* Regeneration of glomerular podocytes by human renal progenitors. *J Am Soc Nephrol* 2009; **20**: 322-332.
146. Sagrinati C, Netti GS, Mazzinghi B*, et al.* Isolation and characterization of multipotent progenitor cells from the Bowman's capsule of adult human kidneys. *J Am Soc Nephrol* 2006; **17**: 2443-2456.
147. Angelotti ML, Ronconi E, Ballerini L*, et al.* Characterization of renal progenitors committed toward tubular lineage and their regenerative potential in renal tubular injury. *Stem Cells* 2012; **30**: 1714-1725.
148. Oliver JA, Klinakis A, Cheema FH*, et al.* Proliferation and migration of label-retaining cells of the kidney papilla. *J Am Soc Nephrol* 2009; **20**: 2315-2327.
149. Oliver JA, Sampogna RV, Jalal S*, et al.* A Subpopulation of Label-Retaining Cells of the Kidney Papilla Regenerates Injured Kidney Medullary Tubules. *Stem Cell Reports* 2016; **6**: 757-771.
150. Humphreys BD. Kidney injury, stem cells and regeneration. *Curr Opin Nephrol Hypertens* 2014; **23**: 25-31.
151. Peired AJ, Sisti A, Romagnani P. Renal Cancer Stem Cells: Characterization and Targeted Therapies. *Stem Cells Int* 2016; **2016**: 8342625.
152. Chaffer CL, Brueckmann I, Scheel C*, et al.* Normal and neoplastic nonstem cells can spontaneously convert to a stem-like state. *Proc Natl Acad Sci U S A* 2011; **108**: 7950-7955.

153. Carnero A, Lleonart M. The hypoxic microenvironment: A determinant of cancer stem cell evolution. *Bioessays* 2016; **38 Suppl 1**: S65-74.
154. Cabarcas SM, Mathews LA, Farrar WL. The cancer stem cell niche--there goes the neighborhood? *Int J Cancer* 2011; **129**: 2315-2327.
155. Shibue T, Weinberg RA. EMT, CSCs, and drug resistance: the mechanistic link and clinical implications. *Nat Rev Clin Oncol* 2017; **14**: 611-629.
156. Huang B, Huang YJ, Yao ZJ*, et al.* Cancer stem cell-like side population cells in clear cell renal cell carcinoma cell line 769P. *PLoS One* 2013; **8**: e68293.
157. Peng L, Hu Y, Chen D*, et al.* Ubiquitin specific peptidase 21 regulates interleukin-8 expression, stem-cell like property of human renal cell carcinoma. *Oncotarget* 2016; **7**: 42007-42016.
158. Khan MI, Czarnecka AM, Lewicki S*, et al.* Comparative Gene Expression Profiling of Primary and Metastatic Renal Cell Carcinoma Stem Cell-Like Cancer Cells. *PLoS One* 2016; **11**: e0165718.
159. Bruno S, Bussolati B, Grange C*, et al.* CD133+ renal progenitor cells contribute to tumor angiogenesis. *Am J Pathol* 2006; **169**: 2223-2235.
160. Addla SK, Brown MD, Hart CA*, et al.* Characterization of the Hoechst 33342 side population from normal and malignant human renal epithelial cells. *Am J Physiol Renal Physiol* 2008; **295**: F680-687.
161. Yamashita M, Hirohashi Y, Torigoe T*, et al.* Dnajb8, a Member of the Heat Shock Protein 40 Family Has a Role in the Tumor Initiation and Resistance to Docetaxel but Is Dispensable for Stress Response. *PLoS One* 2016; **11**: e0146501.

888 **Table 1. Summary of putative CSC markers.**

Sample	*Assay*	*Putative marker of the study*	*Positive markers*	*Negative markers*	*CSC features*	*Reference*
769P	side population		ABCB1	ABCC1, ABCG2	clonogenic, tumorigenicity, resistance to chemo and radiotherapy	Huang et al. [156]
786O	sphere formation assay		CD73		tumorigenicity, resistance to radiotherapy	Song et al. [50]
786O	flow cytometry	Rh123			spheroids in soft agar, proliferation, differentiation, tumorigenicity, resistance to radiotherapy	Lu et al. [73]
786O, 769P, A704, Caki1, Caki2	Flow cytometry	USP21	ALDH		sphere formation, clonogenic, proliferation, invasion	Peng et al. [157]
ACHN	side population		ALDH1	CD105, CD133	sphere formation, self-renewal, tumorigenicity	Ueda et al. [92]
ACHN, Caki1	sphere formation assay		Oct4, Nanog, LIN28, KL4, Zeb1, Zeb2, N-cadherin, Vimentin, CD44, CD24	miR17	sphere formation, self-renewal, differentiation, tumorigenicity	Lichner et al. [72]
ACHN, Caki1	flow cytometry	CD105	CD105, Oct4, Nanog, CD90, CD73	CD24, CD34, CD11, CD19, CD45	spheroids in soft agar, hanging drops	Khan et al. [158]
ACHN, Caki1	MACS		$CD133^+/CD24^+$, Oct4, Notch1, Notch2, Jagged1, Jagged2, DLL1, DLL 4		self-renewal, invasion and migration, tumorigenicity, resistance to chemotherapy (sorafenib and cisplatin)	Xiao et al. [57]
ACHN, Caki1, SMKTR2, SMKTR3,	side population		DNAJB8		tumorigenicity	Nishizawa et al. [104]

RenCa						
ACHN, Caki2	flow cytometry	ALDH1	Oct4, Nanog, Pax2		self-renewal, clonogenic, tumorigenicity	
Caki1, Caki2, 786O, 769P	sphere formation assay		CXCR4		sphere formation, tumorigenicity	Micucci et al. [88]
HEK293T	sphere formation assay		ALDH$^+$, CD44, β-catenin, Notch1, Survivin, Vimentin, N-cadherin, Zeb1, Snail, Slug	CD24	sphere formation, resistance to radiotherapy	Debeb et al. [71]
RCC xenograft	sphere formation assay		CD133/CXCR4		sphere formation, tumorigenicity, resistance to chemotherapy	Varna et al. [58]
RCC26, RCC53	flow cytometry	CXCR4	CXCR4, CD24, CD29, CD44, CD73, Nanog, Oct4, Sox2	CD90, CD105, CD133, CXCR1, Vimentin, β-catenin	sphere formation, tumorigenicity, resistance to chemotherapy	Gassenmeier et al. [87]
RCCs	flow cytometry	CD105	CD105, CD44, CD90, CD73, CD29, Nanog, Oct4, Vimentin, Nestin	CD133	sphere formation, clonogenic, differentiation, tumorigenicity	Bussolati et al. [39]
RCCs	flow cytometry	CD133$^+$/ CD34$^-$	CD73, CD44, CD29, Vimentin		non tumorigenic	Bruno et al. [159]
RCCs	flow cytometry	CD133$^+$/ CD24$^+$	CTR2, Nanog, Oct4, Sox2	CD105, CD90	resistance to chemotherapy	Galleggiante et al. [106]
RCCs	side population		CD133		spheroids in soft agar, differentiation	Addla et al. [160]
RenCa			DNAJB8		side population, sphere formation, tumorigenicity	Yamashita et al. [161]
SK-RC-42	sphere formation assay		Oct4, Nanog, BMI, β-catenin	MHC-II, CD80	sphere formation, tumorigenicity, resistance to radio and chemotherapy	Zhong et al. [120]

890

891

892 **Figure Legend**

893 **Figure 1. Model of tumorigenesis.**

894 This figure illustrates three models of tumorigenesis. The clonal evolution model or stochastic model which
895 implies the presence of a tumor cell population carrying multiple mutations which is transformed over time
896 by selective pressure resulting in tumor heterogeneity and progression. The cancer stem cell model or
897 hierarchical model which proposes that tumor growth and propagation is driven by a small subpopulation
898 of cells with pluriproliferative features namely CSCs. More recently, a unifying model characterized by high
899 tumor heterogeneity, plasticity and complexity has bene proposed. According to this model CSCs can
900 acquire mutations and generate new stem cell branches, on the other hand, tumor cells in the non-CSC
901 subpopulation can undergo EMT and acquire CSC-like features contributing to tumor heterogeneity.
902 Moreover, tumor microenvironment and therapy add another layer of complexity.

903

904 **Figure 2. Identification and isolation of cancer stem cells.**

905 Several potential CSC markers are here depicted. CD105, TβR, CD133, CD44, CD24, CXCR4 and ABCB5 are
906 some of the most studied membranous CSC markers. Whereas, miRNAs, DNAJB8, ALDH1 stand out among
907 the intracellular CSC markers. Based on these markers, FACS and MACS have been adopted as isolation
908 methods for the separation of CSCs from other tumor cells. More recently, other techniques exploiting CSC
909 properties have been developed with the aim to discover potentially new biomarkers such as sphere assay,
910 spheroid and organoid formation and hanging drops.

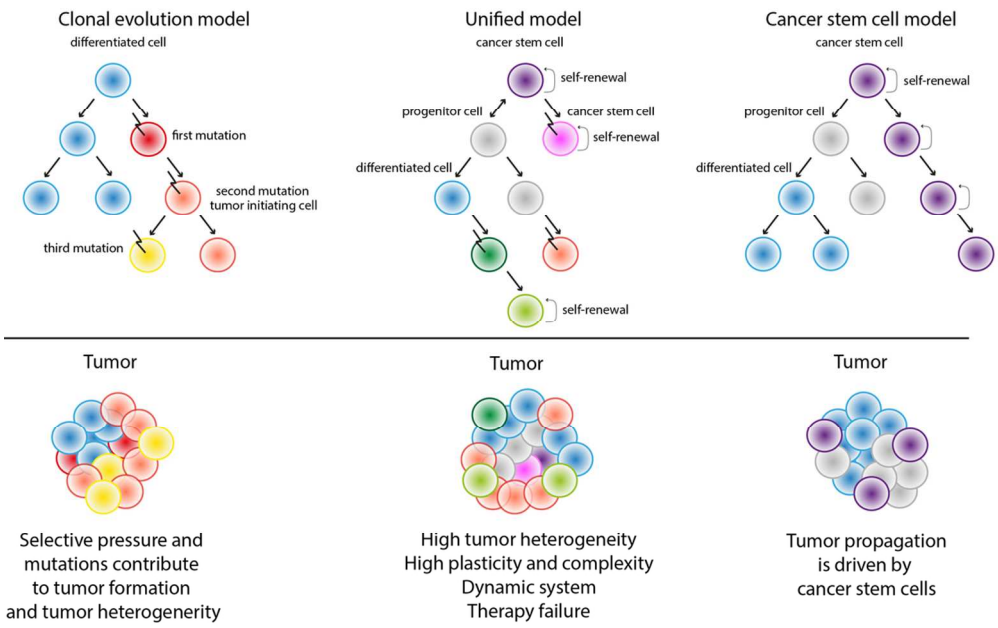

107x68mm (300 x 300 DPI)

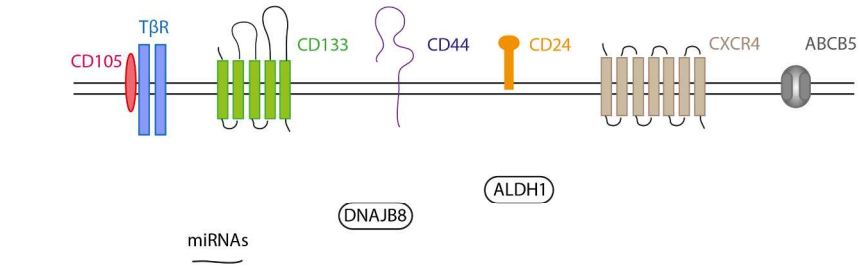

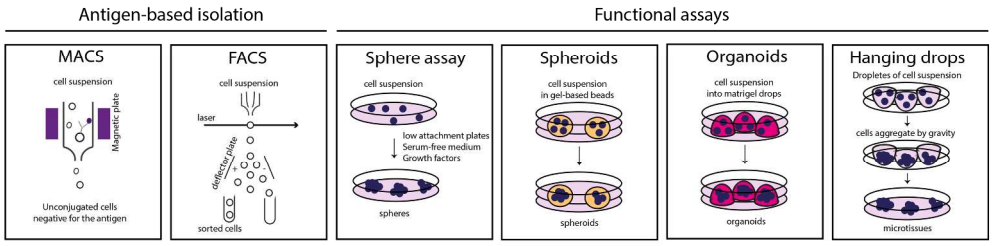

226x144mm (300 x 300 DPI)

Curriculum vitae

Personal information

Claudia Corrò
28.03.1989
Klosbachstrasse 43
CH-8032 Zurich
Claudia.Corro@usz.ch
Claudia.Corro@uzh.ch
Nationality: Italian

Education and Research Experience

11.2013 - Fall 2017 **UNIVERSITY OF ZURICH, Cancer Biology PhD program, Life Science Graduate School Zurich, Zurich, Switzerland**
Ph.D. in Cancer Biology, Prof. Holger Moch research group, Institute of Pathology and Molecular Pathology, University Hospital Zurich
Thesis: "Dissecting Tumor Heterogeneity and Cancer Stem Cell Properties in Clear Cell Renal Cell Carcinoma."

11.2016 - 04.2017 **HARVARD MEDICAL SCHOOL, BRIGHAM AND WOMEN'S HOSPITAL, Boston, Unites States**
Visiting Research Fellow, Prof. Zhe Li research group, New Research Building, Harvard Medical School
Project: "The Role of WNT/β-catenin in Kidney-Derived Organoids."

09.2012 - 07.2013 **IMPERIAL COLLEGE LONDON, London, United Kingdom**
Research Fellow, Prof. Djamgoz Mustafa research group, Faculty of Life Sciences, Division of Cell and Molecular Biology
Project: "A Study of The Voltage-Gated Sodium Channel Mechanisms in Human Breast Cancer: Role of PKA and NHE1."

10.2011 - 07.2013 **UNIVERSITY OF PADUA, Faculty of Life Sciences, Padua, Italy**
M.Sc. in Human Health Biology, 110/110 cum laude (First class with honors)
Thesis: "A Study of The Voltage-Gated Sodium Channel Mechanisms in Human Breast Cancer: Role of PKA and NHE1."
Prof. Djamgoz Mustafa and Prof. Mauro A. Zordan

10.2008 - 11.2011 **UNIVERSITY OF PADUA, Faculty of Life Sciences, Padua, Italy**
B.Sc. in Biology, 110/110 cum laude (First class with honors)
Thesis: "Involvement of Tyrosine Phosphorylation in The Opening of Permeability Transition Pore in Rat Brain Mitochondria."
Prof. Antonio Toninello

09.2003 - 07.2008 **ITAS VENDRAMIN CORNER, Venice, Italy**
Leaving certificate Biology Institute, 100/100
Biology, Chemistry, Biochemistry and Microbiology

Other Relevant Experiences

01.2014 - 01.2016	**Teaching Assistant, Exam Supervisor** UNIVERSITY OF ZURICH, UNIVERSITY HOSPITAL ZURICH, Zurich, Switzerland Pathology (histopathology and macroscopic preparation), Basic Genetics and Molecular Genetics.
01.2007 - 05.2008	**Intern - Food and Water Analyst:** Physical, chemical and microbiological analysis. SAN BENEDETTO S.p.A, Scorzè, Venice, Italy GRANDI MULINI ITALIANI S.p.A, Mestre, Venice, Italy

Awards, Scholarships and Grants

2016 - 2017	**Doc. Mobility Fellowship.** Swiss National Science Foundation SNSF
2016	**Travel Grant** for Keystone Symposia. Hartmann-Müller Foundation
2016	**Research Grant Application** (writing). Swiss National Science Foundation SNSF Main applicant: Prof. Holger Moch
2015	**Ethics Application for Animal Experimentation** (writing). Swiss Federal Veterinary Office FVSO Main applicants: Prof. Lubor Borsig and Prof. Ian Frew
2012 - 2013	**Erasmus Exchange Program.** European Union Scholarship
2011 - 2012	**Outstanding Student Award.** University of Padua

Certifications

2016	**Practical Personalized Medicine.** Competence Center Personalized Medicine UZH/ETH, IT'IS Foundation, International Latsis Foundation
2015 -	**Good Clinical Practice (GCP).** University of Zurich and University Hospital Zurich Center for Clinical Research, Clinical Trial Center
2015 -	**FELASA Accreditation for Animal Experimentation.** University of Zurich, Institute of Laboratory Animal Science
2014	**Project Management for Research.** University of Zurich, Dr. Pamela Alean-Kirkpatrick

Selected Conferences

04.2015	**Speaker** at the **14th Clinical Cancer Research Symposium,** University Hospital Zurich, Zurich, Switzerland
10.2016	Attendee at the Single Cell Analysis Symposium, HMS, Boston, United States
03.2016	**Poster presentation** at the **Keystone Symposia on "Stem Cell and Cancer",** Breckenridge, Colorado, United States
04.2015	Poster presentation at the 6th Cancer Network Zurich PhD Retreat, Emmetten, Switzerland
01.2015	Poster presentation at the 1st Zurich Next Generation Sequencing Symposium
01.2015	**Poster presentation** at the **Charles Rodolphe Brupbacher Symposium**, "Breakthroughs in Cancer Research and Therapy", Zurich, Switzerland
10.2014	**Invited attendee** at the **KOL Digital PCR Congress**, London, United Kingdom

Competences and Skills

Cancer Research Cell/Tissue cultures including primary cultures, Next-generation sequencing, *in vivo* techniques, Flow cytometry, Mass spectrometry, Lineage tracing, CRISPR-cas9, Organoids, Sphere formation assay, Cancer stem cell-related assays, Extracellular vesicles, Transmission electron microscopy, Bisulfide sequencing, Biomarkers in biological fluids (i.e. ctDNA), Ultracentrifugation, Mitochondria isolation, Cloning, Transfection, Molecular and biological techniques and assays

Language Italian: Native
English: Fluent
German: Basic

IT MS Office Suit, Adobe InDesign, Adobe Illustrator, Adobe Photoshop, Fiji, Image J, FlowJo, SigmaStat, GraphPad Prism 5, SPSS and R, CLC Genomic Workbench, Ion Reporter, IGV, Sequencer, UCSC genome browser.
Database consultation: NCBI databases.

Social Volunteer at the **Red Cross Zurich (SRK)**, 2016 –
Volunteer at the **Italian Association for Cancer Research (AIRC)**, 2014 –
Coordinator of weekly research group meetings, USZ, 2014 - 2017
Biological fluids, cancer tissue and living cell biobanking:
Clinical studies in oncology. University Hospital Zurich, 2014 - 2017
Responsible for maintenance of qRT-PCR instruments and introductory courses to new users. University Hospital Zurich, 2014 -2016
Master's student supervisor and lab demonstrator, Imperial College London, 2012 - 2013
Volunteer at the Italian Organization "La Bella Età" in support of elderly people, 2008 – 2010
Catholic youth instructor of 12 – 14 years old students, 2005 - 2007

Personal interests Skiing, Hiking, Swimming, Reading

Publications

Corrò C, Hejhal T, Poyet C, Sulser T, Hermanns T, Winder T, Prager G, Wild PJ, Frew I, Moch H, and Rechsteiner M. *Detecting circulating tumor DNA in renal cancer: An open challenge.* Exp Mol Pathol. 102 (2017), 255-261.

Corrò C and Moch H. *Current updates in biomarker discovery for renal cancer stem cells.* Under revision in The Journal of Pathology: Clinical Research, Sept. 2017.

Corrò C, Bolck HA (these two authors contributed equally to this work), von Teichman A, Pauli C, Chiovaro F, Dettwiler S, Prutek F, Moritz W, Rechsteiner M, Moch H, and Schraml P. *Cancer tissue biobanking at the next level: Establishing patient-derived renal cancer cell cultures as a resource for research and precision medicine.*

Corrò C, Healy ME, Engler S, Schraml P, Bodenmiller B, Weber A, Frew I, Rechsteiner M, and Moch H. *IL-8 and CXCR1 are associated with cancer stem cell-like properties in renal cancer and represent a potential therapeutic target for ccRCC patients.*

ACKNOWLEDGEMENTS

I would like to express my sincere gratitude to Prof. Holger Moch for providing me with the unique opportunity to work on this intriguing project entitled “Dissecting tumor heterogeneity and cancer stem cell properties in clear cell renal cell carcinoma” under his direct supervision. His guidance, encouragement and support were guiding lights throughout the course of my entire Ph.D.

Furthermore, I would like to express my appreciation to each and every Professor and Expert of my Thesis Committee: Prof. Beat Schaefer, Prof. Ian Frew, Prof. Bernd Bodenmiller, and Dr. Markus Rechsteiner for sharing their knowledge and experience, for their inputs and feedbacks. In particular, my heartfelt thank goes to Dr. Markus Rechsteiner. His suggestions, critics and observations were decisive for improving and developing my skills in and outside the academic context.

Many thanks go to my collaborators Prof. Ian Frew, Prof. Lubor Borsig, and Prof. Achim Weber for their input and assistance in designing and performing *in vivo* experiments; to Prof. Bernd Bodenmiller for performing mass cytometry studies; and , finally, to Prof. Peter Wild for supervising and sharing his knowledge on the next-generation sequencing. Our collaboration added a great value to my work.

Dr. Peter Schraml for his valuable advice and contribution to my work.

To Prof. Zhe Li and all the lab members at Harvard Medical School, I thank you for having made my time in the United States such a great experience on both a professional and personal level. Your commitment to the highest standards inspired and motivated me greatly. A special thank goes to Dr. Hubert Pakula for being a great instructor as well as a true friend.

I would like to thank the technical support staff who provided me with excellent assistance in many aspects of the research and administrative work, Dettwiler Susanne, Fabiola Prutek, Martina Storz, Christiane Mittmann, Marcel Glönkler, Andrè Fitsche, Adriana von Teichman, Raquel Herrador, Katharina Mühlbauer, Annette Bohnert, Angela Bürlimann, Norbert Wey, Andre Wethmar, and Monika Bieri. A special thank goes to our secretary Nadja Blöchlinger for her great work and kind support.

I would like to show my gratitude to all the current and former team members of Prof. Alex Solterman, Prof. Achim Weber, and Prof. Peter Wild jointly together with the people from my research group not only for their scientific contribution but also for creating a nice working atmosphere and joyful time outside work. In particular among the members of these teams, I would like to mention Silvia Angori, Aashil Batavia, Elisa Bellini, Dr. Hella Bolck, Dr. Ruben Casanova, Dr. Marc Eammonn Healy, Dr. Anna Honcharova, Dr. Abdullah Kahraman, Dr. Anne-Laure Leblond, Dr. Magdalena Lukamowicz-Rajska, Mohsen Malehmir, Jasna Muhic, Dr. Anna Nowicka, Kathrin Oehl, Chantal Pauli, Dr. Dorothee Pflüger, Dr. Caroline Razafinjatovo, Dr. Melanie Ruf, and Undine Rulle.

To my parents and Dam, whom this work is dedicated to, I would like to express my deepest gratitude for your unconditioned love, for the patience and understanding, for your support and encouragement, and for believing in me. From you, I have learnt the most valuable lessons of my life.

Finally, to all my friends worldwide for having taken the time of making me feel always as part of your lives although international careers lead us far apart from each other.